Driven Precast Prestressed Concrete (PPC) Pile Design and Construction Optimization

ALDOT Project Number: 930-929

Submitted to:

Alabama Department of Transportation
1409 Coliseum Boulevard
Montgomery, Alabama 36110

Prepared by:

Emily Gould, M.S Student
Sriram Aaleti, Ph.D., Associate Professor
Department of Civil, Construction, and Environmental Engineering,
The University of Alabama

Aaron Weatherford, M.S Student
Eric Steward, Ph.D., P.E., Associate Professor
Department of Civil, Coastal, & Environmental Engineering
University of South Alabama

LIST OF ABBREVIATIONS

Organizations:	
AASHTO	American Association of State Highway and Transportation Officials
ACI	American Concrete Institute
ALDOT	Alabama Department of Transportation
ARDOT	Arkansas Department of Transportation
DOT	Department of Transportation
FDOT	Florida Department of Transportation
GDOT	Georgia Department of Transportation
KYTC	Kentucky Transportation Cabinet
LADOTD	Louisiana Department of Transportation and Development
MDOT	Mississippi Department of Transportation
NCDOT	North Carolina Department of Transportation
PCA	Portland Cement Association
PCI	Prestressed/Precast Concrete Institute
SASHTO	Southeastern Association of Highway Traffic Officials
SCDOT	South Carolina Department of Transportation
TDOT	Tennessee Department of Transportation
TxDOT	Texas Department of Transportation
VDOT	Virginia Department of Transportation
WVDOT	West Virginia Department of Transportation
Units of Measure:	
ft.	foot
in.	inch
kip-ft.	kip-feet
klf	kips per linear foot
ksf	kips per square foot
ksi	kips per square inch
mph	miles per hour
pcf	pounds per square foot
psi	pounds per square inch

psf	pounds per square foot
Other:	
ASD	Allowable Stress Design
ed.	Edition
GDM	Geotechnical Design Manual
LF	Load Conversion Factor
Low-Lax	Low Relaxation Prestressing Strand
LRFD	Load and Resistance Factor Design
M	Moment
P	Axial Force
PPCP	Prestressed Precast Concrete Pile
No.	Number
SDM	Structural Design Manual
SF	Safety Factor
Spec	Standard Specifications
Std.	Standard
Typ.	Typical
u.n.o.	Unless Noted Otherwise
VBA	Visual Basic for Applications

TABLE OF CONTENTS

LIST OF TABLES

LIST OF FIGURES

1. Introduction

Driven piles are long, slender foundation elements commonly used to support high-rise buildings and bridges. Piles provide structural support through resistance caused by pile-soil interaction along the embedded portion of the pile shaft and around the cross-sectional area of the pile toe. Pile foundations are commonly used when structures must be elevated or when traditional shallow foundations are unable to provide structural stability due to underlying soil properties. Piles allow structural loads to be transferred from less desirable soils that are highly compressible, expansive, or collapsible to underlying layers with sufficient strength. Driven piles can be made from a variety of materials, including timber, steel, and concrete. Concrete piles, on the other hand, are commonly used for coastal bridge support because of their ability to support heavy loads while also resisting corrosion in saltwater environments.

The Alabama Department of Transportation (ALDOT) frequently uses square prestressed precast concrete (PPC) piles for the foundational support of coastal bridges throughout the southern region of the state. ALDOT currently allows the use of square PPC piles ranging in size from 14 to 36 inches. To aid and expedite the design process for these foundations, ALDOT engineers have a standard table of pile capacities. Having these values as a starting point is useful, however, when these values are compared with those from surrounding state DOTs with similar pile cross-sections and properties, the ALDOT capacities are on the lower end of the spectrum of values. Table 1-1 below shows a comparison between Alabama, Florida, and Georgia DOTs' available axial capacities for different standard prestressed precast piles. The highlighted rows particularly show that Florida's values are nearly three times Alabama's. The origins of the ALDOT standard values are not available at this time, and so the reasoning for the lower capacities has not been well documented. An investigation into these capacities as well as an attempt to increase them is necessary for efficient pile design within ALDOT. If ALDOT's structural axial load limits could be increased, it could result in a potential cost savings, as smaller sized piles could be used in place of larger piles.

Table 1-1: Comparison of Axial Capacities of PPC piles used by different state DOTs.

DOT Specified Pile Axial Capacities (kips)			
Pile Size	Alabama	Florida	Georgia
14 in.	180	550	473
16 in.	240	N/A	636
18 in.	300	900	820
20 in.	360	1100	1006
24 in. Voided	440	1575	1158
30 in. Voided	620	1800	1706
36 in. Voided	820	N/A	2224

To conduct a thorough assessment of the viability of increasing ALDOT's axial load limits for PPC piles, it is necessary to investigate the geotechnical consequences of increasing the load on piles with smaller dimensions. Soil properties have a direct impact on two aspects of pile installation: pile

capacity generation and pile driving-induced stress intensity. Following hammer blows, driving stresses develop as a result of the pile's transient compression, rebound, and elongation. The resistance generated by the pile-soil interaction in relation to the pile's embedded surface area determines its capacity. In general, the capacity of an embedded pile increases in proportion to its area. As a result, pile capacity can be increased by either increasing the size of the piles used or increasing the depth of the piles embedded. As a result, in order to implement smaller piles capable of supporting higher intensity loads, the latter must be driven to deeper levels of embedment, where they can develop the necessary resistance. As the pile's embedment increases, so does the number of hammer blows it receives. Every time the hammer strikes the pile, there is a chance that potentially damaging driving stresses will develop. The primary concern about prolonging pile embedment is the possibility of pile damage caused by increased driving exposure. To increase the axial load limits of square PPC piles, it is necessary to demonstrate the ability to drive piles of varying sizes to greater depths of embedment without sustaining damage.

In addition to driving stresses, the overall cost of using smaller piles to support higher intensity loads must be considered. Allowing increased loads on smaller piles is only beneficial if it results in cost savings. Pile foundations have two major costs: pile material and installation. The cost of piling material is directly proportional to its volume, whereas the cost of installation is proportional to pile embedment depth. As a result, when assessing the potential for cost savings from placing increased loads on smaller sized piles, it is necessary to determine whether a smaller size pile can achieve the resistance required to support higher intensity loads at a depth sufficient to offset the cost savings generated by increased pile length and embedment.

1.1. Research Objectives and Tasks

The objective of the research detailed within this document was to investigate the origins of the ALDOT standard capacities and determine whether the capacities of ALDOT's standard piles could reasonably be increased to allow for more efficient pile usage. To accomplish this goal, several primary tasks were completed.

The first major task was developing a thorough review of the current state of practice within similar DOT offices to understand how their pile capacities were determined. This included developing and administering an online survey to gather pile design information from these organizations. Simultaneously, the current ALDOT design values were closely analyzed to determine likely origins to their values. This included investigating the two different design methodologies that would have been used to arrive at the values in at least some capacity, Allowable Stress Design (ASD) and Load and Resistance Factor Design (LRFD). Within the ASD consideration, the origins of the typical axial pile capacity equation were tracked down and evaluated.

The second major task came from developing a moment-axial interaction diagram program for ALDOT standard PPCPs. This program was developed using Microsoft Excel and Visual Basic for Applications (VBA) coding. These interaction diagrams serve as design aids for showing the theoretically safe thresholds of a pile's combined axial and moment loading. Through this analysis, the available structural capacity of the cross section is visualized, and it is significantly higher than those values provided in the current ALDOT standard pile capacity table. From there, it would be remiss to discuss pile capacity without examining demand, so three prototype bridges were developed for analysis of typical loading pile bents could be expected to experience. The resulting comparison

between capacity and demand showed that for the given loading, the potential capacity of the piles is not currently being fully utilized.

The next task was to determine if smaller sized piles could be safely, and cost effectively installed to a depth of embedment necessary to support higher load intensities using geotechnical modeling and analysis of historic square PPC pile installations in Alabama. The ALDOT Bureau of Materials and Tests provided historical records for 32 test pile installations. The data from the test pile records was used to create an approximate driving system/pile/soil model for each pile installation using GRLWEAP pile analysis software. The research performed using this data can be divided into three primary components: the driving stress and capacity analysis of original test piles, the driving stress and capacity analysis of reduced size piles installed at the same location, and the comparative cost analysis performed on original and reduced size piles.

GRLWEAP modeling and analysis were used to determine the original size of each historic test pile installation included in the pile records. GRLWEAP's driveability program was used to estimate the original test pile capacity as well as the maximum compressive and tensile stresses that would be induced during pile installation. Separate rounds of driveability analysis were carried out with compressive concrete strengths of 5000, 5500, 6000, and 6500 psi. This analysis was carried out to determine the change in driving stresses caused by incremental increases in compressive concrete strength, as well as to determine whether an optimal concrete compressive strength could be chosen to reduce driving stresses. The GRLWEAP estimated maximum driving stresses at each concrete strength were compared to the corresponding allowable stress limits to assess pile integrity. The GRLWEAP predicted capacity resulting from test pile installations was also calculated. In order to assess the accuracy of GRLWEAP pile capacity predictions, the predicted original size pile capacities were compared to the corresponding static load test capacities shown in the pile records.

Reduced size pile analysis involved replacing the original size pile parameters with those of a smaller standard pile size. Reduced pile sizes were tested under identical site conditions as the original size piles. The GRLWEAP-determined capacity of the original size piles served as the baseline capacity for which reduced size piles were required to meet. To achieve the original size pile capacity, the pile embedment needed to be reduced and the length had to be increased. Each reduced-size pile was evaluated using GRLWEAP's driveability program to determine the maximum driving stresses that occur with incremental increases in pile compressive concrete strength. To assess reduced size pile integrity, maximum induced driving stresses were compared to corresponding allowable driving stress limits, just as they were for original size piles. The impact of pile size reduction on allowable driving stresses was assessed by comparing the percentage of achieved allowable stresses between original and reduced size piles.

Based on the research presented within this document and summarized above, the structural capacity of ALDOT piles can be increased substantially from their current values.

2. Background and Literature Review

To successfully design infrastructure structures, engineers must ensure they are supported by strong foundations, in the most literal sense. A foundation is an engineered system used to transmit loads from a structure to the surrounding soil. Typically, foundations are divided into shallow and deep foundations. Examples of shallow foundations include, strip foundations typically used for walls, spread footings typically used under columns, and mat foundations which are concrete slabs covering a larger area to support multiple parts of a structure (Mishra 2018, FHWA 2002). Deep foundations are typically comprised of long structural members embedded deep into the soil. These members can be made of steel, concrete, or timber which are driven into the soil, or cast in place drilled shafts filled with reinforced or unreinforced concrete (Das 2014). Selecting the appropriate type of pile for foundation implementation requires consideration of applied loads, site conditions, and a knowledge of locally available materials (Coduto et al. 2016). Driven piles are the foundation type that is of interest for this research project out of the ones listed previously. Driven piles can be made of steel, timber, concrete, or a combination of the two. Each pile type has distinct advantages and situations in which it performs best. Once a pile foundation has been designed, individual piles are driven into the ground using mechanized hammers. The piles are driven into the soil until they reach the required bearing capacity or the desired tip elevation, as determined by engineering. Once all of the required piles for a group have been driven, a concrete pile cap can be cast to connect the piles.

The geotechnical capacity of a driven foundation pile is determined by two major factors: frictional resistance and bearing resistance. These variables are influenced by the pile's surface area, the cross-sectional area of its bearing surface, and the geological conditions on the site. The structural axial capacity of a pile is determined by its material strength, size, and shape, as well as any preexisting loading conditions, such as prestressed reinforcement in the case of PPCPs. Under certain conditions, a driven pile may extend significantly above the soil surface, acting as a pile bent. In these cases, or when scour occurs at a pile, leaving the pile partially supported, lateral loading conditions for the piles must be carefully considered due to the generation of moments as well as axial loads. This Chapter presents relevant information about piles and the current design and construction practices.

2.1. Prestressed Precast Concrete Piles

To best illustrate the use of PPCPs, it is necessary to first discuss the fundamentals of foundation design before narrowing the discussion to the specific piles investigated in this study. Concrete piles are advantageous over other foundation options in certain situations. Concrete piles are more corrosion resistant than steel, making them more suitable for brackish or saltwater conditions in particular, perform well in compression, so can be subjected to hard driving, and can relatively easily be incorporated directly into a bridge's substructure that is also made of concrete (Das 2014). Concrete also has some disadvantages. Specifically, its well-known poor performance in tension. To increase the tensile capacity of a concrete pile, prestressing is usually incorporated into its cross-sectional design. PPC piles are manufactured prior to installation and often at an off-site location where they are cast through the placement of concrete in an appropriate sized steel form. Typical concrete compressive strengths utilized for PPC pile manufacture range from 5 to 8 ksi (PCI Committee on Prestressed Concrete Piling, 1993). Prior to concrete placement, typical spiral steel cage reinforcement is positioned along the length of the pile about its central axis. Prestressing of the pile is accomplished by implementing tensioned steel strands within the pile form prior to concrete

placement. Once steel reinforcement is positioned, concrete is placed filling the voided area of the form and simultaneously encasing the reinforcing steel. Once the concrete has cured, the tensioned cables are cut off at the pile ends thus supplying a compressive force to the pile. Concrete encasement of reinforcing steel provides protection from externally corrosive environments. The ability to resist corrosion is especially advantageous in the coastal environment due to the presence of salt water. A disadvantage of PPC piles is that they are difficult to lift and transport and their lengths cannot easily be altered. In lifting and transporting PPC piles, measures must be taken to ensure the pile is adequately supported to ensure its tensile stress limits are not exceeded. In terms of the intended final use of the pile, the compressive force from the prestressing diminishes the amount of external axial compression loading that the pile can withstand. However, the incorporation of the prestressing increases the pile's resistance to bending forces from lateral loads, axial load eccentricity, or other tension causing loads.

In terms of project constructability, prestressing is very important to concrete piles. While piles are being driven, the impact force imparted to the pile travels down the pile to its tip in a pulse or wave of energy. What happens during this progression can be problematic if the soil is either too soft or too hard. In the event of soft soil, piles experience tensile stresses after the compression wave reaches the bottom of the pile, and then travels back up the pile, if the surrounding soil does not provide enough resistance to the shaft, then the wave is reverberated as tension. Typically, tensile driving stresses capable of causing damage only to occur within piles in excess of 50 feet in length during soft or irregular driving (PCI Committee on Prestressed Concrete Piling, 1993). Conversely, if soil resistance is too high, then a compression wave travels back up the shaft, then converts to a tension wave after it reaches the pile head and reverberates back down the pile (its second time through that part of the pile). The compression imparted by the prestressing allows the pile to attenuate these tensile driving forces. These driving stress values are either calculated using wave equations or dynamically monitored using advanced measurement systems during driving (Parola 1970).

The allowable driving stresses of a pile is governed by Section 4.5.11 of AASHTO's Standard Specifications for Highway Bridges (AASHTO 2002). The prestressing again diminishes the compression stress allowed on the pile during driving but increases the tensile capacity during driving in normal environments. Prestressing is especially important in severe corrosive environments, where the allowable driving stress in tension is only equal to the concrete compressive stress due to prestressing after all losses (f_{pe}, defined by AASHTO 2002, 4.5.3). Successful PPC pile installation requires the selection of appropriate driving system components under careful considerations of the piles ability to withstand driving stresses.

The cross sections of PPCPs can be a variety of shapes, including round, octagonal, and square (AASHTO 2002, 4.5.20.1). Square cross sections are most frequently used by DOTs in the southeastern United States; thus, a square cross section is to be assumed in this discussion unless noted otherwise. These cross sections typically have an array of longitudinal prestressing steel strands enclosed in spiral wire reinforcement. This array can be circular or square in pattern, depending on the organization's parameters. From examining eleven DOTs' pile details, the square array is most common, typically with 2 to 3 inches of concrete cover on each side of the pile. These strands create uniform prestressing force across the cross section, so as not to cause uneven stress distributions across the pile itself. Piles greater than 24 inches in their primary dimension may have a circular void centered in their cross section to minimize the self-weight of the member, thus improving its structural efficiency. These voids do not run the full length of the pile, but instead terminate a few

feet from the ends of the pile (GDOT 1984). As ALDOT section details are of greatest interest for this project, the following information on them has been reproduced from ALDOT's standard detail sheets (ALDOT 2017a). Figure 2-1 shows the typical cross-sections of ALDOT's voided and non-voided piles. The properties associated with ALDOT's standard piles are reproduced in Table 2-1.

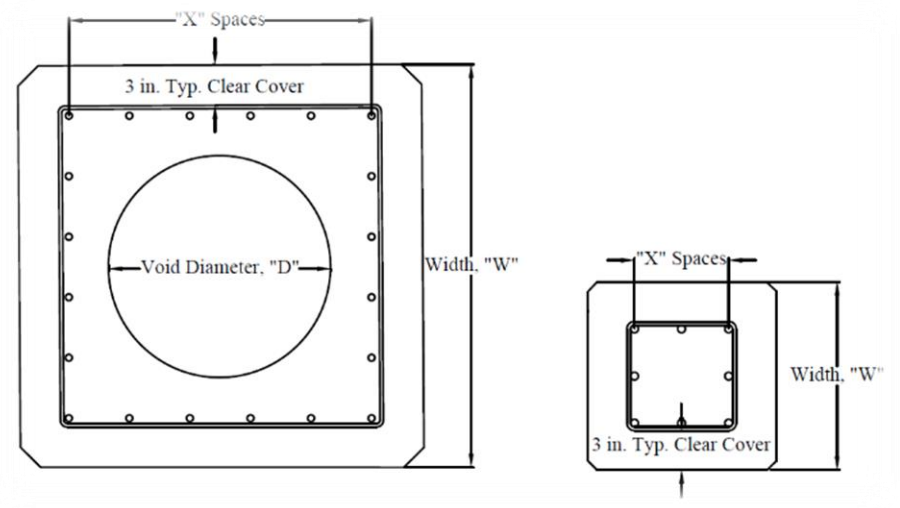

Figure 2-1: Typical ALDOT Voided and Non-Voided PPCP Cross Sections

Table 2-1: ALDOT Standard Pile Properties

ALDOT Standard Pile Properties					
Pile Section Properties			Low Relaxation Strand Details		
Pile Size, "W"	Area of Cross Section, in.^{2}	Void Diameter, "D", in.	No. of Strands	Strand Layout, "X" Spaces	Initial Prestress, psi
14 in.	196	0.00	8	2	1264
16 in.	256	0.00	8	2	968
18 in.	324	0.00	12	3	1147
20 in.	400	0.00	12	3	929
24 in.	489	10.50	16	4	1013
30 in.	686	16.50	20	5	903
36 in.	898	22.50	28	7	966

2.2. Pile to Soil Load Transfer Mechanism

Loads transferred through piles into the surrounding soil are resisted by two components: shaft and toe resistance. As the load is gradually increased, shaft resistance will provide support until the maximum resistance along the shaft is reached. Toe resistance will provide additional support once the shaft resistance has been fully utilized. In general, mobilizing the shaft resistance requires less displacement than mobilizing the toe resistance (Hannigan et al., 2016). The maximum shaft resistance is fully mobilized when the relative displacement between the soil and the pile is 0.2 to 0.3

inches (Das, 2014). Maximum toe resistance is fully mobilized when the tip of the pile has moved 10 to 25 percent of the pile's width or diameter (Das, 2014). A pile is said to be fully mobilized when its entire resistive capacity has been used (Das, 2014). A pile's ultimate load carrying capacity is defined as the maximum load at which it can be fully mobilized. The design load or allowable load that can be placed on a pile is calculated by dividing the pile's ultimate load carrying capacity by a reasonable factor of safety.

The distribution of load between shaft resistance and toe resistance varies depending on soil type and subsurface conditions. Figure 2-2 shows typical load transfer diagrams for different soil types. There is little or no shaft resistance in very weak soils that lies on top of a harder layer (Fig. 2-2a). As a result, toe resistance serves as the primary load support. In cohesive soils, when the toe does not encounter hard strata, shaft resistance carries the majority of the load. Shaft resistance in cohesive soil is caused by soil adhesion to the pile along the length of the shaft. Cohesive soils have adhesive properties that are independent of overburden pressure. As a result, shaft resistance is constant as depth increases (Fig. 2-2b). Toe resistance provides the majority of the load support in cohesionless soils. Shaft resistance in cohesionless soils is caused by friction between the soil and the pile along the length of the shaft. Frictional intensity in cohesionless soil is determined by overburden pressure. Thus, in cohesionless soil, shaft resistance increases linearly with depth (Fig. 2-2c). Though the mechanism of pile-to-soil load transfer can be classified by soil stratigraphy, the short and long term capacities resulting from this load transfer can vary depending on soil composition and the subsequent response to disturbance.

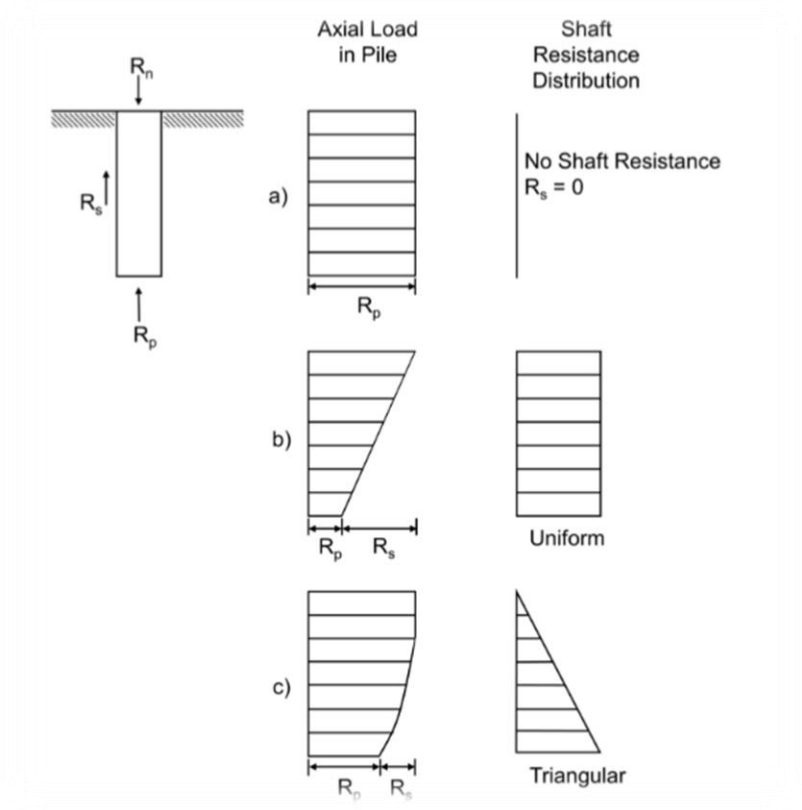

Figure 2-2: Typical pile to soil load transfer (Hannigan et al., 2016).

2.3. Soil Response to Pile Installation

Soil response to pile installation differs significantly between cohesive and cohesionless soil types. Cohesive soil is typically clayed, whereas cohesionless soil is granular. When a pile is driven in cohesive soil, the soil surrounding the pile is disturbed and radially compressed (Hannigan et al., 2016). In cohesive soil, the zone of disturbance is usually contained within one pile diameter of the pile (Hannigan et al., 2016). In saturated cohesive soil, compression within the zone of influence causes high pore pressures and a reduction in soil shear strength (Hannigan et al., 2016). With time, these pore pressures dissipate, the cohesive soil reconsolidates, and shear strength gradually returns. This process of strength restoration is known as "Pile Setup" (Hannigan et al., 2016). In saturated stiff clays, disturbance can cause soil remolding and the loss of historical stress effects.

When a pile is driven into cohesionless soil, the surrounding soil is disturbed and displaced laterally. The resulting zone of disturbance usually extends 3 to 5.5 pile diameters laterally from the pile shaft and 3 to 5 diameters beneath the pile toe (Hannigan et al., 2016). The impact of this disturbance on soil strength and resistance is strongly influenced by the soil's initial density. In loose to medium dense cohesionless soil, pile driving increases the surrounding soil's relative density, resulting in increased shear strength and resistance. However, when loose to medium dense cohesion-less soil is saturated, increasing soil density raises pore water pressure, reducing shear strength and resistance. As a result, there is a temporary trade-off between increased soil density and decreased strength due to increased pore pressure. Porewater pressure gradually decreases, allowing the densified soil to reach its full shear strength capacity. In dense cohesionless soil, pile driving can separate particles, reducing relative density. In saturated dense cohesionless soil, decreasing relative density reduces pore water pressure. The decrease in pore water pressure temporarily increases soil strength. Finally, negative pore pressure subsides, and soil strength decreases in a process known as relaxation (Yang, 1970). Because soil types respond differently to pile installation, pile capacity must be calculated taking long-term soil setup into account. Predicting soil response requires detailed soil parameters obtained through subsurface investigation and in-situ soil testing.

2.4. In-situ Soil Testing

Subsurface exploration is the process of identifying the layers of deposits that lie beneath a proposed structure and their physical characteristics (Das, 2014). Subsurface exploration is primarily used to determine the best type of foundation to support a structure. Subsurface investigation provides foundation design data such as ground water elevation and stratification of soils with corresponding soil strength data. Two types of commonly used in situ soil tests make it easier to collect this information. These tests include the standard penetration test (SPT) and the cone penetration test (CPT).

SPT’s are performed in combination with auger drilled exploratory borings as specified by ASTM D1586 (ASTM, 2011). SPT’s are taken at set intervals of borehole advancement to determine the strength parameters of subsequent soil layers. The primary component of the SPT testing apparatus is the split-spoon sampler. Split spoon samplers consist of a steel driving shoe, a steel casing split along its length, and a coupler used for connection to a drill rod. When a borehole is advanced to a desired depth for testing, drilling equipment is withdrawn, and the sampler is lowered to the bottom of the hole. The sampler is then driven into the soil through blows delivered by dropping a standard 140 pound hammer from a required height of 30 inches. The number of blows required to drive the sampler

to a depth of six inches is recorded. The process is repeated three times at six-inch intervals until the sampler is fully inserted 18 inches into the soil. The soils standard penetration number is the number of blows required to reach the final 12 inches of penetration (N). To reduce inaccuracies, the number of blows associated with the first six inches of penetration are excluded. The resulting N-value is used to quantify soil strength parameters specific to the layer in which it was measured. After complete penetration, the sampler is removed from the boring, and the cylindrical soil sample inside is transported to a geotechnical laboratory for testing. Laboratory testing of the sample provides additional soil strength data and aids in the classification of soil type. SPT testing results are presented as boring logs. Boring logs show a graphic representation of soil layers, along with corresponding soil classification and N values. An example of an SPT boring log is presented in Figure 2-3.

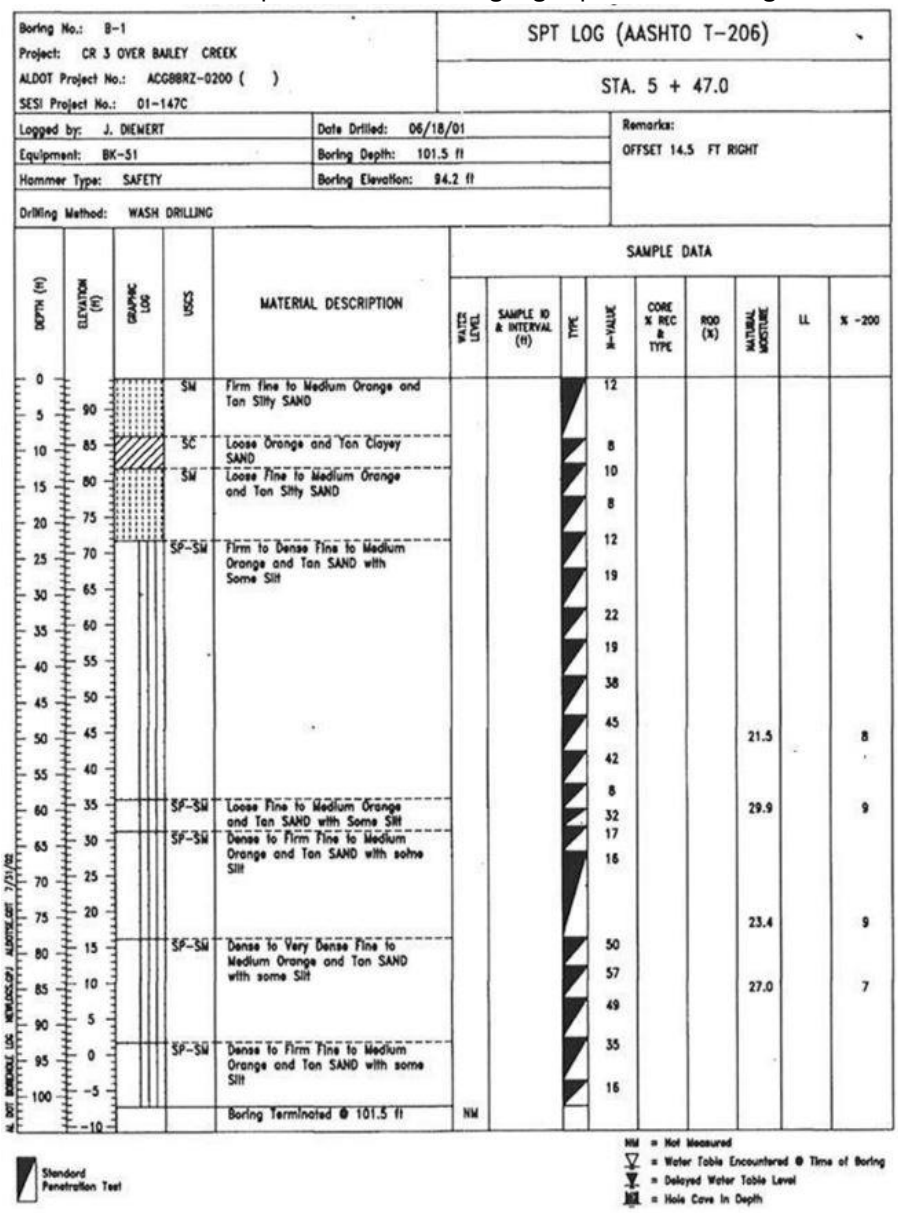

Figure 2-3: Example of a SPT boring log (Provided by ALDOT).

Cone penetration testing (CPT) is performed by hydraulic thrusting of an electrical cone through soil as built in strain gages measure soil resistance. CPT rigs are commonly mounted inside large trucks and operated by a two man crew. One man controls thrusting and oversees data collection while the other adds drill rods as the depth of penetration is increased. Cone configuration includes a 35.7 mm diameter cone-shaped tip with a 60 degree apex angle and a 35.7 mm diameter by 133.7 mm long cylindrical sleeve (Coduto, 2001). As the cone is advanced, two types of resistance are measured: cone resistance and cone side friction. Cone resistance is the total force acting on the cone divided by the area of the cone. Cone side friction is the total frictional force acting on the sleeve divided by the surface area of the sleeve. The values of cone resistance and side friction provide soil behavior data that can be correlated through tables to determine soil type and strength. Cone penetration testing is more cost effective than traditional boring and provides continuous data with depth.

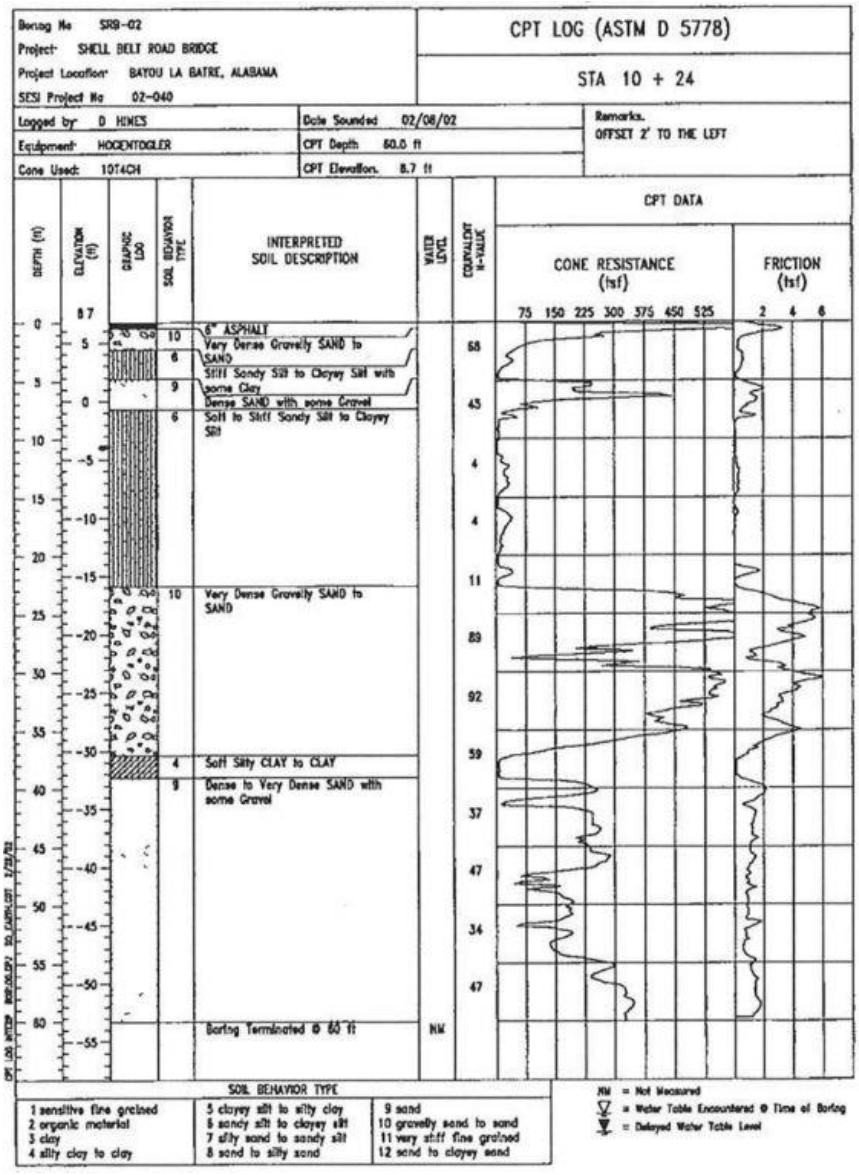

Figure 2-4: Example of a CPT boring log (Provided by ALDOT).

The results of CPT testing are presented in CPT logs. CPT logs provide charts presenting cone tip and side frictional resistance with depth. CPT logs also provide a delineation of soil layers with corresponding soil classification and correlated equivalent N values relating soil strength. An example of an SPT boring log is presented in Figure 2-4**.** Soil strength data acquired by means of insitu soil testing is vital for the selection of pile types and sizes as well as the determination of appropriate components for pile installation.

2.5. Driving System Components

Primary pile driving components include driving rigs, hammers, helmets, and cushions. Driving rigs are cranes mounted on mobile platforms. Cranes are typically attached to a crawler chassis; however, depending on the location and accessibility of the job site, cranes can also be attached to flatbed trucks or barges. Driving rigs are used to position the hammer and pile before driving. Several manufacturers offer pile driving rigs in a variety of sizes and power ratings. When deciding on the best size rig for pile installation, several factors must be considered, including pile size and hammer size. Driving rigs can be equipped with a variety of hammers for pile driving, including drop, air, vibratory, and diesel hammers (Das, 2014). Diesel and air hammers are the two most common hammer types used for square PPC pile installation.

Diesel hammers are made up of a cylinder with a ram and a strike plate. The ram falls, and diesel fuel is injected into the cylinder. The ram compresses the air/fuel mixture until it impacts the striker plate. Upon impact, the air/fuel mixture combusts, forcing the ram upwards to a height from which it falls to deliver a subsequent driving blow to the pile (Coduto et al. 2016). The distance that the ram falls is known as the hammer stroke. Diesel hammers can be either single or double-acting. Double-acting hammers have a cylinder with a closed top. As the ram is propelled upwards, the closed top creates a pressurized chamber above the ram, which limits ram rebound and allows the double-acting hammer to operate at shorter strokes and higher speeds (Coduto el. al. 2016). Diesel hammers are extremely powerful and work well when pile installation involves driving through hard material (Das, 2014). However, this extreme power carries the risk of pile damage. Diesel hammers frequently produce pile driving stresses that exceed the allowable pile driving stress tolerances. The driving force produced by diesel hammers is directly proportional to both the amount of fuel supplied, which affects the hammer stroke, and hammer efficiency. Diesel hammers come with manufacturer-provided specifications for fuel settings and resulting hammer energy. However, actual hammer efficiency can vary significantly, influencing these values. Hammer inefficiency is caused by energy losses within the hammer mechanism. Typically, efficiency declines with hammer use and age. As a result, selecting an appropriate hammer fuel setting requires considering both allowable pile driving stresses and an approximation of actual hammer efficiency. The goal of fuel setting selection is to use the highest fuel setting that reduces installation time while keeping driving stresses below the estimated pile tolerances.

Air hammers use compressed air to deliver driving blows on piles. Air hammers, like diesel hammers, can be both single and double acting. Single-acting air hammers are made up of a cylinder with a piston attached to an external ram. Air within the cylinder is compressed to apply pressure to the piston, which raises the ram to a predetermined height. Upon reaching the set height, an exhaust valve opens, and the hammer falls, delivering a driving blow to the pile (Coduto et al. 2016). Single-acting air hammers operate at fixed strokes, so each blow transfers an equal amount of energy to the pile (Coduto et al. 2016). Double-acting hammers are made up of a cylinder with an internal ram.

Double acting air hammers differ from single acting air hammers in that they use compressed air to lift and accelerate the ram downward, delivering driving blows. As a result, double acting hammers usually have shorter strokes and operate faster than single acting hammers (Coduto et al. 2016).

Pile driving hammers can deliver high intensity blows that can cause damage to both the pile and the hammer itself. As a result, driving accessories that offer protection against these forces are required. These accessories include helmets and cushions. Helmets are typically made of steel and act as the primary interface between hammer and pile. Helmets act as a barrier, protecting the pile from direct impact with the hammer. There are two types of cushions used during pile driving: hammer cushions and pile cushions. Hammer cushions are placed between the hammer and the helmet to reduce the initial impact of each blow while ensuring that the helmet receives an even load. Hammer cushions are typically made of alternating layers of hard materials like aluminum and soft materials like conbest or micarta (Svinkin, 2017). Pile cushions act as a barrier, protecting the pile from direct contact with the helmet. Pile cushions are placed atop the pile to dampen the initial impact of the helmet while ensuring even load distribution to the pile. Common pile cushion configurations include layered oak or plywood cut to match the cross-sectional dimensions of the piles.

Predrilling or jetting is frequently used to facilitate initial pile penetration in order to install concrete piles safely and efficiently. The term predrilling refers to the process of drilling a vertical hole into which the pile will be driven. Jetting is the process of pumping high-pressure water around the pile tip to remove impeding soil and facilitate pile advancement. Predrilling and jetting are typically used when a pile must penetrate hard soil layers that could result in pile damage during standard driving, or when production rates can be increased by reducing the amount of driving required to achieve pile capacity (Coduto et al. 2016). The energy transferred from the driving system to the pile and ultimately resisted by the supporting soil can be modeled and evaluated by means of dynamic analysis.

2.6. Dynamic Analysis

Dynamic analysis refers to the modelling of motions and forces occurring within a pile/soil system as a result of hammer impact. When a hammer impacts the top of a pile, a force pulse is produced that momentarily compresses the top of the pile (Hannigan et al. 2016). The pulse force then travels down the pile towards its toe. The speed with which the force pulse travels is dependent upon the piles elastic modulus and mass density (Hannigan et al. 2016). Soil around the embedded portion of the pile acts to dampen the force pulse. Upon reaching the pile toe, the force reflects back to the pile top as either a tensile or compressive force (Hannigan et al. 2016). The movement of the energy wave along the length of the pile is referred to as wave propagation. If the wave energy is greater than the resistive capabilities of the soil, then the pile is mobilized, and embedment is increased.

Wave equation analysis refers to the complete mathematical representation of a pile installations system including hammer, cushions, helmet, pile, and soil along with an associated computer program for convenient calculation of dynamic motions and forces within the system following ram impact (Hannigan et al. 2016). Wave equation methodology includes modeling of the hammer, helmet, and pile as a series of segments consisting of a concentrated mass and a weightless spring (Hannigan et al. 2016). For the pile segments, spring stiffness and mass values are calculated based on structural properties of the pile material. Hammer and pile cushions are modeled as springs with stiffness values calculated from material cross-sectional area, modulus of elasticity, and thickness (Hannigan et al. 2016). Energy loses in cushion materials and between segments are accounted for by coefficients of restitution. The coefficients range from a value of zero to one. A coefficient of zero indicates a perfectly

plastic collision in which all deformation energy is lost. A coefficient of one indicates a perfectly elastic collision in which all energy is preserved. Static soil resistance is modeled as elastoplastic springs and dynamic soil resistance as dashpots (Hannigan et al. 2016). Typical wave equation models associated with various hammer types are presented in Figure 2-5**.**

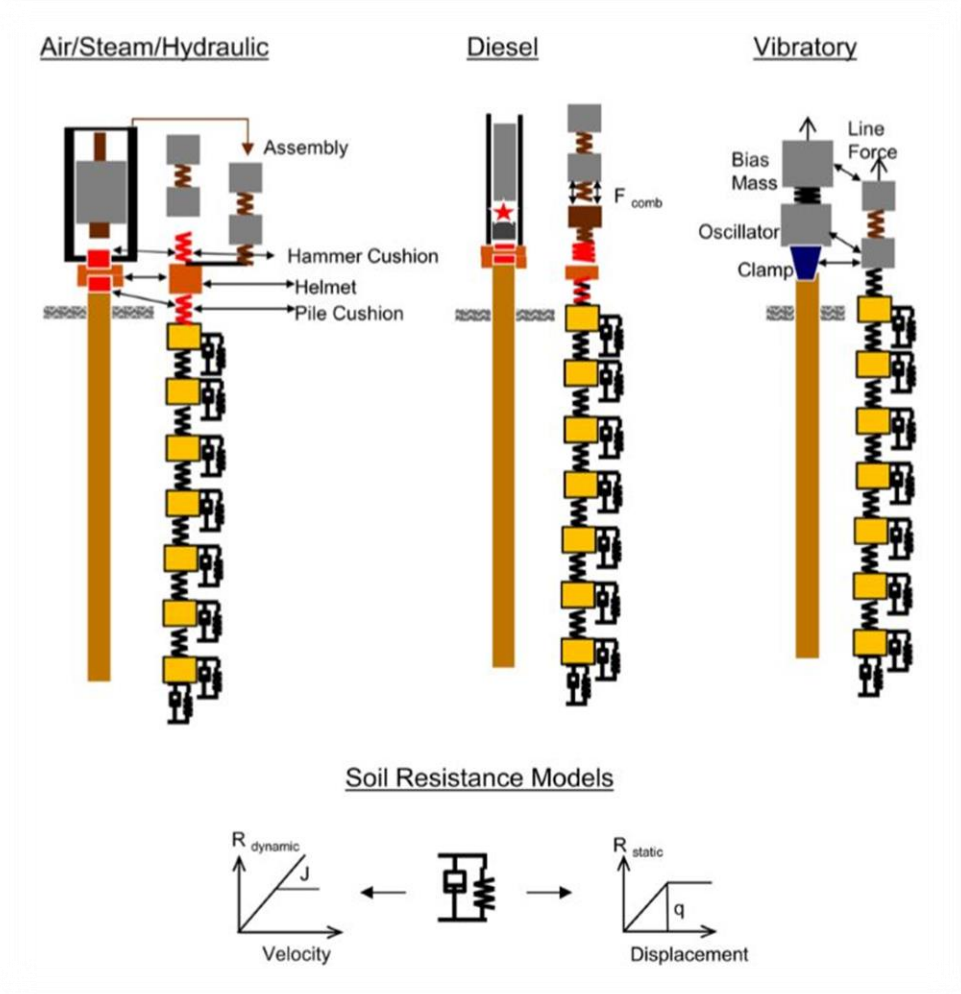

Figure 2-5: Typical wave equation models of various hammer types (Hannigan et al. 2016).

Wave equation analysis begins with a calculated or assumed nominal resistance being distributed about the pile shaft and toe (Hannigan et al. 2016). A ram velocity is then applied to the model. The ram's impact causes a chain reaction of segment displacement. These displacements are resisted by both static and dynamic soil resistance forces. Analysis of the forces acting on each segment allows for the determination of segment acceleration, velocity, and displacement corresponding to each time step. Each subsequent time step is analyzed using updated motion variables resulting from the previous time step (Hannigan et al. 2016). This process is repeated until the pile toe reaches a point of refusal and begins to rebound.

Wave equation analysis can be used over a range of nominal resistances to create a bearing graph relating nominal resistance to pile penetration resistance or blow count (Hannigan et al. 2016). As a result, a bearing graph can be used in the field to calculate nominal resistance based on the number of blows required to achieve a specific depth of penetration. When the blow count corresponding to

the desired nominal resistance is reached, the driving can be stopped. Wave equation analysis also links driving stresses to pile penetration resistance (Hannigan et al. 2016). This allows for the selection of appropriate pile types with material properties that can withstand the driving stress while maintaining the required level of nominal resistance. Wave equation analysis also relates hammer stroke or hammer energy to pile penetration resistance, which corresponds to a given nominal resistance (Hannigan et al. 2016). This helps with the selection of appropriate hammer types, sizes, and strokes. In order to avoid pile damage, these variables should be chosen so that the maximum expected penetration resistance is less than 120 blows per foot (Hannigan et al. 2016).

Several software programs use wave equation analysis for modeling driven pile installation. GRL's Wave Equation Analysis of Pile (GRLWEAP) driving program is a popular tool for pile installation analysis.

2.7. GRLWEAP

GRLWEAP is a software program that utilizes wave equation analysis to simulate motions and forces in a foundation pile when driven by either an impact or vibratory hammer (Pile Dynamics, 2010). GRLWEAP calculates driving resistance, dynamic pile stresses, installation time, and estimates pile capacity based on the observed blow counts corresponding to a given hammer and pile system (Pile Dynamics, 2018). These results can be used to select an appropriate hammer and driving system and also to determine whether a pile will be overstressed at a certain penetration or if refusal will likely occur (Pile Dynamics, 2018). For these reasons, GRLWEAP is primarily used as a pre-installation design tool. Execution of the program requires user supplied inputs corresponding to driving system, pile, and soil parameters that are project specific.

The GRLWEAP driving system consists of a striker plate, hammer cushion, helmet, helmet insert, and, for concrete piles, a pile cushion (Pile Dynamics, 2010). GRLWEAP models the driving system as two non-linear springs, a mass, and a dashpot. The springs represent the ram and hammer cushion, the mass represents the helmet, and the dashpot functions as a vibration dampener (Pile Dynamics, 2010). The GRLWEAP program requires user supplied hammer inputs including hammer type, efficiency, and for diesel hammers, fuel setting and stroke. GRLWEAP contains an in-program database from which hammers can be selected based on manufacturer name and model number. Upon hammer selection, corresponding hammer properties are applied to the analysis. The GRLWEAP program provides recommendations of hammer efficiency based on hammer type. However, the program also recommends these values be altered to reflect actual hammer efficiencies resulting in the field. Hammer and pile cushions are defined within the software by their area, elastic modulus, and thickness (Pile Dynamics, 2010). Helmets are simply defined by their associated mass.

Pile parameters are primarily defined within the program by material composition. GRLWEAP is capable of analyzing timber, steel, and concrete piles. With the selection of pile material type, further pile inputs can be defined including size, length, cross sectional area, perimeter, embedment, elastic modulus, and specific weight. GRLWEAP models the pile by dividing the pile into incremental sections of length with each segment represented by springs, masses, and dashpots (Pile Dynamics, 2010).

GRLWEAP provides several methods for soil data input and analysis. The appropriate method is selected based on the type of insitu testing performed and the extent of available soil data. Each method requires the input of a layered soil profile with specified soil types and strength parameters. GRLWEAP methods of soil data input includes the Soil Type Based Method (ST), the SPT N-value Based Method (SA), the CPT Method, and the API Method. The ST method is the most basic method requiring

only a general input of soil description and classification (Pile Dynamics, 2010). The SA Method is based on soil classification and strength determinations acquired by means of SPT testing and requires the input of soil classification and SPT determined unaltered N values corresponding to soil strength. The CPT Method utilizes soil information obtained through CPT testing and requires the input of tip resistance and sleeve resistance versus depth. The API method is restricted to the evaluation offshore pipe pile installation and requires the input of undrained shear strength for cohesive soils and general density classification of cohesionless soils (Pile Dynamics, 2010). The GRLWEAP program analyzes soil input data by various methods of static analysis to formulate static resistance values associated with individual soil layers and dynamic values corresponding to shaft dampening and toe quake (Pile Dynamics, 2010). GRLWEAP adjusts the dynamic values to provide accurate relationships between the soils response to driving and the spring/dampener model used to represent the soil within the software. The program incorporates both static and dynamic values into its wave equation analysis of pile/soil interaction to reveal the stresses incurred during pile installation as well as the ultimate pile capacity resulting from combined pile shaft and toe resistance.

The GRLWEAP program provides several analysis options including bearing graph, inspectors chart, and drivability analysis. The bearing graph option produces both numerical and graphical outputs that relate capacity, driving stresses, and hammer stroke to blow count (Pile Dynamics, 2018). Bearing graphs are typically used in design to establish the minimum depth of pile embedment necessary for axial load support.

The inspectors chart provides a comparison of stroke versus blow count for a single capacity value. Inspector's charts can be used to determine the required blow count versus variable hammer energy (Pile Dynamics, 2018). Inspector's charts are typically used in the field to determine pile capacity from observed blow counts.

Drivability analysis can generate numerical or graphical estimates of capacity, blow count, and dynamic stresses at various depths of pile embedment. Drivability analysis also considers soil setup using setup and gain/loss factors. These variables enable the simulation of complete or partial loss of soil setup, relaxation effects, and long-term soil resistance. Gain/loss factors control the absolute change of static soil resistance, while setup factors control the relative change of soil resistance between the various soil layers (Pile Dynamics, 2010). GRLWEAP provides rough estimates of these factors based on the soil data entered. Drivability analysis results can be used to calculate the maximum compressive and tensile stresses induced on the pile during installation, as well as the ultimate pile capacities at various depths of penetration. Drivability analysis is commonly used to aid in the selection of the best hammer and driving system parameters for pile installation. However, it can also be used to make an initial estimate of the pile's capacity.

2.8. Load Testing

Pile capacity can be estimated using dynamic analysis, standard static analysis methods, or static load testing. Static load testing is the most accurate among the three methods (Hannigan et al. 2016). Static load testing involves gradually increasing the intensity of an applied axial load on a pile until it has mobilized to an established point of failure. These tests provide data that can be used to verify design, calculate nominal resistance, and analyze deformation response. In the long run, data obtained from static load testing can be implemented into load test databases to aid in the accuracy of future design method calculations and the improved geotechnical design of foundations (Hannigan et al. 2016).

The American Society for Testing and Materials standardized several axial compression load testing procedures (ASTM). These procedures are detailed in ASTM D1143, Standard Test Method for Deep Axial Compressive Load (ASTM, 2013). The most common type of static load testing is axial compression (Hannigan et al. 2016). During static load tests, piles are compressed axially using hydraulic jacking. Jacks are secured to either a beam supported by anchored piles or a weighted platform. Axial compression testing necessitates equipment capable of measuring applied load and corresponding pile movement. Pressure gauges and calibrated load cells are examples of force measurement equipment. The load cell is the primary load measuring device, and the pressure gage provides secondary load data corresponding to jack pressure (Hannigan et al. 2016). Pile movement is measured using a dial gage or a more traditional method that includes a scale, mirror, and wiring system. Dial gages must have at least two inches of travel and a precision of 0.01 inch. Typically, two gages are mounted on reference beams on either side of the beam, at equal distances from the pile head and center.

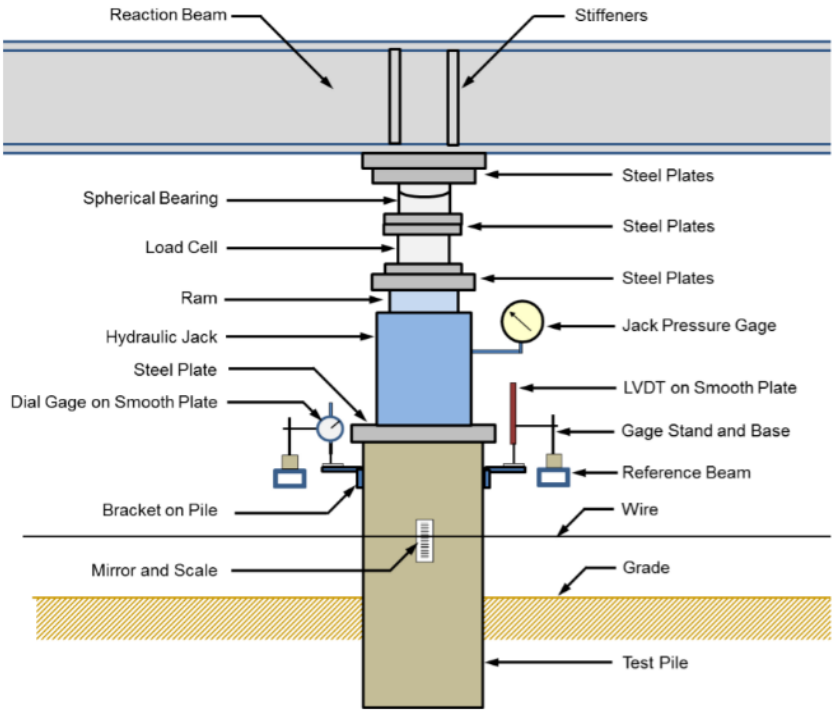

Figure 2-6: Typical static (axial compression) load test setup (Hannigan et al. 2016).

The more traditional scale, mirror, and wiring system measuring method requires a scale precision of 0.01 inches. By this method, a scale atop a mirror is affixed to the pile face. A wire is then run perpendicular to the pile face at a height within the range of the mirrored scale. Manually analyzing the scale reading prior to loading establishes a baseline scale reading that is compared to readings resulting at various load intensities. A typical load test setup diagram is presented in Figure 2-6.

The ultimate load or maximum nominal geotechnical resistance of an axial compressed pile can be either graphically or numerically determined. Each of these approaches require the consideration of elastic deformation of the pile. Elastic deformation is calculated by the following equation (Eq.1).

$$\Delta = \frac{QL}{AE} \qquad \text{(Eq.1)}$$

Where Δ is elastic deformation of the pile, Q is test load, L is pile length below dial gage, A is piling cross-sectional area, and E is elastic modulus of pile material. Ultimate load can be graphically determined using Davisson's offset limit method (Hannigan et al. 2016). Davisson's method requires elastic deformation be plotted along with the load-movement curve. An offset limit line parallel to the elastic deformation line is also plotted. The point at which the offset limit line intersects the load-movement curve is defined as the ultimate load (Hannigan et al. 2016). A typical load-movement curve for an axial compression load test is presented in Figure 2-7. Numerical determination of ultimate load is based on maximum allowable movement of the pile head. The load at which this level of displacement is achieved is defined as the ultimate load.

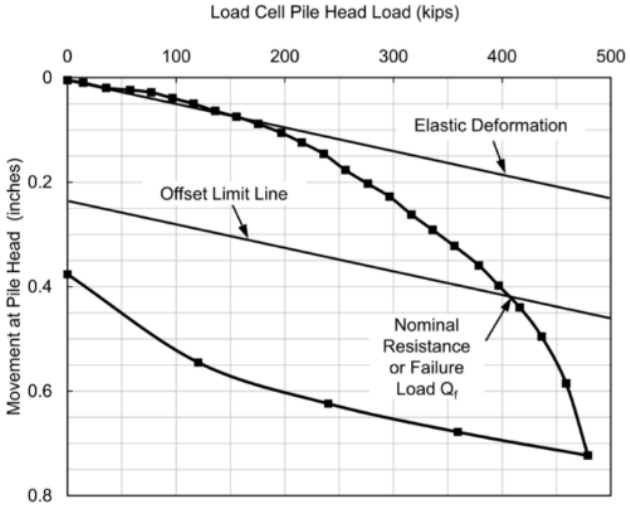

Figure 2-7: Typical load movement curve for axial compression test (Hannigan et al. 2016).

As previously stated, static load testing is widely thought to be the most accurate method of predicting pile capacity. However, it is both time-consuming and expensive. As a result, pile capacity is frequently estimated using static analysis methods. Conveniently, several computer-based programs, including GRLWEAP, use static analysis methods to predict pile capacity. Though convenient, GRLWEAP-generated capacities frequently differ from those determined by static load testing. According to the GRLWEAP manual, GRLWEAP capacity predictions obtained from correlation between wave equation analyses and actual pile driving blow counts typically differ from static load test results, and less than a 10% should never be expected (Pile Dynamic, 2010). Despite being somewhat inaccurate, GRLWEAP generated capacities provide a reasonable estimate of pile capacity, which may be sufficient for some applications.

2.9. Defining Pile Capacity

A pile's capacity can broadly be defined as its ability to resist loading. There are two primary capacity categories that must be satisfied for a pile to have adequate capacity for the task at hand:

- The pile must not fail structurally in supporting its designated load.
- The soil surrounding the pile must provide adequate resistance to the loads of the single pile, as well as the pile group as a whole.

To optimize the design of a pile, it would be recommended to look at each of these parameters individually, to determine which is the primary limiting factor of the capacity of the pile, and then use that limiting capacity as the pile's overall capacity. Additionally, the handling and driving practices for

the piles must not impart sufficient stress to significantly damage the pile. Pile handling and driving practices generally are already moderated separately to try to ensure that they are not the limiting factors of a pile's overall capacity. Thus, further discussion will be focusing on the structural and geotechnical capacities of a pile.

Allowable Stress Design (ASD) and Load and Resistance Factor Design (LRFD) are two common design methodologies used in civil engineering practice. The ASD method has been used for decades to design bridge foundations. However, in the early 2000s, AASHTO and the Federal Highway Administration (FHWA) endorsed LRFD methodology to bring a consistent reliability of design among different elements of a bridge structure, effectively forcing all DOTs to adopt LRFD methodology for foundation design by 2007. (Zickler 2006). ALDOT has only recently fully implemented the LRFD foundation design. Because this transition is still relatively new, there is still some misunderstanding of terms and the use of ASD in design, particularly in geotechnical fields. Thus, the following passages describe both design methodologies, establishing an understanding of both systems and the precise meaning of terms such as "allowable," "ultimate," and "design."

2.9.1. AASHTO's use of Allowable Stress Design

While AASHTO has specified LRFD as mode of designing new projects, ASD is still presented in the 17th edition of the AASHTO Standard Specifications for Highway Bridges (AASHTO 2002). According to the sixth edition of AASHTO LRFD Bridge Design Specifications (AASHTO 2013), bridge engineers for a period of time, had a choice between using ASD methodology found in AASHTO 2002, and LRFD methodology also found in the Spec. However, it has generally been faded out (AASHTO 2013). The AASHTO Specifications for Highway Bridges has been replaced with AASHTO LRFD Bridge Design Specifications, which is currently on its 8th edition, published in 2017 (hereafter referred to as "AASHTO LRFD"). The available most relevant information on AASHTO's ASD design practices from their final bridge specifications incorporating it are presented in the following passages.

2.9.2. ASD Definition of Capacity

AASHTO defined a design pile's ASD capacity as "the maximum load the pile shall support with tolerable movement." The same section of their standard specifications (AASHTO 2002, 4.5.6) goes on to say that when engineers are determining the design pile capacity, they shall consider both the ultimate geotechnical capacity, and the structural capacity of the pile section. Generally, ASD involves determining the theoretical maximum strength of the design element ("ultimate" capacity) then dividing this value by a safety factor and comparing the resulting "allowable" capacity with the loads the element is projected to withstand. These loads are the estimated loads without any additional factors applied to them. The single "factor of safety" or "safety factor" is applied globally in ASD to "compensate for uncertainties from unknown loads or loading conditions, from site variations and from inaccuracies in load determination methods" (Likins 2003).

2.9.3. ASD Geotechnical Pile Capacity

The ultimate geotechnical capacity of the pile (Q_{ult}) is a combination of the pile's ultimate shaft resistance (Q_s) and ultimate tip resistance (Q_T):

$$Q_{ult} = Q_s + Q_T \qquad \text{(AASHTO 2002, eq. 4.5.6.1-1)} \qquad \textbf{Eq.2-1}$$

In some cases, organizations may choose to conservatively consider only the shaft or only the tip capacity based on the soil conditions for the site. The allowable capacity (Q_{all}), which is used as the design capacity of the pile is computed by dividing this ultimate value by a factor of safety (*FS*):

$Q_{all}=Q_{ult}/FS$ (AASHTO 2002, eq. 4.5.6.1-2) **Eq. 2-2**

The factor of safety is determined based on the construction, design, and analysis methods utilized for the pile. AASHTO's corresponding table of safety factors (AASHTO 2002, Table 4.5.6.2A) was replicated in Table 2-2 below.

Table 2-2: AASHTO Geotechnical Safety Factors

Recommended Factor of Safety on Ultimate Geotechnical Capacity Based on Specified Construction Control					
Increasing Construction Control					
Subsurface exploration	[1] X	X	X	X	X
Static Calculation	X	X	X	X	X
Dynamic Formula	X				
Wave equation		X	X	X	X
Dynamic measurement and analysis			X		X
Static load test				X	X
Factor of Safety	3.50	2.75	2.25	[2] 2.00	1.90

[1] X = Construction Control Specified on Contract Plans
[2] For any combination of construction control that includes an approved static load test, a factor of safety of 2.0 may be used.

As this table shows, the factor of safety decreases with increasing levels of construction controls. This is quite understandable, as the better understanding engineers have of a site and the better construction monitoring methods involved, the more confident the engineers can be with the capacity determination.

2.9.4. ASD Structural Pile Capacity

The primary limitation on the structural capacity of a given pile is its allowable stress. The maximum allowable stress for PPCPs is given in Article 4.5.7.3 of the AASHTO Spec (AASHTO 2002). This governing equation for allowable stress on the gross cross section of concrete applies for fully supported piles and is given as:

$0.33\ f_c'-0.27\ f_{pe}$ (AASHTO 2002, 4.5.3) **Eq. 2-3**

In this equation, f_c' refers to the compressive strength of the concrete (ksi), and f_{pe} is the "concrete compression stress due to prestressing after all losses (ksi)" (AASHTO 2002 4.5.3). Piles that do not receive sufficient lateral support from the surrounding soil, are not fully embedded, or otherwise are not fully supported are designed as columns. Brief discussion on slenderness and the column style design of piles can be found in Section 6.7.1 of this document.

2.9.5. Origin of ASD Allowable Stress Equation

While the ASD allowable stress equation for prestressed piles was discovered in a variety of sources, its origins proved difficult to trace. As a result, a portion of this research project involved locating and summarizing the original derivation of this equation. It was particularly important to determine which safety factors had been incorporated.

2.9.5.1. Allowable Stress Equation Derivation

The Portland Cement Association documented the derivation of the often-used allowable stress equation for prestressed concrete in a technical report titled: "Report on Allowable Stresses in Concrete Piles," which was originally published in 1971 (PCA 1971). PCA's derivation of the AASHTO Allowable Stress equation for PPCPs is detailed below (PCA 1971). The variables used in PCA's derivation of the allowable stress in prestressed precast concrete piles are show in Table 2-3.

Table 2-3: Variables used in PCA Allowable Stress Equation Derivation

PCA Allowable Stress Equation Variables		
P_u	=	Ultimate axial load on cross section
A_c	=	Area of concrete
E_p	=	Modulus of Elasticity of prestressing material
f_c	=	Concrete stress
f_c'	=	28-day concrete strength
f_{pe}	=	Effective prestress
f_s	=	Initial prestress (after transfer)
$_s'(loss)$	=	Prestress essentially lost due to concrete reaching ultimate strain
f_{su}	=	Prestress remaining when concrete achieves ultimate strain
ϵ_c	=	Ultimate strain of standard concrete; 0.003

In these calculations, it was assumed that the piles are fully supported, meaning embedded into material that provides sufficient restraint to prevent bending and buckling. To account for accidental eccentricity, an assumption of eccentricity equal to five percent of the cross-section's diameter was incorporated into the derivation of the PCA equation. For square cross-sections in particular, spiral reinforcement was assumed. In 1960 PCA published a report titled "Ultimate Load Tables for Circular Columns" detailing their approach to an improved stress block, being partially parabolic and partially rectangular, with a maximum value of $0.85f_c'$. Similarly, for rectangular cross-sections, PCA published "Ultimate Load Tables for Spirally Reinforced Square Columns" in 1961. Through similar procedures for each, PCA determined that the ultimate load for these types of piles is $P_u=0.734f_c'A_c$, and $P_u=0.750f_c'A_c$ for circular and square cross-sections respectively. Applying a safety factor of 2.2 and dividing each side by the area of the cross section led to allowable stresses of $0.33\,f_c'$ and $0.34\,f_c'$ for circular and square concrete piles.

Moving toward allowable stress equations for prestressed piles involved incorporating the stress imparted by the strands. First, PCA determined how much stress is lost when the pile is loaded, and the concrete strain reaches $\epsilon_c=0.003$ by multiplying this strain by the elastic modulus of the prestressing material. It is worth noting that at this time 30,000,000 psi was used for E_p (units of psi retained to mirror PCA derivation), as opposed to 28,500,000 psi which is the current AASHTO specified value for the modulus of elasticity of prestressing strands (AASHTO 2017, 5.4.4.2). Bars however are assigned a modulus value of 30,000 ksi in the same AASHTO LRFD specifications.

The following equations demonstrate the calculations used in the equations' derivation.

loss in prestress = $f_s' = \epsilon_c * E_p = 0.003 * 30{,}000{,}000 \text{ psi} = 90{,}000 \text{ psi}$ **Eq. 2-4**

PCA assumes the initial prestressing stress in the steel is equal to 70 percent of the material's yield strength. Notably this derivation assumes the use of Grade 250 prestressing material, whereas now Grade 270 is frequently used.

$f_s = 0.70 * 250{,}000 \text{ psi} = 175{,}000 \text{ psi}$ **Eq. 2-5**

The pile having an initial prestress of 175,000 psi progressed to the point where the concrete reaches its ultimate strain, therefore the prestressing material effectively experiences a loss of its stressing.

$f_{su} = f_s - f_s'(loss) = 175{,}000 \text{ psi} - 90{,}000 \text{ psi} = 85{,}000 \text{ psi}$ **Eq. 2-6**

The effective prestress was then calculated assuming 20 percent losses from the original prestress value.

$f_{pe} = (100\% - 20\%) * f_s = 0.80 * 175{,}000 \text{ psi} = 140{,}000 \text{ psi}$ **Eq.2-7**

From there, PCA determined the percent of effective prestress remaining when the concrete reaches its ultimate strength.

$$\%f_{pe} = \frac{f_{su}}{f_{pe}} * 100\% = \frac{85{,}000 \text{ psi}}{140{,}000 \text{ psi}} * 100\% = 60.7\%$$ **Eq. 2-8**

Based on these calculations, PCA determined that 60 percent is a fair estimate of the effective prestress remaining when the concrete reaches its ultimate strain. Combining this determination with the previous ultimate load for circular piles leads to equation for the ultimate load of the cross section. The remaining effective prestress diminishes the compressive strength of the general concrete cross section.

$$P_u = \left(0.734 f_c' - 0.60 f_{pe}\right) A_c$$ **Eq. 2-9**

To put everything in terms of stresses, PCA then divides both sides by A_c.

$$f_c = \frac{P_u}{A_c} = 0.734 f_c' - 0.60 f_{pe}$$ **Eq. 2-10**

PCA method then applies a safety factor of 2.2, the same value as used for traditionally reinforced concrete.

$$f_c = \left(\frac{1}{2.2}\right) * \left(0.734 f_c' - 0.60 f_{pe}\right)$$ **Eq. 2-11**

This final application of the safety factor brings us to the well-known equation for allowable stress in piles: $0.33 f_c' - 0.27 f_{pe}$ (AASHTO 2002, 4.5.7.3). Despite slight differences between circular and square cross sections, PCA conservatively suggests the used of the following equation generally for precast prestressed concrete piles: $f_c = 0.33 f_c' - 0.27 f_{pe}$ (Eq. 2-3).

The primary takeaway from examining the derivation of this allowable stress equation by PCA is that a safety factor of 2.2 was in fact already applied within the derivation of this equation. This means that the resulting values from the application of this equation are in-fact the allowable stresses which have been factored and not ultimate stress values.

2.9.6. **AASHTO's use of Load and Resistance Factor Design.**

As discussed previously, AASHTO and the FHWA sanctioned an official transition from ASD to LRFD in the mid-2000's for DOTs. It is now supposed to be the predominant design methodology employed by these agencies. The majority of the following information comes from AASHTO LRFD, so if not noted otherwise, the numerical citation refers to its section in AASHTO LRFD.

2.9.6.1. *LRFD Definition of Capacity*

In LRFD, different limit states are considered for a structure, including service, strength, and extreme event limit states. Serviceability refers to the structures ability to maintain its function within movement or deformation tolerances. For bridge foundations, service limit states should include consideration for settlement, horizontal movement, overall stability, and scour at the design flood (AASHTO 2017, 10.5.2.1). Strength limit states focus on the ability of the structure to carry the design loads, which are the anticipated loads increased by load factors. Foundations should be evaluated for both their geotechnical and structural resistance in the strength limit state. This includes considering the possible decrease in resistance of the pile if scour occurs, from both geotechnical and structural perspectives (AASHTO 2017, 10.5.3.1). AASHTO lists seven considerations for designing driven pile foundations for strength limit states (AASHTO 2017, 10.5.3.3):

- Axial compression resistance for single piles
- Pile group compression resistance
- Uplift resistance for single piles
- Uplift resistance for pile groups
- Pile punching failure into a weaker stratum below the bearing stratum
- Single pile and group pile lateral resistance
- Constructability, including pile drivability.

In addition to service and strength limit states, extreme event limit states should also be evaluated. Extreme event loading conditions would include vessel impact, flood scour, seismic activity, and other conditions at the discretion of the design engineer (AASHTO 2017, C10.5.4.1). These limit state loading conditions are accounted for with various loading combinations for the structure, and in each case, the "factored nominal" (design) resistance of the structure must meet or exceed the design loads.

2.9.6.2. *LRFD Geotechnical Capacity*

AASHTO LRFD provides the following information regarding the determination of nominal bearing resistance for piles in the strength limit state. This value can be statically determined for estimating pile criteria, but then should be verified in the field with static load tests, dynamic testing, wave equation analysis, or the dynamic formula (AASHTO 2017, 10.7.3.8.6). Static analysis methods are discussed in commentary C10.7.3.3 and Article 10.7.3.8.6a. Additional design considerations would be included for adverse conditions such as scour, down drag, and buoyancy, but the general formula for the design resistance of a pile is calculated as follows:

$$R_R=\phi R_n=\phi_{stat}R_p+\phi_{stat}R_s \qquad \textbf{Eq. 2-12}$$

(AASHTO 2017, 10.7.3.8.6a)

Where:

R_R	=	Factored nominal resistance of footing, pile, micro pile, or shaft (kips)
R_n	=	The nominal pile bearing resistance (kips)
ϕ_{stat}	=	Resistance factor for bearing resistance of a single pile specified in Article 10.5.5.2.3
R_p	$= q_pA_p$	Pile tip resistance (kips)
R_s	$= q_sA_s$	Pile side resistance (kips)
q_p	=	Unit tip resistance of pile (ksf)
q_s	=	Unit side resistance of pile (ksf)
A_s	=	Surface area of pile side (ft.^{2})
A_p	=	Area of pile tip (ft.^{2})

The unit resistances (q_p, q_s) are calculated based on the soil conditions of the site. There is a variety of acceptable methods for calculating these unit resistances, which can be found in 10.7.3.8.6b-g. As the unit resistances rely heavily on existing soil conditions, the primary methods engineers have to increase the pile's geotechnical resistance is to increase the pile's perimeter, length, and/or cross-sectional area at its bearing surface.

Similar to ASD, the factors applied to convert the nominal resistance to the design value are based on types of analysis performed to determine the pile's nominal resistance (AASHTO 2017, 10.5.5.2.3). These values can be found in Table 10.5.5.2.3-1, which has been reproduced below as Table 2-4. This factor does reference Section 5.5.4.2 for other resistance factors, specifically for the structural ones. From this section, the factor for resistance during pile driving is 1.00, while for axial and flexural loading, these factors are determined based on the strain conditions in the cross section being analyzed at its nominal strength (AASHTO 2017, C5.5.4.2).

Table 2-4: Geotechnical AASHTO Resistance Factors

AASHTO LRFD Resistance Factors for Driven Piles (10.5.5.2.3-1)			
Condition/Resistance Determination Method			Resistance Factor
Nominal Bearing Resistance of Single Pile—Dynamic Analysis and Static Load Test Methods, ϕ_{dyn}	Driving criteria established by successful static load test of at least one pile per site condition and dynamic testing* of at least two piles per site condition, but no less than 2% of the production piles		0.80
	Driving criteria established by successful static load test of at least one pile per site condition without dynamic testing		0.75
	Driving criteria established by dynamic testing* conducted on 100% of production piles		0.75
	Driving criteria established by dynamic testing, * quality control by dynamic testing* of at least two piles per site condition, but no less than 2% of the production piles		0.65
	Wave equation analysis, without pile dynamic measurements or load test but with field confirmation of hammer performance		0.50
	FHWA-modified Gates dynamic pile formula (End of Drive condition only)		0.40
	Engineering News (as defined in Article 10.7.3.8.5) dynamic pile formula (End of Drive condition only)		0.10
Nominal Bearing Resistance of Single Pile—Static Analysis Methods, ϕ_{stat}	Side Resistance and End Bearing: Clay and Mixed Soils		
	α-method (Tomlinson, 1987; Skempton, 1951)		0.35
	β-method (Esrig & Kirby, 1979; Skempton, 1951)		0.25
	λ-method (Vijayvergiya & Focht, 1972; Skempton, 1951)		0.40
	Side Resistance and End Bearing: Sand		
	Nordlund/Thurman Method (Hannigan et al., 2005)		0.45
	SPT-method (Meyerhof)		0.30
	CPT-method (Schmertmann)		0.50
	End bearing in rock (Canadian Geotech. Society, 1985)		0.45
Block Failure, ϕ_{b1}	Clay		0.60
Uplift Resistance of Single Piles, ϕ_{up}	Nordlund Method		0.35
	α-method		0.25
	β-method		0.20
	λ-method		0.30
	SPT-method		0.25
	CPT-method		0.40
	Static load test		0.60
	Dynamic test with signal matching		0.50
Group Uplift Resistance, ϕ_{ug}	All Soils		0.50
Lateral Geotechnical Resistance of Single Pile or Pile Group	All soils and rock		1.0
Structural Limit State	Steel Piles	See the provisions of Article 6.5.4.2	
	Concrete Piles	See the provisions of Article 5.5.4.2	
	Timber Piles	See the provisions of Article 8.5.2.2 and 8.5.2.3	
Pile Drivability Analysis, ϕ_{da}	Steel Piles	See the provisions of Article 6.5.4.2	
	Concrete Piles	See the provisions of Article 5.5.4.2	
	Timber Piles	See the provisions of Article 8.5.2.2	
	In all three Articles identified above, use ϕ identified as “resistance during pile driving”		
* Dynamic testing requires signal matching, and best estimates of nominal resistance are made from a restrike. Dynamic tests are calibrated to the static load test, when available.			

2.9.6.3. *LRFD Structural Capacity*

The structural capacity of a pile foundation is dependent upon the pile's axial capacity, as well as its moment capacity and slenderness effects when piles are not fully supported. Additionally, when not fully supported, piles function as columns, whose structural behavior is impacted by the fixity achieved at each end of the structure. The factored axial resistance of a spiral reinforced, biaxially symmetric concrete pile is given in Article 5.6.4.4. The leading 0.85 factor in the P_n equation below serves to limit the compressive strength of the pile in anticipation of unintended eccentricity (AASHTO 2017, C5.6.4.4).

$$P_r = \phi P_n$$

$$P_n = 0.85[k_c f'_c(A_g - A_{st} - A_{ps}) + f_y A_{st} - A_{ps}(f_{pe} - E_p \epsilon_{cu})] \quad \textbf{Eq. 2-13}$$

(AASHTO 2017, 5.6.4.4)

Where:

P_r	=	Factored axial resistance (kip)
P_n	=	Nominal axial resistance (kip)
ϕ	=	Resistance factor specified in Article 5.5.4.2 (see Eq. 2-14)
k_c	=	Ratio of the maximum concrete compressive stress to the design compressive strength of concrete; 0.85 for piles with concrete specified strength less than 10.0 ksi
f_c'	=	Compressive strength of concrete (ksi)
A_g	=	Gross area of cross section (in.^{2})
A_{st}	=	Total area of longitudinal nonprestressed reinforcement (in.^{2})
A_{ps}	=	Area of prestressing steel (in.^{2})
f_y	=	Specified minimum yield strength of nonprestressed reinforcement (ksi)
f_{pe}	=	Effective stress in prestressing steel after losses (ksi)
E_p	=	Modulus of elasticity of prestressing steel (ksi); commonly 28,500 ksi
ϵ_{cu}	=	Failure strain of concrete in compression (in./in.); commonly 0.003

The $E_p\epsilon_{cu}$ term is included to account for the shortening of the pile under the externally applied axial load. This shortening diminishes the compression caused by the prestressing (AASHTO LRFD, C5.6.4.4). In their rendition of the same equation, the American Concrete Institute (ACI) indicates that the prestressing in the steel shall be at least $E_p\epsilon_{cu}$ (ACI 2014, 22.4.2.3). If the prestressing value is less than this, then the *"-$A_{ps}(f_{pe}$-$E_p\epsilon_{cu})$"* term of the equation would actually add to the overall nominal pile capacity, due to the negative term inside the parentheses. Ignoring $E_p\epsilon_{cu}$ results in a conservative estimate of the axial capacity of the pile (AASHTO 2017, C5.6.4.4). For prestressed reinforced axial and flexural capacity considerations, the $0.75 < \phi = 0.75 + \frac{0.25*(\epsilon_t - \epsilon_{cl})}{\epsilon_{tl} - \epsilon_{cl}} \leq 1.0$ **Eq. 2-14** can be used to calculate the resistance factor.

In addition to the pure axial capacity of a pile, it is important that the engineer investigate any bending moments the pile is expected to experience during its service life. This is especially important for pile bent designs when lateral loading is more likely to influence the piles themselves. In these situations, piles are designed similarly to columns. One way engineers can investigate this is by creating axial-moment interaction diagrams, a common analysis practice for column design. These can be created for each standard pile type used by a transportation organization, and then can be used to quickly estimate the suitability of a given pile cross section for a loading condition. A sample

interaction diagram and further discussion on their development can be found in Chapter 5 of this document.

$$0.75<\phi=0.75+\frac{0.25*(\epsilon_t-\epsilon_{cl})}{\epsilon_{tl}-\epsilon_{cl}} \leq 1.0 \qquad \textbf{Eq. 2-14}$$

(AASHTO 2017, 5.5.4.2, 5.3)

Where:

ϕ = Resistance factor

ϵ_t = Net tensile strain in extreme tension steel at nominal resistance (in./in.)

ϵ_{cl} = Compression-controlled strain limit in the extreme tension steel (in./in.)

ϵ_{tl} = Tension-controlled strain limit in the extreme tension steel (in./in.)

Pile bents deserve extra consideration during design, as the issue of slenderness and buckling may present themselves. These parameters are discussed in Section 5.6.4.3 of AASHTO LRFD. These behaviors must also be considered when an embedded pile is not to be considered fully supported, such as when heavy scour is expected, or the depth to fixity is significant. For pile bent analysis as columns, the engineer of record must determine what kind of end conditions the pile is experiencing. Whether the pile is to be considered fixed or pinned in its cap, or where the point of fixity occurs along the embedment length are both crucial pieces of information in this analysis. Advanced software is typically employed in the performance of these calculations.

2.10. Shared Concepts between ASD and LRFD

Despite their differences, there are similarities between ASD and LRFD, some of which are highlighted in the following section.

2.10.1. Definitions

To compare the LRFD notation of design and nominal capacities to the ASD allowable and ultimate capacities, the ultimate capacity in ASD is equivalent to the nominal capacity of LRFD (C10.5.3.1). It follows that the allowable capacity is the factored ultimate capacity in ASD, in the same fashion that the design capacity is the factored nominal capacity in LRFD.

Table 2-5: ASD and LRFD Equivalent Nomenclature

Definitional Equivalency of ASD and LRFD Terms		
ASD	LRFD	Meaning
Ultimate Load/Capacity	Nominal Load/Resistance	The maximum load/resistance/capacity for the element without any safety or load/resistance factors
↓ Apply FS ↓	↓Apply ϕ Factors ↓	Transition Method
Allowable Load/Capacity	Design Load/Resistance	A factored load/resistance/capacity which incorporates a term (FS or ϕ) that accounts for unforeseen increases in the load or decreases in the resistance/capacity of the member

These terms can inadvertently be misused, so it is important to understand their significance with each design methodology. The To compare the LRFD notation of design and nominal capacities to the ASD allowable and ultimate capacities, the ultimate capacity in ASD is equivalent to the nominal capacity of LRFD (C10.5.3.1). It follows that the allowable capacity is the factored ultimate capacity in ASD, in the same fashion that the design capacity is the factored nominal capacity in LRFD.

Table 2-5 is to serve as a guide for understanding the terms. It does not mean that the values calculated for each term will match its counterpart when calculated with the different design methodologies.

2.10.2. Engineer's Ability to Alter Piles' Geotechnical Capacities

AASHTO lists several factors that affect a pile's axial capacity (AASHTO 2002, 4.5.6.1.1). Some of these elements are inherent to the site (through soil properties or environmental conditions) and therefore are considered preset for a given site. Other factors though are under the engineer's control, including the layout of the pile group and construction processes. These AASHTO designated factors and their ability to be controlled by engineers' foundation design process is discussed in Table 2-6.

Table 2-6: Engineers Ability to Affect Geotechnical Factors

Engineers' Control over Factors Affecting Geotechnical Axial Capacities of Piles	
Factors Affecting a Pile's Geotechnical Axial Capacity	Can engineers mitigate the factor through their foundation design for a given site?
The difference between the supporting capacity of a single pile and that of a group of piles;	Yes; Engineers can design foundation groups to minimize group effects
The capacity of underlying strata to support load of pile group	No; Engineers must work around circumstances.
The effects of driving piles on adjacent structures or slopes	Yes; Engineers can work with contractors to develop construction plans minimizing interaction between piles being driven and their surroundings.
The possibility of scour and its effect on axial and lateral capacity;	No; Engineers must work around circumstances.
The effects of negative skin friction or down drag loads from consolidating soil and the effects of uplift loads from expansive or swelling soils;	No; Engineers must work around circumstances.
The influence of construction techniques such as auguring or jetting on capacity;	Yes; Engineers and contractors can control these techniques. DOTs' Standard Specifications may present guidelines on this.
The influence of fluctuations in the elevation of the ground water table on capacity.	No; Engineers must work around circumstances.

In addition to controlling group effects and construction methodology, engineers can work to increase the pile's capacity by increasing the shaft and tip resistances and decreasing the factor of

safety or increasing the resistance factor. For ASD, Figure 2-8 (reproduced from AASHTO 2002, Figure 4.5.4A) clearly delineates the contributions of shaft and tip resistance of a driven pile. Both the side and tip resistances of piles rely heavily on the soil properties in the site. It is beyond the scope of this report to detail how those parameters are determined, aside from saying that geotechnical engineers would apply various methods and engineering judgement to create a reasonably accurate understanding of a given site's soil characteristics.

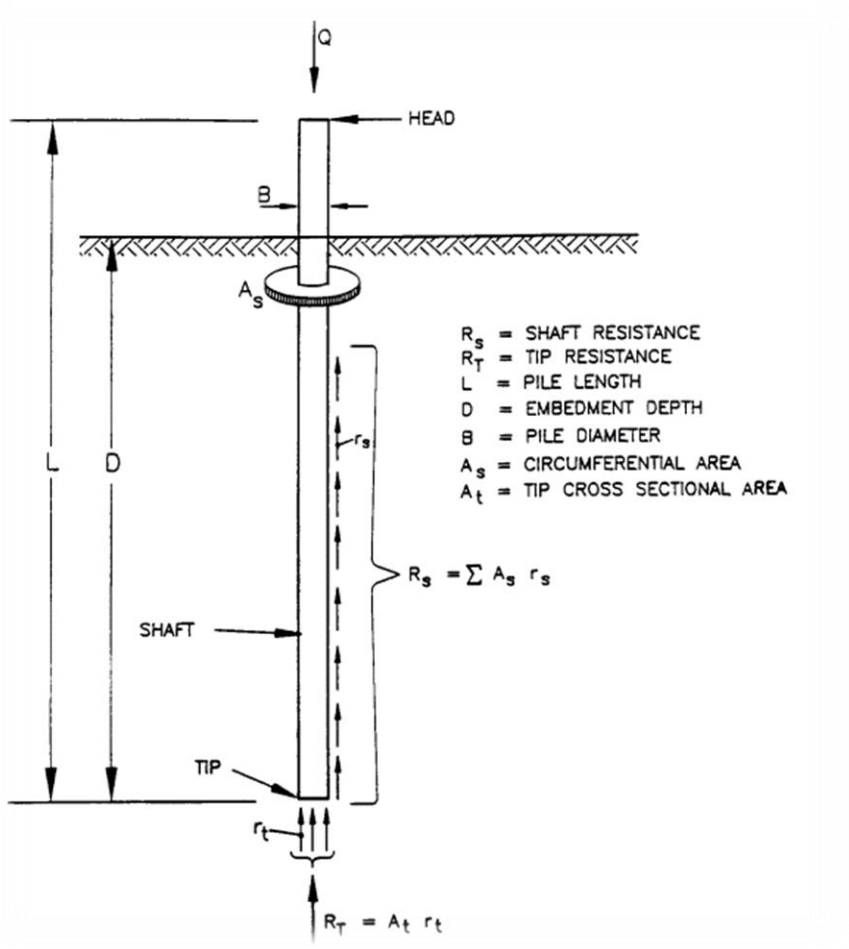

Figure 2-8: ASD Design Terminology for Driven Piles

For ASD, shaft resistance is equal to the circumferential area of the pile (A_s), [the perimeter of the pile (P) times the embedded length of the pile (D)], times the unit side resistance of the soil (r_s). In layered soils, the pile's shaft capacity (R_s) would be taken as the sum of the shaft resistances contributed by each layer of soil:

$$R_s = \sum (A_s * r_s) \qquad \textbf{Eq. 2-15}$$

Any scour, down-drag, or uplift influences would need to be accounted for with these calculations by the geotechnical engineer as well. Therefore, if an engineer wants to increase the shaft capacity of a pile, they can increase the pile length and the perimeter of the pile.

The tip capacity of a pile is governed by the soil's unit compressive resistance (r_t) and the cross-sectional area of the pile tip (A_t). Engineers cannot easily alter the compressive strength of the soil,

thus their primary option for increasing tip capacity is increasing the pile's cross-sectional area at its bearing surface.

The design geotechnical capacity of a pile is equal to the ultimate capacity divided by a factor of safety. By increasing the driving analysis and construction control measures, engineers may use a smaller safety factor, thereby increasing the allowable capacity. AASHTO recommended factors of safety for geotechnical capacity can be found in Table 4.5.6.2A of the Spec, which is found in Table 2-2 of this document (AASHTO 2002).

2.10.3. Engineer's Ability to Alter Piles' Structural Capacities

The primary factors engineers can control which impact a PPCP's structural capacity are its cross-sectional area, prestressing details, concrete strength, fixity at either end, or unbraced length in the case of pile bents. Many of these parameters have pre-set ranges of values for engineers based on the project owner's standard practices and industry availability. However, the available flexibility can be utilized to maximize the strength of a given pile.

Based on survey responses from eleven DOTs in the southeastern United States, DOTs have preset primary dimensions for PPCPs. For square PPCPs, the sizes allowed ranged from 12 to 24 inches in about 2-inch intervals, and then also included 30 and 36 inches. Not all DOTs utilized each pile size, with options likely limited to expedite design proceedings or based on past experience with driving piles of different sizes. Larger piles (24 to 36 inches) often have voids running longitudinally through the middle of the pile to cut down on weight. The ends of the piles are filled in, but the cross-sectional area considered for calculating the axial strength should be taken at a voided section of the pile. The design engineer has some freedom to choose a different sized pile for a given foundation system, and thus can significantly influence the structural capacity of the pile. This analysis of substituting a smaller pile is a part of ALDOT Project 930-929 to be discussed in other reports, rather than in this thesis.

AASHTO specifies a minimum concrete strength of 5,000 psi at 28 days (AASHTO 2002, 4.5.20.1). Engineers can specify higher concrete strengths to achieve greater pile capacities without increasing the volume of concrete used. Engineers should work to understand what strengths of concrete can reliably be produced by local precast industry partners for pile construction.

The minimum effective prestress on the concrete cross section is specified by AASHTO to be at least 700 psi to prevent handling and installation cracking (AASHTO 2002, 4.5.20.2). In pure axial loading conditions, effective prestress decreases the extent of applied loads the pile can handle, but in bending and driving conditions, prestressing increases the pile's capacity. Engineers can conduct structural analysis and create axial-moment interaction diagrams to determine the optimum prestress for the pile, considering construction, driving, and service loading conditions.

When piles are not fully supported, additional structural behavioral considerations must be made. For instance, buckling may need to be considered. In these circumstances, buckling can be mitigated by designing the pile such that is it not considered slender. Slenderness is determined based on the slenderness ratio of the pile, which is acting as a column. This involves increasing the radius of gyration for the pile (r), decreasing its unbraced length (l_u), and/or decreasing its effective length factor (k) in the slenderness ratio equation:

$$SR = \frac{k * l_u}{r} \qquad \textit{(Saatcioglu, n.d.).} \qquad \textbf{Eq. 2-16}$$

The radius of gyration of a pile is a function of its cross-sectional dimensional detailing, which would likely be chosen, and set based on standard pile cross sections, with one already being selected for the pile's axial capacity.

The unbraced length of the pile can be decreased by providing lateral support to the pile, such as through cross members of a bent. The unbraced length would need to be considered in each direction though, so this would have limited effect when looking at a typical column bent in the direction of the roadway. Lateral support transverse to the travel direction of the roadway being supported would be more likely to be provided (Saatcioglu, n.d.).

Engineers can alter the effective length factor by adjusting the degree of fixity for the pile at each end. As the fixity increases from a pinned to a fixed condition, the effective length factor decreases (Saatcioglu, n.d.). As piles are not tied into a structure at each end as columns are, they require additional analysis to determine at what embedment length they achieve fixity (their "depth to fixity). This is determined by geotechnical properties at the site along the length of the pile and is modeled with advanced software such as LPILE. Due to the external factors associated with the toe of the pile, engineers are better able to affect the pile fixity at the head of the pile where it joins the pile or bent cap. The required embedment into the concrete cap is the subject of other research ventures. The Florida DOT offers some insight as to their pile-cap fixity interaction in chapter 3 of their Structural Design Guidelines. By their engineering investigation and judgement, "a 1-foot embedment is considered a pinned head condition" while deeper embedment of 4 feet is required for developing full bending capacity (FDOT 2018c). Additionally, if the pile is voided, it must be solid throughout the 4 feet of embedment as well as for 4 feet below the cap connection (FDOT 2018c). This only applies for their standard, square, up to 30-inch, piles (FDOT 2018c).

2.11. Conclusions on the Meaning of Pile Capacity

The objective of this section was to answer the seemingly simply question, "What is pile capacity?" To answer this, both the fundamental principles of piles and analytical capacities have been discussed. A pile does not have a single capacity. As discussed, piles have both geotechnical and structural capacities, as well as installation limitations. A pile's capacity should be its lowest capacity between geotechnical, structural, and installation parameters. The engineer should use their judgment to determine which capacity is the limiting factor, and work around that value.

3. Survey of Standard DOT Practices

Consolidated information regarding the state of practice for square precast prestressed concrete pile (PPCP) usage by different state departments of transportation is presented in this chapter. The following information relies heavily upon survey responses from each of the southeastern DOTs approached for information, as well as their respective structural design manuals (SDMs), geotechnical design manuals (GDMs), standard specifications, and pile detail drawings. Additionally, this chapter compares these agencies' practices with those detailed in the American Association of State Highway and Transportation Officials (AASHTO) Standard Specifications for Highway Bridges (17th Edition, also referred to as AASHTO Spec) and LRFD Bridge Design Specifications (8th Edition, also referred to as AASHTO LRFD). A summary of the information gathered and its meaning in the context of this research project is presented in the following sections.

3.1. Survey Administration

For the project this thesis is tied to, it was important to reach out to various DOTs and they were asked to provide information regarding their usage of PPCPs. DOTs were selected for inclusion in the survey based on their geographic proximity to Alabama, as well as their joint membership in the Southeastern Association of State Highway Transportation Officials (SASHTO). This regional association was relied upon for likely producing similar geotechnical conditions as well as an increased likelihood of response and information sharing in the spirit of their camaraderie within SASHTO. Representatives from member states within the continental United States were sent a link to an online survey produced using Qualtrics, a survey program provided to University of Alabama students and faculty for such purposes. This survey was designed to take about half an hour to complete and provided ample opportunities for respondents to upload any relevant files their DOT employs in their pile design process. The survey was a combination of multiple-choice style questions as well as free response, and within each section, users had the opportunity to add any comments and elaborate on their responses. These questions primarily served to request information regarding the DOTs' current design documents, pile usage, and structural and geotechnical considerations in their pile designs. Some of this information was available online for the DOTs, but as the volume of available resources varied between DOTs, and to confirm that the online information was in fact that which is currently used in practice within the organization, the respondents were asked to provide this information.

The level of survey completeness varied between respondents, and in some cases, the information appears to be slightly contradictory. However, this survey was immensely beneficial in understanding DOTs current state of practice, as well as acting to fulfill one of the project objectives for ALDOT. A blank survey is provided in Appendix A to show the questions asked and the style in which they were asked.

3.2. Survey Respondent Information

To understand the practices of surrounding transportation agencies, as well as Alabama's, a survey was distributed to engineering professionals from 13 state organizations. These states were chosen due to their relatively similar geographic region, the southeastern continental US, in hopes that they would provide the most relevant information. The following states were consulted, and their transportation organizations' standard abbreviations are listed here: Alabama (ALDOT), Arkansas

(ArDOT), Florida (FDOT), Georgia (GDOT), Kentucky (KYTC), Louisiana (LaDOTD), Mississippi (MDOT), North Carolina (NCDOT), South Carolina (SCDOT), Tennessee (TDOT), Texas (TxDOT), Virginia (VDOT), West Virginia (WVDOT). Responses were received from all 13 agencies. Rather than a "Department of Transportation," Kentucky's state transportation agency is called its "Transportation Cabinet," and Louisiana has a "Department of Transportation and Development." For the purpose of this document, "DOT" is taken in a broad sense to include these state transportation agencies.

3.3. Pile Properties

Based on survey responses and other DOT resources such as structural design manuals and pile detail sheets, the following information was collected. Where applicable, the question or statement which prompted the response is included for clarity. In some instances, there were contradictions between the available resources for a given represented state. Those are generally and explained in the notes associated with each table.

3.3.1. Types of Piles Used

Representatives from West Virginia and Kentucky indicated that they do not use prestressed precast concrete piles, so these agencies will be excluded from the following discussion. This research project is focused on the optimization and use of square precast prestressed concrete piles (PPCPs), so that will be the focus of this discussion; however, it is important to note that many DOTs use other types of piles.

In addition to square PPCPs and steel cross sections, Alabama permits cylindrical concrete piles. One Louisiana respondent stated that their DOT does not use steel piles, but other LADOTD respondents confirmed that they do. North Carolina allows a wide range of pile types, including LDOEP (Large Diameter Open-Ended Piles), Concrete Cylinder Piles, Composite Piles, and FRP (Fiber-Reinforced Polymer) Piles. One Texas respondent stated that timber piles are used, whereas the other did not. Similarly, Virginia's survey responses were mixed, with one respondent stating that "timber piles are only used on rare occasions..." Virginia, like Alabama, allows the use of cylindrical piles, but VDOT's are specifically post-tensioned concrete. VDOT is also looking into piles made of stainless steel and carbon fiber strands for use in tidal or brackish water splash zones. Table 3-1 summarizes the pile types utilized for the DOTs under consideration.

Table 3-1: Pile Types Used by different DOTs in Southeast region.

DOT Reponses Regarding Pile Type												
Please Check all Driven Pile Types Your DOT Utilizes:	State DOT	AL	AR	FL	GA	LA	MS	NC	SC	TN	TX	VA
	PPCPS	X	X	X	X	X	X	X	X	X	X	X
	Steel (Tube or Rectangular Pipe or H Piles)	X	X	X	X	X	X	X	X	X	X	X
	Timber Piles				X	X		X			X	X
	Other	X						X				X

3.3.2. Typical or Allowable Prestressed Precast Concrete Pile (PPCP) Dimensions

All of the DOTs surveyed used at least some piles of the same gross dimensions as ALDOT. In general, it seems like smaller diameter piles, such as 12-inch and 14-inch ones, are allowed in limited capacities for relatively light loading conditions, or non-critical structures (FDOT 2018c, Table 3.5.1-1). South Carolina released an official memorandum in 1993 stating that the use of 14-inch piles was to be discontinued effective immediately, and it cited cracking problems during installation as the primary cause (Meetze 1993). GDOT similarly removed 12-inch piles from their Bridge Design Manual in 2015, though the particular reason was not available (GDOT 2017). On the other end of the spectrum, the 30-inch and 36-inch piles are not used by as many DOTs as the more moderately sized ones. Based on the number of DOTs that use them, 16-, 18-, and 20-inch piles appear to be the most frequently used.

A Florida respondent said that 18-inch to 36-inch piles are most typical for them. The Georgia SDM indicates additional pile sizes are allowed that were not mentioned in the survey response (GDOT 2017, marked with an * in Table 3-2), so perhaps the respondent was indicating that 14-inch to 20-inch piles were the most commonly used sizes, rather than the only allowable sizes. Louisiana and North Carolina notably allow a 12-inch pile. North Carolina respondents indicated that 30-inch and 36-inch piles are used, but their drawings for these piles could not be found at this time. Virginia respondents did not indicate that a 12-inch pile was typical or allowable, but the details for one were found with other pile details, so perhaps it is allowed but not typical. Table 3-2 summarizes the PPCP dimensions each DOT appears to use.

Table 3-2: Square PPCP Primary Dimensions Used

DOT Reponses Regarding Pile Sizes												
Typical or Allowable Square Pile Gross Dimensions:	State DOT	AL	AR	FL	GA	LA	MS	NC	SC	TN	TX	VA
	14 in.	X	X	X	X	X	X			X		X
	16 in.	X	X	X	X	X	X	X		X	X	X
	18 in.	X	X	X	X	X	X		X	X	X	X
	20 in.	X	X	X	X	X	X	X	X		X	X
	24 in.	X	X	X	*	X	X	X	X		X	X
	30 in.	X		X	*	X	X	X				
	36 in.	X		X	*	X	X	X				
	Other:					X		X				

3.3.3. Concrete Strength

Concrete strength is one of the primary factors in determining a PPCP's capacity. Two critical events occur at which a specified concrete strength must be achieved. These occur, 1) at the transfer and release of the prestressing strands during construction and 2) at the actual driving and erection of the piles. The latter value is typically given in terms of a pile's 28-day strength. Based on survey responses, many DOTs allow piles to be driven earlier than 28 days after casting as long as the pile's 28-day strength has been reached.

3.3.3.1. Strength at Transfer/Release

The typical release strength of concrete specified for these piles is 4,000 psi. Louisiana requires a slightly higher value at 4,500 psi based on their survey response. On the other hand, South Carolina

requires a slighter lower value at 3,500 psi (SCDOT 2014). Tennessee's survey response did not provide the release strength for their PPCPs, but their pile detail sheets do specify 4,000 psi (TDOT 1990). Florida has a specialized 30-inch high moment PPCP design that requires a concrete release strength of 6,500 psi (FDOT 2016)). NCDOT has one survey response that is different from what other sources indicate, with a significantly lower value of 3,000 psi, however that same respondent also indicated 4,000 psi, as did the other respondent. Virginia also had a slight discrepancy, where the pile detail sheet indicated a lower value (3,500 psi) than survey responses (4,000 psi) (VDOT 2016). This information is summarized in Table 3-3, with an asterisk indicating information found for the DOT that did not come from the survey. The transfer or release strength used for PPCPs by the Mississippi DOT could not be found at this time.

Table 3-3: Specified Transfer Concrete Strength

DOT Reponses Regarding Concrete Release Strength												
Concrete Strength Used at Release / Transfer of Prestress:	State DOT	AL	AR	FL	GA	LA	MS	NC	SC	TN	TX	VA
	3,000 psi							*				
	3,500 psi								*			*
	4,000 psi	X	X	X	X			X		*	X	X
	4,500 psi					X						
	Other:			*								

3.3.3.2. Strength at 28 Days

All DOTs that responded to this prompt indicated a minimum required concrete strength of at least 5,000 psi for PPCPs. The Mississippi representative did not provide an answer to this question, and the information could not be found at this time in the available MDOT material. As 5,000 psi is the minimum AASHTO specified concrete strength for PPCPs at the time of driving, this will be assumed for future analysis with Mississippi piles (AASHTO 2017, 5.12.9.4). Similarly, South Carolina and Tennessee representatives did not provide this information; however, 5,000 psi is specified in their respective pile detail sheets (SCDOT 2014, TDOT 1990).

Table 3-4: Specified 28-Day Concrete Strength

DOT Reponses Regarding Concrete 28-Day Strength												
Allowable / Required Concrete Strength (f_c' at 28 days):	State DOT	AL	AR	FL	GA	LA	MS	NC	SC	TN	TX	VA
	5,000 psi	X	X		X		*	X	*	*	X	X
	5,500 psi											
	6,000 psi			X		X		X				
	6,500 psi			X								
	7,000 psi											
	7,500 psi							X				
	8,000 psi											
	8,500 psi			X								
	Other:											

Florida's specialized 30-inch high moment pile design requires a significantly higher 28-day strength of 8,500 psi (FDOT 2018). As this special case does not align with the current scope of investigation, it is noted here, but is not discussed further. With the NCDOT survey respondents, one source indicated 5,000 psi and 6,000 psi as the requisite or allowed concrete strengths, while other

sources indicate 7,500 psi is the standard required concrete strength for the same piles. As 7,500 psi was more consistent across the other two NCDOT responses and available pile details, that value shall be considered the required value for future analysis (NCDOT 2017). Table 3-4 summarizes this information, including asterisks where the information was not available directly from the survey.

3.3.4. Prestressing Details

What sets PPCPs distinctly apart from other concrete piles is their prestressed reinforcement. While prestressing does not increase the pure axial capacity of a pile (it has quite the opposite effect), it does improve the pile's strength in other loading conditions. AASHTO suggests a minimum effective prestress (stress after losses) on the cross section of at least 0.7 ksi to "prevent cracking during handling and installation" (AASHTO 2017, 5.12.9.4.3). Additionally, when piles experience eccentric or lateral loads that cause bending moments, the prestressing can help increase the bending capacity of the pile.

3.3.4.1. Strand Material Types

All of the surveyed DOTs allow low-relaxation (low-lax), Grade 270 strands to be used while few allow Grade 250 or stress-relieved strands to be used. Georgia's standard pile drawing provides details for both grades, but it is unknown which strands are currently used (GDOT 1984). Based on the standard practices and industry trends demonstrated by other DOTs, it is likely the Grade 250 material is less frequently used. One VDOT respondent indicated that stress-relieved strands are used, however, another respondent and the pile detail sheets indicate only low-relaxation strands are used. This information is provided in Table 3-5, with asterisks indicating where the information was in conflict, or materials may be used, but likely are not the primary choice.

Table 3-5: Strand Material Classification

DOT Reponses Regarding Prestressing Strand Materials												
Allowable Prestressing Strand Material Properties:	State DOT	AL	AR	FL	GA	LA	MS	NC	SC	TN	TX	VA
	Stress Relieved Strand	X	X							X		*
	Low-Lax Strand	X	X	X	X	X	X	X	X	X	X	X
	Grade 270	X	X	X	X	X	X	X	X	X	X	X
	Grade 250		X		*					X		

3.3.4.2. Strand Diameter

Most DOTs surveyed allow 0.5-inch diameter strand to be used in their PPCPs, with Georgia as the only exception. Their standard pile detail sheets indicate only 7/16-inch diameter strand is used (GDOT 1984). This difference was considered minor enough to still allow comparison with other DOTs' 0.5-inch strand piles. A North Carolina respondent indicated that "Other" diameters of strands are used but provided no additional information. One VA respondent indicated that 7/16-inch strand is used, however, other sources indicate only 0.5-inch diameter strand is used for the same organization. This information is summarized in Table 3-6 with asterisks indicating information that appeared to be outlying as opposed to the standard practice.

Table 3-6: Strand Diameters Used by different DOTs.

DOT Reponses Regarding Prestressing Strand Diameter												
Prestressing Strand Diameter Allowed in Piles:	State DOT	AL	AR	FL	GA	LA	MS	NC	SC	TN	TX	VA
	3/8 in.			X						X		
	7/16 in.		X	X	X					X		*
	0.5 in.	X	X	X		X	X	X	X	X	X	X
	0.6 in.			X				X				
	Other:							*				

4. Design Procedures and Calculations

A primary focus of this research venture is understanding and potentially improving the standard pile capacities listed in the ALDOT structural design manual. To understand DOTs practices in this area, DOTs were asked whether they used a table of standard pile capacities, and if so, how were those values calculated and where could they be found. Of the DOTs surveyed, only six states currently use standardized pile capacity values in a publicly available format (Alabama, Florida, Georgia, Mississippi, Texas, and Virginia). Louisiana used to have a standard table, but it has been removed from more recent editions of their SDM (LADOTD 2017). North Carolina's survey respondent indicated that the state has a series of moment-axial interaction diagrams for their use, but those are only for in-house use. The available information surrounding the provided pile capacities for each of the six DOTs is discussed below. Following this information, some AASHTO based capacity calculations have been carried out, and those values are compared with the DOTs' values. Several figures and tables have been provided to help facilitate direct comparison between similar piles from each DOT.

4.1. DOT Practices

Within this section, the available information regarding each list of PPCP pile capacities from DOTs is presented on a state-by-state basis. As previously noted, the states that have PPCP capacities available, and thus will be discussed here, are Alabama, Florida, Georgia, Mississippi, Texas, and Virginia.

4.1.1. Alabama

The values presented in Table 10-2 of the ALDOT SDM are taken as the maximum factored design loads for fully embedded individual piles (ALDOT 2017b). Pile bents are to be designed separately as columns, rather than having their capacities given in a table. The origin of these standard values is currently a topic of this research venture.

Size of Pile	Maximum Factored Design Load Allowed
14-inch Square	90 tons
16-inch Square	120 tons
18-inch Square	150 tons
20-inch Square	180 tons
24-inch Square	220 tons
30-inch Square	310 tons
36-inch Square	410 tons

Table 10-2
Maximum Factored Design Load per Pile for Prestressed Piling

Figure 4-1: ALDOT Table of Pile Capacities

4.1.2. Florida

It is not a table of standard pile capacities, but FDOT has a list of maximum driving resistances, found in Table 3.5.12-1 of their SDM, under the title "Maximum Pile Driving Resistance."

Table 3.5.12-1 Maximum Pile Driving Resistance

Pile Size[1]	Resistance (tons)
14 inch	200
18 inch	300
20 inch	360
24 inch	450
30 inch	600
54 inch concrete cylinder	1550
60 inch concrete cylinder	2000

1. See *SDG* 3.5.1.F for applicability.

Figure 4-2: FDOT Table of Maximum Driving Resistance

The governing equation they utilize for required nominal bearing resistance is:

$$\frac{Factored\ Design\ Load + Net\ Scour + Down\ Drag}{\phi} < R_n \qquad (FDOT\ 2018c) \qquad \textbf{Eq. 4-1}$$

This equation can be rearranged to show that the factored design load must be less than the factored pile resistance after the resistance is diminished for scour and down drag effects: *Factored Design Load* < ϕR_n *- (Net Scour + Down Drag)*.

3.5.6 Resistance Factors [10.5.5]

Delete *LRFD* [Table 10.5.5.2.3-1] and substitute *SDG* Table 3.5.6-1 for piles.

Table 3.5.6-1 Resistance Factors for Piles (all structures)

Pile Type	Loading	Design Method	Construction QC Method	Resistance Factor, φ
Driven Piles with 100% Dynamic Testing	Compression	Davisson Capacity	100% Dynamic Testing[1]	0.75
			100% Dynamic Testing[1] & Static Load Testing	0.85
			100% Dynamic Testing[1] & Statnamic Load Testing	0.80
	Uplift	Skin Friction	100% Dynamic Testing[1]	0.60
			100% Dynamic Testing[1] & Static Uplift Testing	0.65
Driven Piles with ≥5% Dynamic Testing	Compression	Davisson Capacity	Driving criteria based on Dynamic Testing and Analysis	0.65
			Driving criteria based on Dynamic Testing and Analysis & Static Load Testing	0.75
			Driving criteria based on Dynamic Testing and Analysis & Statnamic Load Testing	0.70
	Uplift	Skin Friction	Driving criteria based on Dynamic Testing and Analysis	0.55
			Driving criteria based on Dynamic Testing and Analysis & Static Uplift Testing	0.60
All piles	Lateral (Extreme Event)	FBPier[2]	Standard Specifications	1.00
			Lateral Load Test[3]	1.00

1. With analysis of at least 10% of Piles in all Bents and Footings. Ensure all soil conditions encountered are analyzed.
2. Or comparable lateral analysis program.
3. When uncertain soil conditions are encountered

Figure 4-3: FDOT Table of Resistance Factors

Put another way, the factored driving resistance of the pile must exceed the factored load demand as well as the negative effects of scour and down drag. The load factor is to be taken from SDM Table 3.5.6-1, depending on the construction practices in place (FDOT 2018s)

The SDM's following section (3.5.12.B) states that R_n is typically the required driving resistance, and that the "nominal bearing resistance values given in the Pile Data Table must not exceed the following values unless specific justification is provided and accepted…." Further, in 3.5.12.D, the values in the table are described as being based on upper bound driving resistance of typical driving equipment. It is also stated that the values "should not be considered default values for design" as the values listed may not be achievable based on the soil conditions at the site. This information indicates that these pile resistances used are heavily based on geotechnical and driving behavior, rather than the pure structural bearing capacity of a fully embedded pile (FDOT 2018c).

To compare the FDOT nominal bearing resistances to the AASHTO design axial capacities based on the cross section details of the pile, they must be factored. Based on Table 3.5.6-1 (FDOT 2018c), for compression of piles, the worst resistance factor that would be used would be 0.65, corresponding to "Driven Piles with ≥ 5% Dynamic Testing" and "Driving criteria based on Dynamic Testing and Analysis." The following table has the published resistance, as well as its corresponding factored resistance.

Table 4-1: FDOT Maximum Nominal and Factored Resistance

FDOT Maximum Pile Resistances			
Pile Type	Resistance, R_n, tons	Resistance Factor, ϕ	Factored Resistance, ϕR_n, tons
14 in.	200	0.65	130
18 in.	300	0.65	195
20 in.	360	0.65	234
24 in.	450	0.65	293
30 in.	600	0.65	390

In addition to this table of maximum driving resistances, FDOT also has published moment-axial interaction diagrams for their PPCPs. These can be found in the document *Instructions for Design Standards,* specifically within the section "Index 20600 Series Concrete Piles" (FDOT 2018a). The approximate axial capacities of the piles can be read from these diagrams, and they are summarized in the table below. These are the highest values seen for DOT listed pile capacities in this research venture. FDOT's 14-inch pile interaction diagram is replicated here to give an example of the information available and its format. These values will be used in future comparisons and discussion. Creating a standard moment axial interaction diagram is generally a purely structurally based process, and so these values are more likely to be representative of the piles' structural capacity without geotechnical consideration. Table 4-2 shows the estimated pile capacity from the available interaction diagrams, read to the nearest 25 kips, and then converted to tons.

Table 4-2: FDOT Capacities from Interaction Diagrams

Estimated FDOT Capacities from Interaction Diagrams		
Pile Type	Design Load, ϕP_n, kips	Design Load, ϕP_n, tons
14 in.	550	275
18 in.	900	450
20 in.	1100	550
24 in.	1575	788
30 in.	1800	900

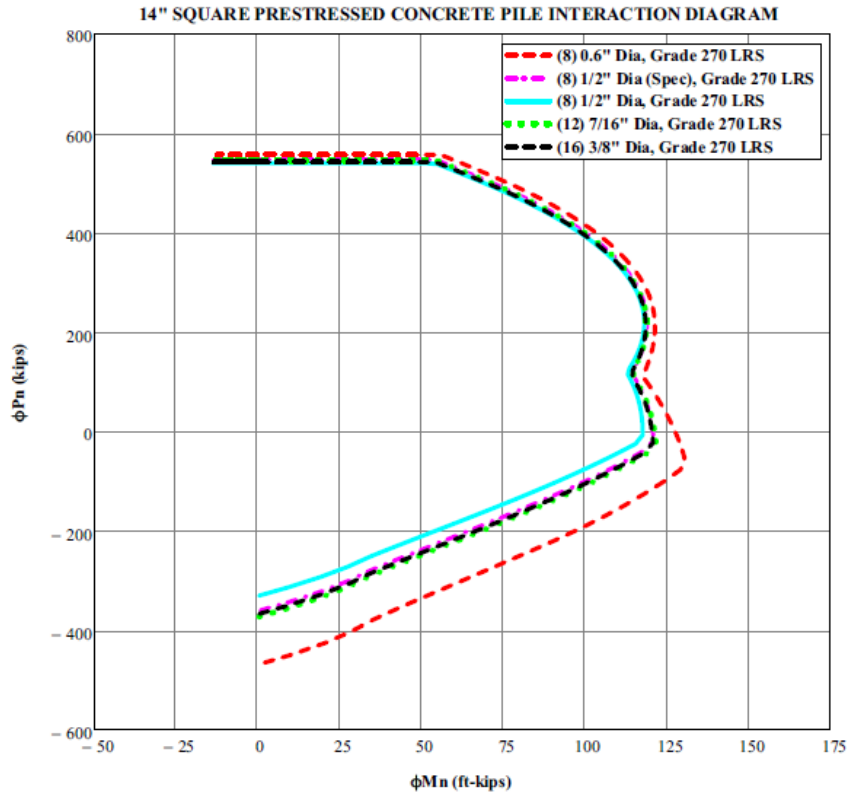

Design Assumptions:

- Concrete compressive strength $f'_c = 6$ ksi.
- Modulus of elasticity of prestressing strands, $E_p = 28{,}500$ ksi.
- Resistance factor ϕ based on AASHTO LRFD 5.5.4.2.1 (0.75 compression controlled, 1.0 tension controlled)
- All piles assumed to have spiral ties.
- Strand sizes and strand patterns used to create interaction curves correspond with those indicated in Index 20614.

Figure 4-4: Representative FDOT Interaction Diagram

When designing pile foundation systems, FDOT geotechnical engineers use preliminary loading conditions to estimate axial resistance versus tip elevation and provides the structural engineer with this information as well as soil properties for lateral loading analysis. The structural engineer then completes the design, as it is primarily their responsibility, and the geotechnical engineer reviews it.

4.1.3. Georgia

Georgia notably has some of the highest listed capacities for their respective PPCPs. These values are found in Table 4.2.2.4-1 of their SDM, which is replicated below as Figure 4-5, and apply to continuously supported piles constructed in accordance with their standard pile details (GDOT 2017). These values are deemed the "Max. Factored Structural Resistance, P_R," and are given in kips, so they were converted to tons for this comparison. GDOT's Bridge Foundation Investigation Template indicates that these values come from a 2013 official interdepartmental correspondence (GDOT 2016). This letter indicates that the values were calculated based on the fifth edition of AASHTO LRFD (Rabun, 2013).

Table 4.2.2.4-1 Properties for PSC piles (LRFD)

Pile Size	Stress Limits			Max. Factored Structural Resistance, P_R (kips)
	Compression (ksi)	Tension (ksi)		
		Normal	Severe	
14" SQ PSC	3.214	1.248	1.036	473
16" SQ PSC	3.457	1.005	0.793	636
18" SQ PSC	3.623	0.839	0.627	820
20" SQ PSC	3.573	0.889	0.677	1006
24" SQ PSC, VOID	3.519	0.943	0.731	1158
24" SQ PSC	3.662	0.800	0.588	1464
30" SQ PSC, VOID	3.553	0.909	0.697	1706
30" SQ PSC	3.561	0.901	0.689	2224

Figure 4-5: GDOT Listed Pile Capacities

A survey response indicates that these values are based solely on structural axial capacity, and were calculated by following, more specifically, Sections 5 and 6 of the AASHTO LRFD Bridge Design Specifications. In reviewing these sections, equation 5.6.4.4-2 is most likely the one used to determine the factored axial resistance of the piles. Calculations carried out in 2013 used the fifth edition of AASHTO LRFD, but this particular equation does not appear to have changed through the current 8th Edition. The SDM indicates that a resistance factor of 0.75 should be employed for the piles (GDOT 2017). When this equation and a 0.75 resistance factor is applied to each standard GDOT pile, the resulting values are the same as those listed in GDOT's Table 4.2.2.4-1 (GDOT 2017). This is excellent corroborating evidence to the statement that these are the maximum factored structural values, as it positively identifies the procedure used to calculate the standard values used by GDOT and that those values are purely structural in nature. Further discussion on these calculations occurs later in Section 4.3 of this document.

Careful examination of available documents revealed a slight discrepancy regarding GDOT's pile capacity table. The last two rows of values are supposedly for a 30-inch voided square pile and a 30-inch square pile. GDOT's Geotechnical Bureau's Bridge Foundation Investigation Template includes what looks like a very similar table (GDOT 2016). This is replicated in Figure 4-6 below. However, it also includes the details for a 12-inch pile, and rather than the last row being for a 30-inch non-voided pile, it is for a 36-inch voided pile. The stress limits and maximum factored structural resistance

correspond with those listed in GDOT's SDM Table 4.2.2.4-1. GDOT's survey response did not offer any indication that pile sizes larger than twenty inches are typically used or allowed to be used, so it did not work to indicate which interpretation of the discrepancy is correct. The standard pile details sheet (GDOT 1984) however, also indicates 30-inch and 36-inch piles that are voided, with only the 24-inch pile having solid and voided options. This aligns with our current understanding that GDOT's Table 4.2.2.4-1's last row should in fact be for a 36-inch voided pile, rather than a 30-inch solid one.

PSC Piles

f'c = 5.0 ksi, piles fabricated in accordance with GA STD. 3215

Pile Size	Stress Limits			Max. Factored Structural Resistance, P_R (kips)
	Compression (ksi)	Tension (ksi)		
		Normal	Severe	
12" SQ. PSC	3.310	1.152	0.940	352
14" SQ. PSC	3.214	1.248	1.036	473
16" SQ. PSC	3.457	1.005	0.793	636
18" SQ. PSC	3.623	0.839	0.627	820
20" SQ. PSC	3.573	0.889	0.677	1006
24" SQ. PSC, void	3.519	0.943	0.731	1158
24" SQ. PSC	3.662	0.800	0.588	1464
30" SQ. PSC, void	3.553	0.909	0.697	1706
36" SQ. PSC, void	3.561	0.901	0.689	2224

Figure 4-6: GDOT Pile Capacity Table from Investigation Template

4.1.4. Mississippi

The MDOT structural design manual contains a limited discussion on piles. The primary pile information provided in the body of the text (rather than the attached detail drawings) is a range of values to be used for the "ultimate capacity" of prestressed concrete piles under intermediate bents. This information is found in the "Intermediate Bents" section of the SDM, specifically on page 26 (MDOT 2010). The available information is found Figure 4-7 below.

2. For pile supported intermediate bents, piles should be placed under bearings as nearly as possible. But, DO NOT use pile spacings of less than 1" increments. The number of piles used under each bearing should be determined by the capacity of the piling used. For prestressed concrete piling the following range for ultimate capacity should be used:
   a. 14"x14" - 45-48 tons
   b. 16"x16" - 55-60 tons
   c. 18"x18" - 70-75 tons

Figure 4-7: MDOT Pile Ultimate Capacity Ranges

Notably, the values given are said to be the "ultimate capacity" of the piles. If that is the case, typically, "ultimate" values are factored to yield "allowable" ones in the case of ASD or are considered the nominal (unfactored) strength of a pile. Based on these technical definitions of ultimate, these capacities would be decreased for the allowable or design capacities. As the discussion does appear in the "Intermediate Bent" section, it is possible that these values apply to piles that form bents rather than fully embedded ones. This could explain the lower values seen. The survey response for Mississippi unfortunately does not offer further explanation of these values, and in fact indicates that MDOT does not use a table or list of standard capacities for PPCPs.

4.1.5. Texas

In the TxDOT geotechnical design manual, Table 5-2 provides "Maximum Allowable Pile Service Loads" for abutments and trestle bents and pile footings (TxDOT 2018). The pile footing values are used for this report and capacity comparison, as other DOTs' values are taken to be for fully supported piles. In the description for the table, the GDM indicates that these are the structural loads that can be relied upon without more thorough structural investigation, and that soils often cannot provide this level of resistance. The table is provided as Figure 4-8 below, and the description as Figure 4-9.

Table 5-2: Maximum Allowable Pile Service Loads

Size	Maximum Length	Abutments and Trestle Bents	Footings (per Pile)
16 in.	85 ft.	75 ton	125 tons
18 in.	95 ft.	90 tons	175 tons
20 in.	105 ft.	110 tons	225 tons
24 in.	125 ft.	140 tons	300 tons

Figure 4-8: TxDOT Listed Pile Capacities

Service Loads

See the following table for maximum piling length and structural loads recommended without conducting a detailed structural analysis. Many soils are not capable of developing these maximum loads. Before final structural design, review the soil information to verify the ability of the foundation to develop desired maximum loads.

Figure 4-9: Excerpt from TxDOT GDM

Conversely, one survey response seems to indicate that the capacity is based on the geotechnical capacity for the piles. When prompted with "If your DOT uses a table or list of standard PPCP pile capacities, please explain what precisely is meant by those values. Are they listed in terms of LRFD design capacities?" the individual replied, "Capacity listed is the maximum allowable axial value. This is based on geotechnical capacity for the piles." When asked which of the following characteristics are incorporated into the standard capacity values of the piles, the respondent checked the boxes for structural axial capacity, geotechnical capacity specific to the site, and general soil conditions of the region. According to the same respondent, when asked how the standard capacity values were calculated they responded: "TxDOT uses a local method, which utilizes the Texas Cone Penetrometer. So, the capacities were derived using ASD." These further muddles whether these capacities are structural or geotechnical based. Based on the GDM description though, these values are taken as the structural capacities of the pile.

4.1.6. Virginia

Virginia's listed capacities come from their GDM Table 9-10, as "Typical Pile Loads" for concrete piles. This table lists a "Min", "Max", and "Prelim. Design**" category (VDOT 2011). The "**" footnote indicates that these values are the "minimum preliminary design load to be investigated for structural/geotechnical capacity and economics." These values accordingly fall between the

minimum and maximum values listed in the GDM table and represented by the two-tone bars in the following pile capacity comparison figures. This table is represented in Figure 4-10.

Two of the three respondents for VDOT indicated they were not sure if a table of standard values was used, and the third said no, one was not used. This information therefore appears not to be used frequently. One respondent laid it out as follows: "The pile capacities at most of our PPCP sites are dictated by the geotechnical resistance that can be achieved, while not overstressing the pile during installation. At the same time, we count on some percentage of 'soil set-up.' Therefore, a standard table of capacities (resistances) would not make sense for us." Based on these responses and the verbiage of the table presented in the GDM, these capacities listed are typical pile loads that serve as guidelines rather than strict parameters for engineering design.

TYPICAL PILE LOADS
Table 9-10

Nominal Size (in.)	Type of Pile (Typical capacity – Tons)									
	Timber	Driven Shell (CIP)		Concrete			Steel H (friction)***		Steel H (EB)****	
		Min	Prelim. Design**	Min	Prelim. Design**	Max	Min	Prelim. Design**	Prelim. Design**	Max *****
10	20	35	50	35	50	70	20	30	9.0 (Gr. 36 steel)	12.0 (Gr. 36 steel)
12	24*	42	60	42	60	96	24	36		
14	28*	49	70	49	70	112	28	42		
16	32*	56	80	56	80	128			12.5 (Gr. 50 steel)	16.5 (Gr. 50 steel)
18				63	90	144				
20				70	100	160				
22				77	110	176				
24				84	120	192				

* Requires timber pile sizes to be specified.

** Minimum preliminary design load to be investigated for structural/geotechnical capacity and economics.

Figure 4-10 – VDOT Listed Pile Capacities

4.2. Summary of Standard Pile Capacities

With regards to using standardized pile capacity tables, most of the DOTs surveyed indicated that they do not follow that practice. The pile capacities for those that do, (Alabama, Georgia, Mississippi, Texas, and Virginia) are summarized in the charts below. Florida is also included in this, as although the survey responses did not indicate that standard capacities were used, a table of standard resistances and moment-axial interaction diagrams were found in their current design resources. Similarly, VDOT is included as despite survey responses not indicating the use of a standard capacity table, as one was found in their GDM. The available standard values could mean different things to each DOT. Discussion on this matter preceded this section of this document, and additional possible explanations are included following this one.

Figure 4-11 contains a plot of the listed capacities for DOTs' PPCPs that are also utilized by ALDOT. Figure 4-12 similarly provides the available listed PPCP capacities, but for larger piles. These piles are generally voided unless noted otherwise in the body of the figure. GDOT has both a voided and a non-voided 24-inch pile, hence the two different marked likes for its entry. As ALDOT only allows a voided 24-inch pile, later comparison will focus on GDOT's voided 24-inch pile.

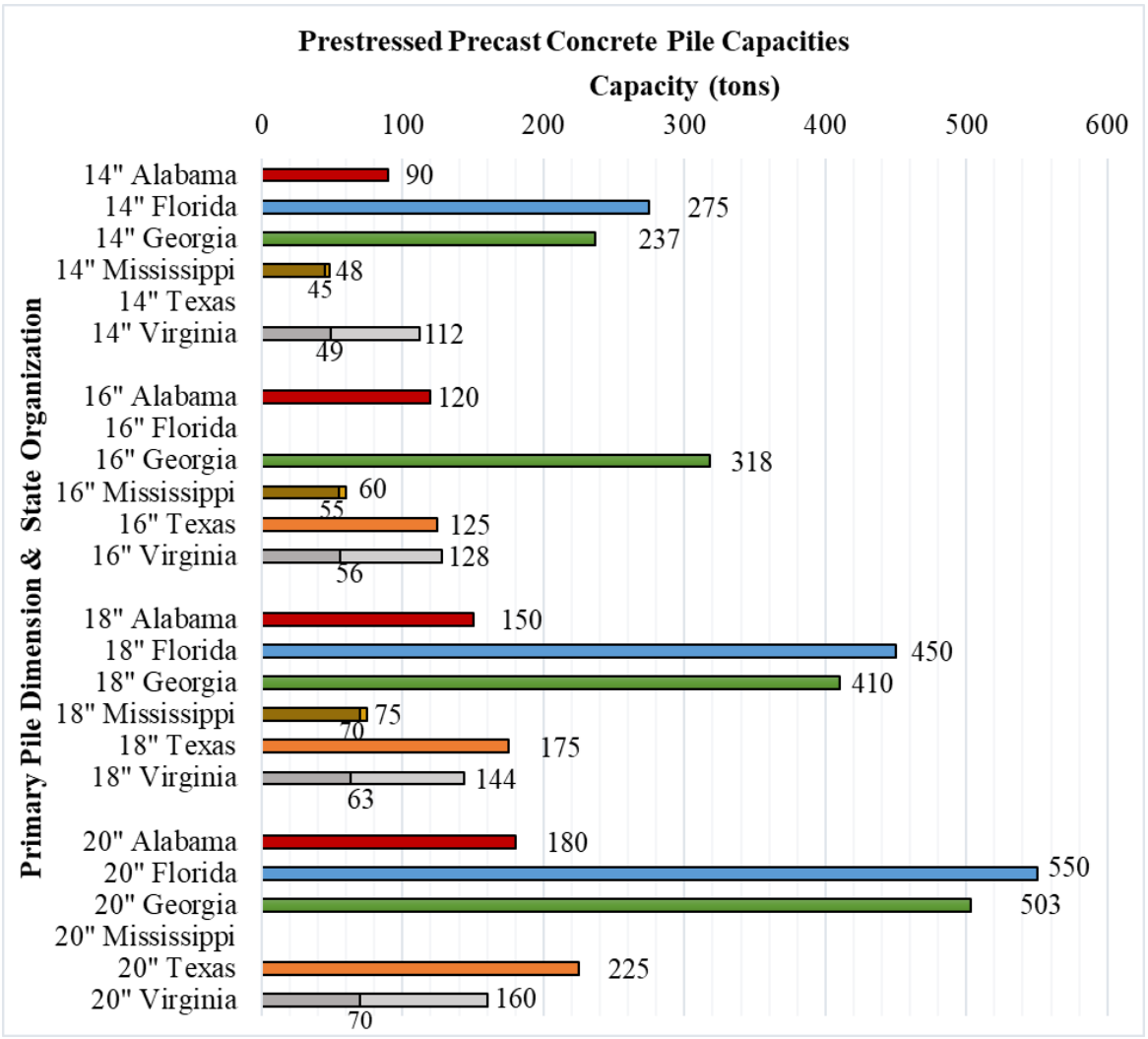
Prestressed Precast Concrete Pile Capacities
Capacity (tons)
0
100
200
300
400
500
600
Primary Pile Dimension & State Organization
14" Alabama
14" Florida
14" Georgia
14" Mississippi
14" Texas
14" Virginia
16" Alabama
16" Florida
16" Georgia
16" Mississippi
16" Texas
16" Virginia
18" Alabama
18" Florida
18" Georgia
18" Mississippi
18" Texas
18" Virginia
20" Alabama
20" Florida
20" Georgia
20" Mississippi
20" Texas
20" Virginia
90
275
237
48
45
112
49
120
318
60
55
125
128
56
150
450
410
75
70
175
144
63
180
550
503
225
160
70

Figure 4-11: 14-inch to 20-inch PPCP Listed Capacities

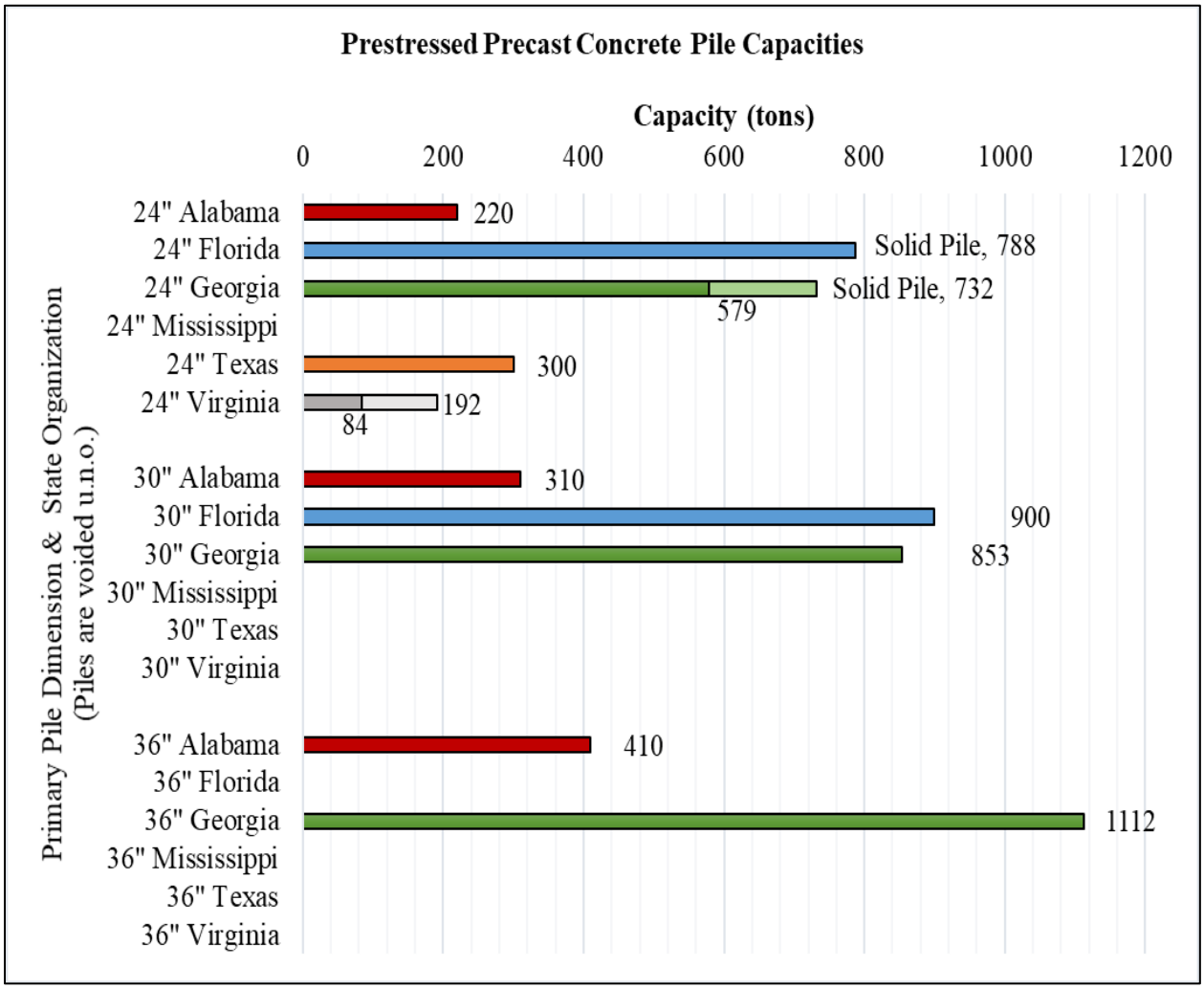

Figure 4-12: 24-inch to 36-inch PPCP Listed Capacities

4.3. Pile Analysis – AASHTO Calculations and DOT Capacities

As seen in the previous discussion, DOT listed capacities can have various meanings. To put them on a more level playing field and look at the analytical structural strength of the pile cross sections, Article 5.6.4.4 of AASHTO LRFD was used to estimate the factored axial structural resistance of the pile types from each DOT that are the most similar to those employed by ALDOT. This equation provides the factored axial resistance of a spirally reinforced, biaxially symmetric concrete pile. A brief description of this equation was reproduced previously within this document from AASHTO LRFD as] Eq. 2-13.

To implement this equation, some assumptions had to be made. For example, concrete strength information could not be found for Mississippi at this time, so it was assumed to have a specified 28-day concrete strength of 5.0 ksi, which is consistent with the AASHTO-specified minimum value (AASHTO 2017, 5.12.9.4). If prestressing loss information was not available, 20 percent losses were assumed, and this was the case for Alabama, Arkansas, Mississippi, North Carolina, and Tennessee.

Interestingly, during the structural axial capacity calculations, the effective prestress of some piles fell below the suggested 0.7 ksi minimum found in Article 5.12.9.4.3 of AASHTO LRFD. For example, Georgia's f_{pe} value for the concrete was calculated to be 0.627 ksi for its 18-inch pile. Georgia's loss information was provided though, and the final capacity answers match those listed in their structural design manual. Based on this information, GDOT appears to have taken advantage of the commentary provision for Article 5.12.9.4.3, indicating that this value, which serves to help prevent cracking during handling and installation, may be lowered at the discretion of the project Owner. Arkansas' piles also showed this phenomenon for their 16-, 18-, and 20-inch piles. In this case, it may be due to a difference in rounding, as the values were 0.678, 0.689, and 0.682 respectively, or their actual loss percentage may be lower than the assumed 20 percent. If a DOT provided initial and effective prestress information, as was the case for Florida, South Carolina, and Virginia, then the approximate losses were calculated based on those values and the percent decrease between them. Louisiana had the lowest losses, with their percentages calculated based on the difference between the initial prestress and the given 90 days level of prestress. Those DOTs that provided some loss information showed losses between about 10 and 22 percent.

Table 4-3 shows the result of this analysis for all PPCP-using DOTs considered in this study. In Table 4-3, the colors indicate if the calculated axial design capacities are higher (green), lower (orange), or approximately equal to (yellow) the Alabama values for the given pile type. Not every DOT uses piles matching those used by ALDOT, so when a DOT does not use an equivalent pile, their values are considered not applicable, and their cells are marked with grey. For example, Florida does use a 24-inch pile, but it is not voided, whereas Alabama's is. As this added cross sectional area would have a significant impact on the axial capacity of the pile, Florida's 24-inch non-voided pile is not included in the analysis here. However, piles with different sized voids were still allowed, as categorically, they are still "voided". Additionally, Georgia's use of 7/16-inch diameter strands did not preclude them from consideration, though that was considered, and it did affect their area of prestressing steel within each pile.

Table 4-3: Design Structural Capacities of Piles

Pile Design Capacities Based on AASHTO LRFD Bridge Design Specifications (5.6.4.4)												
State DOT		Calculated Axial Design Capacity (tons)										
		AL	AR	FL	GA	LA	MS	NC	SC	TN	TX	VA
Square PPCP Primary Dimension (in.)	14	234	242	288	237	280	234	N/A	N/A	242	N/A	246
	16	315	319	N/A	318	359	315	488	N/A	315	316	N/A
	18	392	403	486	410	468	392	N/A	400	399	400	402
	20	495	499	585	503	572	495	764	494	N/A	488	487
	24	599	N/A	N/A	579	699	600	N/A	N/A	N/A	N/A	N/A
	30	851	N/A	953	853	980	851	N/A	N/A	N/A	N/A	N/A
	36	1106	N/A	N/A	1112	1286	1107	N/A	N/A	N/A	N/A	N/A

Notably, most of the values calculated are higher than Alabama's for the given pile size. As one equation was used to calculate the nominal capacity values for each set of inputs, changing just one variable can have a significant impact on the axial design capacity of the pile. AASHTO LRFD axial

capacity equation was reproduced previously in] Eq. 2-13 for convenience and consideration with the following discussion breaking down the key variables.

The following variables are assumed to be the same values across all piles considered for the DOTs: ϕ (0.75), k_c (0.85), A_{st} (0 in.^{2}), f_y (N/A), E_p (28,500 ksi), and ϵ_{cu} (0.003). The gross areas of solid piles were taken as the same for each pile type, and as per standard practice, the chamfers on the corners of the piles were not considered. The gross area for voided piles did have some variation across DOTs for a given pile due to differences in void diameter. For those piles with the same gross area though, that leaves the following variables as the primary catalysts of change: f_c', A_{ps}, and f_{pe}. The table below gives examples of each of these variables for an 18-inch pile, and the resulting design axial resistance, as most DOTs utilize this pile type. The color scheme from Table 4-3 is applied to Table 4-4 for easier visualization of information.

Table 4-4: Design Axial Resistance and Selected Variables

Comparing Design Axial Resistances of DOT Piles					
State	Concrete Strength (Compared to AL) f_c', ksi	Area of Prestressing Steel (Compared to AL) A_{ps}, in.^{2}	Effective Prestress in strands (Compared to AL) f_{pe}, ksi	Design Axial Resistance P_r kips	tons
AL	5.0	1.836	161.96	783	392
AR	Same, 5.0	Lower, 1.377	Higher, 162.09	807	403
FL	Higher, 6.0	Higher, 2.448	Lower, 132.35	972	486
GA	Same, 5.0	Lower, 1.380	Lower, 147.18	820	410
LA	Higher, 6.0	Same, 1.836	Higher, 181.06	936	468
MS	Same, 5.0	Same, 1.836	Higher, 162.09	783	392
NC	N/A	N/A	N/A	N/A	N/A
SC	Same, 5.0	Lower, 1.377	Higher, 170.59	799	400
TN	Same, 5.0	Lower, 1.530	Higher, 162.11	799	399
TX	Same, 5.0	Lower, 1.530	Lower, 160.56	800	400
VA	Same, 5.0	Same, 1.836	Lower, 144.71	804	402

This information shows the different values of these variables used by DOTs and their resulting axial structural pile capacities. Engineers can consider changing each of these three variables to achieve higher design capacities for their piles and doing so can have tremendous results. Alabama's capacity is notably behind most of the other DOTs based on their pile details. Still looking at the 18-inch pile scenario, if the Alabama pile's concrete strength is consistently increased to 6.0 ksi, its resulting factored resistance jumps up to about 958 kips, an increase of about 22 percent. This opportunity for optimization is available to engineers and may be considered by ALDOT for pile optimization moving forward.

4.4. Pile Analysis – Given Values for Capacity Compared to Calculated Capacities

Calculating the AASHTO LRFD design axial capacities found in Table 4-4 was a beneficial step in understanding the structural capacities of the DOTs' piles. Some DOTs provide standardized pile

capacities in their official literature. However, even given these values, it is not always immediately clear what they are meant to represent. Some language has been muddled between design methodology definitions and the common English meaning of the words. For example, Alabama provides a table with the Maximum Factored Design Load Allowed. In LRFD terminology, a design load is one which has already been factored. In ASD, allowable capacities are taken to mean ultimate capacities divided by a safety factor. In this way, this five-word title could mean a variety of things.

As ASD was widely used by DOTs prior to the LRFD transition, the AASHTO allowable stress equation for PPCPs, $f_c = 0.33f_c' - 0.27f_{pe,}$ has been applied to the DOTs' pile details to determine an allowable capacity based on the stress in the pile. The derivation of this equation does include a safety factor of 2.2 (PCA 1971), making it in fact the allowable stress and not the ultimate stress for the pile. The allowable stress resulting from the preceding equation was multiplied by the gross area of the pile to arrive at these capacities found in Table 4-5.

To better understand how the listed capacities from DOTs relate to their analytical AASHTO capacities, Table 4-5 has been prepared including the AASHTO LRFD design axial capacity, AASHTO ASD allowable capacity, the DOTs' listed values, and then the listed values divided by the AASHTO LRFD and ASD values. As Florida has two sets of listed values, they have an additional row in their part of Table 4-5.

Table 4-5: Comparison of DOT Pile Capacities

Comparison of Listed and Calculated DOT Pile Capacities								
State Org.	Value Type	Primary Square Pile Dimension						
		14 in.	16 in.	18 in.	20 in.	24 in.	30 in.	36 in.
AL	AASHTO - LRFD Design Axial Capacity (tons)	234	315	392	495	599	851	1106
	AASHTO - ASD Allowable Stress Capacity (tons)	135	184	227	290	350	499	647
	Listed - "Maximum Factored Design Load Allowed" (tons)	90	120	150	180	220	310	410
	Listed/LRFD	0.38	0.38	0.38	0.36	0.37	0.36	0.37
	Listed/ASD	0.67	0.65	0.66	0.62	0.63	0.62	0.63
FL	AASHTO - LRFD Design Axial Capacity (tons)	288	N/A	486	585	N/A	953	N/A
	AASHTO - ASD Allowable Stress Capacity (tons)	168	N/A	277	342	N/A	552	N/A
	Listed - "Maximum Pile Driving Resistance" with Factor Applied (tons)	130	N/A	195	234	N/A	390	N/A
	Listed - Interaction Diagrams	275	N/A	450	550	N/A	900	N/A
	Listed Resistance / LRFD	0.45	N/A	0.40	0.40	N/A	0.41	N/A
	Listed - Interaction /LRFD	0.96	N/A	0.93	0.94	N/A	0.94	N/A
	Listed – Interaction /ASD	0.78	N/A	0.70	0.68	N/A	0.71	N/A

Comparison of Listed and Calculated DOT Pile Capacities								
State Org.	Value Type	Primary Square Pile Dimension						
		14 in.	16 in.	18 in.	20 in.	24 in.	30 in.	36 in.
GA	AASHTO - LRFD Design Axial Capacity (tons)	237	318	410	503	579	853	1112
	AASHTO - ASD Allowable Stress Capacity (tons)	134	184	240	293	336	497	648
	Listed – "Max. Factored Structural Resistance" - Tons	237	318	410	503	579	853	1112
	Listed/LRFD	1.00	1.00	1.00	1.00	1.00	1.00	1.00
	Listed/ASD	1.76	1.73	1.71	1.71	1.72	1.72	1.72
MS	AASHTO - LRFD Design Axial Capacity (tons)	234	315	392	495	600	851	1107
	AASHTO - ASD Allowable Stress Capacity (tons)	135	184	227	290	350	350	647
	Listed - "Range for Ultimate Capacity" – Upper Value (tons)	48	60	75	Not Given	Not Given	Not Given	Not Given
	Listed/LRFD	0.21	0.19	0.19	N/A	N/A	N/A	N/A
	Listed/ASD	0.36	0.33	0.33	N/A	N/A	N/A	N/A
TX	AASHTO - LRFD Design Axial Capacity (tons)	N/A	316	400	488	N/A	N/A	N/A
	AASHTO - ASD Allowable Stress Capacity (tons)	N/A	184	234	284	N/A	N/A	N/A
	Listed - "Maximum Allowable Pile Service Loads" (tons)	N/A	125	175	225	N/A	N/A	N/A
	Listed/LRFD	N/A	0.40	0.44	0.46	N/A	N/A	N/A
	Listed/ASD	N/A	0.68	0.75	0.79	N/A	N/A	N/A
VA	AASHTO - LRFD Design Axial Capacity (tons)	246	N/A	402	487	N/A	N/A	N/A
	AASHTO - ASD Allowable Stress Capacity (tons)	140	N/A	231	286	N/A	N/A	N/A
	Listed - "Typical Capacity" (tons)	112	N/A	144	160	N/A	N/A	N/A
	Listed/LRFD	0.46	N/A	0.36	0.33	N/A	N/A	N/A
	Listed/ASD	0.80	N/A	0.62	0.56	N/A	N/A	N/A

Comparing Alabama's listed values to the AASHTO values indicate that some sort of additional factors have been applied to reduce the calculated ASD or LRFD capacities, if that is how they were originally calculated. Across the different pile types, the listed to AASHTO ratios are fairly consistent, which may indicate an external factor was applied to the calculated values as a lump sum manner of

accounting for transportation stress, driving stress, and/or geotechnical variability. Further discussion of ALDOT piles' capacities is found in Section 4.5 of this document.

The most definitive result from this table comparison comes from Georgia's considered piles. The AASHTO LRFD values effectively match the listed "Max. Factored Structural Resistance" found in their SDM. This shows that Georgia's standard values used are structural in nature, for axially loaded, fully embedded columns. No additional considerations appear to be made for other structural implications, such as lateral loading and slenderness effects, or geotechnical limitations applied. This means that when Georgia engineers are evaluating possible foundation plans, if the geotechnical conditions do not prove to be the limiting factor, they have the ability to utilize the full design capacity of the piles under the right circumstances.

The Florida interaction diagram capacities are quite close to those calculated using AASHTO LRFD methodology. The interaction diagram values are each slightly lower than the calculated values. The level of accuracy between them, as well as the available information from the FDOT resources indicate that the interaction diagrams were based on the AASHTO LRFD structural capacity of axially loaded piles. The slight discrepancies between the AASHTO LRFD values calculated by this research team and those taken from the interaction diagrams may very well come from the manner in which the interaction diagrams were read. The researcher viewing the diagrams had to estimate a value and tended to err on the side of conservatively not overstating the pile capacity from the diagrams. Once the calculations were carried out, the interaction diagram could be revisited to see if the estimate can be refined to be closer to the interaction diagram values. This was not carried out at this phase to preserve the integrity of the original estimate. Now that more relevant information is available through FDOT's interaction diagrams, the listed maximum driving resistances do not warrant further investigation at this time during attempts to ascertain the structural capacities of Florida piles.

Based on the AASHTO calculations, MDOT's piles have significantly higher structural capacity than those currently listed for 14-, 16- and 18-inch piles. As mentioned previously, the information surrounding these listed values is rather scarce. From the calculations and comparison above, it can again be seen that there are fairly consistent ratios between the listed values and AASHTO calculated ones. MDOT values are about one quarter of LRFD values, and about one third of ASD values. It is possible that additional factors were applied to previously calculated MDOT AASHTO values to arrive at those listed, however what those factors are or how they were determined remains unknown at this time.

The available information from Texas causes some comparison difficulty within the table. Their table of pile values claims to include the maximum allowable pile service loads. Service loads in LRFD tradition refer to the unfactored loads accounted for on the pile. It is unknown if that is how it is meant to be taken in this context. Conversely, in ASD, "allowable" does refer to a factored value. The load ratios are somewhat consistent, but not conclusively.

As discussed previously, the Virginia capacity values do not appear to be heavily relied upon by VDOT engineers based on the survey responses received on the matter. Additionally, the comparison between the calculated AASHTO values and the listed maximum typical capacities yields a wide spread of ratios, indicating a more substantial lack of consistency between the listed and calculated values.

4.5. Possible Explanations of ALDOT Pile Capacities

The primary goal of this research venture is to understand the derivation of the currently used ALDOT pile capacities listed in the current ALDOT bridge design manual, which are presented in Table 4-6 below. While meeting with the ALDOT project advisory committee, it was discussed that the current listed values were arrived at by multiplying previously listed values based on ASD methodology with a factor. Therefore, it is particularly important to evaluate the AASHTO ASD calculated values and the ALDOT provided values. We then are able to look to correlations within the data and develop plausible explanations for how the current standard values were produced.

To develop these explanations, various theories were considered. The critical background information leading to these theories has been presented previously. The following passages primarily focus on how this information has been pulled together to create credible explanations of ALDOT's existing pile capacity values.

Table 4-6: ALDOT Currently Listed Pile Capacities

ALDOT Standard Pile Capacities from SDM Table 10-2	
Size of Pile	Maximum Factored Design Load Allowed
14-inch	90 tons
16-inch	120 tons
18-inch	150 tons
20-inch	180 tons
24-inch*	220 tons
30-inch*	310 tons
36-inch*	410 tons
*Pile cross section has circular void	

4.5.1. AASHTO ASD Based ALDOT Pile Capacities

While AASHTO has transitioned to LRFD, their ASD equations are still available in previous editions of their publications. For instance, the Standard Specifications for Highway Bridges (17th ed.) includes discussion of Allowable Stresses in Piles in Section 4.5.7.3 (AASHTO 2002). This equation was discussed at length in Section 2.9.1 of this document. To calculate the ASD pile capacities, the effective prestress across the pile must be calculated. As detailed information regarding the losses in prestress in piles was not available for ALDOT's pile design methodology at this time, twenty percent losses were assumed for this analysis. This assumption and others for the following calculations are recorded below in Table 4-7.

Table 4-7: Assumptions for ALDOT Allowable Stress Capacity Calculations

Assumptions Used to Calculate ALDOT Piles Allowable Stress Capacities	
Property	Assumption Made
Concrete Strength (f_c')	5,000 psi, ALDOT typical concrete strength for piles
Concrete Elastic Modulus (E_c)	$120{,}000 * K_1 * w_c{}'^{2.0} * f_c{}'^{0.33}$, ksi **Equation 4-2** K_1=1.0, w_c' =0.150 kcf (AASHTO 2017, 5.4.2.4)
Prestressing Steel Elastic Modulus (E_s)	28,500 ksi (AASHTO 2017, 5.4.4.2)
Humidity	75%
Strand Type	Grade 270, Low Lax, 0.5-inch diameter
Prestressing Losses	20%
Pile Type	Fully Embedded, Pretensioned

Next, the load strength for a given prestressed pile was calculated using the AASHTO/PCA equation for allowable stress. After tracking down the original source of this equation, we found that a safety factor of 2.2 had been incorporated into its original derivation (PCA 1971). The allowable stress was then multiplied by the gross area of the pile to determine the maximum allowable load, as per AASHTO Standard Spec 4.5.7.3. The calculations for the ASD allowable load for ALDOT piles is found in Table 4-8 below.

Table 4-8: Calculating ASD Capacities of ALDOT Piles

AASHTO ASD Load Strength of ALDOT PPCPs			
Size of Pile	Allowable Compressive Stress (ksi)	Gross Area of Pile (in.^{2})	Maximum Allowable Load, (tons) "AASHTO ASD Pile Capacity"
	$f_c = 0.33\, f_c' - 0.27\, f_{pe}$,	A_g	$P_u = f_c * A_g * \frac{1\ ton}{2000\ lbs}$
14 in.	1.377	196	135
16 in.	1.441	256	184
18 in.	1.402	324	227
20 in.	1.449	400	290
24 in.*	1.431	489	350
30 in.*	1.455	686	499
36 in.*	1.441	898	647
*Pile cross section has circular void			

Now that these values have been calculated, theories can be developed to correlate the ALDOT values to ASD values, and then consider transitions to LRFD values. The primary theory which has been developed is explained in the following passages.

4.5.2. Comparing AASHTO ASD to ALDOT 2008 ASD Pile Capacities

In addition to the current ALDOT list of standard pile capacities (ALDOT 2017b), values from ALDOT's 2008 structural design manual are available (ALDOT 2008). These values provide an important stepping-stone to understanding the current ALDOT values. Table 4-9 shows the calculated AASHTO ASD capacity, then the 2008 and 2017 ALDOT values and the ratio of the 2017 capacities to the 2008 ones. The final two columns compare AASHTO's ASD calculated values to the 2008 and 2017 ALDOT values respectively.

Table 4-9: Comparing AASHTO ASD to ALDOT Loads

Conversion Theory Development Part 1: Ratio of AASHTO ASD to ALDOT Listed Capacities						
Size of Pile	AASHTO ASD Capacity (tons)	ALDOT Capacity			Comparing AASHTO ASD to ALDOT	
		2008 Maximum Design Load (tons)	2017 Maximum Design Load (tons)	Ratio of 2017 to 2008 Design Loads	Ratio of AASHTO ASD to ALDOT 2008	Ratio of AASHTO ASD to ALDOT 2017
14 in.	135	60	90	1.50	2.25	1.50
16 in.	184	80	120	1.50	2.30	1.53
18 in.	227	100	150	1.50	2.27	1.51
20 in.	290	120	180	1.50	2.42	1.61
24 in.*	350	160	220	1.38	2.19	1.59
30 in.*	499	190	310	1.63	2.63	1.61
36 in.*	647	250	410	1.64	2.59	1.58
*Pile cross section has circular void			Average Ratio:	1.52	2.38	1.56

When comparing the 2017 ALDOT capacities to those from 2008, the ratio interestingly is consistently 1.5 for the non-voided piles. The 2017 SDM states that resistances were "increased by an assumed average load factor γ, of 1.45." This passage does not clearly state what the resistances were before they were increased, but page 20 of the 2008 SDM does specify that Service Load Design method (Allowable Stress Design) is the design method to be employed at this time for structural design. Thus, these 2008 values should be taken as ALDOT's ASD allowable loads (ALDOT 2008). Based on the 2017 SDM's statement, that the loads were increased by a factor of 1.45, we would expect that the ratio of 2017 LRFD to 2008 ASD values to be 1.45 (ALDOT 2017b). However, this is not consistently the case.

In the 2008 manual, these loads are specifically stated to be "for foundation (footing) piles only." It goes on to say that loadings would be less for pile bents. The 2017 manual carries the same note. Based on this, it seems unlikely that these loads are limited based on pile bent behavior. Perhaps a certain level of moment is assumed to be acting in addition to axial loading, but that is not mentioned in the manuals. In the AASHTO ASD equation derivation by PCA, an accidental eccentricity of loading for an individual pile was assumed to be 0.05 times the thickness of the member (PCA 1971). Thus, the loads calculated by ASD should only be decreased for their axial-only capacity if greater than five percent eccentricity is expected.

To examine the likely transition chronologically, we then take the ratio of the AASHTO ASD calculated values to the ALDOT 2008 values. This column then shows that there is a factor of at least 2.0 between the AASHTO ASD values and the 2008 ALDOT ones.

Notably, these values are close to the assumed safety factor already incorporated into the AASHTO equation. In the AASHTO Spec there is no discussion on factors of safety for axial capacity of piles (AASHTO 2002). Instead, the listed allowable stresses are given as the "allowable" or factored equations. This is already taken care of within the capacity equation. Comparatively, for geotechnical axial capacity for piles, factors are specified to be between 1.9 and 3.5 depending on the level of site exploration and construction controls (AASHTO 2002, Table 4.5.6.2A). For drilled shafts, factors of safety are said to be at least 2.0 when the design was based on a load test on the site, while a minimum factor of 2.5 is specified for other cases with normal levels of field quality control (AASHTO 2002, 4.6.5.4).

Based on the preceding discussion, it is possible that, when calculating the ASD capacity of the piles, an additional safety factor was used. The ratio being 2.0 or more falls within the other AASHTO provided safety factors for the geotechnical capacity of pile foundations.

This theory about what is essentially a geotechnical safety factor being applied to the structural capacity of the pile is supported by consideration of static load testing of piles. Typically, when a static load test would be applied, it would strive to achieve 200 percent of the design load for the pile (FHWA 2006). If the geotechnical capacity of the pile is set by utilizing the full allowable structural capacity of the pile, then this could present an issue during the load testing. To ensure that there would not be a geotechnical-based failure, this pile would be loaded to twice its geotechnical capacity. However, if this geotechnical capacity was set equal to the structural capacity, this would mean that the structural capacity of the pile was also exceeded. This is not a desirable circumstance. To prevent this issue, it is possible that in the derivation of the ALDOT listed pile capacities, the values were cut in half, in anticipation of them experiencing static load testing of twice this value. If that is true, then these piles with a listed capacity that is half of their "true" capacity would see a maximum of 200 percent of half of their capacity during a load test, and thus would only ever see 100 percent of their true design capacity. The AASHTO Specifications' safety factors for ultimate geotechnical capacity are replicated within this document as Table 2-2 for reference.

4.5.2.1. AASHTO ASD to ALDOT ASD Conversion Theory with Factor of 2.2

Table 4-10 looks closer at the theory that the values were factored again or reduced for geotechnical reasons and experiments with the application of an additional factor. As the value of 2.2 was assumed in the derivation of the AASHTO equation, that value is assumed here again as a reasonable starting point. From Table 4-10, we can see that the ASD values with an additional factor fall rather closely to the 2008 ALDOT loads. In particular, most times the ASD value divided by 2.2 results in a value greater than the ALDOT ones, with the only exception being for the 24-inch pile. The slight variations could be due to minor changes in assumptions (such as more detailed loss calculations) or rounding and reductions applied at the engineers' discretion. Notably the voided piles have larger variances, so perhaps additional considerations were made due to their voided nature, or their larger size.

Table 4-10: Applying Safety Factor of 2.2 to AASHTO ASD Capacities

Applying Safety Factor of 2.2 to AASHTO ASD Calculated Values					
Size of Pile	AASHTO ASD Capacity (tons)	Add Safety Factor of 2.2	AASHTO ASD/2.2 (tons)	ALDOT 2008 Maximum Design Loads for PPC Piles (tons)	Percent Difference between ASD/2.2 and ALDOT 2008
14 in.	135	/2.2 =	61	60	2.2
16 in.	184	/2.2 =	84	80	4.4
18 in.	227	/2.2 =	103	100	3.1
20 in.	290	/2.2 =	132	120	9.4
24 in.*	350	/2.2 =	159	160	0.6
30 in.*	499	/2.2 =	227	190	17.7
36 in.*	647	/2.2 =	294	250	16.2
*Pile cross section has circular void			Average % Difference:		7.7

4.5.2.2. AASHTO ASD to ALDOT ASD Conversion Theory with Factor of 2.25

Table 4-11 shows the same calculations as Table 4-10, but with 2.25 being the assumed safety factor instead. This factor appears as the safety factor for geotechnical pile capacity when wave equation and dynamic measurement and analysis are applied as construction controls on the foundation. The resulting comparison in Table 4-11 shows smaller percent differences, with the same pattern of outliers as when a factor of 2.2 was assumed in Table 4-10.

Table 4-11: Applying Safety Factor of 2.25 to AASHTO ASD Capacities

Applying Safety Factor of 2.25 to AASHTO ASD Calculated Values					
Size of Pile	AASHTO ASD Capacity (tons)	Add Safety Factor of 2.25	AASHTO ASD/2.25 (tons)	ALDOT 2008 Maximum Design Loads for PPC Piles (tons)	Percent Difference between ASD/2.25 and ALDOT 2008
14 in.	135	/2.25 =	60	60	0.0
16 in.	184	/2.25 =	82	80	2.2
18 in.	227	/2.25 =	101	100	0.9
20 in.	290	/2.25 =	129	120	7.1
24 in.*	350	/2.25 =	156	160	2.8
30 in.*	499	/2.25 =	222	190	15.4
36 in.*	647	/2.25 =	288	250	14.0
*Pile cross section has circular void			Average % Difference:		6.1

4.5.2.3. Selecting a Conversion Factor for Proposed AASHTO to ALDOT ASD

The differences between the ASD doubly factored values and the 2008 ALDOT ones could likely be the result of the same differences in assumptions or applications of engineering judgement as discussed following Table 4-10. Thus, because of its smaller average percent difference, our theory has developed to consider the application of a factor of 2.25 rather than 2.2.

4.5.3. Comparing ALDOT 2008 ASD Values to 2017 ALDOT Standard Capacities

Now that the first transition of AASHTO ASD to ALDOT 2008 ASD values has been addressed and a transition factor of 2.25 has been selected as the best and most logical fit, we move on to determining what factor was applied to convert from the 2008 ALDOT ASD values to the current ALDOT 2017 listed capacities. Two different conversion factors are considered, 1.45 and 1.5, and these possible conversions are discussed in the following paragraphs.

4.5.3.1. ALDOT 2008 to ALDOT 2017 Conversion Theory with Factor of 1.45

To get from 2008 ALDOT ASD values to those found in the current (2017) SDM, ALDOT might have multiplied the 2008 values by a factor of 1.45. This conversion factor was explicitly mentioned in the ALDOT SDM, and therefore provides a decent starting point. Table 4-12 shows these calculations and the resulting percent difference between the 2008 values with the new factor and the current 2017 LRFD values. Here the percent differences again are not huge, but it is noteworthy that the increase of 1.45 resulted in values lower than the current 2017 listed capacities. We believe it is unlikely that ALDOT engineers would choose to round up after selecting a factor of 1.45, perhaps they selected a larger factor to begin with.

Table 4-12: Applying Factor of 1.45 to ALDOT 2008 PPCP Capacities

Increasing 2008 ALDOT Capacities by a Factor of 1.45					
PPCP Type	ALDOT 2008 ASD Capacity (tons)	Increase by 1.45	ALDOT 2008 ASD*1.45 (tons)	ALDOT 2017 Maximum Design Loads for PPC Piles (tons)	Percent Difference between (2008 ALDOT*1.45) and (2017 ALDOT)
14 in.	60	*1.45 =	87	90	3.4
16 in.	80	*1.45 =	116	120	3.4
18 in.	100	*1.45 =	145	150	3.4
20 in.	120	*1.45 =	174	180	3.4
24 in.*	160	*1.45 =	232	220	5.3
30 in.*	190	*1.45 =	276	310	11.8
36 in.*	250	*1.45 =	363	410	12.3
*Pile cross section has circular void			Average % Difference:		6.1

4.5.3.2. ALDOT 2008 to ALDOT 2017 Conversion Theory with Factor of 1.5

In the previous section, a factor of 1.45 was applied in compliance with the available information in ALDOT's SDM. However, as this resulted in unconservative values, we next try the same approach but with a slightly larger factor of 1.5.

Table 4-13 : Applying Factor of 1.5 to ALDOT 2008 PPCP Capacities

Increasing 2008 ALDOT Capacities by a Factor of 1.5					
PPCP Type	ALDOT 2008 ASD Capacity (tons)	Increase by 1.5	ALDOT 2008 ASD*1.5 (tons)	ALDOT 2017 Maximum Design Loads (tons)	Percent Difference between (2008 ALDOT*1.5) and (2017 ALDOT)
14 in.	60	*1.5 =	90	90	0.0
16 in.	80	*1.5 =	120	120	0.0
18 in.	100	*1.5 =	150	150	0.0
20 in.	120	*1.5 =	180	180	0.0
24 in.*	160	*1.5 =	240	220	8.7
30 in.*	190	*1.5 =	285	310	8.4
36 in.*	250	*1.5 =	375	410	8.9
*Pile cross section has circular void			Average % Difference:		3.7

From the last column of Table 4-13 we see that in applying factor of 1.5, the percent difference for the smaller piles is essentially zero. The larger piles have larger percent differences. Similar nonconformity was seen for the larger and voided piles in Table 4-10 and Table 4-11 when considering a conversion factor between the AASHTO ASD and ALDOT 2008 values. Again, this discrepancy may be the result of a different conversion factor being applied to increase the capacities for the larger piles.

4.5.4. Conversion Attempts using Direct Transmission

To follow up from these two separate conversion steps, direct transmission from AASHTO ASD to ALDOT 2017 values was calculated by applying a safety factor of either 2.2 or 2.25 and then increasing the capacity by 1.45 or 1.5. This direct transmission brings our values close to ALDOT's 2017 current listed capacities. The following tables show direct attempts at transmission between AASHTO ASD capacities and 2017 ALDOT Values. These rely on the application of safety factors of 2.2 or 2.25 (SF) to transition to ALDOT 2008 values, and then increases of 1.45 or 1.5 (load conversion factor, LF) to arrive at the final 2017 ALDOT values. The percent differences between the calculated (AASHTO ASD/SF*LF) approximation of 2017 ALDOT values and the actual posted 2017 ALDOT values is presented in the final column of each table, with the average percent difference following. Table 4-14 provides a key and summary of each case's combination of factors as well as which of the following tables focus on that case.

Table 4-14: Factor Combinations for Conversion of AASHTO ASD to ALDOT LRFD

Direct Conversion of Pile Capacity Factor Combinations			
Table Case #	Table Number	Safety Factor (SF)	Load Conversion Factor (LF)
1	Table 4-15	2.2	1.45
2	Table 4-16	2.2	1.5
3	Table 4-17	2.25	1.45
4	Table 4-18	2.25	1.5

Table 4-15: Direct Transmission AASHTO ASD to ALDOT LRFD with 2.2 and 1.45

Case 1: Direct Transmission from AASHTO ASD to ALDOT 2017 (using 2.2 and 1.45)							
PPCP Type	AASHTO ASD Capacity (tons)	Add Safety Factor of 2.2	AASHTO ASD/2.2 (tons)	Increase by 1.45	AASHTO ASD/2.2 * 1.45	ALDOT 2017 Capacity (tons)	Percent Difference between (ASD/2.2* 1.45) and ALDOT 2017
14 in.	135	/2.2 =	61	*1.45 =	89	90	1.1
16 in.	184	/2.2 =	84	*1.45 =	121	120	1.1
18 in.	227	/2.2 =	103	*1.45 =	150	150	0.3
20 in.	290	/2.2 =	132	*1.45 =	191	180	6.0
24 in.*	350	/2.2 =	159	*1.45 =	231	220	4.7
30 in.*	499	/2.2 =	227	*1.45 =	329	310	5.9
36 in.*	647	/2.2 =	294	*1.45 =	426	410	3.9
*Pile cross section has circular void				Average % Difference:			3.3

Table 4-16: Direct Transmission AASHTO ASD to ALDOT LRFD with 2.2 and 1.5

Case 2: Direct Transmission from AASHTO ASD to ALDOT 2017 (using 2.2 and 1.5)							
PPCP Type	AASHTO ASD Capacity (tons)	Add Safety Factor of 2.2	AASHTO ASD/2.2 (tons)	Increase by 1.5	AASHTO ASD/2.2 * 1.5	ALDOT 2017 Capacity (tons)	Percent Difference between (ASD/2.2*1. 45) and ALDOT 2017
14 in.	135	/2.2 =	61	*1.5 =	92	90	2.2
16 in.	184	/2.2 =	84	*1.5 =	125	120	4.4
18 in.	227	/2.2 =	103	*1.5 =	155	150	3.1
20 in.	290	/2.2 =	132	*1.5 =	198	180	9.4
24 in.*	350	/2.2 =	159	*1.5 =	239	220	8.1
30 in.*	499	/2.2 =	227	*1.5 =	340	310	9.3
36 in.*	647	/2.2 =	294	*1.5 =	441	410	7.3
*Pile cross section has circular void				Average % Difference:			6.3

Table 4-17: Direct Transmission AASHTO ASD to ALDOT LRFD with 2.2 and 1.45

Case 3: Direct Transmission from AASHTO ASD to ALDOT 2017 (using 2.25 and 1.45)							
PPCP Type	AASHTO ASD Capacity (tons)	Add Safety Factor of 2.25	AASHTO ASD/2.25 (tons)	Increase by 1.45	AASHTO ASD/2.25 * 1.45	ALDOT 2017 Capacity (tons)	Percent Difference between (ASD/2.25* 1.45) and ALDOT 2017
14 in.	135	/2.25 =	60	*1.45 =	87	90	3.4
16 in.	184	/2.25 =	82	*1.45 =	119	120	1.2
18 in.	227	/2.25 =	101	*1.45 =	146	150	2.5
20 in.	290	/2.25 =	129	*1.45 =	187	180	3.8
24 in.*	350	/2.25 =	156	*1.45 =	226	220	2.5
30 in.*	499	/2.25 =	222	*1.45 =	322	310	3.7
36 in.*	647	/2.25 =	288	*1.45 =	417	410	1.7
*Pile cross section has circular void				Average % Difference:			2.7

Table 4-18: Direct Transmission AASHTO ASD to ALDOT LRFD with 2.25 and 1.5

Case 4: Direct Transmission from AASHTO ASD to ALDOT 2017 (using 2.25 and 1.5)							
PPCP Type	AASHTO ASD Capacity (tons)	Add Safety Factor of 2.25	AASHTO ASD/2.25 (tons)	Increase by 1.5	AASHTO ASD/2.25 * 1.5	ALDOT 2017 Capacity (tons)	Percent Difference between (ASD/2.25* 1.5) and ALDOT 2017
14 in.	135	/2.25 =	60	*1.5 =	90	90	0.0
16 in.	184	/2.25 =	82	*1.5 =	123	120	2.2
18 in.	227	/2.25 =	101	*1.5 =	151	150	0.9
20 in.	290	/2.25 =	129	*1.5 =	193	180	7.1
24 in.*	350	/2.25 =	156	*1.5 =	233	220	5.9
30 in.*	499	/2.25 =	222	*1.5 =	333	310	7.1
36 in.*	647	/2.25 =	288	*1.5 =	431	410	5.1
*Pile cross section has circular void				Average % Difference:			4.0

Table 4-19 provides a summary of the primary observations made from the factor combinations in the cases. Larger piles had larger percent differences in all cases except Case 3. Perhaps the loss assumptions made are less applicable to the larger piles. Alternatively, where the calculated values for voided piles are larger than those used by ALDOT, perhaps more conservative rounding was used by ALDOT engineers, due to the perhaps perceived greater importance the larger piles would have. The logic could have been that because these piles would be seeing larger loads, it is justifiable to round down even more conservatively than in other cases. This would make Cases 2 and 4 the most likely cases. None of the currently used values exceed the calculated ones, and the larger piles values are

rounded down more significantly in these cases. Then, between those two combinations, Case 4's estimates are closer to ALDOT's 2017 values, so it is the current preferred theory of transmission. The factors of 2.25 and 1.5 were also selected as favorable when the transitions were considered separately, which further supports their selection.

Table 4-19: Summary of Direct Transmission Results

Summary of Direct Transmission Results			
Table Case #	Safety Factor (SF)	Load Conversion Factor (LF)	Observations
1	2.2	1.45	• 1.45 matches what is given in SDM. • 2.2 matches assumed safety factor in ASD equation derivation. • Some values were lower than current ALDOT values. • Relatively small percent differences (second lowest average percent difference)
2	2.2	1.5	• 1.5 matches the observed change between 2008 and 2017 values. • 2.2 matches assumed safety factor in ASD equation derivation. • In each case, the calculated values were greater than the current ALDOT ones, indicating that conservative rounding could have been applied. • Greatest average percent difference
3	2.25	1.45	• 1.45 matches what is given in SDM. • 2.25 resulted in smaller percent differences than 2.2. • Some values were lower than current ALDOT values. • Most even percent differences, resulting in the smallest average percent difference.
4	2.25	1.5	• 1.5 matches the observed change between 2008 and 2017 values. • 2.25 resulted in smaller percent differences than 2.2. • In each case, the calculated values were greater than the current ALDOT ones, indicating that if used, conservative rounding could have been applied

4.5.5. Final Conclusions on Possible Explanation of Standard PPCP Capacity Origins

After incorporating and comparing ALDOT's 2008 pile capacity values, it is the current working theory that ALDOT calculated the AASHTO ASD allowable capacity, applied an additional safety factor of about 2.25, and then to convert from the 2008 ASD values to the 2017 LRFD ones, increased the axial capacities by about 1.5. This theory is based on examining and comparing the values found for

ALDOT in 2008 and 2017 with the AASHTO ASD calculations and is strongly supported by the preceding sections.

It is possible that the derivation of the Alabama DOT's PPCP pile capacities is permanently lost to the past. However, with the above plausible theories, ALDOT engineers may have a better understanding of their opportunities to allow increased structural capacities of piles. The following discussion focuses on developing tools to assist with potential improvements by ALDOT engineers.

5. Pile Analysis through Creation of Moment Axial Interaction Diagrams

As previously mentioned, a particular goal of this research has been the development of moment-axial interaction diagrams for ALDOT's PPCPs. The process based on first principles and a spreadsheet program developed for this purpose are detailed in this chapter.

5.1. Background

Moment-axial interaction diagrams are essential tools for engineers designing column-like structures. For these structural members, the primary considered structural failure methods would be either in compression (by an applied concentric axial load, P), flexure (generated by a moment, M), or a combination of the two. Moment-axial interaction diagrams are also known as M-P diagrams and may be referred to as such in this document for brevity. These diagrams plot the points of compression failure, flexure failure, and points in between to create a threshold of values, beyond which failure should be expected. These nominal values can then be factored to generate design curves for a given cross section. Once these curves are generated, engineers can use the diagrams for preliminary sizing consideration of members for given loading conditions.

In practice, engineers may generate and use these types of figures for design purposes. The design of the shear reinforcement, such as spacing of ties, or pitch of spirals in not included in this discussion, neither are other detailing requirements. The program developed for creating these M-P diagrams for this project uses Microsoft Excel 2016 and Visual Basic for Applications (VBA).

5.2. Developing M-P Diagrams

To generate these diagrams, some fundamental assumptions were made. First, we are assuming a linear strain distribution along the depth of section in the direction of bending (thereby adopting the "plane-sections remain plane" assumption). Second, we are assuming that there is perfect bond between concrete and strands, i.e., strain compatibility between the concrete and the prestressing strands exists. Third, the total compression force in the cross section under combined axial and bending moment can be calculated using an equivalent rectangular stress block distribution for the compression stress in the concrete (Nawy 1995). These three assumptions are commonly used in analysis of reinforced concrete members.

Interaction diagrams are developed based on a series of design points selected by the developer to plot the approximate capacity based on relevant code standards of practice. This can be done with as few as two points (the axial compression limit, and the flexural capacity of the member), or as many as the engineer wishes. With an increase in the number of points used, the smoothness of the capacity curves increases. If only the pure axial capacity and flexure capacity were used to represent the M-P diagram, the diagram would then consist of a straight line drawn between the two. This would be conservative, as it does not account for the interplay between axial and moment capacities. For example, in most cases, a "nose" can be seen on the diagrams where the moment carrying capacity increases when some axial load is applied. To draw a line directly between the axial and moment capacity values would cut out this increase in moment capacity as a result of the member experiencing axial compression.

5.2.1. Primary User Interface and Inputs

The user inputs for this program are discussed in the following passages. To facilitate easy use of the developed program, a sheet has been included in the workbook for "Typical Inputs." This includes input columns for each standard ALDOT PPCP, as well as a user-defined option. The primary categories of these inputs are section details, concrete properties, and prestressing properties. These inputs also vary in their nature as being either values that users plug in directly or being calculated or determined as a function of the program itself. In these situations, the origins of these equations or values is described below. For simple user inputs, the reasoning for their use or typical values are provided as well. The major assumptions and inputs used for developing our interaction diagrams for ALDOT piles in particular are discussed below.

The sheet "Pile Analysis Inputs" gives users the option to autofill the inputs based on the "Typical Inputs" sheet. Should they choose not to, there are certain inputs that they can edit, while others are calculated within the program itself. These user input values that may be changed are identified with a dashed border and differing cell color. The remaining cells are populated through the pile analysis process and are considered derived inputs. Users are also presented with the option to run the pile analysis, or clear the program's outputs, generated diagrams, and inputs. These clearing functions cannot be undone, so users are met with a confirmation option prior to the actions of the program being carried out.

5.2.2. Section Properties

For the general section properties of the piles, these values are predominantly pulled directly from those provided in ALDOT's standard drawing "Precast Prestressed Concrete Piles," namely PSCP-1 (ALDOT 2017a). Low-relaxation strands seem to be the standard of current practice, so the values that correspond to that strand type were used. When calculating the area of concrete for the piles, the chamfer areas and prestressing strand areas were not subtracted from the total concrete area. This appears to be an acceptable simplifying assumption for ALDOT's practice, based on the listed "Area of Normal Cross Section" values on the same standard drawing. Concrete cover for the cross sections is also incorporated in determining the depth to the initial strand layer in the direction of bending, and in establishing the analytical location of each subsequent strand layer.

Some of the larger ALDOT piles are voided, removing excess material to reduce the pile weight and cost. A circular void is described in PSCP-1, and it is assumed to be centered in the cross section. The void start and end locations are each determined based on the ALDOT specified void diameter. This void presents an interesting programming challenge for computing the concrete force in the section with a varying neutral axis depth (c). As the neutral axis moves down in the cross section (in the direction of bending), it starts to include portions of the void. The rectangular equivalent stress block depth, ($a= \beta_1 * c$), can fall above the void, within the top half of the void, below the void's center, or below the void entirely. This results in a concrete stress block with an atypical effective width and centroid location. Thus, for each of these scenarios of the location of the equivalent rectangular stress-block's depth, a composite body series of equations had to be developed to find the area and geometric centroid.

The strand layout for all the piles used by ALDOT for their bridge foundations is also provided in PSCP-1 document (ALDOT 2017a). The concrete cover is also specified within PSCP-1 as being 3 inches. However, the depth to the center of each strand layer had to be approximated based on the concrete cover, spiral shear reinforcement diameter, prestressing strand diameter, and the number

of spaces available. Essentially the first strand layer depth was determined, then the center-to-center spacing was derived and added to the first layer depth to find the second layer location. The spacing was then added to the second layer to find the third layer location and so on for all remaining layers. Even though the maximum number of strand layers for ALDOT low-relaxation current pile designs is eight, the program has been developed to accommodate up to 10 strand layers. Whether the pile can contain that many layers and satisfy all other detailing requirements, remains a judgement call for any designer engineers and falls outside the scope of this research venture.

5.2.3. Concrete Material Inputs

The inputs used for the concrete materials are industry standard values. They are summarized in the table below to indicate what values were used in the derivation of the moment-axial interaction diagrams generated for ALDOT piles. Some relevant rationale and citation information is additionally provided in Table 5-1 for the reader's convenience.

Table 5-1: Program Inputs for Concrete

Concrete Material Program Inputs			
Input	Abbreviation	Value Used	Rationale
Concrete Strength	f_c'	5 ksi	ALDOT specifies use of 5 to 6 ksi concrete for piles. (ALDOT 2017b, SDM, Table 5-1)
Weight of Concrete	w_c	0.150 kcf	(AASHTO 2017, Table 3.5.1-1 & C3.5.1)
Ultimate Strain of Concrete	ϵ_c	0.003 (in./in)	For strength and extreme limit states, for normal weight concrete up to 15 ksi, the maximum usable strain in unconfined concrete is taken as 0.003 in the extreme compression fiber. (AASHTO 2017, 5.6.2.1)
Modulus of Elasticity (derived)	E_c	4592 ksi	$E_c = 120{,}000 * K_1 * w_c^{2.0} * f_c'^{0.33}$ **Eq. 5-1** K_1 = the correction factor for aggregate, taken as 1.0 (AASHTO 2017, Eq. 5.4.2.4-1)
Stress Block Factor (derived)	β_1	0.8 for 5 ksi concrete	$\beta_1 = 0.85 - \frac{0.85 * f_c' * 1000 - 4000}{1000}$ (for concrete with f_c' between 4 and 10 ksi) **Eq. 5-2** (AASHTO 2017, 5.6.2.2; ACI 2014, Table 22.2.2.4.3) Notably, for our consideration, the magnitude of the rectangular stress block distribution is taken to be: *0.85*f'c* (Also supported by AASHTO 2017, 5.6.2.2)

5.2.4. Prestressing Properties

Similar to the concrete material properties, rather standard properties were used for the prestressing strand reinforcement. This information can be seen in Table 5-2 below.

Table 5-2: Program Inputs for Prestressing

Prestressing Reinforcement Material Program Inputs			
Input	Abbreviation	Value Used	Justification
Grade of Prestressing	F_u	270 ksi	ALDOT specifies the use of Grade 270 strands for PPCPs on PSCP-1
Modulus of Elasticity	E_s	28,500 ksi	(AASHTO 2017, 5.4.4.2)
Yield Strength	F_y	243 ksi	Yield Strength for Grade 270 strand = 90% of F_u (AASHTO 2017, Table 5.4.4.1-1)
Yield Strain	ϵ_{py}	0.0085 (in./in)	For Grade 270 strand, the yield strain is 0.0085. (PCI 2010, Design Aid 15.3.3)
Strand Diameter	D_{strand}	0.5 in	ALDOT specifies the use of 0.5 in. diameter strands for PPCPs on PSCP-1
Compression strain limit	ϵ_{cl}	0.002 (in./in)	(AASHTO 2017, 5.6.2.1)
Tension strain limit	ϵ_{tl}	0.005 (in./in)	(AASHTO 2017, 5.6.2.1)
Ties or Spiral shear reinforcement	*T or S*	Spiral	Only spiral reinforcement is considered for this program. This is used in determining the axial compressive capacity of the pile. (ALDOT 2017a PSCP-1) (AASHTO 2017, 5.6.4.4-2) (ACI 2014, R21.2.2)
Effective Prestress	f_{pe}	-162 ksi	An assumption of 20% lump sum losses were applied to the initial prestress values given in PSCP-1. Further details for ALDOT PPCP loss calculations were not available.
Total Effective Prestress force on all strands	P_e	Varies	$P_e = f_{pe} * (total\ area\ of\ all\ strands)$ **Eq. 5-3**
Strain in concrete from prestress	ϵ_{ce}	Varies, (in./in.)	$\epsilon_{ce} = \frac{\left(\frac{\lvert P_e \rvert}{A_{concrete}}\right)}{E_c}$ **Eq.5-4**
Effective prestressing strain	ϵ_{pe}	Varies, (in./in.)	$\epsilon_{pe} = \frac{P_e}{A_{strands} * E_s}$ **Eq. 5-5**

5.2.5. Design Point Selection and Calculations

For our analysis, five points were selected for developing the M-P diagram for each pile section. They occur when the strain at the extreme fiber in compression reaches 0.003 in./in. (representing the failure as stipulated in the design codes), would be expected for each of the following circumstances:

A) Pure axial compression, no moment is applied.
B) When the neutral axis is equal to the depth of the cross section
C) A balanced condition when the steel in the bottom of the member reaches yielding in tension, as the concrete is reaching ultimate strain in compression.
D) The point where the axial load is equal to half of the balanced condition's axial load.
E) Pure flexural loading, no axial load applied.

Each of these points is then plotted on a graph with the horizontal (X-) axis being the moment capacity, and the vertical (Y-) axis being the axial capacity. Within the program we have created, the derivation of each point is considered separately, with some overarching reasoning. Point A for pure compression was determined using AASHTO's specified formula, while the others were determined through the application of strain compatibility and equilibrium. It is worth reiterating that the moment-axial interaction diagrams generated by this program are not influenced by slenderness. A methodology for approximate evaluation of slenderness effects is provided in AASHTO LRFD 5.6.4.3 and is briefly discussed in Section 6.7.1 of this document.

5.2.5.1. Point A - Pure Axial Compression

To determine a PPCP's factored axial resistance, AASHTO conveniently supplies an equation for this critical value. For spiral reinforced doubly symmetric members, (such as our PPCPs) made of normal weight concrete, up to 10 ksi in strength, the applicable axial capacity equations are provided in] Eq. 2-13.

5.2.5.2. Points B-E – Strain Compatibility and Equilibrium Conditions

Aside from the pure compression case (Point A), four additional design points are calculated. For each of these four points, their derivation includes several similar steps. The program has been developed so that a neutral axis condition is set, and then the strain in the strands is calculated based on that condition. From those strains, the stresses are then calculated, and used to determine the force acting at each strand layer location. The force in the concrete is then calculated based on the same neutral axis parameter. The axial capacity of the cross section is then taken as the summation of the force in the concrete and the forces acting in the strands. The moment capacity of this cross section for the given point is then calculated by taking the moment of these respective forces (strand layers and concrete) about the plastic centroid of the member.

The differing neutral axis conditions are what creates the difference between each of these four points. For Point B, the initial condition is set such that the neutral axis depth is equal to the depth of the cross section, indicating that the entire cross section is in compression. For Points C, D, and E, an iteration loop is utilized to find the neutral axis location based on equilibrium of forces in the cross section. Ideally, the tolerances for defining convergence for equilibrium iterations would be zero. However, for computational purposes, this is not entirely feasible, so a reasonable tolerance of 0.1 kips is allowed in each case. Point C's loop function served to determine the neutral axis point at which the steel strain in the lowest strand layer is equal to the yielding strain of the steel. This yielding of steel while the concrete achieves its ultimate strain creates the balanced point for the cross section. Point D's loop function conversely alters the neutral axis point based on the parameter of the axial

capacity being equal to one-half of the axial capacity determined for Point C. For Point E, a loop is again used, but this point is determined based on the axial capacity (the summation of the strand forces and the concrete force) being equal to approximately zero.

5.2.5.3. Applying Reduction Factors

Each of these capacities for axial and moment combinations is then factored using resistance factors as per AASHTO LRFD recommendations. The pure compression resistance factor is taken as 0.75, as it is compression controlled. The resistance factors for the other points, however, are determined based on the net tensile strains in the extreme row of prestressing strands from the compression face, using Eq. 2-14 presented in Chapter 2. The net tensile strain in the extreme tension steel, ϵ_t, is calculated by determining the strain in the extreme tensile strand (the lowest strand in the cross section), then subtracting the strain in the strands as a result of the prestressing force (a negative value), and then adding the strain in the concrete initially generated by the effective prestress force. This calculated reduction factor is then applied to both the axial and moment values for each design point.

5.2.6. Outputs

After inputting their desired parameters, the user then presses the "Run Pile Analysis" button embedded in the "Pile Analysis Inputs" sheet to run the previously described analysis procedures. From there, two primary output sheets available to the program user.

The first, "Pile Analysis Output" includes the calculated strain, stress, and force values for each strand layer, for each calculation point. Additionally, the force for the concrete is displayed for these points. The appropriate reduction factors and maximum and net strain values in the prestressing strands are also presented along with the calculated neutral axis depth. For the circumstance of voided piles, the centroid of the equivalent stress block may be a value of interest, so a small table presents that information as well. The most important element of this page though is the buttons that generate the M-P interaction diagrams corresponding to the calculated points. The user has the option to plot the points in units either of kip-ft. or kip-in. for the moment values.

In the second output sheet, "Capacity Demand Comparison", the user has the opportunity to plot interaction diagrams with up to ten pile demand combinations. This allows the user to directly see where their demand falls compared to the threshold created by the factored interaction diagram. Engineering judgement should certainly be used in checking these demands versus the capacity, especially if these demand values fall near to threshold plotted by the charts.

5.2.7. Results

Based on the procedures and inputs previously discussed, moment-axial interaction diagrams were generated for each standard ALDOT PPCP. A representative diagram is shown below for a 14-inch PPCP. Diagrams for all other ALDOT PPCP standard sizes can be found in Appendix B. To check the trends exhibited by our developed program, we were able to compare our results with a program developed by the Prestressed/Precast Concrete Institute (PCI), and the following discussion documents the correlation we saw. After developing interaction diagrams for each standard ALDOT PPCP size, we then took those values and plotted all of the diagrams on a single chart so that it could be used to estimate required pile size for specified demands. This chart also shows the current ALDOT standard values for PPCPs. From those calculations, a table of possible new ALDOT standard values was created, Table 5-3. These values would need thorough review and approval from ALDOT engineers

before use and implementation, but for this analysis are used to demonstrate the potential increase identified herein. Additionally, in Table 5-4, it is apparent that these changes bring ALDOT pile capacities much closer to their neighboring DOTs'.

Table 5-3: Possible New ALDOT PPCP Capacities

Possible New ALDOT Standard Capacities		
Pile Size	Factored Axial Capacity	
	kips	tons
14-inch Pile	468	234
16-inch Pile	631	315
18-inch Pile	783	391
20-inch Pile	989	494
24-inch V. Pile	1200	600
30-inch V. Pile	1702	851
36-inch V. Pile	2214	1107

Table 5-4: Comparing ALDOT Possible Values with Current Values and Other DOTs

Possible New ALDOT Standard Capacities				
Pile Size	Alabama		Florida	Georgia
	Current	Possible		
14-inch Pile	180	468	550	473
16-inch Pile	240	631	N/A	636
18-inch Pile	300	783	900	820
20-inch Pile	360	989	1100	1006
24-inch V. Pile	440	1200	1575	1158
30-inch V. Pile	620	1702	1800	1706
36-inch V. Pile	820	2214	N/A	2224

5.2.8. M-P Diagram for 14-inch ALDOT PPCP

This diagram found in Figure 5-1 was created using values calculated in Moment-Axial Interaction Diagram Generator (v9.3) for a standard ALDOT 14-inch PPCP.

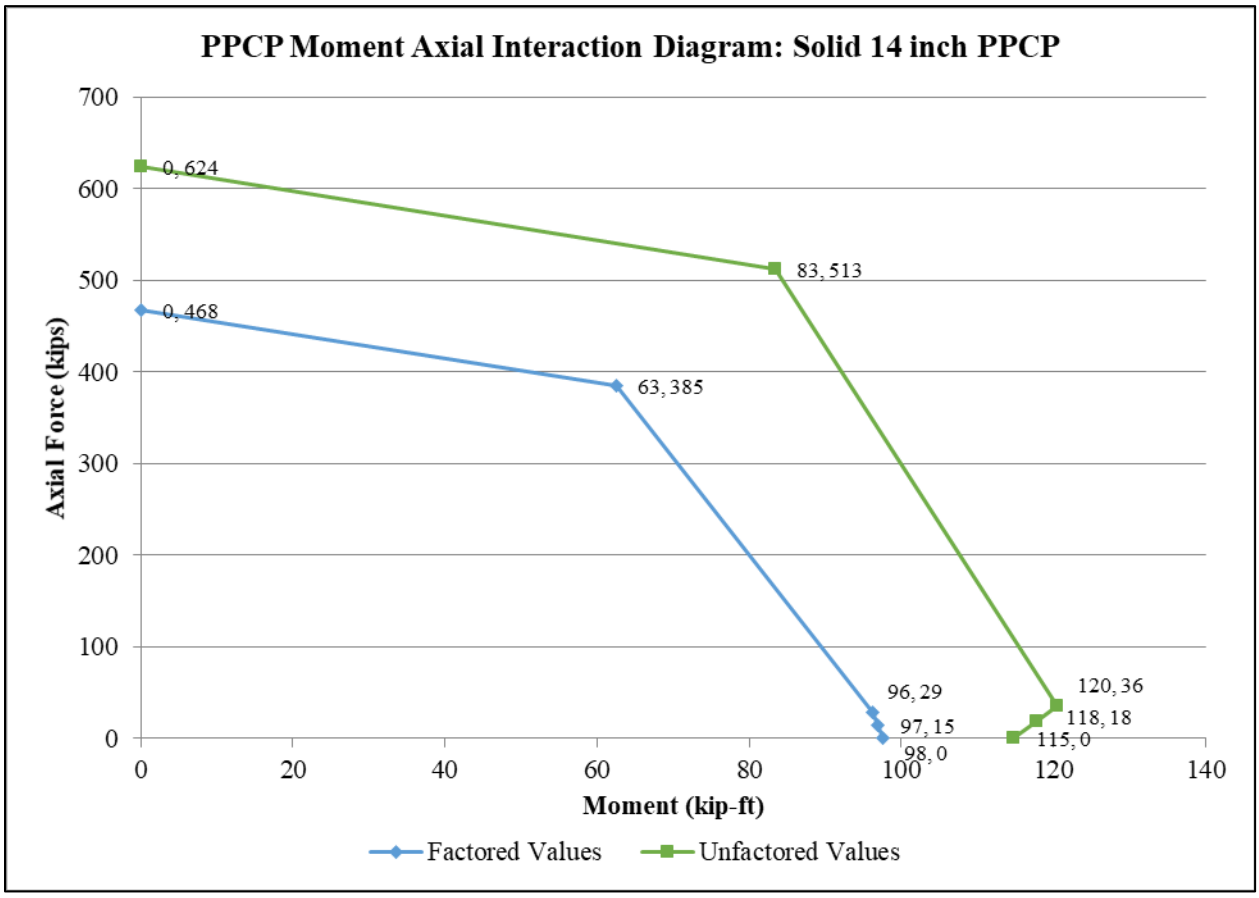

Figure 5-1: Sample ALDOT M-P Diagram for 14 in. PPCP

5.2.9. Comparison with available PCI Software

PCI has developed a program to similarly generate M-P diagrams for PPCPs. It is titled "PCI Prestressed Concrete Pile Interaction Diagram Spreadsheet" and version 1.2.15 was utilized in the following comparison (PCI 2015). The inputs for the PCI workbook are approximately equal to the inputs used in the Moment-Axial Diagram Generator. Using the PCI program, we can plot our A-E points for the same cross section. As is shown below, significant correlation can be seen between our generated diagram points and PCI's. The most prominent difference is that our pure compression point already includes a reduction that theirs only incorporates with the "Maximum Axial Load" line. This simplification should be conservative as our line from Point A to Point B would still fall within their threshold curve. Comparatively, if we used the pure axial compression value for Point A and drew a straight line to Point B, we would see that line would at least partially fall outside the PCI curve. Thus, we have decided to utilize the already reduced pure compression value for Point A in our diagrams. This comparison and substantial correlation with industry-accepted software validates the use of our program for our desired purpose.

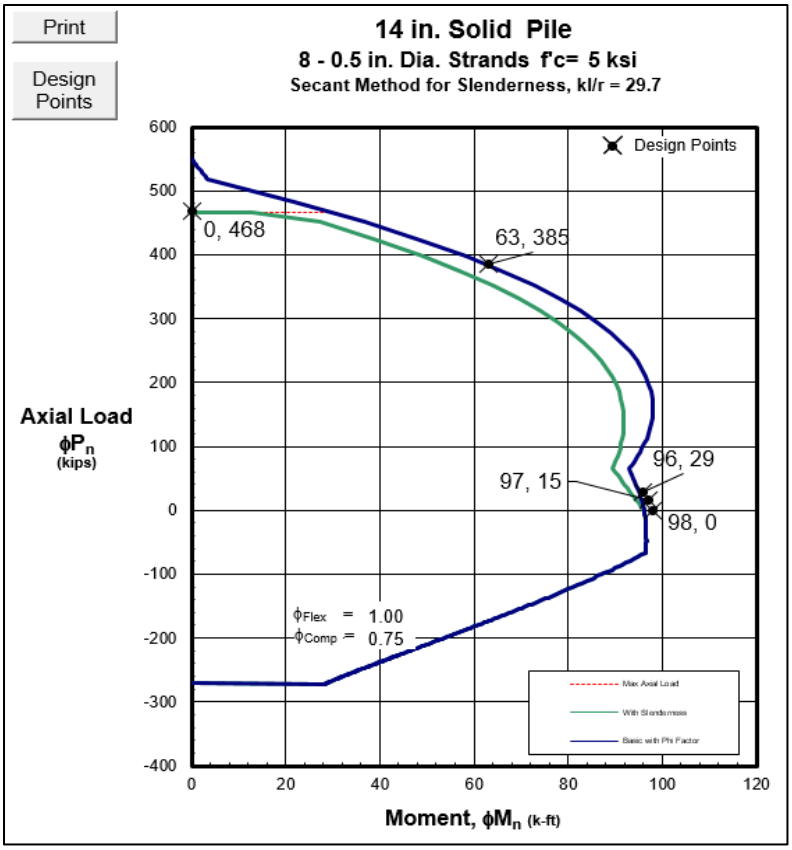

Figure 5-2: PCI M-P Diagram for 14 in. PPCP

5.2.10. ALDOT Interaction Diagrams with Listed Standard Capacities

After determining the five plotting points for each of ALDOT's standard PPCPs, each pile's interaction diagram was plotted on the same chart so that they can easily be compared. This is provided in Figure 5-3 below. Additionally, a tabulated account of each ALDOT PPCP's generated five plotting points is provided in Table 5-5. In addition to these values, the current ALDOT standard capacities have been plotted on this diagram for easy comparison.

Table 5-5: Considered Points for Moment-Axial Interaction Diagrams

Point	Factored Values For M-P Diagrams (Generator v9.3) (P in kips, M in kip-ft)													
	14 in.		16 in.		18 in.		20 in.		24 in.		30 in.		36 in.	
	P	M	P	M	P	M	P	M	P	M	P	M	P	M
A	468	0	631	0	783	0	989	0	1200	0	1702	0	2214	0
B	385	63	539	93	654	136	849	185	965	321	1329	623	1645	1076
C	29	96	109	145	112	216	214	295	330	506	567	939	746	1557
D	15	97	60	149	60	221	121	306	195	547	352	1044	464	1756
E	0	98	0	150	0	224	0	291	0	485	0	813	0	1385

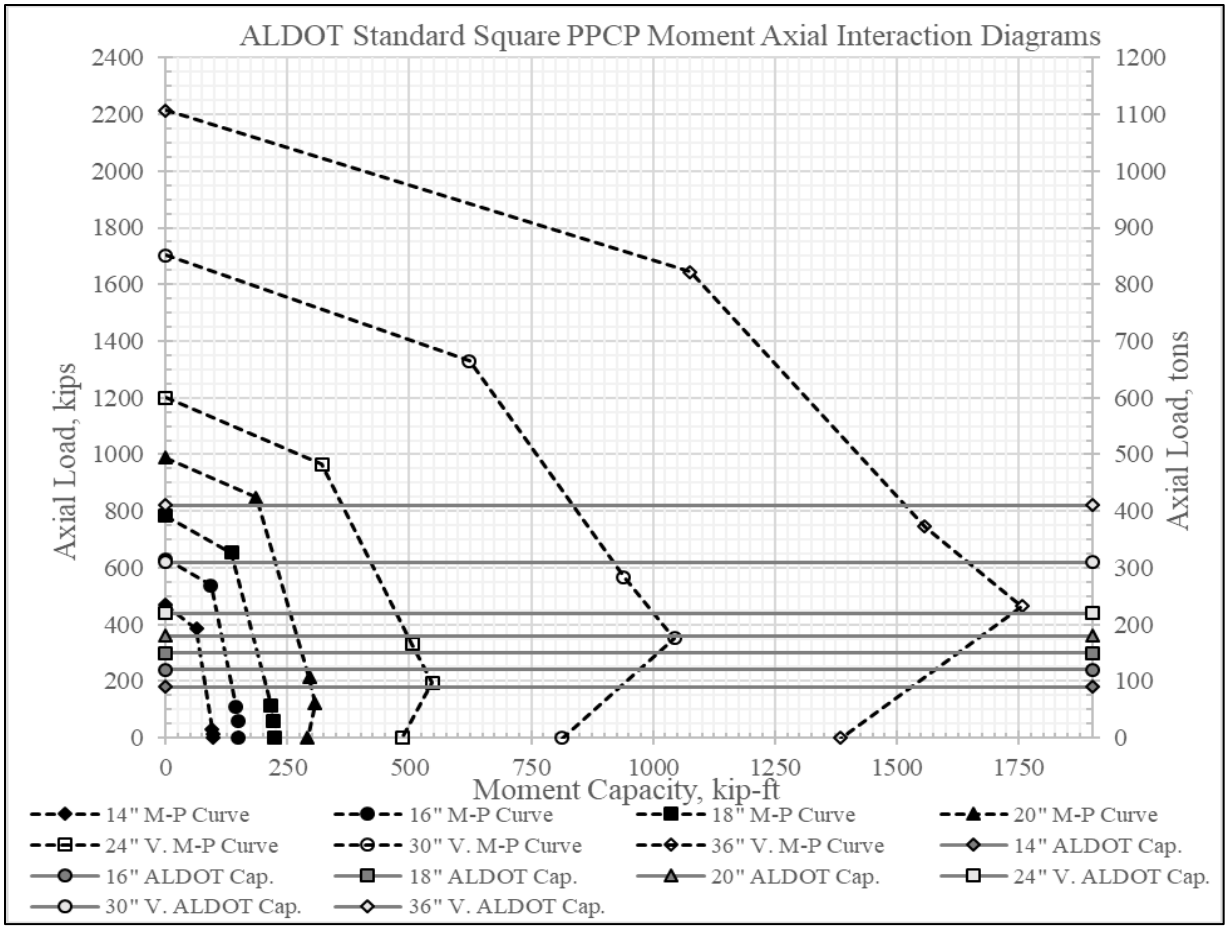

Figure 5-3: Moment-Axial Interaction Diagram for All Considered ALDOT PPCPs

6. Examining Pile Demands

While the primary consideration for this research relates to the capacity of ALDOT's PPCPs, this Chapter focuses on expected demands on typical bridges that utilize PPCPs as foundation elements. To make any recommendations regarding design capacities that one can use, it is certainly worth considering the moment demands on these piles that could reasonably be expected in typical bridges. Within this section, brief discussion of current AASHTO LRFD bridge loading (HL-93) is presented, as well as particular analysis based on three different prototype bridges which utilize pile bents for their substructure. While the axial loading of piles would be similar if a bridge was supported by a pile bent, or if the piles supported a hammerhead or similar style pier instead, the moments experienced by the piles would likely be substantially different. Pile bents would have piles which are directly exposed to lateral loading and extend significantly beyond the lateral support supplied by their embedment in the ground. These are the focus of our prototype bridge analysis.

6.1. Introduction to Bridge Loading

Bridges undergo a variety of loads that must be considered in the design of their foundations. These loads can be broken into permanent loads, transient loads, and extreme loads. Permanent loads include the dead loads of the bridge structure itself, such as the weight of the deck, traffic barriers, and girders, in addition to geotechnical pressures and internal forces in the structure such as creep, post-tensioning, and shrinkage. Transient loads meanwhile include those imparted by passing cars, trucks, and pedestrians in addition to wind and water pressures. Extreme events include earthquakes and impact loading from blasts, ice, vehicles, and vessels.

Designers rely on local and national specifications to estimate these loads. AASHTO's LRFD Bridge Design Specifications (AASHTO 2017) walk users through these load types and give state DOTs the opportunity to supplement these requirements. For the analysis conducted as part of this study, some load conditions are not considered. Of primary concern are the structural dead loads and vehicular, wind, and water live loads. Each of these will be discussed further in sections below during load path elaboration. For ALDOT bridges, the SDM states that AASHTO LRFD's loading parameters shall be followed unless specified otherwise. Notably ALDOT's SDM specifies the addition of a dead load for metal stay-in-place forms with 15 psf to include both the forms and the concrete within. For vessel and scour loading, ALDOT "has no additional considerations beyond those covered in the AASHTO LRFD Bridge Design Specifications". However, these loading types are case specific and are not considered for generalized or typical bridges. Thus, extreme event loading was removed from consideration for this analysis. For the purpose of this analysis, scour is also not being considered. The goal of this portion of the research conducted is to get a general understanding of the order of magnitude of loads that would be experienced, and not for the design of special cases.

6.2. Loads and Load Path

The following discussion serves to explain the loads considered for this particular analysis for pile bents for a straight, non-skew, deck and girder style bridge with multiple spans crossing a waterway. The loads this design bridge experiences include permanent and transient loads. For our particular analysis, three different prototype bridges were examined. Each had a span length of fifty feet and had two, four, or six total lanes of travel. Throughout the general discussion of the loads and load path, particular mention of how these loads were applied to the prototype bridges will be addressed.

6.2.1. Permanent Loads

To determine the dead loads resulting from the bridge's superstructure, first the elements' geometry must be specified. From the top of the superstructure, working our way down, we will consider the parapet barriers, the deck, stay-in-place formwork, and the girders. On each side of the roadway, there is assumed to be one barrier wall. For analysis purposes, this barrier's cross section is approximated as a trapezoid, with adjustable height and base dimensions. ALDOT's standard barrier is found on their standard detail drawing I-131 (ALDOT 2015). Thus, a barrier height of 2 ft.-8in., a base width of 1ft.-4 ½ in., and a top width of 6 in. are assumed. These estimations are used to provide an approximation of the barrier's cross-sectional area. For analysis purposes, ALDOT's SDM allows the barrier loads to be taken as distributed evenly across the girders (ALDOT 2017b).

In addition to these parapets, sidewalks can be included in the analysis. Their curb height and width can be altered to suit the design bridge. Additionally, the number of sidewalks can be determined by the designer. The depth of the sidewalk is multiplied by its width, to get the cross-sectional area of each sidewalk. For the prototype bridges, no true sidewalks were incorporated, however a gutter was effectively added by including a "sidewalk" on each side of the road with zero thickness. This allowed for the width of the gutter to be accounted for in the deck width without adding concrete area for a raised sidewalk.

Moving downward through the superstructure, typical deck thickness for ALDOT projects is found in their SDM Figure 9-1 and then the deck width is determined. This is based on the number of design lanes, times the design lane width (typically 12 feet), plus the width of any sidewalks (or gutters), and the base of both barriers. This width is then multiplied by the deck thickness to get the cross-sectional area of the deck. For the prototype bridges, a conservative deck thickness of 10 inches was assumed, as was a 12-foot design lane width.

To determine the line loads created by the barriers, sidewalks, and the bridge deck, the cross-sectional area of each element is determined, as described above, and that is then multiplied by the concrete density, which for these purposes is assumed to be 150 pcf.

Additionally, stay-in-place metal formwork is specified for consideration by ALDOT. This load of 15 psf is considered to act for the entire length and width of the deck. Similarly, any additional wearing surface load is calculated based on the cross-sectional area (anticipated thickness of surface, including resurfacing, times the total width of the design lanes) being multiplied by a density of 140 pcf for the bituminous layers (AASHTO 2017 SDM, Table 3.5.1-1). For the prototype bridges, the metal formwork was incorporated with the dead loads, as was an assumed 3-inch thick wearing surface in each design lane.

The loads produced by the barriers, sidewalks, deck, stay-in-place formwork, and wearing surface are all considered vertical gravity loads which transfer to and are distributed across the bridge girders. As we are most interested in the reactions at the support points for the girders, and are not designing the deck or girders themselves, more refined analysis is not warranted. It is worth noting that despite the similar load path, the wearing surface loads have a different load factor than other structural components, so they must be treated separately when factoring the loads.

For the girders, ALDOT's SDM permits the use of the following AASHTO-PCI standardized girder cross-sections: Type I, Type II, BT-54, BT-63, and BT-72 (ALDOT 2017b). These are the girder types currently allowed in the analysis program. These standard designs have standard cross-sectional areas that were incorporated into the analysis program (PCI 2011, Appendix B-7). Similar to the other

concrete structural elements, the area of the girder is then multiplied by the density of the concrete to determine the weight of each girder. For the prototype bridges, based on their span length being 50 feet and the information available in ALDOT's standard drawings, Type II girders were assumed. Additionally, for this analysis, the center-to-center spacing of these girders was assumed to be six feet. To simplify the analysis, within the pile bent, a pile was assumed to act under the centerline of each girder.

When the bridge is considered dead load discontinuous, the girders are considered simply supported on each end of the span. At each end of the girder, the bent or pier cap must support half of the girder weight, in addition to its even share of the barrier, sidewalk, deck, formwork, and wearing surface load, divided by two (as that load is also distributed to each end for the supports). One must keep in mind that each support under consideration is supporting loads from the span on either side, so these girders point loads from each span at a support location must be combined. As the span lengths could vary on each side of the support, the analysis code is written to allow for varying lengths of the span in determining these reactions, however for the prototype bridges, even 50-foot spans are assumed on each side of the analyzed support.

These girder point loads are then transmitted directly through the bearings to the pier or pile bent cap. This cap, as well as the pier shaft or exposed piles that form the bent, produce additional structural dead load. The developed program was designed to estimate the external loading of the bent system, and thus the self-weight of the piles is not currently incorporated. For the estimated load on the piles within the bent though, a bent cap self-weight was estimated based on ALDOT's standard drawing PCA-2840-CP and the factored and separately applied to the bent as a line load acting transverse to the roadway (ALDOT 2015).

6.2.2. Transient Loads

The transient loads require analysis that is more complicated and follow more complicated load path than the permanent gravitational loads. The major categories of transient loads are those imparted by bridge users (standard vehicles, trucks, tandems, braking forces, pedestrians) and those imparted by the environment (through wind and water).

6.2.2.1. Loads Imparted by Bridge Users

The primary function of a bridge is to aid in the transportation of people and goods from one point to another. As vehicles and pedestrians traverse the bridge to accomplish this goal, they impart the vehicular live loading of the bridge.

6.2.2.1.1. Lane Live Load – Article 3.6.1.2.4 of AASHTO LFRD

The loading suggested by AASHTO LRFD to model these vehicles is a combination of a design lane load, as well as a design vehicle load, with this combined vehicle loading being known as HL-93 (AASHTO 2017, 3.6.1.2.1). In the absence of additional, site specific lane load conditions, the recommended design lane load is 0.64 klf across the longitudinal length of the bridge, and transversely, taken as being distributed over a 10.0 foot portion of the design lane (AASHTO 2017, 3.6.1.2.4). For the prototype bridges, the total equivalent lane load from each lane within the tributary area of the support (half the span lengths in either direction) was determined. This was divided by 10 and applied as a distributed load across 10.0 feet of each lane of the bent.

6.2.2.1.2. Design Vehicle Load – Article 3.6.1.2 of AASHTO LRFD

To account for larger vehicles, a design truck and a design tandem are also considered in the vehicular live loading of the bridge. The truck is idealized as an 8-kip front axle, followed 14 feet later by a 32.0 kip second axle. A third axle supporting 32.0 kips is spaced between 14 and 30 feet behind the second one. This spacing between the second and third axles is typically varied to produce maximum force effects on the bridge. Transversely, the wheels of the truck are spaced 6 feet apart (AASHTO 2017, 3.6.1.2.2). The tandem is a simpler vehicle, with only two axles, spaced 4 feet apart and each supporting 25.0 kips. As with the truck load, transversely, the centers of the wheels are spaced 6 feet apart (AASHTO 2017, 3.6.1.2.3).

6.2.2.1.3. Vehicular Live Load Assumptions

For the lane live load and the design vehicle loading, some simplifications were made with regards to their placement on the prototype bridge. The 10.0-foot lane live load started 1.0 foot from the left most edge of the design lanes and then was reasonably spaced across the other lanes as well. Between the truck and the tandem, the truck supplies a greater gravity load, and thus it was the vehicle we used. We assumed that the worst-case scenario for truck loading would be when the centroid of the axle loads passes over the support, and thus we applied the total truck load to the support over two point loads, representative of its left and right tires. This was applied to each design lane. Additional analysis varying the precise transverse location of the lane live load start and stop locations, or the truck axle load points were not considered for the given prototype bridge. This depth of analysis was not warranted for the level of detail that was desired, thereby justifying these simplifications.

When considering these loads together, generally each lane is loaded with the design lane load, as well as a design truck or tandem. When investigating negative moment zones and reactions at interior supports, then 90 percent of two design trucks are typically considered to act on either side of the support, with at least 50.0 feet between the lead axle of one truck and the rear axle of the other. This load is to be combined with 90 percent of the design lane load (AASHTO 2017, 3.6.1.3.1). While this is typical for AASHTO bridge analysis, this surpasses the general load approximation that was needed for this research, and so it was not considered.

6.2.2.1.4. Pedestrian Loading – Article 3.6.1.6 AASHTO LRFD

While not adding "vehicular" load, pedestrian load must also be considered in live loads, and can be considered an active "lane" of traffic. Foot traffic loading is given in Section 3.6.1.6 of AASHTO LRFD as a pressure of 0.075 ksf for all sidewalks on the bridge greater than two feet in width. For the purpose of the following discussion on moment magnification factors, pedestrian live load in a sidewalk is considered a "loaded lane" (AASHTO 2017, C3.6.1.1.2). As the prototype bridges have no sidewalks, pedestrian loading was not considered.

6.2.2.1.5. Multiple Presence and Dynamic Allowance Factors – Articles 3.6.1 & 3.6.2 AASHTO LRFD

To account for the likelihood of a given number of lanes being loaded, in Section 3.6.1.1.2, AASHTO LRFD suggests several multiple presence factors that can be applied to the vehicular and pedestrian live loads. Table 3.6.1.1.2-1 provides these values (AASHTO 2017). When considering only one lane

to be loaded, the vehicular load of that lane is increased by a factor of 1.2. Comparatively, when considering three or more lanes to be loaded, the load can be reduced by a factor of 0.65. Diminishing the loads due the reduced likelihood of multiple lanes being loaded is an optional step, while increasing the load for a single lane is mandatory. As we are looking to conservatively estimate the loading on a support system, we will not be reducing loads by the multiple presence factor. However, when we consider braking force (to be discussed later), we are only assuming one lane of the two-lane prototype bridge is being loaded (with vehicles that are braking), and so we do implement the multiple presence factor of 1.2 for the braking force.

Another modification for vehicular loads comes in the form of the dynamic load allowance. To account for the dynamic nature of the moving truck and tandem, the gravity loads of these design vehicles are increased by 33 percent for most limit states for the consideration of all bridge components aside from deck joints. For our consideration, it is noteworthy that AASHTO LRFD specifies that the dynamic load allowance does not need to be applied for "foundation components that are entirely below ground," due to the assumed dampening effects of the soil (AASHTO 2017, 3.6.2.1, and C3.6.2.1). However, this effect is still applied for the prototype bridges, as the foundations are not entirely below ground.

6.2.2.1.6. Braking Force – Article 3.6.4 AASHTO LRFD

In addition to their vertical gravity loads, braking force loads are also considered for the vehicles traversing the bridge. Braking force is taken to act along the travel direction of the roadway, and 6 feet above it. It is applied in each of the perceived maximum number of lanes in the roadway that would be travelling the same direction, and for the prototype bridges, this means one-half of the design lanes. The magnitude of this force is taken as the larger of a) 25 percent of the axle weights of the design truck or tandem, or b) 5 percent of the design truck or tandem plus the lane load. It is up to the analyst to determine which case governs and appropriately apply it to the relevant lanes, including the multiple presence factor on this load as well.

The braking force produces an in-plane moment, which is then resisted by a force couple supplied by the supports (FDOT 2011). The moment arm is defined as the height of the girders, deck, and wearing surface, plus six feet to the theoretical location of the force. Taking the moment about one of the spans' supports results in a vertical reaction in the opposite support equal to: the braking force times the moment arm, divided by the span length between the two supports. To satisfy vertical force equilibrium, the opposite support would be generating a vertical force as a result of the braking force, but that is ignored for this analysis.

To satisfy force equilibrium in the longitudinal direction of the bridge, each support is assumed to resist one-half of the horizontal breaking force as a shear load transmitted through the bearing pads of the bridge. More detailed analysis of the bearing pads could be conducted to examine load transmission, but for this simplified consideration, full transmission of the longitudinal load is considered to occur at the top of the bent.

For the 2-lane bridge under consideration, the multiple presence factor is applied to the braking forces, as we would be considering only one lane loaded, and for that, the multiple presence factor is not optional, but mandatory. Comparatively, for the four and six lane bridges, the multiple presence factor is not used to reduce the assumed braking force as at least two lanes are loaded in the braking scenario.

6.2.2.1.7. Other Superstructure Loading

Other horizontal vehicular forces, such as loads on railings, vehicular collisions, and centrifugal forces are not currently considered in the prototype analysis. The gravity and vehicular and loads are transmitted through the deck, to the girders, and eventually to the bent cap.

6.2.2.2. *Loads Imparted by the Environment*

AASHTO LRFD includes discussion on both wind and water loads experienced by a bridge as a result of its environment. Each of these categories has a variety of possible loading conditions, only some of which are included in this analysis.

6.2.2.2.1. Wind Load on Live Load – Article 3.8.1.3 AASHTO LRFD

Starting from the top and working our way down, first we have wind load acting on the live load. Essentially this force is specified by AASHTO LRFD as 0.10-klf acting for the full length of the roadway, six feet above its surface, transverse to the travel direction. This approximates the load seen from wind pressure acting on a hypothetical line of mixed vehicles traversing the roadway. Depending on the wind direction, transverse and longitudinal components can be separated and applied simultaneously to the bridge. For the prototype bridges, wind was only assumed to be acting transverse to the roadway. The live load force was assumed to be transmitted from the vehicles to the roadway, to the girder, and through the bearing pad to the pile bent. For simplified analysis, the equivalent force from the tributary area of the support was applied to the windward edge of the pile bent in the transverse direction to the roadway.

6.2.2.2.2. Wind Load on Superstructure Transmitted to Substructure – Article 3.8.1.2.3a AASHTO LRFD

Next, we have the wind load on the superstructure. As we are most interested in the wind load on the superstructure that is transmitted to the substructure, AASHTO LRFD Section 3.8.1.2.3 is of particular interest. It specifies that the wind pressure, times a skew coefficient (based on the wind's angle of attack, found in Table 3.8.1.2.3a-1), times the depth of the bridge produces the load from the superstructure which is transmitted to the substructure.

Wind pressure (P_z) can be calculated based on AASHTO LRFD's equation 3.8.1.2.1-1:

$$P_z(in\ ksf)=2.56*10^{-6}*V^2*K_z*G*C_D \qquad \textbf{Eq. 6-1}$$

The wind velocity (V, in mph) is taken as the 3-second design gust speed, which can be approximated using AASHTO's wind maps for the United States for the Strength III load combination. For other combinations, Table 3.8.1.1.2-1 provides the appropriate wind speed to use. Strength V is the primary wind load combination considered for the prototype bridges, and its assumed velocity is 80 mph. The pressure exposure and elevation coefficient (K_z) is calculated based on the anticipated structure height (but not less than 33.0 feet) and the level of obstructions in the surrounding area that would serve to break up the wind pressure. For all combinations except Strength III and Service IV, this is taken as 1.0. For these two specific combinations, AASHTO Equations 3.8.1.2.1- (2, 3, or 4) are used based on the estimated wind exposure category. The gust coefficient, (*G*), can be taken as 1.0 for most

load combinations, with the exception of Strength III and Service IV, where Table 3.8.1.2.1-1 is to be used instead. From this table, for all structures aside from sound barriers, *G* is to be taken s 1.0. The drag coefficient, (C_D), can either be determined from a structure specific study, or be found in Table 3.8.1.2.1-2 (AASHTO 2017). For superstructures, the windward coefficient is to be taken as 1.3, while for substructures, this value should be 1.6. Utilizing each of these variables, the wind pressure can be calculated and then applied to the superstructure at its mid-depth, and as though acting along the longitudinal axis of the roadway. For our simplified model of the prototype bridge, this load is instead transmitted as a point load at the windward most point of the pile bent.

6.2.2.2.3. Wind Load on Substructure – Article 3.8.1.2.3b AASHTO LRFD

Moving on down, we have the wind loading on the substructure. The substructure's wind pressure is calculated using the same formula as the superstructure's (AASHTO 2017, 3.8.1.2.3b). The height of the structure used in the K_z equation for the substructure wind pressure can be the same value used in approximating the superstructure's wind pressure (AASHTO 2017, 3.8.1.2.1). The height used in this equation should never be taken as less than 33.0 feet due to turbulence effects below that point (AASHTO 2017, C3.8.1.2.1). This consideration was built into the load analysis program to assume a height of 33.0 feet if the specified height is less than this amount. Similar to superstructure wind loads, these loads should be broken into transverse and longitudinal components if the winds angle of attack is skewed. These pressures are taken to act on the exposed area of the substructure and should be analyzed as such (AASHTO 2017, 3.8.1.2.3.b). For the prototype bridges, this load was applied as a distributed load on the exposed length of each pile in the bent. For the wind load acting on the pile bent cap, this load is taken as a point load on the windward most joint of the bent.

6.2.2.2.4. Vertical Wind Load – Article 3.8.2 AASHTO LRFD

Interestingly, in addition to these horizontal wind forces, the bridge should also be considered to have a vertical wind load that may cause overturning effects for Strength III and Service IV load combinations. These loads are 0.020 ksf and 0.010 ksf respectively, acting for the full width of the deck, and applied at the windward quarter-point of the deck (AASHTO 2017). For this analysis, vertical wind load is not considered, as it would be acting against the prevailing gravity loads, thereby decreasing the axial loads.

6.2.2.2.5. Water Loads – Article 3.7 AASHTO LRFD

In addition to wind pressures, AASHTO loads suggest the consideration of water loads for static pressure, buoyancy, stream pressure, and wave loads. For the prototype bridges assumed to be crossing a body of water, buoyancy is not considered due to the geometry of the bridge components. Rather than static pressure, stream pressure is considered, as that would likely produce a greater force with the limited depth of water assumed. For the prototype bridges, the body of water was assumed to be five feet deep, and the stream pressure was calculated as 0.0063 k/sf. This water pressure was converted to a point load and applied at the mid-stream height on each pile in the bent.

6.2.2.3. Extreme Loads

AASHTO provides provisions for extreme event loading including earthquakes, ice collision, check flooding, and vessel or vehicle collision. Originally, vessel collision was considered within the analysis for the prototype bridges. This loading was calculated based on the minimum vessel impact for substructure design, which is an empty hopper barge. The input parameters were estimated based on available information. This information was not fully pursued as these loading conditions will be a special case and not expected for routine bridges.

6.3. Limit States and Load Combinations

LRFD analysis involves the consideration of various limit states emphasizing different theoretical load conditions. Those named in AASHTO's LRFD Bridge Design Specifications are categorized into four groups: Strength, Extreme Events, Service, and Fatigue.

The five strength load cases include the nominal dead load of the structure amplified by various factors. Strength I, II, and V also include live load of the bridge. Water and stream loads are considered in all strength cases, but wind load on the structure is only considered for III and V, while wind load on live load is only considered in V. For our analysis of the prototype bridges, Strength I and V were selected as the load cases for our analysis based on their emphasis of dead, live, and wind loading. Strength III would likely result in greater wind loading, but it completely discounted live loading, so it is not included at this time.

Extreme event loading focuses on events outside of the typical daily loading of the bridge. Extreme Event- I load pertains to the incorporation of seismic loading, while Extreme Event II includes provisions for blast loading, ice collision, vehicular collision, or vessel collision. These atypical incidents are each to be considered separately as applicable or at the discretion of the owner. The extreme event loading was excluded from the prototype bridge analysis, as these load cases will be very specific to a bridge.

Service limit states pertain to the behavior of the bridge elements rather than strictly their ability to safely support the factored expected loads. For these four combinations, permanent loads are all taken to be their nominal values. Live loading is incorporated for all but Service IV, but their load factors for I, II, and III are 1.0, 1.3, and 0.8 respectively. Water load is considered for all service limit states, but wind load varies in its application. These limit states are applied to investigate deflection (I), yielding and slippage of connections for steel elements (II), crack control analysis of prestressed girders (III), and tension crack control in prestressed columns (IV). Our analysis of the prototype bridges is currently only concerned with the anticipated structural loading of the bent, so service loading is not currently considered.

The two fatigue limit states relate to a bridge's load induced fatigue life, over either an infinite or a finite timeframe. The load factors associated with these combinations are equal to or smaller than the already selected strength limit states, and long term or cyclic loading is not a primary consideration for this analysis. Therefore, the fatigue limit states are not included in the prototype bridge analysis.

Based on the load factors implemented for each limit state, the limit states of Strength I, Strength V, and Extreme Event II were initially selected for the generalized analysis for the prototype bridges. Extreme Event II has since been dropped from primary comparisons due to limited available information.

6.4. Design Bridge Parameters

Aside from the design parameters previously discussed, a few more assumptions were made in the development of the prototype bridges. Of the most relevant are the load continuity of the girders and the depth to fixity for the piles. ALDOT's structural design manual provides notice that girders are to be designed as being simply supported between supports for both dead and live load considerations. Thus, girders were assumed to be simply supported at each bent cap for the prototype analysis. We consistently considered the pile bases fixed at a certain depth, based on the depth to fixity equation given in AASHTO LRFD's commentary and originally based on Davisson and Robinson's work (AASHTO 2017, C10.7.3.13.4-2). Medium submerged sand was assumed, which resulted in an estimated depth to fixity of about 10 feet for 20-inch piles. This depth to fixity was therefore assumed for all of the prototype bridges.

6.5. Application of Load Combinations and Model Analysis

Once the relevant loads were determined and factored as described in the preceding sections, the prototype bridges were modeled and analyzed for each considered load case.

6.5.1. Model Analysis

Of the software available for simplified analysis of prototype bridge bents, a combination of Microsoft's Excel and RISA-2D were utilized. The process for creating the models and then applying the considered loads is described in the following paragraphs. The standard two-lane prototype bridge model is shown below in Figure 6-1.

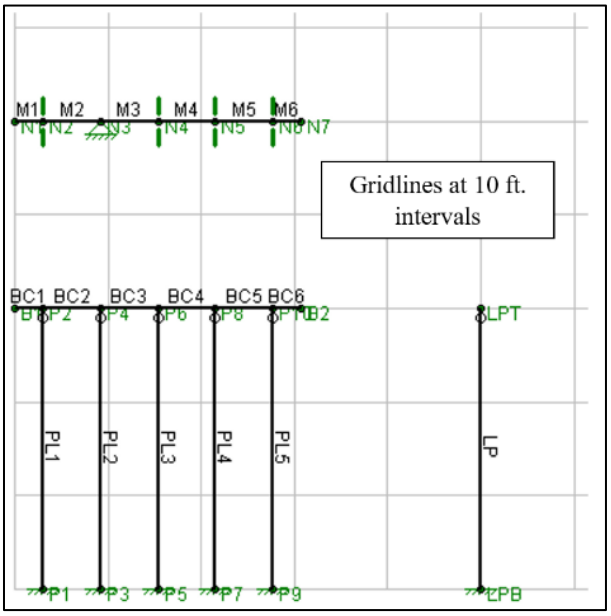

Figure 6-1: RISA Model for Simplified Two-Lane Prototype Bridge

6.5.1.1. Creating RISA Simplified Prototype Bridge Models

To analyze a simplified pile bent, three separate model components were created for each bridge model. The first is a continuous indeterminate beam representing the superstructure of the bridge, supported vertically at each girder location, (with one support being a pin for stability purposes), with each end of the beam extending representing the deck overhang area. Girders were spaced at

approximately 6 feet on center, with the edge overhangs being equal to one-half of the spacing between girders. The properties of the members were not a concern for the analysis of this part of the model as long as they were equal across each included member for distribution purposes. Figure 6-1 shows the standard simplified deck and girder model for the two-lane bridge.

Next, the pile bent was developed for the bridge. The two-lane bridge model bent can be seen in Figure 6-1. The bent cap of the bridge was assumed to be the same width as the deck, and as the piles and girders are set to line up, the bent cap members (BC1 – BC6) mirror those of the deck and girder model. For these prototype bridge models, the pile members (PL1 – PL5 in Figure 6-1) are 30 feet long. This assumes of the piles extending 20 feet above the ground and having 10 feet of embedment until they reach a point of fixity. The fixity is represented at the lower nodes of the pile members (joints P1, P3, P5, P7, P9) with a small horizontal line and hash marks. When the connection between the pile and the bent is considered a pin (allowing rotation at the joint), a small circle appears below the joint (P2, P4, P6, P8, P10). This is the case in Figure 6-1. When fixity is assumed, this circle is not present.

Unlike the deck and girder model, the substructure member properties are of greater concern for force and moment distribution. For these members, their geometric and material properties were calculated based on reasonable estimates from available ALDOT information. For these members, (the piles and their bent cap), their gross moment of inertia was reduced by a factor to account for some cracking during loading. This provision was incorporated from ACI 318-14, Table 6.6.3.1.1(a), and resulted in a decrease in the columns' gross moment of inertia by a factor of 0.7, and the bent cap beam's moment of inertia being reduced by a factor of 0.35. These provisions were determined based on traditional reinforced concrete, rather than prestressed members, but it is believed that these reductions were conservative and sufficient for our analysis.

The third component of the model is a representation of the bent consolidated as would be seen looking at the bridge spans in elevation view. This model is designed to be used to primarily consider horizontal loads acting along the longitudinal axis of the prototype bridge in addition to gravity loads. The single member, LP in Figure 6-1, was given an area and moment of inertia equivalent to the summation of those values for all of the piles in the bent. The base fixity is consistently assumed, and while the top is released in rotation, this has no effect on the analysis of the member.

Once these principles were applied to develop the two-lane bridge model, four- and six-lane models were created in a similar manner. The standard models for these two prototype bridges are presented in Figure 6-2 and Figure 6-3.

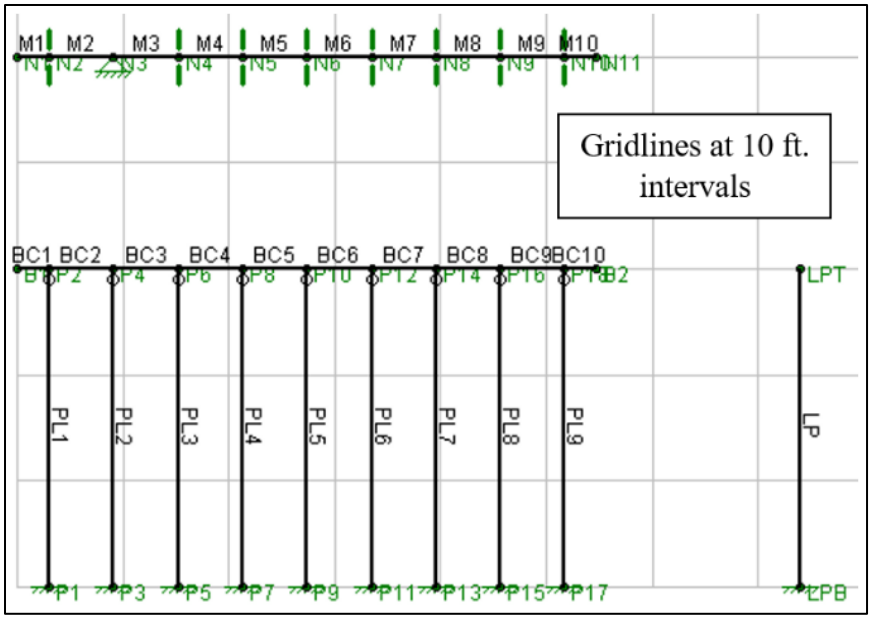

Figure 6-2: RISA Model for Simplified Four-Lane Prototype Bridge

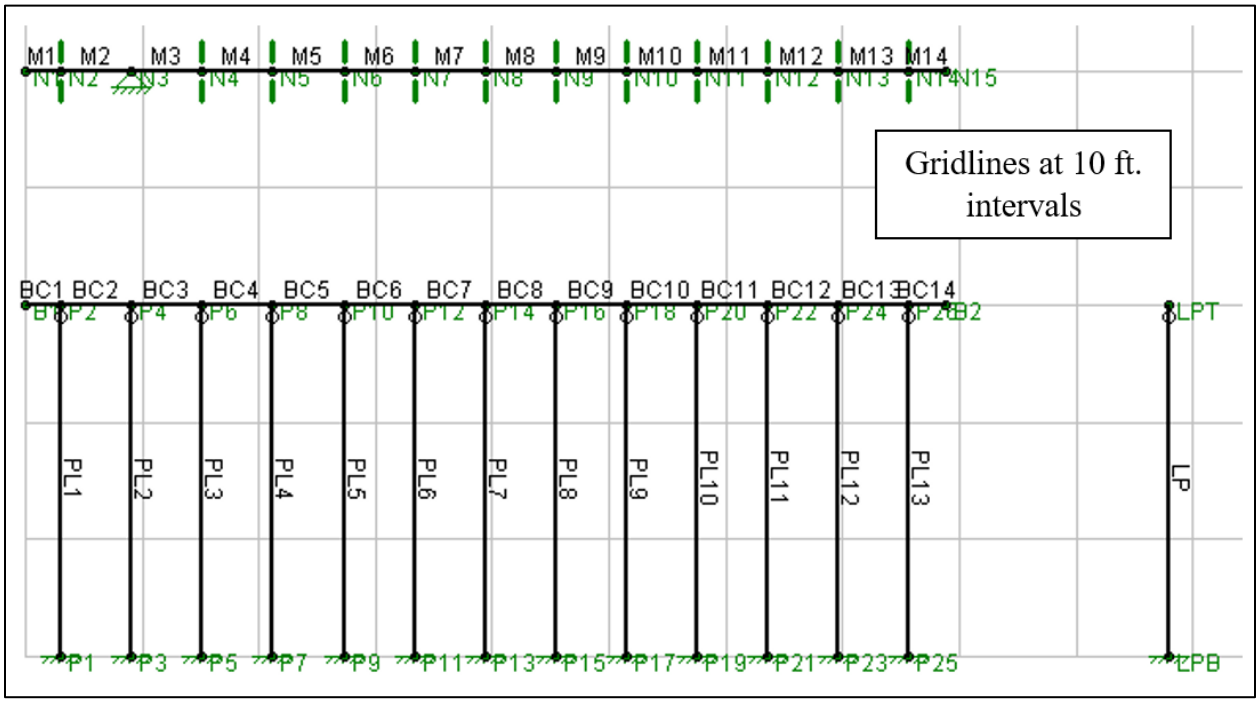

Figure 6-3: RISA Model for Simplified Six-Lane Prototype Bridge

After these standard models were created for each prototype bridge, the different load combinations were applied to the models for analysis.

6.5.1.2. Load Analysis with RISA Models

For each prototype bridge, the load combinations of Strength I and Strength V were applied in separated versions of each bridge's standard model. Similar procedures for applying the loads and then analyzing the bridges were applied for each case, and those procedures are summarized here.

RISA 2D allows for the application of three different types of loads that were used in this analysis: joint loads, point loads, and distributed loads. Therefore, in each loading case, the loads to be applied had to be categorized as one of these three types and their location of application determined. This input information was determined in spreadsheet (one for each bridge type) and then input to RISA for analysis. This methodology was developed to take advantage of being able to copy and paste load information into the RISA software.

To work through these spreadsheets, first the loads experienced by the bridge had to be determined (the methodology of which was discussed in previous sections). Then these factored loads were categorized for the superstructure model as joint loads, point loads or distributed loads. Each load case (Strength I and Strength V) did have a different combination of load factors which were incorporated in the load determination for the given case. While some analysis software has the capability to apply load factors within the model, that was not an option for our educational license of RISA-2D, so these different load cases were manually applied to different saved copies of each standard prototype bridge. Having different files for each load case of each prototype also enabled easy modifications to the members without having to change the load conditions from analysis to analysis, (for example changing the fixity condition or the pile dimensions).

The superstructure dead load (including barriers, sidewalks/gutters, deck material, stay-in-place formwork, wearing surface, and the girders self-weight) were applied as equal joint loads at the theoretical girder locations (the "N" nodes in Figure 6-1, Figure 6-2, and Figure 6-3). Additionally, half of the girder nodes received additional vertical loading from the braking force moment. To determine how much of the total braking force each of these girders would experience, the total braking force was divided by the total number of girders ("x"). The center girder then experienced 1/x of the force, and the remaining girders on that side of the bridge each experienced 2/x of the force. This resulted in a logical distribution of the full braking vertical force on half of the bridge.

The point and distributed loads involved more analysis to place within the model. The location of these loads is stated in relation to the member it is occurring on, as opposed to a global model coordinate system. For example, we could not say that the distributed lane live load starts 4 feet from the edge of the model component and extends for 10 feet, but rather that it starts 1.35 feet into member M2, proceeds to the end of that member, stops, and then continues 5.29 feet into M3. Each axle location and distributed lane load for the superstructure members were determined based on this system.

Once this information for the superstructure was tabulated, it could be copied into each of RISA's input locations for each of the respective loading types. With this information applied (load type, location, direction, and magnitude), we could solve for the reactions at each of the girder support points (N1 – N15 for the six-lane bridge for example). These reactions were then copied back to Excel as loads to apply to the joints of the pile bent portion of the model.

In addition to the reactions from the bridge girders (with the load direction having been flipped to represent a downward force), the pile bent experienced stream pressure, which was applied to each pile as an effective point load at mid-depth of the water feature, and a distributed load for the bent

cap's self-weight for Strength I analysis. Strength V analysis also incorporated horizontal joint loads for the wind load transmitted from the superstructure, the wind load on the bent cap, and the wind load on live load. A distributed wind load was also applied to each pile within the bent from the theoretical water height to the top of the pile for Strength V Analysis. Once these loads and locations were tabulated, they were carried back to RISA for analysis.

For each bent, this analysis was carried out twice per load case: once with the tops of the piles considered fixed in the pile bent, and then again with them considered pinned connections. This enables comparison with both fixity conditions and determination how moment and axial load distribution varied as a result.

In addition to the pile bent analysis previously described the analysis for the consolidated bent was carried out in a similar manner. Once the girder reactions were determined for the given load case, they were summed and applied to the LPT joint in each model. The weight of the pile bent cap was also applied to this joint. The only other load applied for this consolidated bent was the horizontal braking force also as a joint load at the top of the bent. The resulting reactions generated at the base of this bent (joint LPB) would be distributed across the piles in some manner, but the particulars of that analysis are beyond the current consideration of the analysis, namely due to the fact that analysis was carried out in two dimensions rather than three for the level of analysis we needed. The results of this analysis are discussed in the following passages.

6.6. Comparing Moment – Axial Capacities with Demands

Based on the analysis described above, we can see that under these loading applications, the pile capacity does not approach the demand. For particular consideration, observe the following moment-axial interaction diagram. This includes two, four, and six, lane bridges, with load combinations Strength I and Strength V in our analytical model. Key combinations from the structural analysis were selected and plotted based on which values provided the most extreme axial load, moment, or combination of the two which would bring the plotted point nearest to the previously determined threshold for moment and axial combined capacity. This information is summarized in Table 6-1 and Figure 6-4. The pile analysis name seen below is representative of the number of lanes in the analysis, then the load combination, and then the fixity assumed (fixed base – fixed top, or fixed base – pinned top).

Table 6-1: Bent Loading Combinations

Bent Loading Combinations			
Pile Demand Combinations		Axial, P	Moment, M
Pile Analysis Name		kips	kip-ft.
1	2-S1-FP	268	1
2	2-S1-FF	173	7
3	2-S5-FP	231	88
4	2-S5-FF	229	47
5	4-S1-FP	332	1
6	4-S1-FF	328	3
7	4-S1-FF	185	9
8	4-S5-FP	279	63
9	6-S1-FF	391	4
10	6-S5-FP	328	43

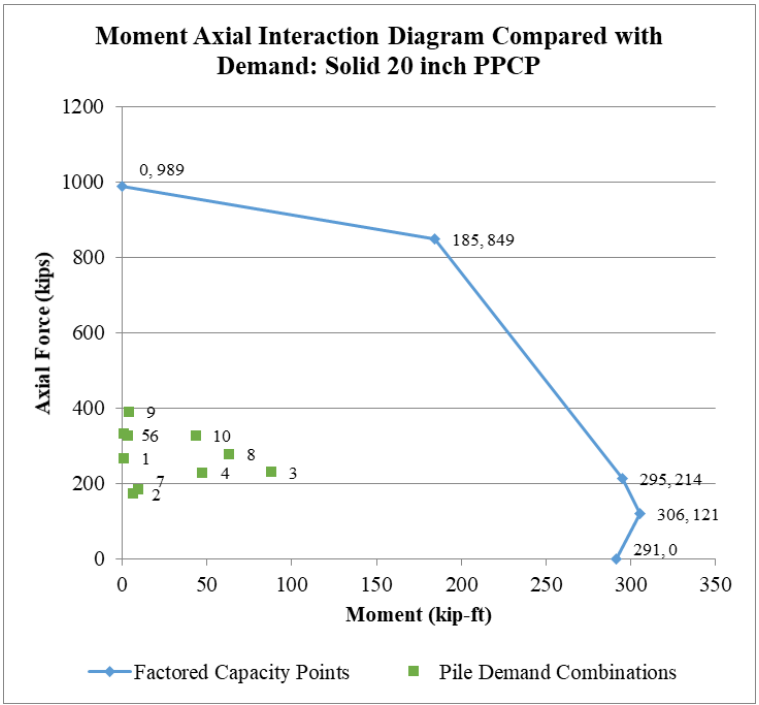

Figure 6-4: Comparing Demand with Capacity

6.7. Axial and Moment Distribution with Varying Pile Size

Beyond the 20-inch pile bent which was originally considered, we additionally examined what would happen in our model if we substituted smaller piles into the same loading scenario. The only changes were made to the piles' area and effective moment of inertia. The loads including the self-weight of the bent cap and wind and stream horizontal forces were not modified so that any observed changes in moment and axial distribution were a result of the pile properties and not due to decreasing loads (smaller surface area would mean smaller wind and water pressure, as well as likely a smaller bent cap). This comparison was carried out for each considered load case, number of lanes, and pile fixity condition. The comparison can be seen in its entirety in Appendix C, but an excerpt is provided in the following table as well. While 18- and 16- inch piles were also considered in the comparison, they are removed from the following table for brevity.

Table 6-2: Pile Reactions with Size Change

Comparing Pile Reactions for Two-Lane Bridge with Pile Size Change									
Two Lane - Strength I Case							Trend Moving Down in Pile Size		
Two Lane Bridge - Fixed Base, Pinned Top									
	20 in.			14 in.					
	X, k	Y, k	M, k-ft.	X, k	Y, k	M, k-ft.	X	Y	M
P1	-0.052	167.197	0.656	-0.052	170.773	0.656	=	+	=
P3	-0.052	264.759	0.656	-0.052	255.663	0.656	=	-	=
P5	-0.052	224.767	0.656	-0.052	235.885	0.656	=	+	=
P7	-0.052	267.607	0.656	-0.052	258.358	0.656	=	-	=
P9	-0.052	170.334	0.656	-0.052	173.987	0.656	=	+	=
LPB	-37.800	1094.700	1134.000	-37.800	1094.700	1134.000	=	=	=
Max Bent	0.052	267.607	0.656	0.052	258.358	0.656			
Two Lane Bridge - Fixed Base, Fixed Top									
	20 in.			14 in.					
	X, k	Y, k	M, k-ft.	X, k	Y, k	M, k-ft.	X	Y	M
P1	0.544	169.388	-5.423	0.229	171.748	-2.284	-	+	+
P3	0.006	262.591	-0.042	-0.003	254.851	0.039	-	-	+
P5	-0.047	224.705	0.488	-0.050	235.525	0.506	-	+	+
P7	-0.110	265.374	1.109	-0.101	257.512	1.012	-	-	-
P9	-0.655	172.606	6.560	-0.337	175.030	3.370	+	+	-
LPB	-37.800	1094.700	1134.000	-37.800	1094.700	1134.000	=	=	=
Max Bent	0.655	265.374	6.560	0.337	257.512	3.370			
Two Lane - Strength V Case									
Two Lane Bridge - Fixed Base, Pinned Top									
	20 in.			14 in.					
	X, k	Y, k	M, k-ft.	X, k	Y, k	M, k-ft.	X	Y	M
P1	-3.119	153.174	87.749	-3.119	155.927	87.729	=	+	-
P3	-3.119	228.311	87.732	-3.119	221.307	87.725	=	-	-
P5	-3.118	197.528	87.718	-3.119	206.089	87.722	=	+	+
P7	-3.118	230.509	87.709	-3.118	223.387	87.720	=	-	+
P9	-3.118	155.591	87.705	-3.118	158.404	87.718	=	+	+
LPB	-29.160	965.114	874.800	-29.160	965.114	874.800	=	=	=
Max Bent	3.119	230.509	87.749	3.119	223.387	87.729			
Two Lane Bridge - Fixed Base, Fixed Top									
	20 in.			14 in.					
	X, k	Y, k	M, k-ft.	X, k	Y, k	M, k-ft.	X	Y	M
P1	-2.513	145.139	40.662	-2.852	147.037	43.326	-	+	+
P3	-3.177	229.431	47.289	-3.112	223.035	45.93	+	-	-
P5	-3.213	197.481	47.637	-3.157	205.812	46.376	+	+	-
P7	-3.264	226.032	48.145	-3.187	220.39	46.674	+	-	-
P9	-3.426	167.031	49.76	-3.284	168.841	47.646	+	+	-
LPB	-29.160	965.114	874.800	-29.160	965.114	874.800	=	=	=
Max Bent	3.426	229.431	49.760	3.284	223.035	47.646			

There were noticeable changes for the bents with regards to the maximum axial load a single pile experienced when the pile size was changed. For the Strength I case, the maximum axial load decreased by about 9 to 16 kips for fixed-pinned piles and 7 to 13 for fixed-fixed ones as the pile size decreased from 20 inches to 14 inches across the two to six lane bridge scenarios. Similarly, for the Strength V combination, the maximum axial load within the piles of the bent decreased by 7 to 12 kips for fixed-pinned conditions and 6 to 10 kips for fixed-fixed piles. The largest change in each case again came from the six-lane bridge. This makes sense, as this is theoretical bridge has the greatest number of piles, so we would expect the effects of changing each pile's size to be most evident where there are the most piles in use.

With the fixed-pinned condition, the maximum moment seen in a pile bent showed effectively no change in the Strength I combination, and similarly showed less than 1 kip-ft. of change for the Strength V combination when the pile size was changed from 20 inches down to 14 inches. When the piles are considered fixed at each end, the maximum moment experienced within the bent for Strength I decreased by up to about 6 kip-ft. for the six-lane bridge. For Strength V in the same scenario, the maximum moment decreased by up to about 4 kip-ft. as the pile size went from 20 inches down to 14 inches. This maximum change again came from the six-lane bridge scenario.

While these changes in axial and moment distribution are observed, compared to the anticipated capacities of these piles, the variation does not appear to be significant.

6.7.1. Regarding Slenderness

It is worth noting that the moment-axial interaction diagrams were developed for fully supported piles, and that the load analysis was developed for a pile bent. There was no direct accommodation made for slenderness effects or moment magnification at this time. However, the following discussion shows how a representative moment magnification factor may be calculated, and the result of that calculation for the given analytical six-lane bridge with a pile bent of 13 piles.

For the approximate evaluation of slenderness effects, we can follow AASHTO LRFD Section 5.6.4.3. This passage indicates that for members with slenderness ratios $\left(\frac{Kl_u}{r}\right)$, less than 22, slenderness may be neglected. For members with slenderness ratios less than 100, a magnification factor may be applied to the moment to account for this slenderness. The approximate slenderness reduction factors (K) are in accordance with the American Institute of Steel Construction's listed values for fixed base with top free to translate horizontally but not rotate for the fixed-fixed pile condition (Case C), and for the fixed-pinned pile condition, Case E is used, meaning that translation and rotation are both free (AISC 2016, Table C-A-7.1). These result in a factor of 1.0 and 2.0 respectively.

For our analytical bridge, the slenderness ratio is as follows:

For Fixed-Fixed:

$$\left(\frac{Kl_u}{r}\right) = \left(\frac{1.0*(30\text{ ft.}*12\text{ in./ft.})}{\sqrt{((20\text{ in.})(20\text{ in.})^3/12)\,/(20\text{ in.})^2}}\right) = 62.4 \qquad \textbf{Eq. 6-2}$$

For Fixed-Pinned:

$$\left(\frac{Kl_u}{r}\right) = \left(\frac{2.0*(30\ \text{ft.}*12\ \text{in./ft.})}{\sqrt{((20\ \text{in.})(20\ \text{in.})^3/12)\ /(20\ \text{in.})^2}}\right) = 124.7 \qquad \textbf{Eq. 6-3}$$

We cannot apply the moment magnification method to the fixed-pinned pile bent, as its slenderness ratio exceeds the limit of 100. More advanced consideration would be necessary. As the primary objective of our research focused on the capacity consideration for the piles, rather than the demand, we will progress with examining only the approximate method of analysis for moment-magnification of the fixed-fixed bent condition.

What we are most interested in seeing is a representative value for the moment magnification factor, δ_b. This can show for the given loading scenario, how much the calculated moment should be amplified to incorporate slenderness considerations. Based on the fixed-fixed analysis for the six-lane bridge with 20-inch piles, δ_b ranges from 1.05 to 1.10. We can see from the analysis that the magnification is by up to about ten percent. Reflecting this finding on Figure 6-4, the slenderness does not appear to be particularly significant in this scenario. This cannot be said for all bridge layouts or loading conditions, certainly, but it gives a reference point for the current analysis and fits the scope of this work.

Table 6-3:Magnification of Moment for Slenderness Consideration

Moment Magnification for Slenderness Effects		
M_c :	Magnified Moment (kip-ft.) $M_c = \delta_b M_{2b} + \delta_s M_{2s}$ **Eq. 6-4**	(AASHTO LRFD, 4.5.3.2.2b-1)
M_{2b}:	Moment on compression member due to factored gravity loads that result in no appreciable sidesway, (kip-ft.)	Varies
M_{2s}:	Moment on compression member due to factored lateral or gravity loads that result in sidesway greater than l_u/1500, (kip-ft.)	The lateral deflection of the top joints of our piles in the fixed-fixed scenario is about 0.14 inches. The unbraced length of this member is 30 feet. Thus the deflection (0.14 in.) is less than the unsupported length divided by 1500 (0.24 in.), and so we will take M_{2s} as zero.
δ_b:	$\delta_b = \frac{C_m}{1-\left(\frac{P_u}{\phi_K P_e}\right)} \geq 1.0$ **Eq. 6-5**	(AASHTO LRFD, 4.5.3.2.2b-3) C_m taken as 1.0
δ_s:	$\delta_s = \frac{1}{1-\left(\frac{\Sigma P_u}{\phi_K \Sigma P_e}\right)}$ **Eq. 6-6**	(AASHTO LRFD, 4.5.3.2.2b-4) Not computed as M_{2s} = 0
P_u:	Factored Axial Load Applied, (kips)	Varies
P_e:	Euler Buckling Load, (kips) $P_e = \frac{\pi^2 EI}{(Kl_u)^2}$ **Eq. 6-7**	(AASHTO LRFD, 4.5.3.2.2b-5) For 5 ksi concrete, 20-in. piles, fixed-fixed condition, and unbraced length of 30 ft: $P_e = \frac{\pi^2 EI}{(Kl_u)^2} = \frac{\pi^2(4592\ \text{ksi})(13{,}333\ \text{in.}^4)}{(1.0*360\ \text{in.})^2} = 4662.6$ kips
ϕ_K:	Stiffness Reduction Factor	0.75 for concrete members

6.8. Pile Analysis Summary and Conclusions

Throughout this document, many elements of pile capacity have been addressed. First, by examining the current design practices of various southeastern DOTs, we have shown the current state of practice in the industry for these piles. Based on those practices, we calculated the theoretical structural axial-only capacity of the piles. From here, we examined these values to eventually present viable explanations for the origins of ALDOT's table of standard pile capacities.

Moving beyond the pure axial capacities of the piles, we developed moment-axial interaction diagrams for each of ALDOT's standard piles. Not only do we have these figures as design aids and deliverables, but also the program used to create them has been prepared and may be used for preliminary evaluation of potential changes to the pile standard details. When the ALDOT listed pile capacities are plotted along with the moment-axial interaction diagrams in Figure 5-3, we can again see that these values are significantly smaller than the full analytical capacity curves that we developed when axial capacity is the prevailing loading encountered.

Next, we needed something to compare with these capacities, so three prototype bridges were created and modified AASHTO loading was applied. This enabled us to see that under Strength I and Strength V limit states, the moment and axial loading of these piles in the prototype bents fell well within the created moment-axial interaction diagram for the 20-inch ALDOT standard pile. From the plot of these demand combinations and the capacity curve in Figure 6-4, we can see that the estimated capacity far exceeds the estimated loading of these theoretical two-, four-, or six-lane bridges. While this particular comparison is only valid for the theoretical loading previously discussed, it does go to show that for this consideration there is a comfortable margin between demand and capacity. Slenderness was not accounted for in the development of the capacity curves, however, the engineers using these resources can use alternate methods to account for the second order effects generated within pile bents, such as the moment magnification factor discussed in Section 6.7.1. For the fixed-fixed prototype bents, this slenderness factor would only magnify the moment by about ten percent, and the plotted demand points for the load combinations considered still would fall within the capacity curve of the 20-inch standard ALDOT pile. Additionally, we conducted basic analysis to see if the moment or axial load distribution varied significantly within a bent when the pile size was changed. From our analysis, there were changes in the distribution, but they are not considered significant at this time.

From this portion of our investigation, we determined that the listed axial structural strength of ALDOT's piles could likely be increased at the discretion of ALDOT engineers.

7. Geotechnical Analysis Methods and Procedures

7.1. Acquiring and Organizing Data

Investigating the feasibility of altering ALDOT's current square PPC pile axial load limits began with the acquisition of 32 test pile records provided by ALDOT. These records contained data corresponding to the installation of square PPC piles of various sizes including 14, 16, 20, 24, 30, and 36 inch in the coastal region of the State of Alabama. Each test pile was labeled with a rather lengthy ALDOT project ID. To promote efficient communication, each test pile was assigned a Pile ID ranging from 1 to 32. Table 7-1 serves as a reference to link each pile ID with its corresponding ALDOT project ID. The location of each test pile was provided within the reports in the form of Global Positioning System (GPS) coordinates. These coordinates were used to develop a map indicating the approximate location of each test pile installation. The resulting map is presented in Figure 7-1.

Table 7-1: Pile ID/ALDOT ID correlation

Pile ID	ALDOT ID
1	BR-0213(501) Pile #1
2	BR-0213(501) Pile #6
3	ACGBBR-4915 (200) Pile #5
4	BR-0193(500) Pile #6
5	BR-0913(500) Pile #10
6	STPMB-7509(600) Pile #4
7	NHF-7571 (600) Pile #NA
8	IM MGF 65 I (252) Pile #8 Bent 14NBR
9	IM MGF 65 I (252) Pile #8 Bent 4NBR
10	BRZ-4900 (204) Pile #3
11	ACSTPAA-1702(904) Pile #5
12	ACSTPAA-1702(904) Pile #52
13	ACSTPAA-1702(904) Pile #42
14	ACGBBRZ-0200(206) SITE #3-Bent 2 RT
15	ACGBBRZ-0200(206) SITE #3-Bent 2 WB RT
16	ACGBBRZ-0200 (206) Bent #3
17	USA Project 930-839R Mobile River 36"
18	USA Project 930-839R Mobile River 24"
19	STPAAF-EOAPF-BRF-I010(301) Pile #2
20	ACSTPAA-1702(904) Pile #25
21	ACSTPAA-1702(904) Pile #50
22	ACSTPAA-1702(904) Pile #35
23	ACSTPAA-1702(904) Pile #25
24	ACSTPAA-1702(904) Pile #15
25	ACSTPAA-1702(904) Pile #70
26	ACSTPAA-1702(904) Pile #55
27	HPP1702(905) Pile #NA
28	ACSTPAA-1702(904) Pile #30
29	ACSTPAA-1702(904) Pile #14
30	ACSTPAA-1702(904) Pile #59
31	ACBRZ58307-ATRP(001) Pile #7
32	ACBRZ58307-ATRP(001) Pile #3

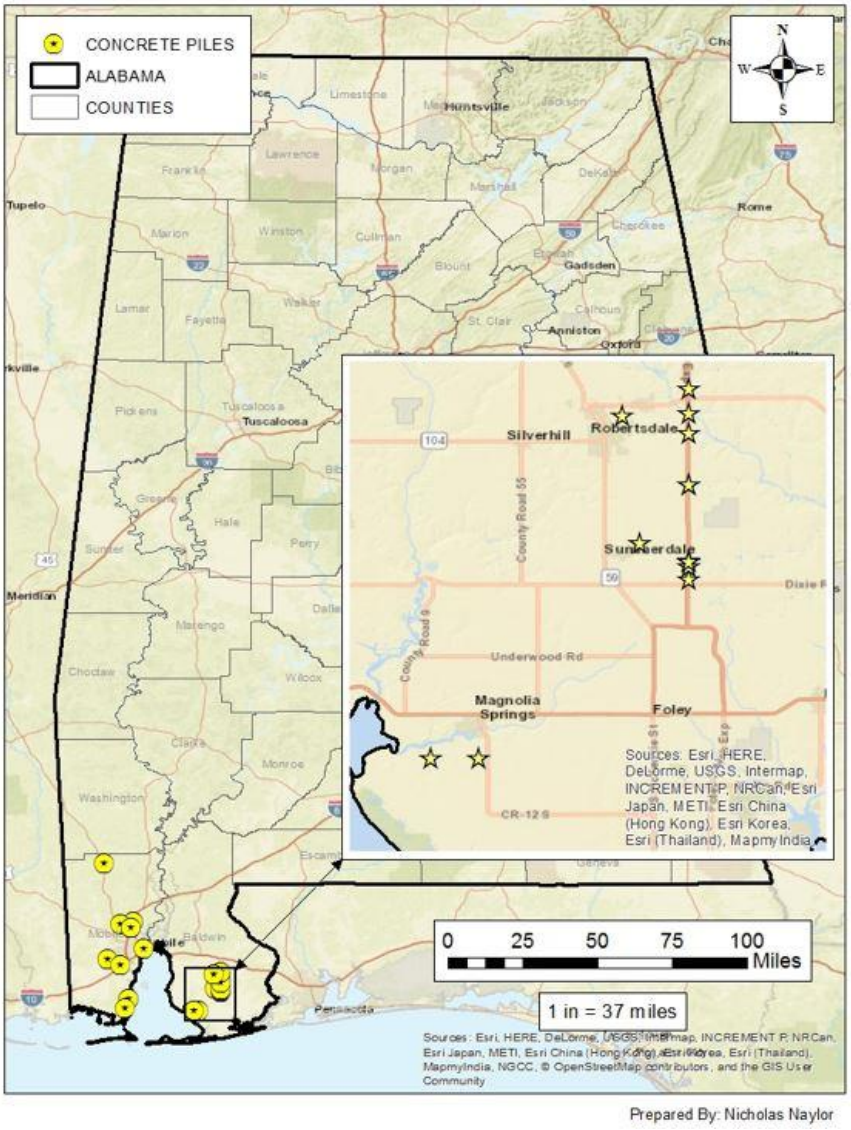

Figure 7-1: Map of test pile installation sites (Naylor, 2018).

GRLWEAP was selected as a primary research tool due to its efficiency in modeling pile installations and its ability to estimate driving stresses and pile capacity. GRLWEAP is also commonly used by ALDOT personnel for pile installation design. Initial research efforts focused on developing an understanding of the data provided within the test pile records and identifying which components were required inputs of the GRLWEAP program. Each test pile record contained an inspector driving log, static load test pile loading record, and soil boring logs. Relevant data contained within these documents can be separated into three categories: driving system information, pile information, and soil information.

7.2. GRLWEAP Driving System Information

GRLWEAP Driving system information includes hammer type as well as hammer and pile cushion parameters. GRLWEAP contains an in-program database of various types of hammers. Of the thirty-two test pile installations, only two were installed using air hammers, while the remaining piles were

installed using diesel hammers of various sizes. Conveniently, each type of hammer utilized in the thirty-two pile installations was included within the GRLWEAP database. Upon selection of a specific hammer from the database, default hammer parameters were generated from the database within the GRLWEAP program. For air hammers, the program assigned a default parameter for hammer efficiency. For diesel hammers, default parameters of efficiency, pressure, and stroke were automatically generated by the software. In an effort to validate these parameters, the Alabama Department of Transportation's Material's and Testing Bureau was consulted. The bureau revealed that based on experience, most hammers possess an actual efficiency rating of approximately 75 percent. Therefore, in an attempt to improve model accuracy, the hammer efficiencies corresponding to each pile installation were set to 75%. For Diesel hammers, pressure is directly proportional to the amount of fuel supplied to the hammer. The GRLWEAP program enables incremental fuel/pressure adjustment by the selection of one of four available fuel settings. These fuel settings are labeled Max-3, Max-2, Max-1, and Max with Max-3 providing the least amount of fuel and Max the highest. In an effort to accurately model each pile installation, the fuel setting that produced GRLWEAP predicted blow counts that most closely replicated blow counts presented in the corresponding inspector driving log was selected and utilized. For each analysis, the pressure resulting from the selected fuel setting was held constant while the stroke was allowed to vary. An example of the hammer parameters section of the GRLWEAP input display is presented in Figure 7-2.

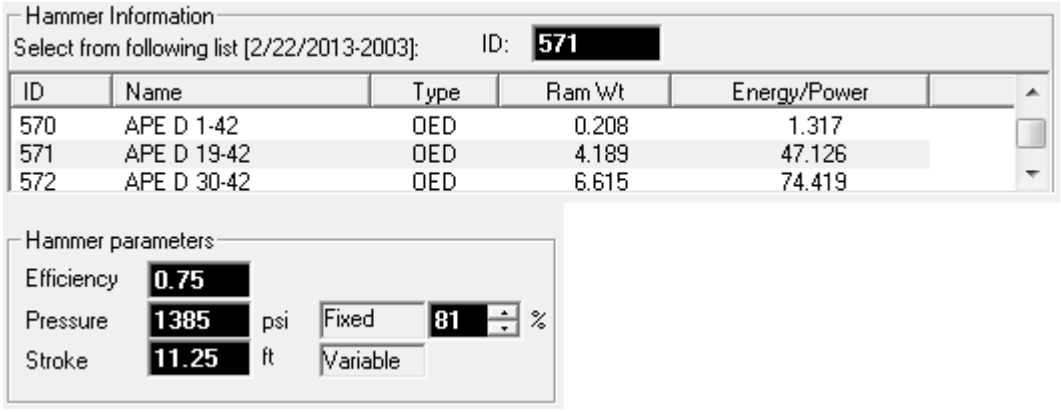

Figure 7-2: GRLWEAP hammer parameter input screen.

Acquiring the necessary inputs for hammer and pile cushion parameters proved challenging. The test pile records simply provided helmet weight along with hammer and pile cushion material type, area, and thickness. Therefore, the required hammer and pile cushion parameters of elastic modulus, coefficient of restitution, and stiffness remained unknown. Acquiring these parameters again required input from ALDOT's pile inspection department. The department revealed these parameters are typically provided within the pile driving and equipment data form associated with each pile installation. However, these data forms were not provided within the test pile records and could not be located within ALDOT's database. Therefore, the department suggested the utilization of GRLWEAP's default parameter database for the generation of unknown hammer and pile cushion parameters. This method of acquiring unknown cushion parameters became standard practice for the ensuing research. An example of the cushion information section on the GRLWEAP input display is presented in Figure 7-3.

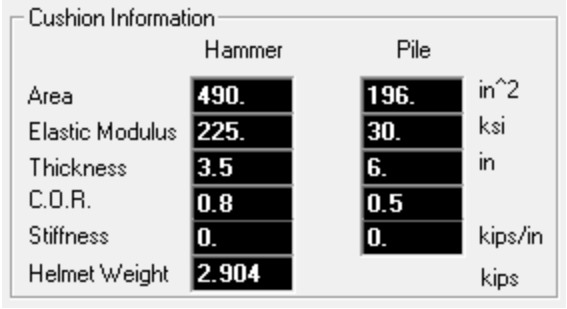

Figure 7-3: GRLWEAP cushion parameter input screen.

7.3. Pile Information

Pile information provided within the test pile records included pile size, length, and embedment. GRLWEAP required additional pile parameters including section area, toe area, elastic modulus, and specific weight. The parameters of section and toe area corresponding to each size pile were acquired through an ALDOT supplied table of square concrete pile properties. The cross sectional area presented in this table corresponded to the GRLWEAP input of toe area, while the voided area corresponded to the GRLWEAP input of section area. Section and toe areas associated with square PPC pile sizes 24 inches and larger differed due to voided cross sections. The ALDOT supplied table of concrete pile properties is presented in Table 7-2.

Table 7-2: ALDOT supplied table of square PPC pile properties (Acquired from ALDOT

Pile Size	Cross Sectional Area	Voided Area	Number of Strands (a)	Effective Prestress (b)	Comp Stress (c)	Tensile Stress (c)
14”	196 (in)2	solid	8	1011.4	3.24	1.22
16”	256 (in)2	solid	8	774.3	3.48	0.99
18”	324 (in)2	solid	12	917.7	3.33	1.13
20”	400 (in)2	solid	12	743.4	3.51	0.96
24”	576 (in)2	489 (in)2	16	810.7	3.44	1.02
30”	900 (in)2	686 (in)2	20	722.4	3.53	0.93
36”	1296 (in)2	898 (in)2	28	772.6	3.48	0.98

NOTES:

a) # of strands based on low relaxation (lolax) strand

b) effective prestress is in unit of PSI

c) compressive & tensile stresses are in units of KSI

- stresses are based on 5,000 psi design concrete mix

The pile parameter of elastic modulus was calculated based on compressive concrete strength and the specific weight of concrete was assumed to be 150 pcf, as is standard for reinforced concrete. The pile information section on the GRLWEAP input display is presented in Figure 7-4.

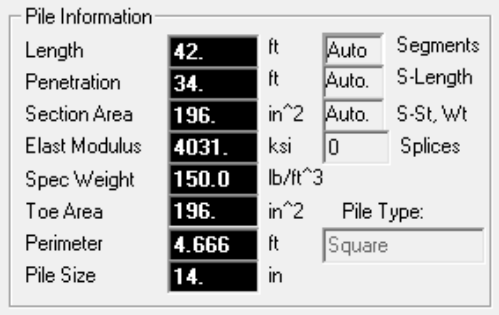

Figure 7-4: GRLWEAP pile parameter input screen

7.4. Soil Information

Soil information was derived directly from boring logs provided within the test pile records and applied to the GRLWEAP program using the SA Method of soil analysis. The SA method was selected due to 30 of the 32 pile records containing SPT boring logs. The remaining two records contained CPT boring logs. In an effort to perform consistent analysis, the SA Method was also utilized for these pile installations by the application of correlated N values contained within the CPT boring logs. Often, multiple boring logs were presented within each record. In such cases, the boring log in closest proximity to the pile installation site was utilized. Analysis of the boring logs allowed for the delineation of soil layering by depth, classification, and strength based on SPT N-values. Soil classification was assigned based on descriptions provided within the boring logs. Soil strength was assigned based on unaltered N values derived from SPT's as is standard geotechnical practice. Through analysis of inspector driving logs, it was determined that for each pile installation, initial pile penetration was facilitated prior to driving by either drilling or jetting. The appropriate way to account for the reduction of soil strength resulting from disturbance within the depth of initial penetration was determined through review of related literature. Poulos and Davis (1980), reported that shaft resistance should be reduced by 50 percent of the originally calculated resistance in the jetted zone. McClelland et al. (1969) reported that a decrease in shaft resistance over a predrilled depth can range from 50 to 85 percent (Hannigan et al., 2016). In accordance with these findings, N values corresponding to soils within the predrilled or jetted depths were reduced by 50 percent.

An additional parameter required by GRLWEAP software and presented within a boring log is the depth of the water table. However, in 7 of the 32 pile reports, no indication of water depth was provided. In such cases, ALDOT personnel suggested the conservative approach of setting the depth of the water table equal to the elevation of the ground surface. GRLWEAP also required an input value for effective overburden pressure at grade. Effective overburden pressure at grade results when fill material is placed atop the site prior to pile installation. No indication of fill material was presented within the pile reports. Therefore, effective overburden pressure at grade was set at zero ksf for each model. Having acquired all necessary soil information, the delineated soil profile was applied to the GRLWEAP program. Implementation of the delineated soil profile resulted in the automatic generation of GRLWEAP predicted values of unit shaft and toe resistance resulting from pile/soil interaction within each soil layer upon pile penetration. Likewise, GRLWEAP calculated quake and dampening values resulting about the pile shaft and toe.

Setup factors associated with each soil layer were generated by the SA method of soil analysis. Setup factors indicate the anticipated strength gain or reduction resulting from soil disturbance. The

GRLWEAP program utilizes setup factors to calculate gain/loss factors which indicate the soil resistance resulting about the pile shaft and toe at various stages of soil remolding. A gain/loss factor of 1 indicates no change in soil strength during driving and therefore negates the temporary alteration of pile capacity occurring after installation. A gain/loss factor less than 1 indicates a soil setup scenario in which soil resistance is reduced during driving and increases with time following pile installation. A gain/loss factor greater than 1 indicates a soil relaxation scenario in which soil resistance increases during driving and reduces with time following pile installation. (Hannigan et al., 2016). The program calculates the shaft gain/loss factor as the inverse of the set up factor associated with the most sensitive soil layer existing about the pile shaft. The toe gain/loss factor is held at 1, due to an assumed minimal soil disturbance occurring about the pile toe.

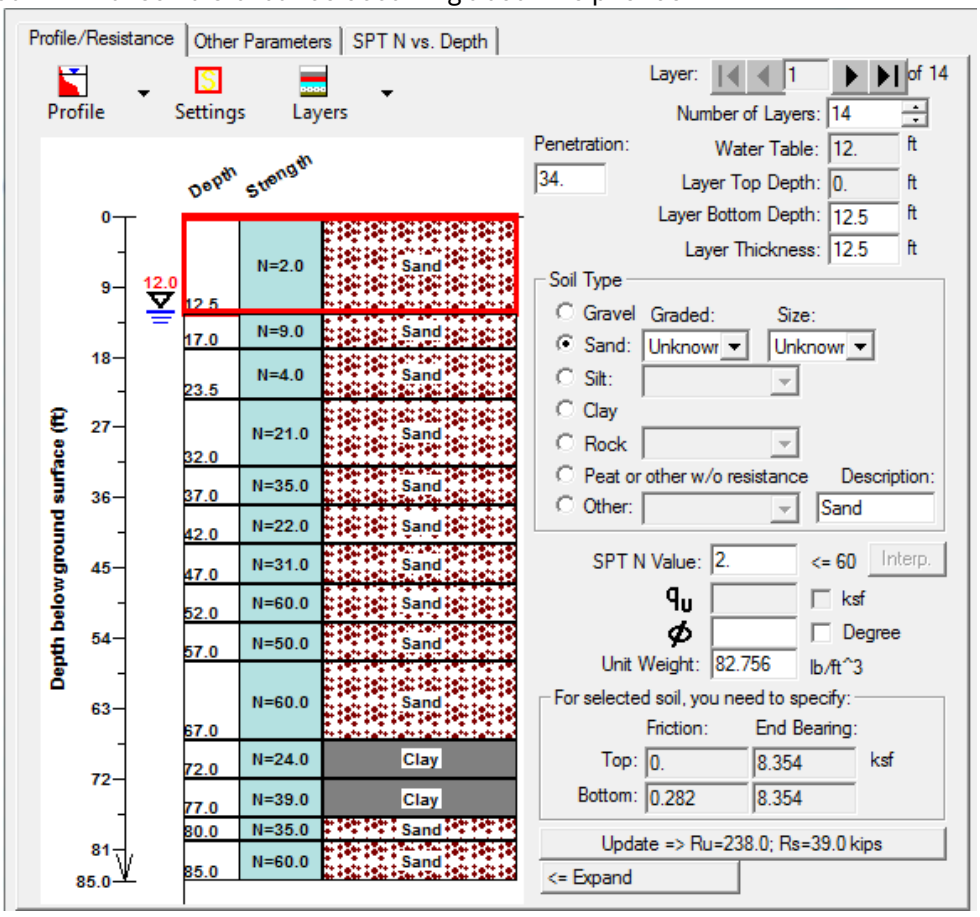

Figure 7-5: GRLWEAP SA Method soil input screen

Two primary goals of analysis were the determination of maximum compressive and tensile driving stresses resulting during driving and the long term ultimate capacity of the pile. Accomplishing these goals required two rounds of analysis: First, driving stresses were analyzed under GRLWEAP predicted gain/loss factors to account for the change in soil strength occurring during driving. Second, ultimate pile capacity analysis was conducted by setting the shaft and toe gain/loss factors to 1. Setting the gain/loss factors to 1, produced the actual long term pile capacity resulting after the resistance altering effects of soil disturbance had subsided; therefore, providing a more consistent estimate of long term pile capacity. The soil parameter sections of the GRLWEAP program are presented in Figure 7-5 and Figure 7-6.

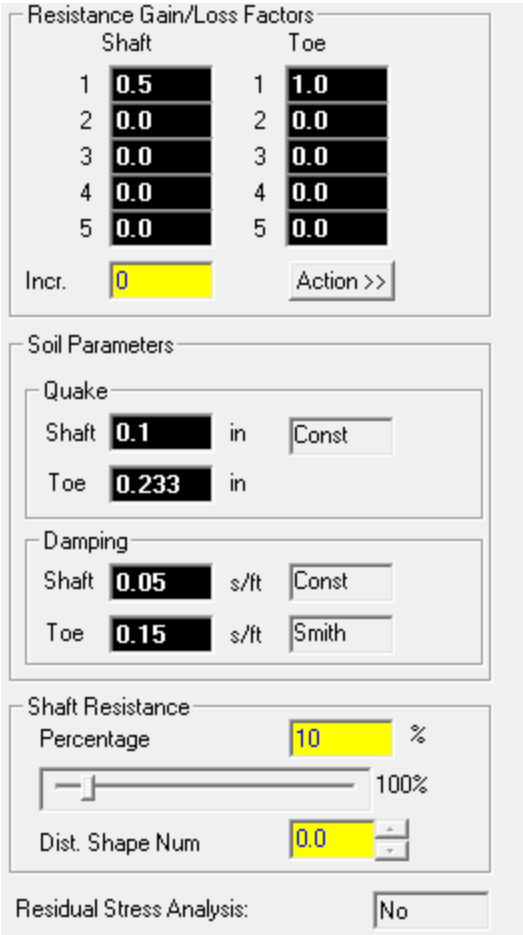

Figure 7-6: GRLWEAP soil parameter input screen

Two capacity values, including design load and static load test capacity, were acquired from each test pile record for comparison with GRLWEAP generated capacities. Design loads were generated by ALDOT and provided within inspector driving logs. Design loads were doubled to account for factor of safety capacity reduction. Static load test capacity, or ultimate pile capacity, was acquired from Davisson offset analysis of load movement curves generated from load tests performed upon each test pile.

7.5. Execution of GRLWEAP Analysis

Following the acquisition of all necessary GRLWEAP input parameters, each test pile was analyzed using GRLWEAP's drivability analysis program. Utilizing wave equation analysis, the program facilitated two primary components of research including driving stress analysis and ultimate pile capacity determination. The analysis performed through the GRLWEAP drivability program can be separated into two sections. The first section focused on the replication of maximum driving stresses incurred during and the ultimate long term capacity resulting from the modelled installation of each test pile. Execution of the drivability program, under GRLWEAP predicted gain/loss factors generated the compressive and tensile driving stresses resulting at specified two foot intervals along the entire depth of embedment. A secondary research goal focused on the evaluation of maximum driving stresses resulting at altered compressive concrete strengths. Standard variations of concrete pile

properties including compressive concrete strength and corresponding allowable stresses were provided based on the survey results. The estimated allowable compressive and tensile stress limits for ALDOT piles is presented in Table 7-3. Though ALDOT does not currently allow the use of 12 inch square PPC piles, evaluating the effectiveness of 12 inch pile utilization was included as a goal of research. Due to a lack of ALDOT 12 inch square PPC pile data, 12 inch pile parameters were acquired from the Louisiana Department of Transportation and Development.

GRLWEAP drivability analysis was performed upon each test pile at each recommended compressive concrete strength including 5000, 5500, 6000, and 6500 psi. The maximum compressive and tensile driving stresses produced during driving of each pile at each concrete strength were recorded. The average change in maximum driving stress resulting from incremental increases in compressive concrete strength was calculated. The maximum driving stresses occurring during each pile installation were then compared to the UA provided allowable stress limits corresponding to each compressive concrete strength. Following the determination of maximum driving stresses, shaft and toe gain/loss factors were set to 1 and the long term GRLWEAP predicted capacity of each pile was determined. The long term GRLWEAP predicted pile capacity was then compared to static load test and twice the design load capacities presented in the pile records to evaluate the accuracy of GRLWEAP capacity predictions.

The second section of GRLWEAP analysis focused on evaluating the effectiveness of replacing original test pile sizes with reduced pile sizes at original installation sites. To facilitate this analysis, original test pile sizes were replaced with piles one standard size smaller according to the ALDOT recommended pile properties guide in Figure 10. In an effort to create the most accurate model, reduced pile size analysis was performed with hammer types and driving system parameters consistent with those commonly utilized for each specific pile size as determined from the historical test pile records. With appropriate GRLWEAP input parameters in place, decreased pile sizes were evaluated within the original soil profile to determine the length of additional embedment required to achieve the GRLWEAP generated capacity of the original size test pile. If a reduced pile size was incapable of achieving original size test pile capacity within the available depth of boring, the terminal soil layer was extended to a depth at which original test pile capacity could be achieved. The resulting embedment of the reduced pile size was recorded for comparison with original test pile size embedment. Following embedment determination, pile length was altered to achieve a pile top elevation consistent with that of original test pile installation. Driving stress analysis was then performed on reduced pile size installations. Driving stresses were evaluated at two foot intervals along the established altered depth of embedment at each recommended compressive concrete strength of 5000, 5500, 6000, and 6500 psi. Consistent with the first section of analysis, the maximum compressive and tensile driving stresses incurred were recorded and the average change in driving stress resulting from each incremental increases in compressive concrete strength was calculated. The maximum driving stresses occurring during each pile installation were then compared to the UA provided allowable stress limits corresponding to each concrete strength.

Table 7-3: Estimated allowable compressive and tensile stress limits for ALDOT square PPC piles.

Pile Size	Concrete Strength (psi)	Estimated Allowable Stress Limit (psi)	
		Compression	Tension
12 inch	5000	3476	986
	5500	3901	996
	6000	4326	1006
	6500	4751	1016
14 inch	5000	3165	1297
	5500	3583	1314
	6000	4002	1330
	6500	4422	1345
16 inch	5000	3392	1071
	5500	3813	1085
	6000	4234	1098
	6500	4656	1111
18 inch	5000	3251	1211
	5500	3670	1227
	6000	4090	1242
	6500	4511	1256
20 inch	5000	3421	1041
	5500	3842	1055
	6000	4264	1069
	6500	4686	1081
24 inch	5000	3356	1106
	5500	3776	1121
	6000	4198	1135
	6500	4619	1148
30 inch	5000	3444	1018
	5500	3865	1032
	6000	4287	1045
	6500	4709	1058
36 inch	5000	3393	1069
	5500	3814	1084
	6000	4235	1097
	6500	4657	1110

The determination of reduced size pile length and embedment was used to facilitate comparative cost analysis. Estimated material and installation costs associated with various sized square PPC piles were acquired from a regional pile driving contractor. They provided per linear foot of material and installation costs for each analyzed pile size. These values are presented in Table 7-4. Utilizing these values, the total cost associated with original test pile and reduced pile size installation was calculated. These values were compared to determine if a monetary benefit could result from the utilization of reduced size piles. In order to observe any trends that might exist between soil type and driving stresses, each pile installation was categorized based on the predominant soil type existing about the pile shaft and the pile tip. Soil at the tip of the pile was simply identified as the soil type existing at the terminal depth of pile embedment. Soil along the shaft was determined by a 35% to 65%

criteria. If a particular soil type, either sand or clay, comprised 65% or more of soil composition about the pile shaft, then that soil was selected as the predominant shaft soil type. If either soil type comprised 35% and 65% of soil composition about the shaft, then the soil was considered mixed. The soil categories are presented in Table 7-5.

Table 7-4: Material and installation cost associated with square PPC piles (Daniel, 2018)

Pile Size (in)	Material Cost/LF ($)	Installation Cost/LF ($)
12	$20.00	$13.50
14	$27.00	$15.00
16	$32.00	$17.00
18	$43.00	$21.00
20	$50.00	$32.00
24	$75.00	$55.00
30	$95.00	$70.00
36	$125.00	$85.00

Table 7-5: Soil classification categories (Pement, 2017)

Soils Encountered	1	2	3	4	5	6
Soil at Tip	Sand	Sand	Sand	Clay	Clay	Clay
Soil along Shaft	Sand	Clay	Mixed	Sand	Clay	Mixed

7.6. Results and Discussion of The GRLWEAP Analysis

The results of the driving stress and capacity analysis conducted upon the existing test piles are reported. Driving stress results include the GRLWEAP estimated maximum compressive and tensile driving stresses occurring during test pile installation, the change in maximum driving stresses resulting from incremental increases in compressive concrete strength of the pile, and a comparison of maximum driving stresses to allowable driving stress limits. GRLWEAP predicted test pile capacity was determined and each test pile was categorized based on soil type. A discussion of these results is provided in this section.

7.6.1. Driving Stress Determination of the Installed Test Piles

Each original pile was analyzed utilizing GRLWEAP generated gain/loss factors to determine maximum driving stresses. The maximum compressive and tensile driving stresses resulting from each modelled pile installation were acquired from GRLWEAP numeric output. An example of GRLWEAP numeric output is provided in Figure 7-7.

Alabama Department of Transportation
B1

Nov 29 2018
GRLWEAP Version 2010

Gain/Loss 1 at Shaft and Toe 0.500 / 1.000

Depth ft	Ultimate Capacity kips	Friction kips	End Bearing kips	Blow Count blows/ft	Comp. Stress ksi	Tension Stress ksi	Stroke ft	ENTHRU kips-ft
12.0	18.7	7.3	11.4	2.0	1.204	-0.220	3.65	15.2
14.0	60.0	8.8	51.2	7.4	1.507	-0.179	4.29	11.7
16.0	61.3	10.1	51.2	7.6	1.514	-0.180	4.30	11.6
18.0	34.2	11.5	22.7	3.1	1.388	-0.242	3.98	14.2
20.0	35.5	12.8	22.7	3.2	1.398	-0.244	4.00	14.1
22.0	36.9	14.1	22.7	3.3	1.410	-0.248	4.02	14.0
24.0	135.0	15.6	119.4	27.1	1.695	-0.057	4.90	9.2
26.0	136.5	17.1	119.4	27.7	1.700	-0.058	4.91	9.1
28.0	138.2	18.8	119.4	28.3	1.702	-0.058	4.92	9.1
30.0	140.0	20.6	119.4	28.9	1.708	-0.056	4.93	9.0
32.0	141.9	22.5	119.4	29.7	1.714	-0.054	4.94	9.0
34.0	223.3	24.3	199.0	60.2	1.807	-0.135	5.26	8.7

Max. Tensile Stress

Max. Compressive Stress

Figure 7-7: GRLWEAP numeric output

Initially, each test pile was analyzed using the design compressive concrete strength of 5000 psi. It is important to note that though the test pile design specifications called for a compressive concrete strength of 5000 psi, the actual compressive concrete strength of the piles may have varied as it is not uncommon for pile manufacturers to utilize higher compressive concrete strength than required. If and to what extent the actual compressive concrete strength of the test piles exceeded design concrete strength specifications is unknown. Therefore, the possible variation between the design and the actual compressive concrete strength of the piles is a potential source of error within this study. Due to the lack of actual pile concrete strength data, the known design compressive concrete strength of 5000 psi was established as the baseline value from which the piles were analyzed. As such, the maximum compressive and tensile driving stresses obtained utilizing 5000 psi concrete were estimated to be those that most closely matched the driving stresses induced during the actual test pile installations. These stresses were also utilized as the baseline values from which the change in driving stress resulting from incremental increases in compressive concrete strength could be evaluated. Following the establishment of baseline stresses, each pile was reevaluated at incremental increases in compressive concrete strength including 5500, 6000, and 6500 psi. The maximum driving stresses resulting from each incremental increase in concrete strength were determined and recorded. These values were compared to the stresses occurring at the design compressive concrete strength of 5000 psi and used to calculate the percentage change in maximum compressive and tensile driving stress resulting at each increase in compressive concrete strength. Table 7-6 presents the estimated maximum compressive driving stress occurring during each pile installation utilizing 5000 psi concrete as well as the percentage change in maximum compressive driving stress occurring at each increase in compressive concrete strength. The average percentage change in compressive driving stress resulting from each increase in compressive concrete strength is also presented. A positive percentage change indicates an increase in compressive driving stress, whereas a negative

percentage change indicates a decrease in compressive driving stress. Table 7-6 reveals that for all but three of the original test piles (Pile 3, Pile 11, and Pile 30), increasing the compressive concrete strength of the pile resulted in a slight increase in maximum compressive driving stress. On average, increasing the compressive concrete strength of the pile from 5000 psi to 5500, 6000, 6500 psi resulted in small increases in compressive driving stress. Therefore, it is important to note, that increasing compressive concrete strength does not necessarily result in a reduction of compressive driving stresses.

Table 7-6: Comparison of compressive driving stresses when the compressive concrete strength of the test pile is increased.

Size (in)	Pile ID	Original Concrete Compressive Strength (psi)	Change in Concrete Compressive Strength (psi)		
		5000	5500	6000	6500
		Maximum Compressive Driving Stress (ksi)	Percent Change in Compressive Driving Stress (%)		
14	1	1.807	0.50%	0.89%	1.38%
	7	1.826	0.38%	0.77%	0.82%
	10	2.47	0.12%	0.12%	0.12%
	14	2.238	0.31%	0.67%	0.98%
	15	1.559	0.45%	0.77%	0.83%
	16	1.724	0.35%	0.99%	1.39%
	19	2.798	2.82%	2.32%	2.32%
	31	2.389	1.00%	2.05%	2.72%
	32	2.415	1.12%	2.11%	2.98%
		Avg.	**0.78%**	**1.19%**	**1.51%**
16	4	1.854	0.54%	1.13%	1.40%
	6	2.219	1.17%	3.15%	5.00%
	11	2.014	-0.25%	-0.55%	-0.70%
	12	1.592	0.75%	0.82%	1.19%
	13	1.504	0.40%	0.80%	1.33%
	21	1.662	0.42%	0.72%	1.14%
	27	1.783	0.56%	1.07%	1.29%
		Avg.	**0.51%**	**1.02%**	**1.52%**
20	5	1.844	0.38%	0.60%	0.87%
	20	1.367	0.51%	0.66%	0.80%
	22	1.453	0.48%	0.76%	1.10%
	23	1.415	0.28%	0.64%	0.92%
	24	1.216	0.33%	0.66%	0.99%
	25	1.758	0.57%	0.40%	0.74%
	26	1.231	0.24%	0.73%	0.97%
	28	1.262	0.32%	0.63%	0.87%
	29	1.415	0.35%	0.78%	1.06%
	30	2.2	-0.27%	-0.50%	-0.91%
		Avg.	**0.32%**	**0.53%**	**0.74%**
24	2	1.936	0.46%	0.93%	1.39%
	3	1.809	-0.33%	-0.66%	-0.94%
	18	2.095	0.67%	1.43%	2.00%
		Avg.	**0.27%**	**0.57%**	**0.82%**
30	8	1.705	0.53%	1.00%	1.35%
	9	1.975	0.56%	1.16%	1.72%
		Avg.	**0.54%**	**1.08%**	**1.54%**
36	17	2.039	0.69%	1.37%	1.86%
		Avg.	**0.69%**	**1.37%**	**1.86%**

Table 7-7 presents the estimated maximum tensile driving stresses occurring during each original test pile installation utilizing 5000 psi concrete, as well as the percentage change in maximum tensile

stress occurring at each adjustment in compressive concrete strength. The average change in maximum tensile driving stress resulting from each increase in compressive concrete strength is also presented.

Table 7-7: Comparison of tensile driving stresses when the compressive concrete strength of the test pile is increased.

Size (in)	Pile ID	Original Concrete Compressive Strength (psi)	Change in Concrete Compressive Strength (psi)		
		5000	5500	6000	6500
		Maximum Tensile Driving Stress (ksi)	Percent Change in Tensile Driving Stress (%)		
14	1	0.25	-3.60%	-7.60%	-12.00%
	7	0.573	1.92%	-2.09%	0.70%
	10	0.174	-10.34%	-9.77%	-4.02%
	14	0.77	2.08%	4.03%	3.90%
	15	0.614	-0.81%	-0.98%	-3.26%
	16	0.938	0.75%	0.85%	1.39%
	19	0.929	3.34%	4.95%	6.46%
	31	0.517	0.77%	1.16%	1.74%
	32	0.968	1.76%	3.31%	4.03%
		Avg.	**-0.46%**	**-0.68%**	**-0.12%**
16	4	0.301	5.98%	8.64%	9.30%
	6	0.35	-4.00%	0.29%	2.57%
	11	0.175	2.29%	4.00%	7.43%
	12	0.485	-4.54%	-8.66%	-12.99%
	13	0.203	-2.96%	-7.39%	-9.85%
	21	0.772	0.91%	0.65%	0.65%
	27	0.718	2.09%	2.92%	2.79%
		Avg.	**-0.03%**	**0.06%**	**-0.02%**
20	5	0.527	3.61%	8.35%	11.01%
	20	0.333	0.00%	-2.10%	-3.60%
	22	0.635	0.16%	0.31%	0.31%
	23	0.484	-0.41%	-1.45%	-2.69%
	24	0.622	1.77%	3.38%	4.82%
	25	0.598	1.17%	1.84%	2.01%
	26	0.484	0.21%	-1.24%	-2.07%
	28	0.08	-3.75%	-7.50%	-12.50%
	29	0.532	-0.19%	-0.19%	-0.75%
	30	0.994	-0.10%	-0.50%	-0.80%
		Avg.	**0.25%**	**0.09%**	**-0.43%**
24	2	0.425	4.24%	6.59%	8.47%
	3	0.562	2.85%	4.63%	6.41%
	18	0.333	4.50%	8.41%	11.11%
		Avg.	**3.86%**	**6.54%**	**8.66%**
30	8	0.211	-4.27%	-7.11%	-9.00%
	9	0.716	-2.65%	-5.17%	-7.82%
		Avg.	**-3.46%**	**-6.14%**	**-8.41%**
36	17	1.092	2.66%	4.85%	6.87%
		Avg.	**2.66%**	**4.85%**	**6.87%**

Table 7-7 indicates a varied response of maximum tensile driving stress to incremental increases in the compressive concrete strength of the pile. For some of the test piles, an increase in compressive concrete strength resulted in increased tensile driving stress; for others, an increase in compressive concrete strength resulted in decreased tensile driving stress. The one consistency for all evaluated piles was that the variation in tensile driving stress resulting from incremental increases in compressive concrete strength were relatively small. Therefore, varying the piles compressive

concrete strength had minimal impact upon maximum tensile driving stress occurring during pile installation.

The results of the maximum driving stress analysis performed on each original size pile utilizing varying compressive concrete strengths indicate that increasing compressive concrete strength at increments of 500 psi from 5000 to 6500 psi, on average, results in a slight increase in both the compressive and tensile driving stresses. However, the percentage by which maximum driving stresses vary with increased concrete strength is very small. Therefore, increasing the compressive concrete strength of the pile would likely have a minimal impact upon the maximum driving stresses induced during pile installation.

7.6.2. Comparison of Maximum Driving Stress to the Allowable Stress Limits of the Installed Test Piles

The maximum driving stresses resulting at each compressive concrete strength were compared to the estimated allowable stress limits associated with each pile size at each compressive concrete strength. The results of this comparison are provided in Figures 7-8 to 7-19 indicating the percentage of allowable stress achieved during each pile installation at each concrete strength. These figures are separated by pile size (14”, 16”, 20”, 24”, 30”, and 36”) and stress type (Compressive or Tensile). The percentage of allowable compressive stress achieved during each test pile installation is presented in Figure 7-8 to Figure 7-13. The percentage of allowable tension achieved during each original test pile installation is presented in Figure 7-14 to Figure 7-19, grouped by pile size.

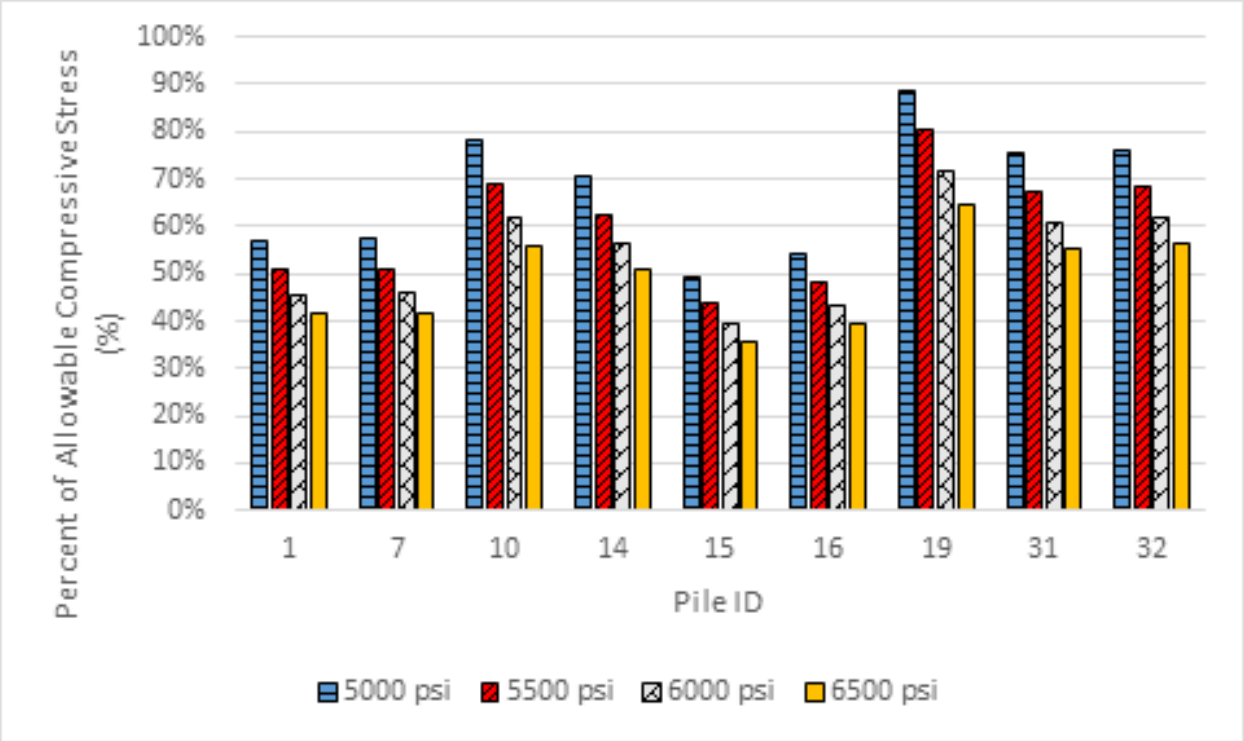

Figure 7-8: Percentage of allowable compressive stress achieved during 14 inch test pile installations.

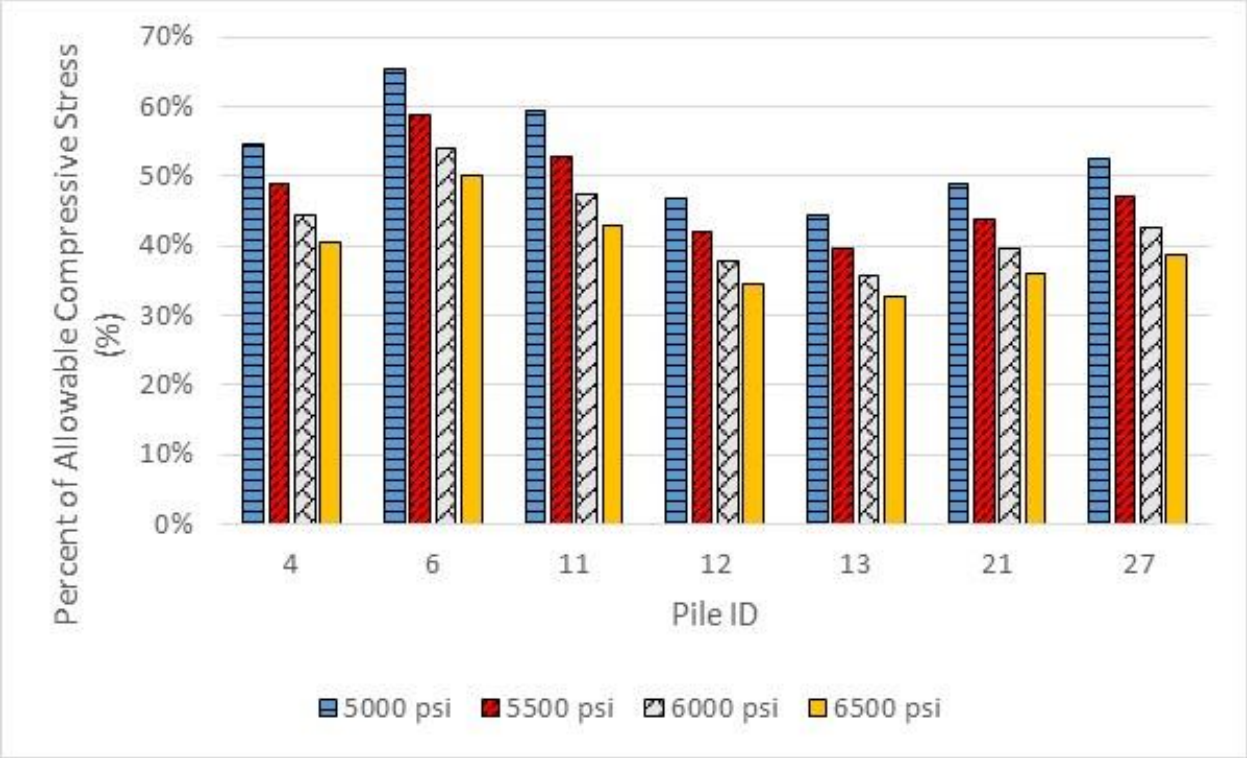

Figure 7-9: Percentage of allowable compressive stress achieved during 16 inch test pile installations.

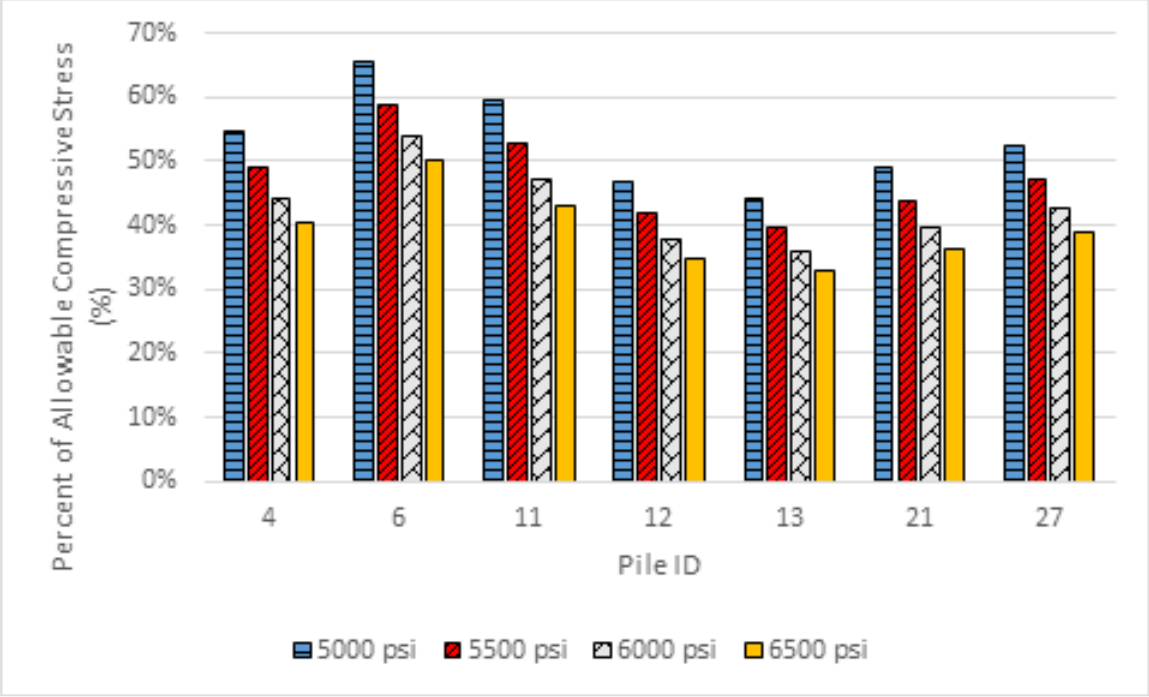

Figure 7-10: Percentage of allowable compressive stress achieved during 20 inch test pile installations.

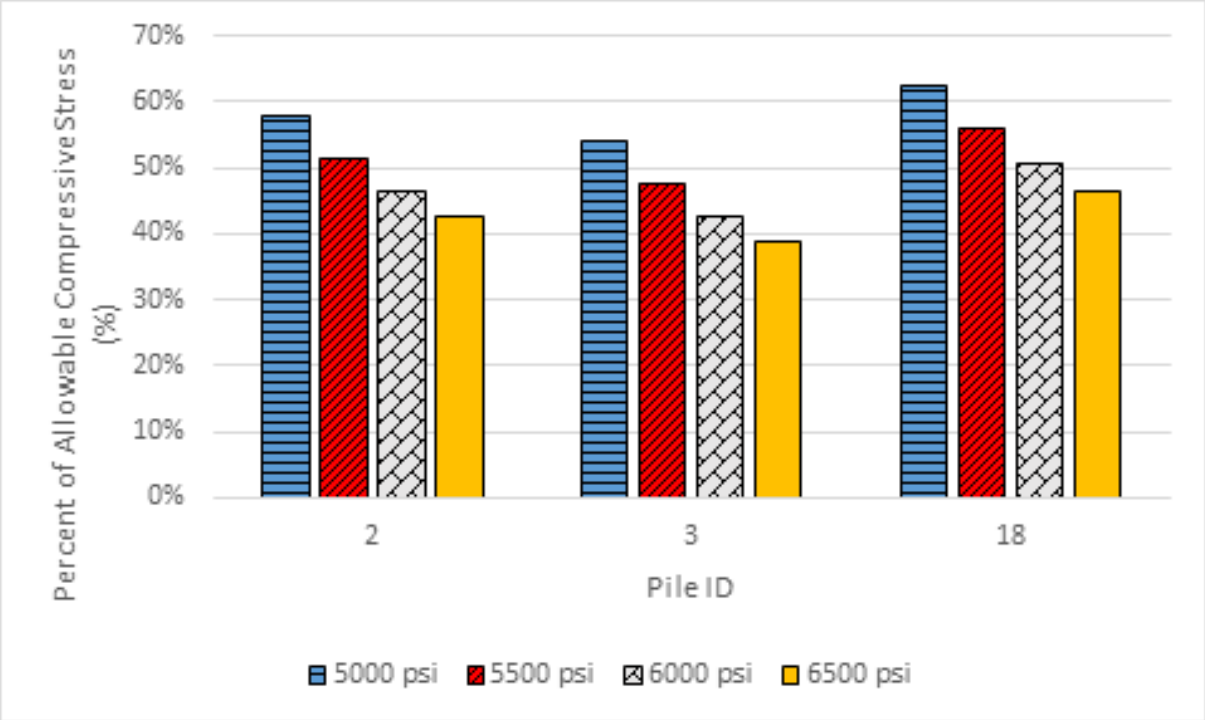

Figure 7-11: Percentage of allowable compressive stress achieved during 24 inch test pile installations.

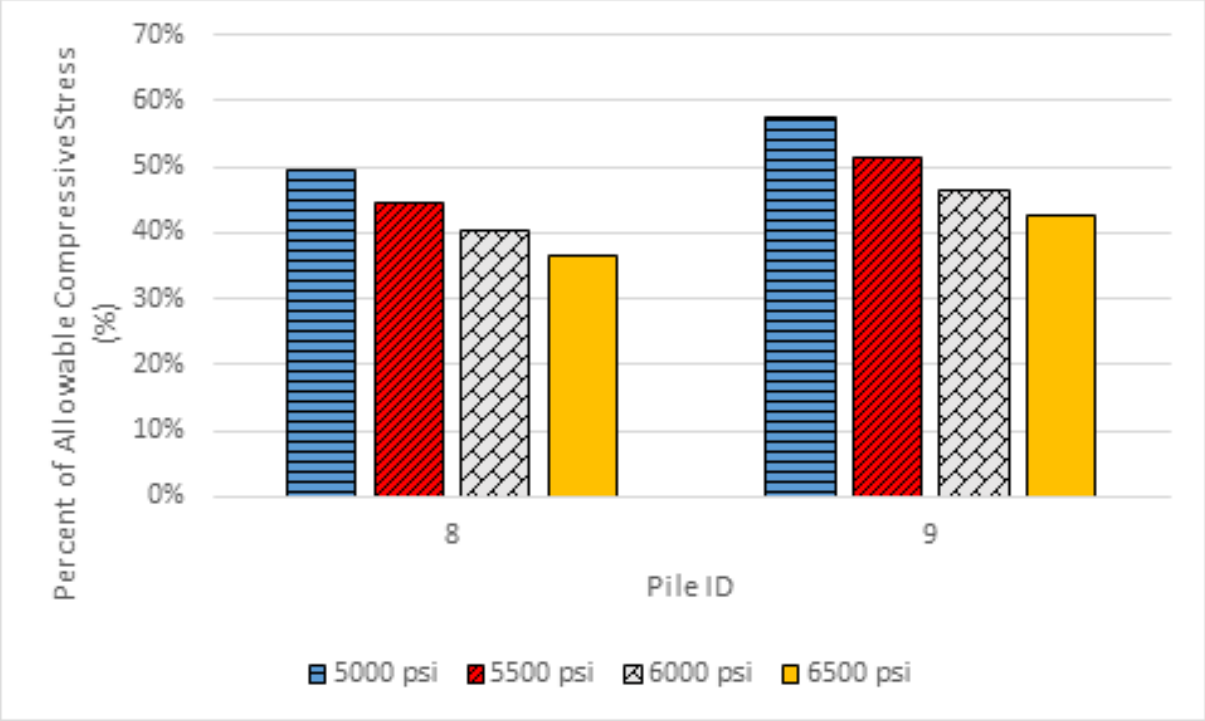

Figure 7-12: Percentage of allowable compressive stress achieved during 30 inch test pile installations.

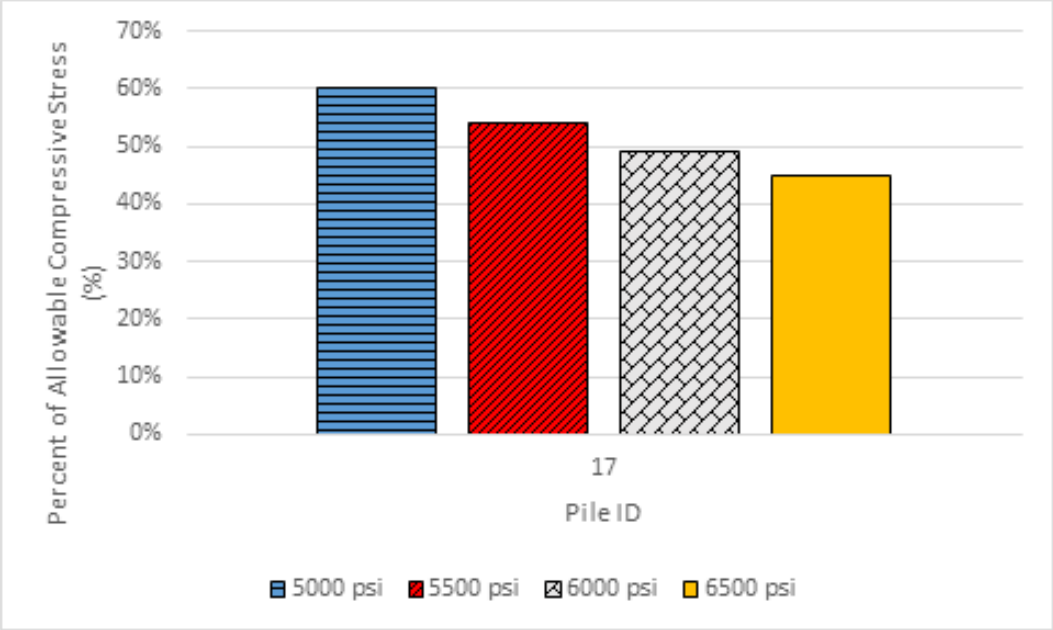

Figure 7-13: Percentage of allowable compressive stress achieved during 36 inch test pile installations.

Figure 7-8 through Figure 7-13 reveal that none of the original test piles experienced maximum compressive driving stress exceeding estimated allowable compressive stress limits. Furthermore, the majority of the test piles experienced maximum compressive driving stress that fell well short of exceeding estimated allowable compressive stress limits. Therefore, results indicate that the piles could potentially have been driven at increased intensity without jeopardizing pile integrity. The results also reveal, for each test pile installation, the percentage of achieved allowable compression decreased as compressive concrete strength increased. This trend is attributed to the fact that increasing the compressive concrete strength of the pile had a more pronounced impact upon the piles allowable compressive driving stress limit than it did the actual maximum compressive driving stress incurred by the pile during installation. On average, a 500 psi increase in compressive concrete strength increased the allowable compressive stress limit of the test piles by 11.3 percent, while the maximum compressive driving stress incurred by the pile only increased by 0.41 percent. As a result, the percentage of achieved allowable compression decreased with each increase in compressive concrete strength.

Figure 7-14 through Figure 7-19 reveal that all test piles except for the single 36 inch pile (17) incurred maximum tensile stresses within allowable tensile driving stress limits. With the exception of 20 inch Pile 30 and 36 inch Pile 17, all test piles experienced maximum tensile driving stress that fell well short of exceeding estimated allowable tensile stress limits. Pile 17 represented the largest and only 36 inch pile evaluated within this study and is also the only test pile to have exceeded allowable tensile driving stress limits. It is important to note that pile 17 was a research pile installed for research purposes only. As such, pile 17 was not installed for use as a structural support member. Therefore, the fact that pile 17 exceeded allowable tensile stress limits was not considered critical as the pile was not installed for the support an actual structure.

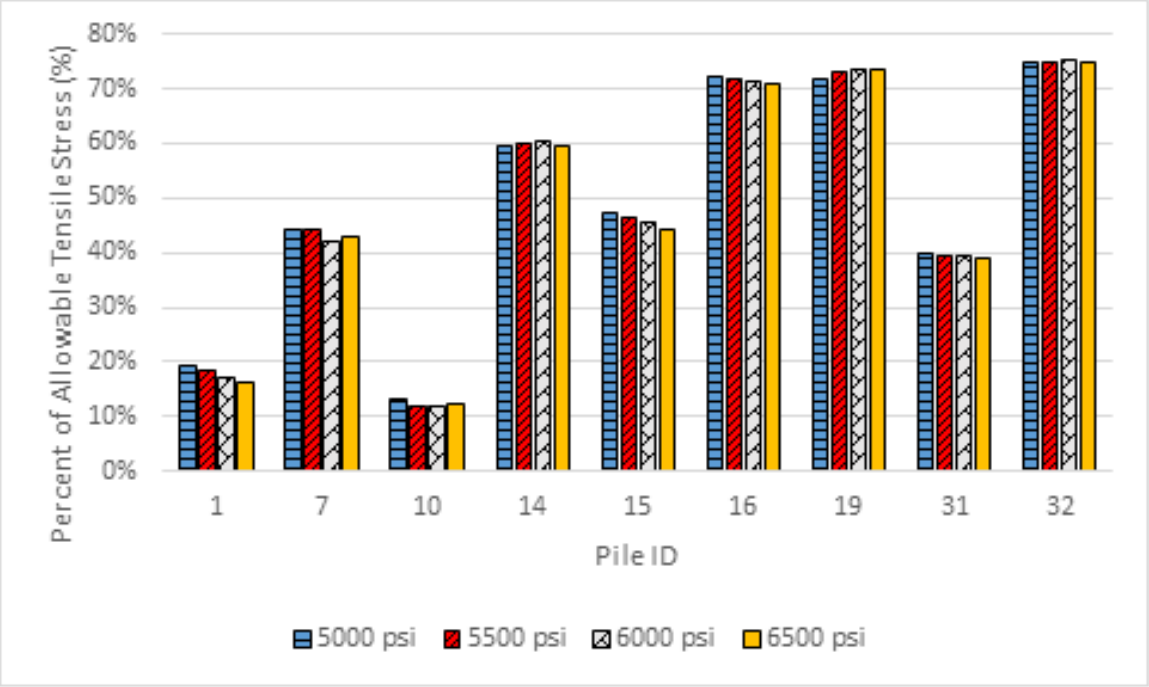

Figure 7-14: Percentage of allowable tensile stress achieved during 14 inch test pile installations.

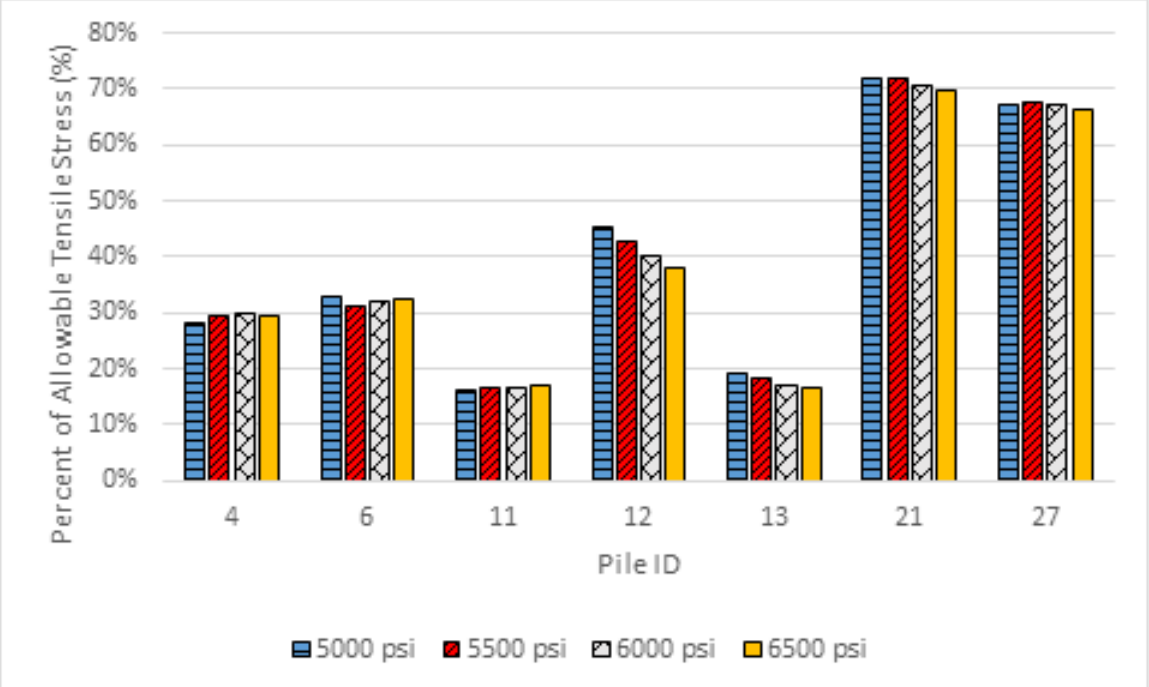

Figure 7-15: Percentage of allowable tensile stress achieved during 16 inch test pile installations.

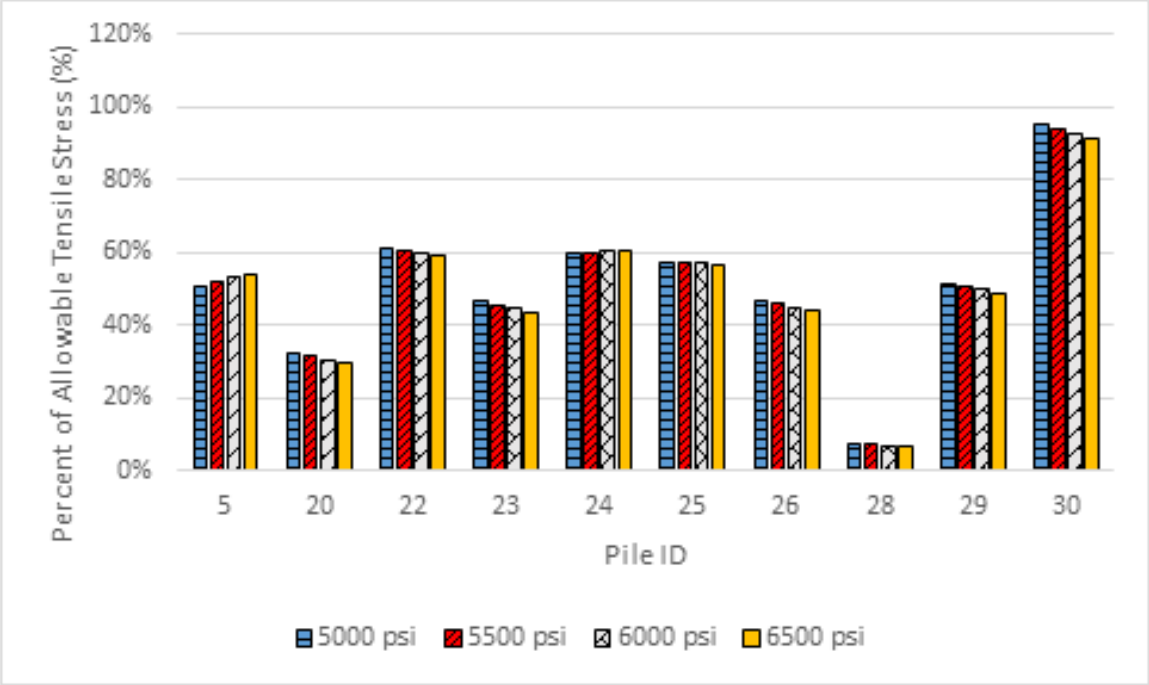

Figure 7-16: Percentage of allowable tensile stress achieved during 20 inch test pile installations.

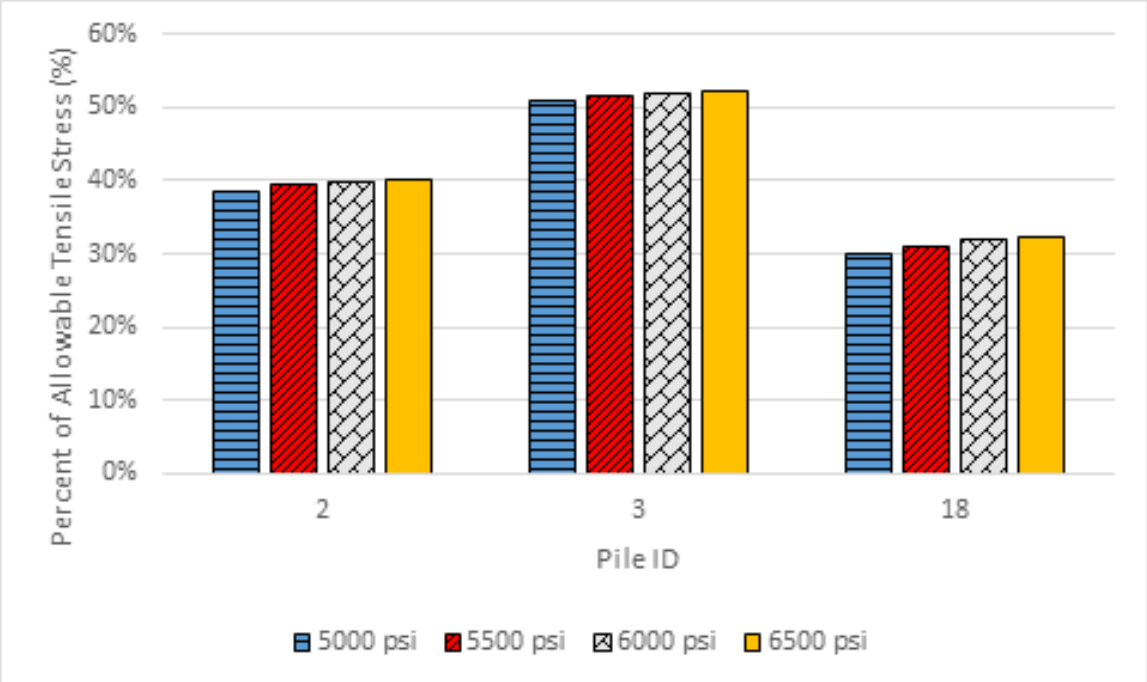

Figure 7-17: Percentage of allowable tensile stress achieved during 20 inch test pile installations.

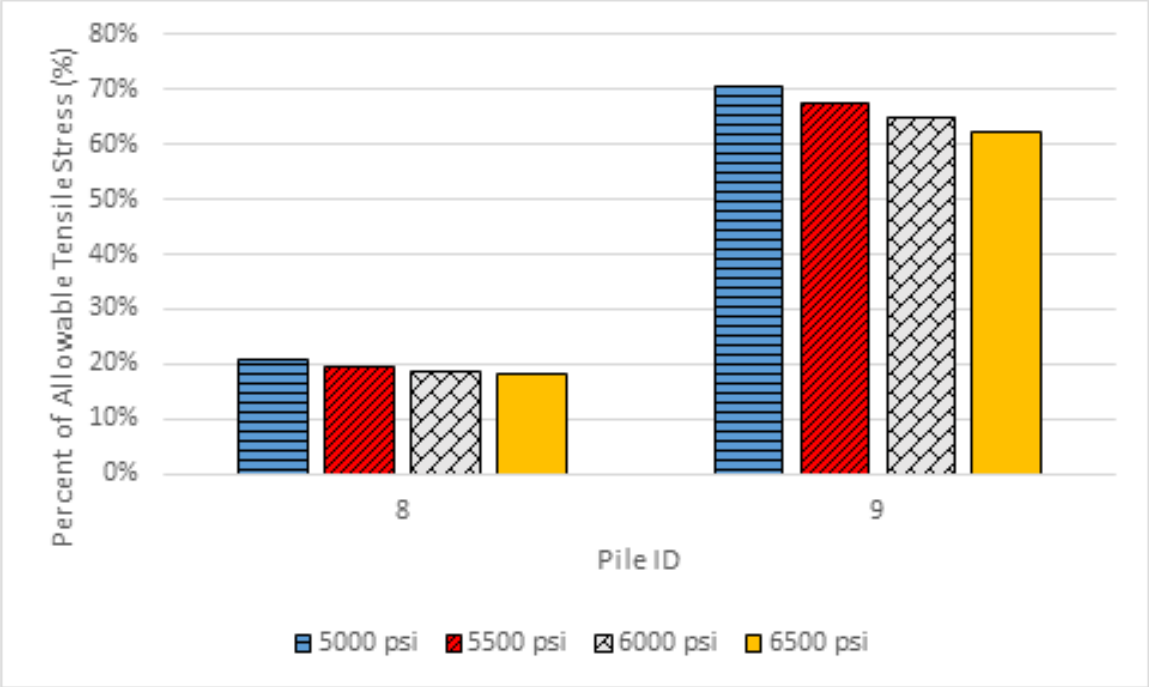

Figure 7-18: Percentage of allowable tensile stress achieved during 30 inch test pile installations.

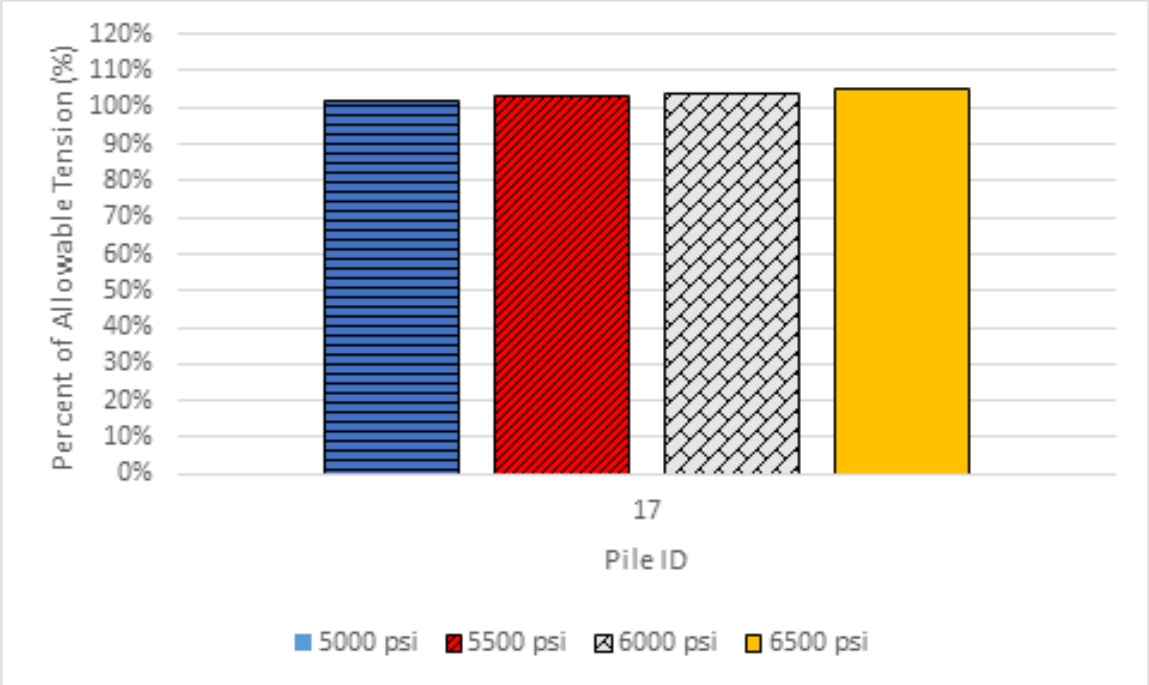

Figure 7-19: Percentage of allowable tensile stress achieved during 36 inch test pile installations.

The observed change in the percentage of achieved allowable tension resulting at incremental increases in concrete strength was less uniform than that of achieved allowable compression. In response to incremental increases in compressive concrete strength, the percentage of achieved

allowable tension increased for 24 inch test piles, decreased for 30 inch test piles, and fluctuated between increasing and decreasing values for 14, 16, and 20 inch test piles. This varied response can be attributed to subtle changes in both the allowable tensile stress limits and maximum tensile driving stresses resulting at each incremental increases in concrete strength. On average, a 500 psi increase in compressive concrete strength increased the allowable tensile stress limit of the test piles by 1.3 percent and the maximum tensile driving stress incurred by the pile by 0.11 percent. Therefore, the percentage of achieved allowable tension varied little with increased compressive concrete strength.

The driving stress analysis performed on the test pile installations revealed that the maximum driving stresses incurred during installation were often well below allowable stress limits. Therefore, it may be possible to generate increased pile capacity through extending pile embedment without subjecting the pile to damaging driving stresses.

7.6.3. Pile Capacity Determination of the Installed Test Piles

The determination of the GRLWEAP predicted capacity of original test piles was primarily conducted to establish baseline capacities that could be utilized to evaluate the feasibility of installing reduced size piles to achieve original test pile capacity. In addition to satisfying the needs of reduced size pile analysis, the determination of GRLWEAP generated capacities presented an opportunity to evaluate the accuracy of GRLWEAP capacity predictions. GRLWEAP numeric output served as the primary source from which ultimate pile capacity values were obtained. Each test pile was initially analyzed at shaft and toe gain/loss factors of 1 to determine GRLWEAP predicted ultimate pile capacity. In an attempt to validate the accuracy of GRLWEAP pile capacity predictions, the GRLWEAP predicted ultimate capacity of each test pile was compared to design and static load test capacities provided within the pile driving records obtained from ALDOT. Static load tests are often compared with twice the design loads in the state of Alabama, so this study will utilize this value as a point of comparison. The results of this comparison are presented in Figure 7-20 to Figure 7-25, separated by pile size.

The GRLWEAP manual indicates that GRLWEAP capacity predictions obtained from correlation between wave equation analyses and actual pile driving blow counts typically vary from static load test results by at least a 10 percent difference (Pile Dynamics, 2010). Therefore, it was anticipated that the GRLWEAP generated capacities would vary from those provided within the pile records. The results of capacity comparison revealed that on average, GRLWEAP predicted capacity exceeded twice the design load capacity by 34.2 percent and exceeded the static load test capacity by 8.1 percent. Static load testing is generally considered the most accurate estimator of pile capacity. Therefore, the comparison of GRLWEAP predicted pile capacity to static load test capacity served as the primary means of accessing the accuracy of GRLWEAP pile capacity predictions. This comparison revealed GRLWEAP generated pile capacity to be within 8.1 percent of corresponding static load test determined pile capacity; therefore, indicating GRLWEAP to be an adequate predictor of pile capacity.

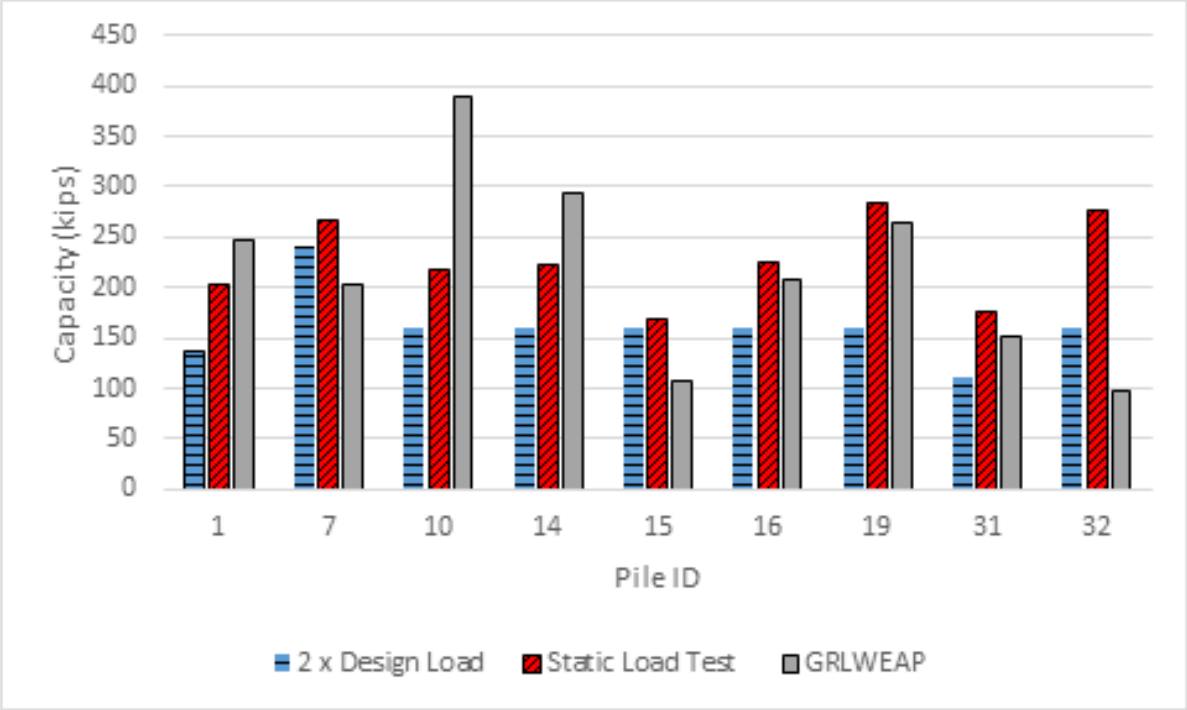

Figure 7-20: Test pile capacity comparison of 14 inch piles

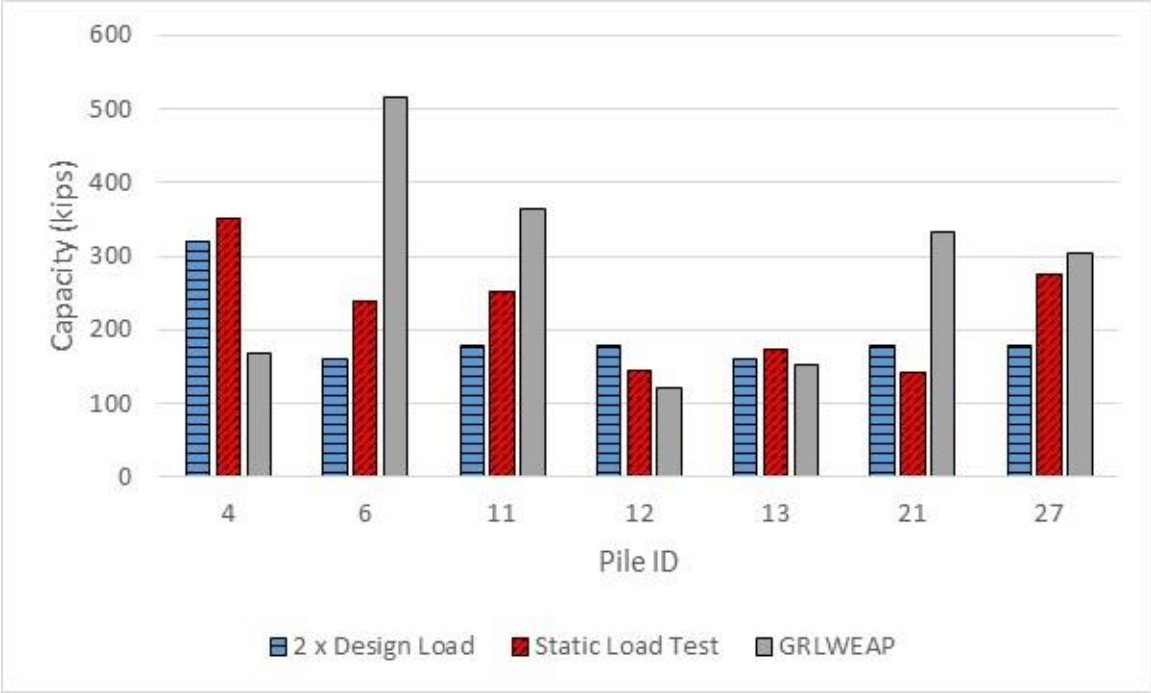

Figure 7-21: Test pile capacity comparison of 16 inch piles

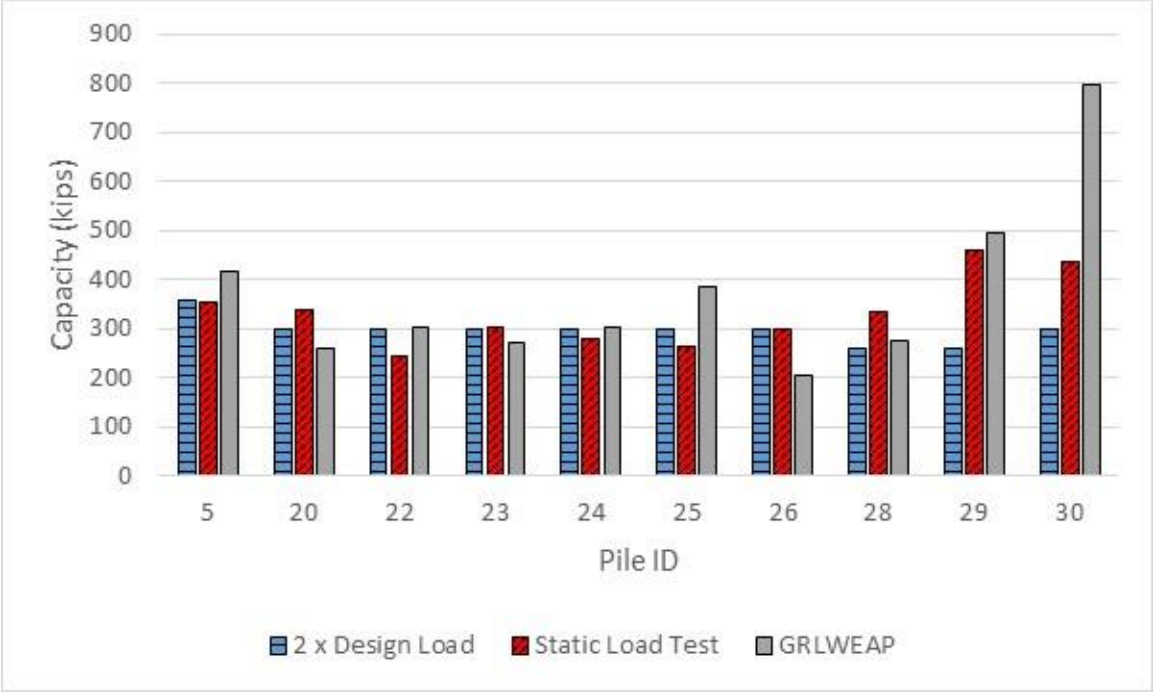

Figure 7-22: Test pile capacity comparison of 20 inch piles

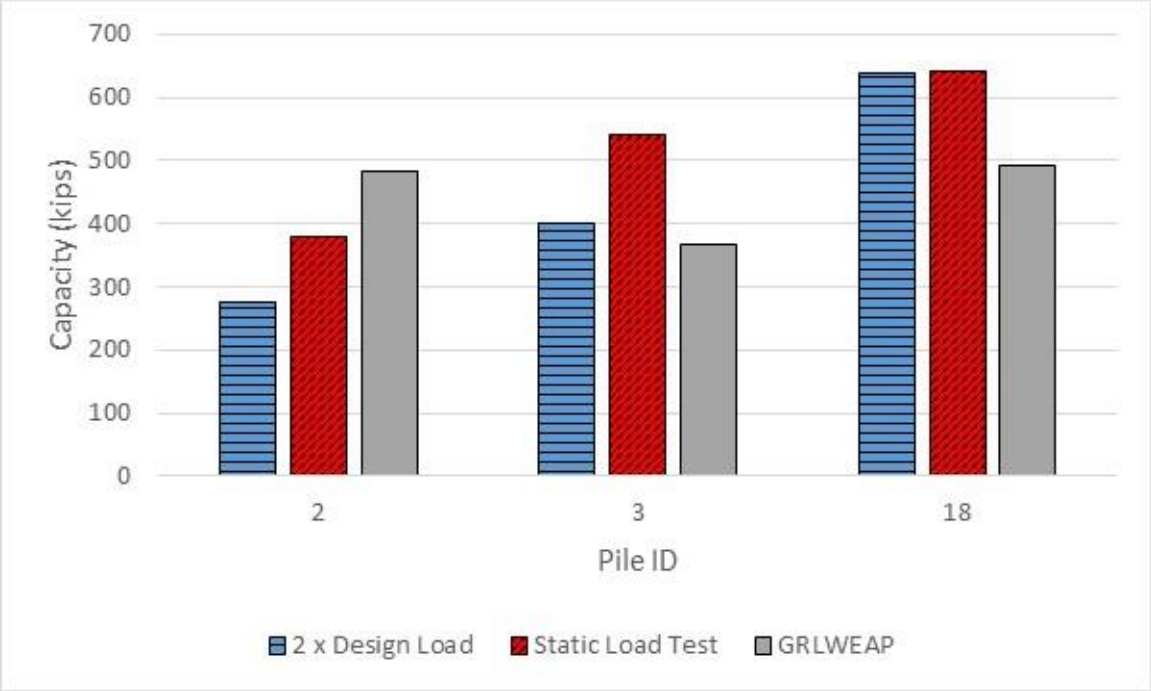

Figure 7-23: Test pile capacity comparison of 24 inch piles

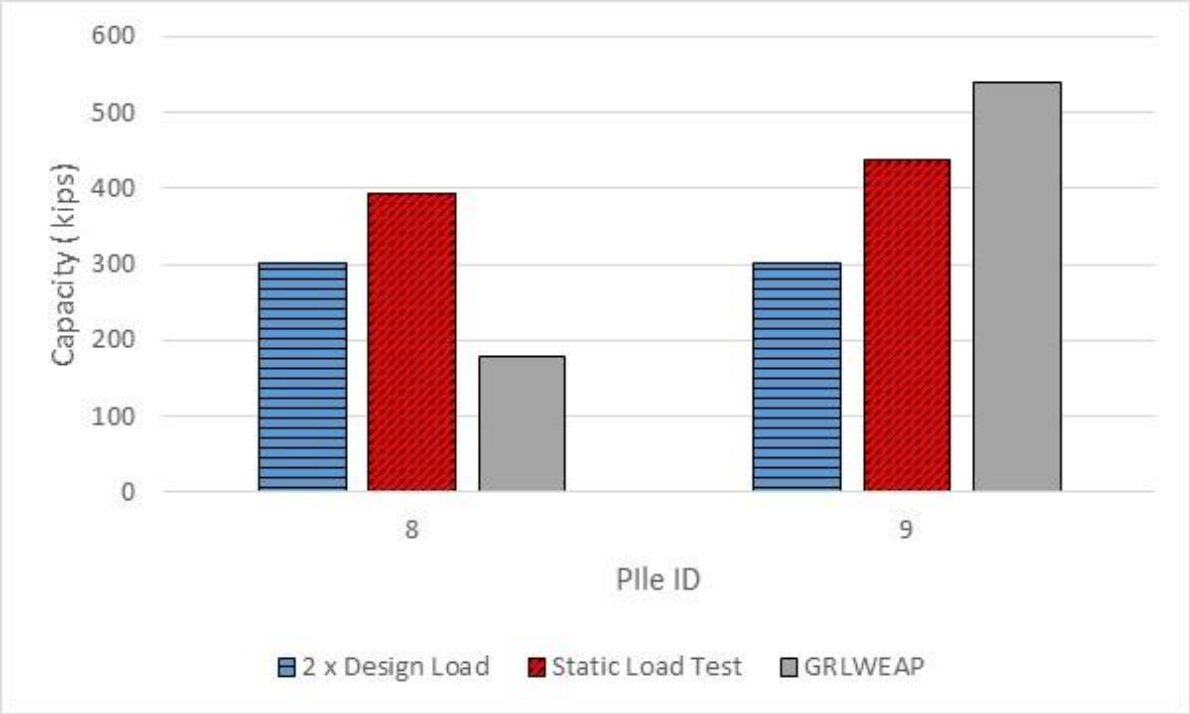

Figure 7-24: Test pile capacity comparison of 30 inch piles

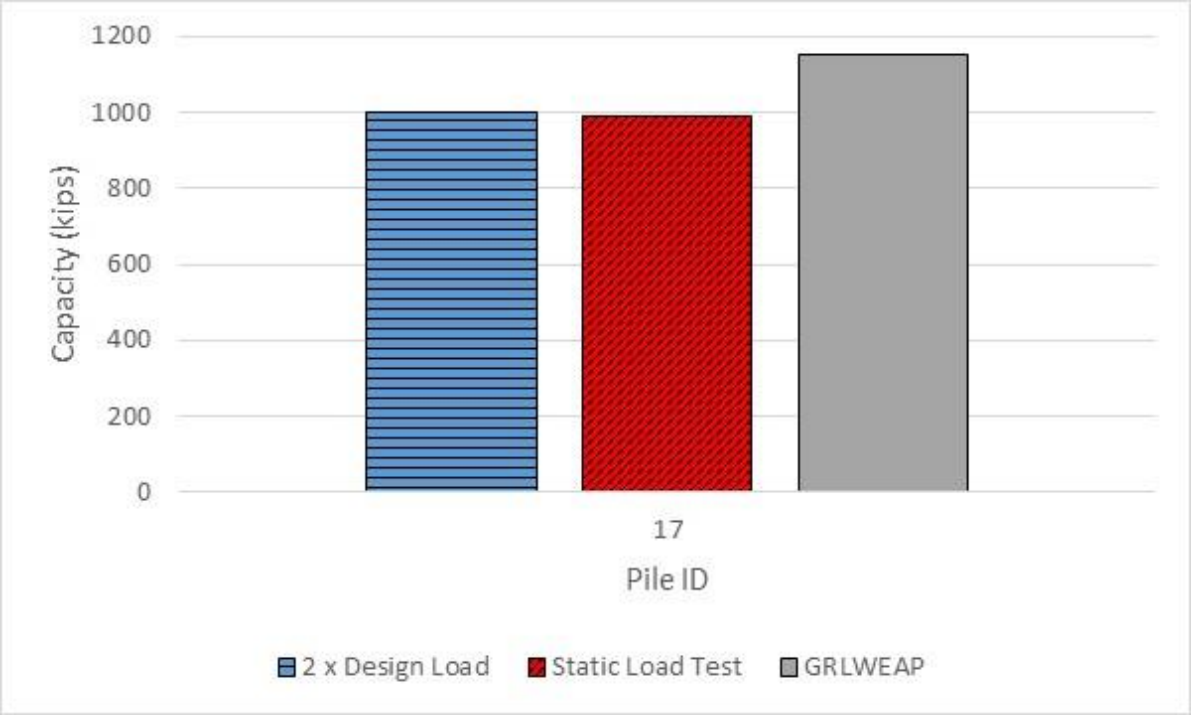

Figure 7-25: Test pile capacity comparison of 36 inch piles

In an effort to assess the adequacy of current ALDOT PPC pile axial load limits, the GRLWEAP predicted and static load test capacities of each test pile were compared to ALDOT allowable axial load limits specified for each pile size. This comparison is presented in Figure 7-26 to Figure 7-31, separated by pile size.

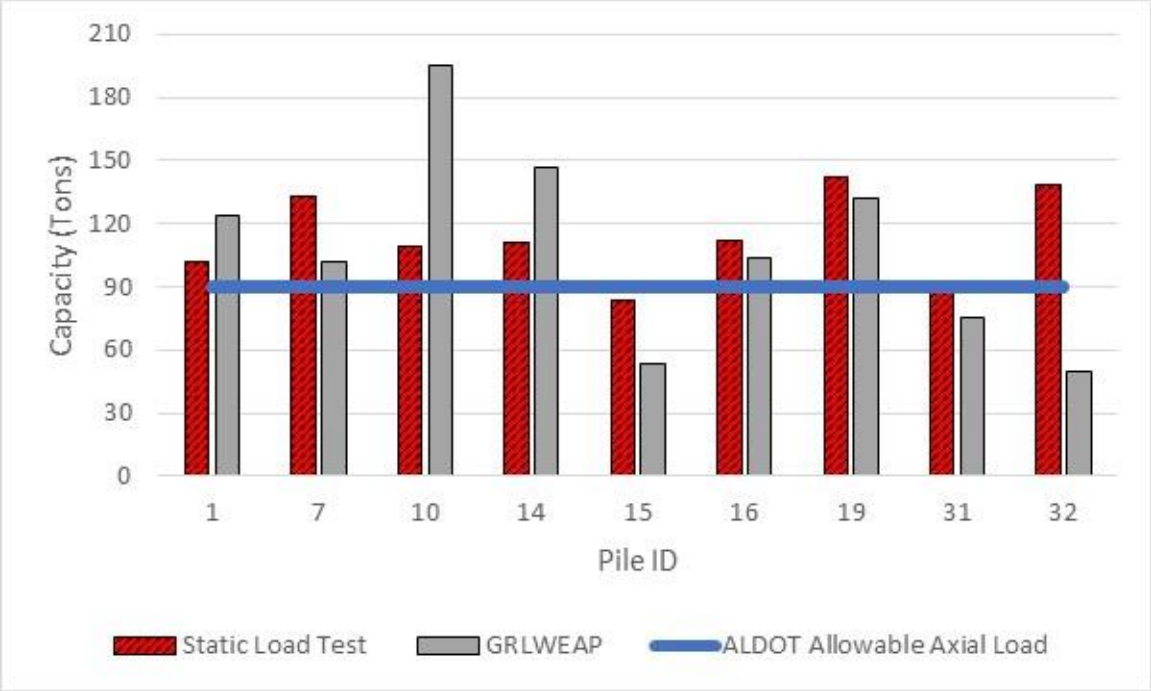

Figure 7-26: Comparison of 14 inch test pile capacity to ALDOT allowable axial load limit.

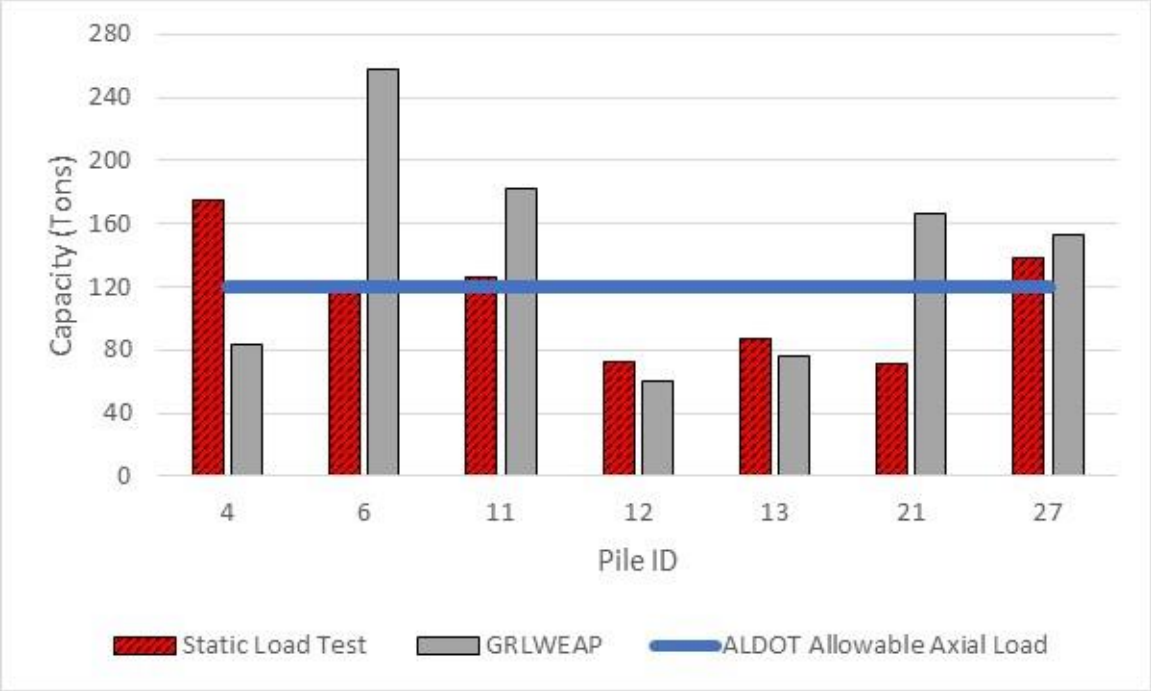

Figure 7-27: Comparison of 16 inch test pile capacity to ALDOT allowable axial load limit.

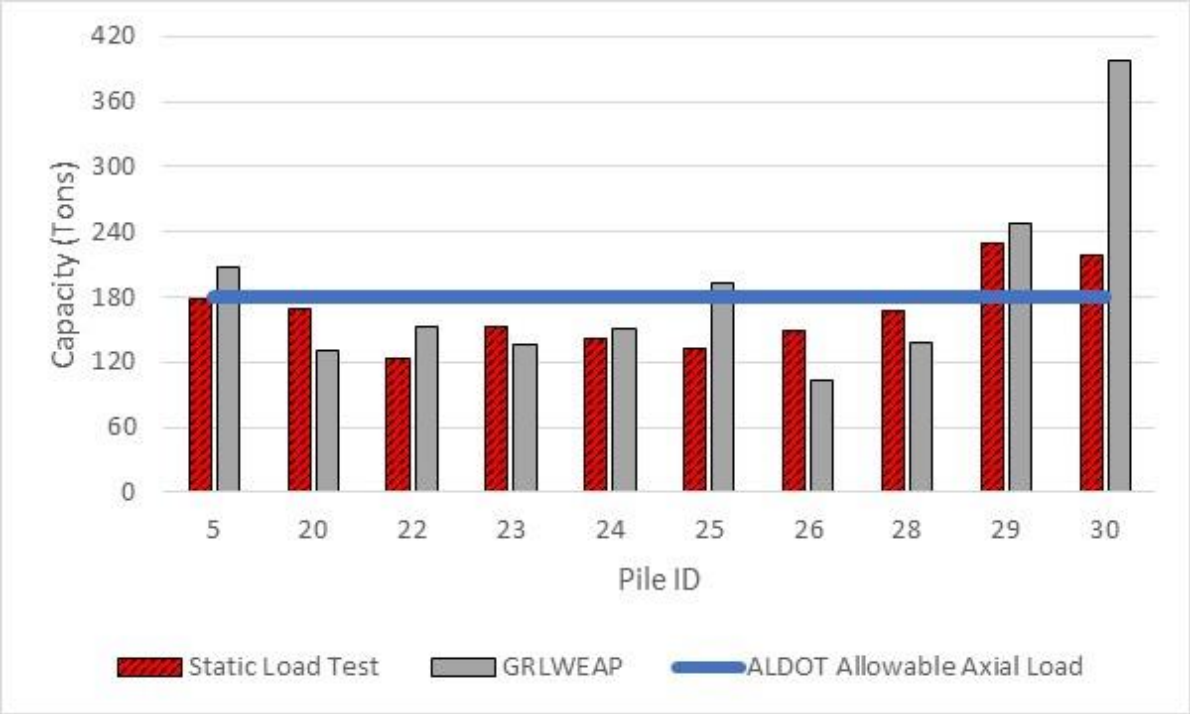

Figure 7-28: Comparison of 20 inch test pile capacity to ALDOT allowable axial load limit.

Figure 7-29: Comparison of 24 inch test pile capacity to ALDOT allowable axial load limit.

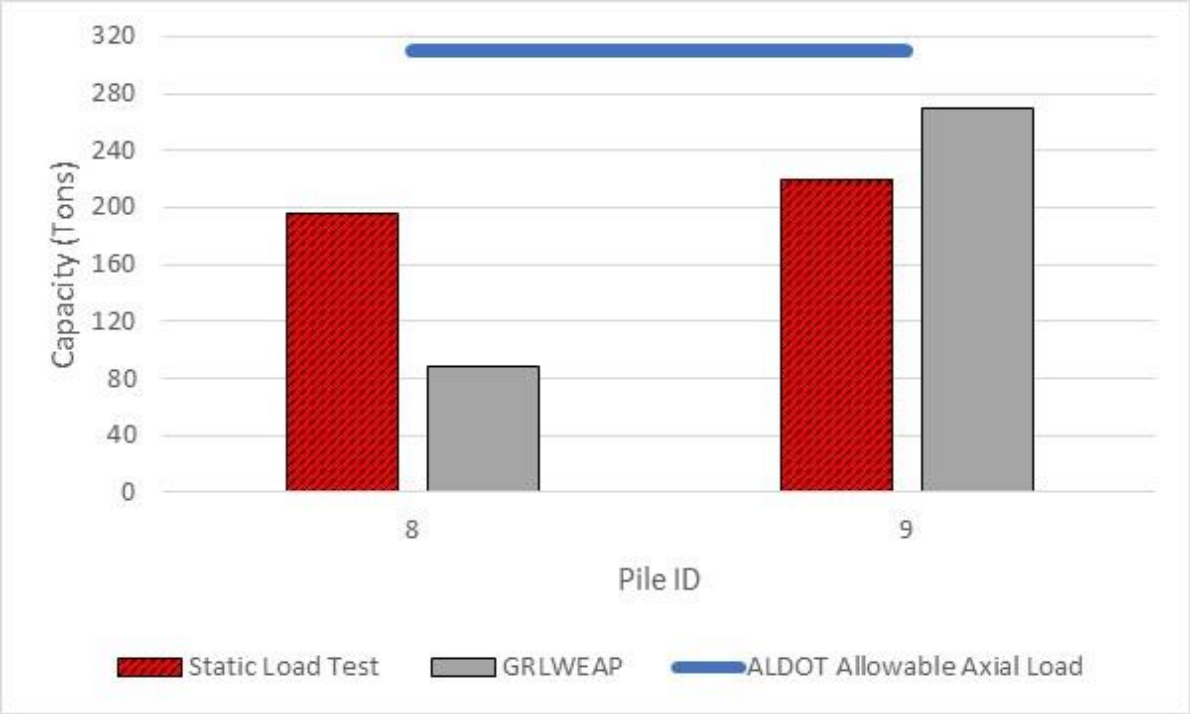

Figure 7-30: Comparison of 30 inch test pile capacity to ALDOT allowable axial load limit.

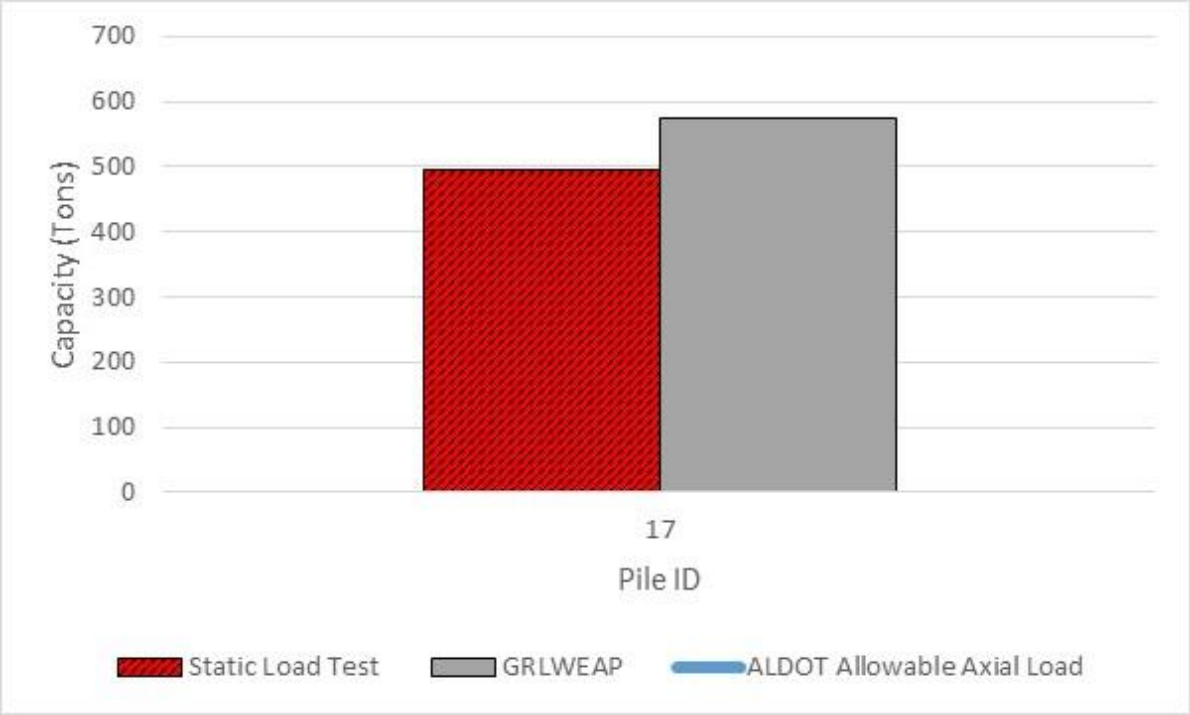

Figure 7-31: Comparison of 36 inch test pile capacity to ALDOT allowable axial load limit.

Based on Figure 7-20 to Figure 7-25, geotechnical design load is about half of the tested capacity values. As such, the efficiency of design between the geotechnical resistance and the structural load capacity is similar. Also, there appears to be room for increase of the structural load capacity limits,

especially with those piles that have values near the allowable load lines indicated by Figure 7-26 to Figure 7-31.

Each original test pile was categorized based on the soil type about the pile toe and the predominant soil type along the embedded pile shaft as indicated by Table 7-5. Table 7-8 presents the soil type based categorization of each installed test pile. The categorization of each pile by soil type was performed to potentially identify any correlations that might exist between soil type and driving stress. Twenty-three of the existing thirty-two test piles were categorized as soil type 1, which reveals the majority of the soil along the shaft of the pile is sand and the pile also tips in sand. Of the remaining nine piles, five were categorized as soil type 3 (majority of the shaft encounters clay, but tips in sand), three were categorized as soil type 4 (tips in clay, yet the majority of the shaft encounters sand), and one was categorized as soil type 6 (majority of the shaft encounters clay and also tips in clay). An interesting observation was made as a result of soil type categorization involving the fact that four of the existing piles were tipped in clay. Tipping of a pile in a clay material when layers of dense sand are present near the depth of the pile tip is often not standard geotechnical engineering practice. For this reason, it is believed that the soil stratigraphy of the sites corresponding to these particular pile installations was altered by cut or fill at some point after soil boring logs were drilled, but before the piles were installed. These presumed site modifications were not specified within the pile records and therefore were not implemented into the analysis. This raises a potential error in the analysis. After consultation with ALDOT personnel, it was determined that accurate depictions of the site surfaces after the boring logs were generated could not be acquired.

Table 7-8: Classification of soils encountered along the shaft and at the toe of each test pile.

Size (in)	Pile ID	TOE	Shaft		Type
			Sand %	Clay %	
14	1	Sand	100	0	**1**
	7	Sand	100	0	**1**
	10	Sand	100	0	**1**
	14	Sand	100	0	**1**
	15	Sand	100	0	**1**
	16	Sand	47	53	**3**
	19	Sand	100	0	**1**
	31	Sand	44.6	55.4	**3**
	32	Sand	44.6	55.4	**3**
16	4	Sand	68.75	31.25	**1**
	6	Sand	87.3	12.7	**1**
	11	Sand	100	0	**1**
	12	Sand	76.7	23.3	**1**
	13	Sand	100	0	**1**
	21	Sand	72.2	27.8	**1**
	27	Sand	94	6	**1**
20	5	Sand	60.8	39.2	**3**
	20	Clay	53.1	46.9	**6**
	22	Sand	80	20	**1**
	23	Sand	100	0	**1**
	24	Sand	66.5	33.5	**1**
	25	Clay	88.6	11.4	**4**
	26	Clay	76.5	23.5	**4**
	28	Sand	100	0	**1**
	29	Sand	92.4	7.6	**1**
	30	Sand	56.1	43.9	**3**
24	2	Sand	100	0	**1**
	3	Sand	100	0	**1**
	18	Sand	100	0	**1**
30	8	Clay	85.1	14.9	**4**
	9	Sand	100	0	**1**
36	17	Sand	100	0	**1**

7.7. Driving Stress Results of the Reduced Sized Piles

Following the analysis of original test pile installations, reduced size piles were similarly analyzed as if they were installed at the same locations. This analysis required that each reduced size piles length and embedment be adjusted so that reduced size pile could achieve original test pile capacity. GRLWEAP software was used to estimate reduced size pile capacity. Due to smaller cross-sectional area, reduced size pile embedment had to increase in order to achieve original test pile capacity. Once the appropriate length and embedment of the reduced size pile was established, maximum driving stresses were again determined. Maximum driving stresses were then analyzed to evaluate the change in maximum driving stresses resulting from incremental increases in the

compressive concrete strength of the pile. The maximum driving stresses incurred by each pile at each analyzed compressive concrete strength were then compared with corresponding allowable driving stress limits. The percentage of allowable compressive and tensile driving stress achieved by original and reduced sized piles utilizing 5000 psi concrete was also compared.

7.7.1. Determination of the Pile Lengths of the Reduced Size Piles

The analysis of reduced pile sizes required that GRLWEAP input parameters be set to those of a pile size smaller than those of original test piles to allow consistency throughout the analysis. Even though ALDOT does not allow 12 inch square PPC piles, 14 inch test piles were still analyzed at a reduced 12 inch size to evaluate the effectiveness of 12 inch pile utilization.

With appropriate parameters input into the GRLWEAP program, each reduced size pile was evaluated to determine the depth of embedment required to achieve the capacity of the original test pile at the same location. Consistent with original test pile capacity determination, gain/loss factors were set to 1 for the determination of reduced pile size embedment at which original test pile capacity could be achieved. The reduced size pile capacity often exceeded that of the original test pile due to the variability in resistance resulting from subsequent soil layers. However, the depth at which the original test pile capacity was achieved or exceeded was established as the required depth of embedment for the reduced size pile. The results of the reduced size pile analysis are presented in Table 7-9 which provides a comparison of reduced size pile capacity and embedment with that of the original test piles.

The embedment depth, and subsequently, the overall length of the reduced size piles were determined. Table 7-10 reveals that embedment depth was increased as the cross-sectional area of the pile was reduced, as anticipated. However, some piles required a significant increase in embedment, likely due to incomplete soil profile data and potential altering of the ground surface between boring and pile installation. For some of the piles, increased embedment resulted in a change of soil type classification. Table 7-10 provides the comparison of the soil type encountered by the original test piles to that of the reduced sized piles at the extended embedment required to achieve original test pile capacity.

Table 7-9: Original versus reduced pile size capacity and embedment depth.

Size (in)	Original Pile Size			Reduced Pile Size			Change in	
	Pile ID	Capacity (kips)	Emb. Depth (ft)	Size (in)	Capacity (kips)	Emb. Depth (ft)	Capacity (kips)	Emb. Depth (ft)
14	1	247.6	34	12	318.6	47.5	71	13.5
	7	203.1	43		210	48	6.9	5
	10	390.1	30.7		393.7	87.7	3.6	57
	14	292.9	46.5		343	78.5	50.1	32
	15	106.2	38		228.8	44	122.6	6
	16	206.7	69		206.9	75	0.2	6
	19	263.8	59		267.2	77	3.4	18
	31	150.9	46		244.3	73	93.4	27
	32	98.7	65		244.2	73	145.5	8
16	4	167.1	32	14	212.4	39.6	45.3	7.6
	6	514.7	47		518.4	78	3.7	31
	11	364.8	32		371.6	63	6.8	31
	12	121.3	45		239.1	48	117.8	3
	13	152	37		153.8	42	1.8	5
	21	333.6	57.6		334.9	94	1.3	36.4
	27	305.4	50		306	71	0.6	21
20	5	415.9	48.44	18	431.3	79	15.4	30.56
	20	259.7	66		265.9	71	6.2	5
	22	305.2	75		310.8	95	5.6	20
	23	271.3	55		273.5	64	2.2	9
	24	302.7	65.5		305.3	90	2.6	24.5
	25	387.2	79		392.2	101	5	22
	26	206.2	68		208	72	1.8	4
	28	275.1	46		277.9	55	2.8	9
	29	494.3	65.4		748.1	68	253.8	2.6
	30	795.6	66		798.2	97.5	2.6	31.5
24	2	482.8	35	20	792.2	48	309.4	13
	3	365.8	34		903.7	48	537.9	14
	18	493.2	71		494.4	85	1.2	14
30	8	178	26.5	24	184	28	6	1.5
	9	539	52.6		565.1	62	26.1	9.4
36	17	1150.4	83.5	30	1161.7	126	11.3	42.5

Table 7-10: Soil type classification of reduced pile sizes

Original Pile						Reduced Pile					
Size (in)	Pile ID	TOE	Shaft		Type	Size (in)	Pile ID	TOE	Shaft		Type
			Sand %	Clay %					Sand %	Clay %	
14	1	Sand	100	0	1	12	1	Sand	100	0	1
	7	Sand	100	0	1		7	Sand	100	0	1
	10	Sand	100	0	1		10	Sand	97.7	2.3	1
	14	Sand	100	0	1		14	Sand	100	0	1
	15	Sand	100	0	1		15	Sand	100	0	1
	16	Sand	47	53	3		16	Sand	50	50	3
	19	Sand	100	0	1		19	Sand	100	0	1
	31	Sand	44.6	55.4	3		31	Sand	51	49	3
	32	Sand	44.6	55.4	3		32	Sand	51	49	3
16	4	Sand	68.75	31.25	1	14	4	Sand	62.2	37.8	3 *
	6	Sand	87.3	12.7	1		6	Sand	92.4	7.6	1
	11	Sand	100	0	1		11	Sand	100	0	1
	12	Sand	76.7	23.3	1		12	Sand	78.2	21.8	1
	13	Sand	100	0	1		13	Sand	100	0	1
	21	Sand	72.2	27.8	1		21	Clay	48.4	51.6	6 *
	27	Sand	94	6	1		27	Sand	95.8	4.2	1
20	5	Sand	60.8	39.2	3	18	5	Sand	76	24	1 *
	20	Clay	53.1	46.9	6		20	Clay	49.3	50.7	6
	22	Sand	80	20	1		22	Clay	70.5	29.5	4 *
	23	Sand	100	0	1		23	Sand	100	0	1
	24	Sand	66.5	33.5	1		24	Clay	53.3	46.7	6 *
	25	Clay	88.6	11.4	4		25	Clay	69.3	30.7	4
	26	Clay	76.5	23.5	4		26	Clay	72.2	27.8	4
	28	Sand	100	0	1		28	Sand	88.2	11.8	1
	29	Sand	92.4	7.6	1		29	Sand	92.7	7.3	1
	30	Sand	56.1	43.9	3		30	Sand	70.3	29.7	1 *
24	2	Sand	100	0	1	20	2	Sand	100	0	1
	3	Sand	100	0	1		3	Sand	79.2	20.8	1
	18	Sand	100	0	1		18	Sand	100	0	1
30	8	Clay	85.1	14.9	4	24	8	Sand	81.5	18.5	1 *
	9	Sand	100	0	1		9	Sand	100	0	1
36	17	Sand	100	0	1	30	17	Sand	84.9	15.1	1

Note: (*) indicates a change in soil type from original to reduced pile sizes

Comparison of original test and reduced size pile soil types revealed that the extended embedment corresponding to reduced pile sizes caused the soil type classification of seven reduced size piles to vary from that of the original test pile. Therefore, the soil composition surrounding these seven piles was significantly altered as embedment was increased. It was also noted that six of the reduced size piles achieved original test pile capacity at a depth in which the pile was tipped in clay, which is often not common practice. However, the embedment of these piles was not altered due to a primary goal of research being the determination of the exact depth of embedment at which the reduced size pile could achieve the capacity of the original test pile.

7.7.2. Driving Stress Determination of the Reduced Size Piles

Following the determination of reduced size pile embedment, the length of each reduced size pile was established as to produce a pile top elevation consistent with that of the corresponding original test pile. The driving stress analysis of the reduced size piles was then performed utilizing GRLWEAP generated gain/loss factors. Driving stresses resulting from reduced size pile installation were initially

analyzed using the design compressive concrete strength of 5000 psi. The maximum compressive and tensile driving stresses resulting at 5000 psi compressive concrete strength were recorded and utilized as the baseline values from which the change in driving stress resulting from incremental increases in compressive concrete strength could be evaluated. Following the establishment of baseline driving stresses, each reduced size pile was reevaluated at incremental increases in compressive concrete strength including 5500, 6000, and 6500 psi. The maximum driving stresses resulting from each increase in compressive concrete strength were determined and recorded. These values were then compared to the maximum driving stresses occurring at the compressive concrete strength of 5000 psi and used calculate the percentage change in maximum compressive and tensile driving stress resulting from each increase in compressive concrete strength. Table 7-11 presents the maximum compressive driving stress occurring during each reduced size pile installation utilizing 5000 psi concrete as well as the percentage change in maximum compressive driving stress occurring at each adjustment in compressive concrete strength.

Table 7-11: Comparison of maximum compressive driving stresses when the compressive concrete strength of the reduced size pile is increased.

Size (in)	Pile ID	Original Concrete Compressive Strength (psi)	Change in Concrete Compressive Strength (psi)		
		5000	5500	6000	6500
		Maximum Compressive Driving Stress (ksi)	Percent Change in Compressive Driving Stress (%)		
12	1	2.648	-0.23%	-0.19%	-0.49%
	7	2.18	0.60%	0.78%	1.01%
	10	2.782	-0.14%	-0.14%	-0.18%
	14	2.237	0.04%	0.18%	0.58%
	15	2.275	-0.31%	-0.40%	-0.70%
	16	2.15	0.47%	0.93%	1.63%
	3	2.735	0.15%	-0.04%	-0.11%
	31	2.129	0.66%	1.13%	1.27%
	32	2.138	0.56%	1.12%	1.45%
		Avg.	**0.20%**	**0.37%**	**0.49%**
14	4	1.995	0.55%	1.00%	1.00%
	6	2.325	-0.43%	-0.86%	-1.33%
	11	2.286	-0.39%	-1.18%	-1.49%
	12	2.001	0.50%	0.75%	1.15%
	13	1.959	0.26%	0.66%	0.87%
	21	2.068	0.73%	1.11%	1.64%
	27	1.783	0.56%	1.07%	1.29%
		Avg.	**0.25%**	**0.36%**	**0.45%**
18	5	2.029	0.44%	0.79%	1.18%
	20	1.571	0.32%	0.45%	0.83%
	22	1.607	0.81%	1.31%	1.62%
	23	1.581	0.44%	0.82%	1.14%
	24	1.171	0.43%	0.85%	1.37%
	25	1.658	0.54%	0.97%	1.33%
	26	1.505	0.47%	0.86%	1.26%
	28	1.56	0.26%	0.58%	0.83%
	29	2	-0.10%	-0.10%	-0.35%
	30	2.136	0.05%	0.05%	-0.09%
		Avg.	**0.37%**	**0.66%**	**0.91%**
20	2	1.802	-0.22%	-0.55%	-0.83%
	3	1.63	0.31%	0.74%	1.04%
	18	1.532	0.46%	0.78%	1.70%
		Avg.	**0.18%**	**0.32%**	**0.64%**
24	8	1.678	0.60%	0.89%	1.25%
	9	1.927	0.47%	0.78%	1.45%
		Avg.	**0.53%**	**0.84%**	**1.35%**
30	17	2.136	0.94%	1.78%	0.14%
		Avg.	**0.94%**	**1.78%**	**0.14%**

Table 7-11 reveals that increasing the compressive concrete strength of pile resulted in slight variations in maximum compressive driving stress. Some piles responded to increased concrete strength with slight increases in maximum compressive driving stress, while others responded with slight decreases in maximum compressive driving stress. The Results indicate that varying the compressive concrete strength of pile from 5000 psi to 6500 psi has minimal impact upon compressive driving stress. Table 7-12 provides a summary of Table 14 and presents the average percentage change in maximum compressive driving stress for all reduced size piles resulting from increasing the compressive concrete strength of the pile from 5000 psi to 5500, 6000, and 6500 psi.

Table 7-12: Average percentage change in maximum compressive driving stress when the compressive concrete strength of the pile is increased.

Change in Concrete Compressive Strength (psi)		
5500	6000	6500
Avg. Percent Change in Compressive Driving Stress (%)		
0.30%	0.51%	0.66%

Table 7-12 reveals that on average, increasing the compressive concrete strength of pile from 5000 psi to 5500, 6000, 6500 psi results in small increases in compressive driving stress. Table 7-13 presents the maximum tensile stress occurring during each reduced size pile installation utilizing 5000 psi concrete as well as the percentage change in maximum tensile driving stress occurring at each increase in compressive concrete strength. Table 7-13 indicates a varied response of maximum tensile driving stress to incremental increases in the compressive concrete strength of the pile. For some of the piles, an increase in compressive concrete strength resulted in increased tensile driving stress; for others, an increase in compressive concrete strength resulted in a decrease in tensile driving stress. The one consistency for all evaluated piles was that the variation in tensile driving stress resulting from incremental increases in compressive concrete strength were relatively small. Therefore, varying the compressive concrete strength of the pile had minimal impact upon maximum tensile driving stresses induced during pile installation.

Table 7-14 provides a summary of Table 7-13 and presents the average percentage change in maximum tensile driving stress for all reduced size piles resulting from increasing the compressive concrete strength of the pile from 5000 psi to 5500, 6000, and 6500 psi. The results of the maximum driving stress analysis performed on each reduced size pile utilizing varying concrete compressive strengths were consistent with those corresponding to original test piles. On average, the results indicate that increasing concrete compressive strength at increments of 500 psi from 5000 to 6500 psi results in a slight increase in both maximum compressive and tensile driving stresses. However, the percentage by which driving stresses varied with increases in compressive concrete strength is very small. Therefore, increasing the compressive concrete strength of the pile would likely have minimal impact upon the maximum driving stresses induced during pile installation.

Table 7-13: Comparison of maximum tensile driving stresses when the compressive concrete strength of the reduced size pile is increased.

Size (in)	Pile ID	Original Concrete Compressive Strength (psi)	Change in Concrete Compressive Strength (psi)		
		5000	5500	6000	6500
		Maximum Tensile Driving Stress (ksi)	Percent Change in Tensile Driving Stress (%)		
12	1	0.451	-1.11%	-3.10%	-4.21%
	7	0.524	-2.48%	-5.92%	-8.78%
	10	0.834	1.32%	3.60%	5.40%
	14	0.733	1.36%	3.96%	6.55%
	15	0.65	-2.00%	-6.31%	-8.15%
	16	1.058	0.19%	0.85%	1.32%
	3	0.796	2.51%	4.27%	6.16%
	31	1.019	1.18%	2.26%	2.55%
	32	1.053	0.95%	2.47%	2.94%
		Avg.	**0.21%**	**0.23%**	**0.42%**
14	4	0.776	1.03%	0.90%	1.42%
	6	0.36	2.78%	3.89%	3.06%
	11	0.896	1.12%	2.34%	3.68%
	12	0.696	0.86%	0.86%	0.57%
	13	0.611	1.31%	2.29%	3.11%
	21	0.917	1.20%	2.73%	4.25%
	27	0.718	2.09%	2.92%	2.79%
		Avg.	**1.48%**	**2.28%**	**2.70%**
18	5	0.745	1.34%	1.88%	2.68%
	20	0.387	-4.13%	-9.30%	-15.25%
	22	0.703	1.85%	1.85%	2.99%
	23	0.508	-1.38%	-5.91%	-8.66%
	24	0.584	1.88%	1.88%	4.79%
	25	0.672	1.64%	3.12%	4.32%
	26	0.553	-1.63%	-5.42%	-8.32%
	28	0.358	-0.84%	-1.68%	-1.96%
	29	0.644	2.02%	1.09%	0.47%
	30	0.845	0.47%	1.07%	1.18%
		Avg.	**0.12%**	**-1.14%**	**-1.77%**
20	2	0.213	0.47%	0.47%	0.47%
	3	0.33	2.12%	3.64%	4.85%
	18	0.292	5.48%	9.93%	14.04%
		Avg.	**2.69%**	**4.68%**	**6.45%**
24	8	0.503	1.79%	4.37%	4.77%
	9	0.671	2.53%	3.43%	4.32%
		Avg.	**2.16%**	**3.90%**	**4.55%**
30	17	1.095	2.56%	4.93%	7.21%
		Avg.	**2.56%**	**4.93%**	**7.21%**

Table 7-14: Average percentage change in maximum tensile driving stress when concrete strength of the reduced size pile is increased.

Change in Concrete Compressive Strength (psi)		
5500	6000	6500
Avg. Percent Change in Tensile Driving Stress (%)		
0.89%	1.04%	1.27%

7.7.3. Comparison of Maximum Driving Stress to the Allowable Stress Limits of the Reduced Size Piles

The maximum driving stresses incurred by each reduced size pile at each compressive concrete strength were then compared to their corresponding allowable stress limits. The results of this comparison are provided in Figure 7-32 to Figure 7-43 indicating the percentage of allowable stress achieved during each pile installation at each compressive concrete strength. These figures are separated by pile size (12”, 14”, 18”, 20”, 24”, and 30”) and stress type (Compressive or Tensile). The percentage of allowable compressive stress achieved during each pile installation is presented in Figure 7-32 to Figure 7-37.

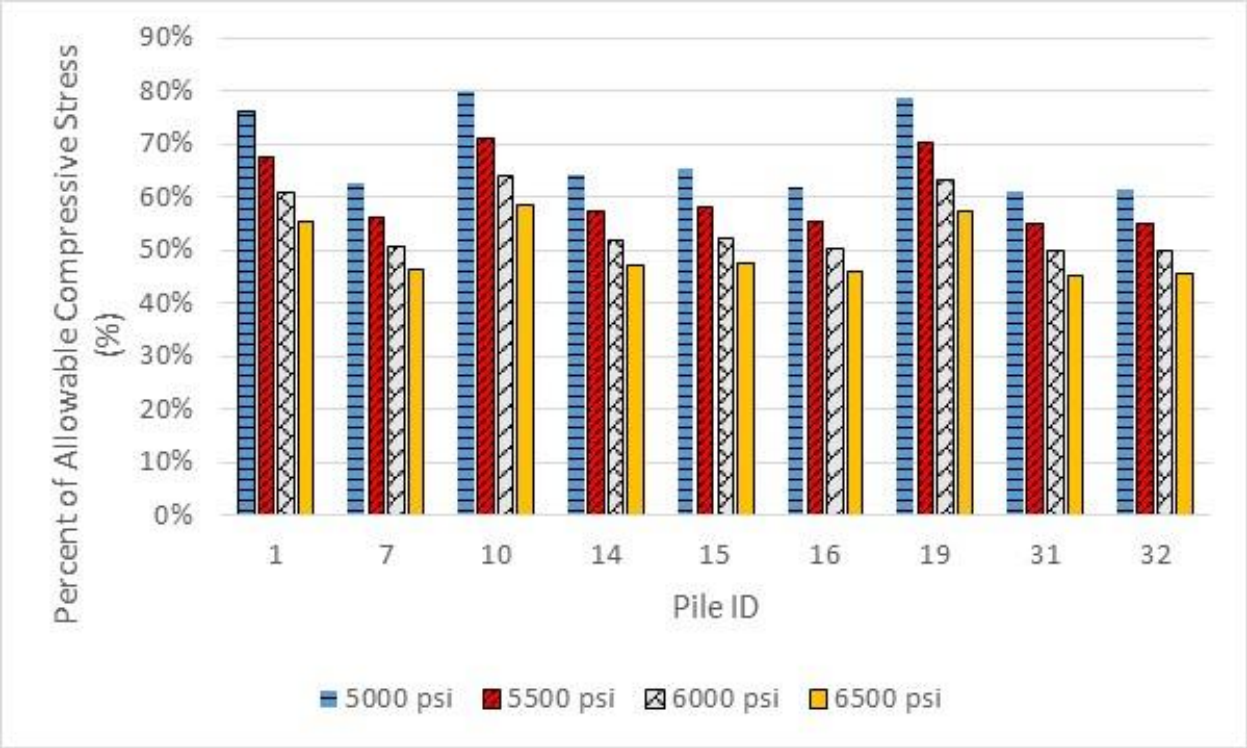

Figure 7-32: Percentage of allowable compressive stress achieved during 12” inch reduced size pile installations.

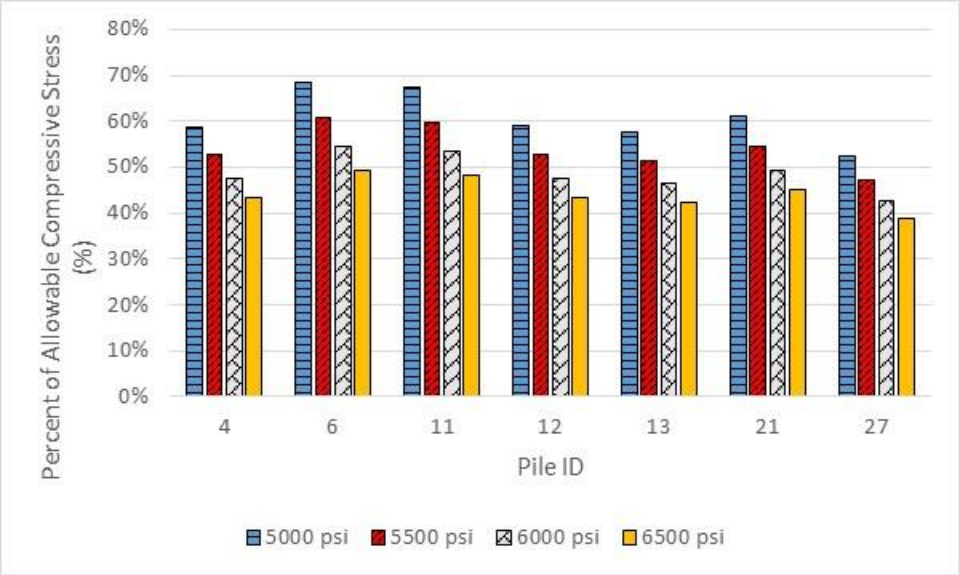

Figure 7-33: Percentage of allowable compressive stress achieved during 14" inch reduced size pile installations.

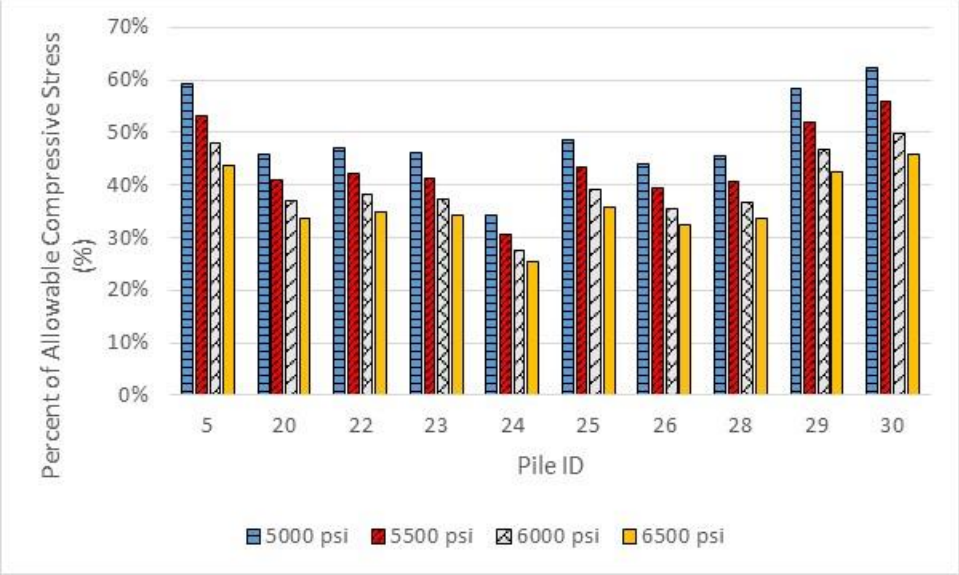

Figure 7-34: Percentage of allowable compressive stress achieved during 18" inch reduced size pile installations.

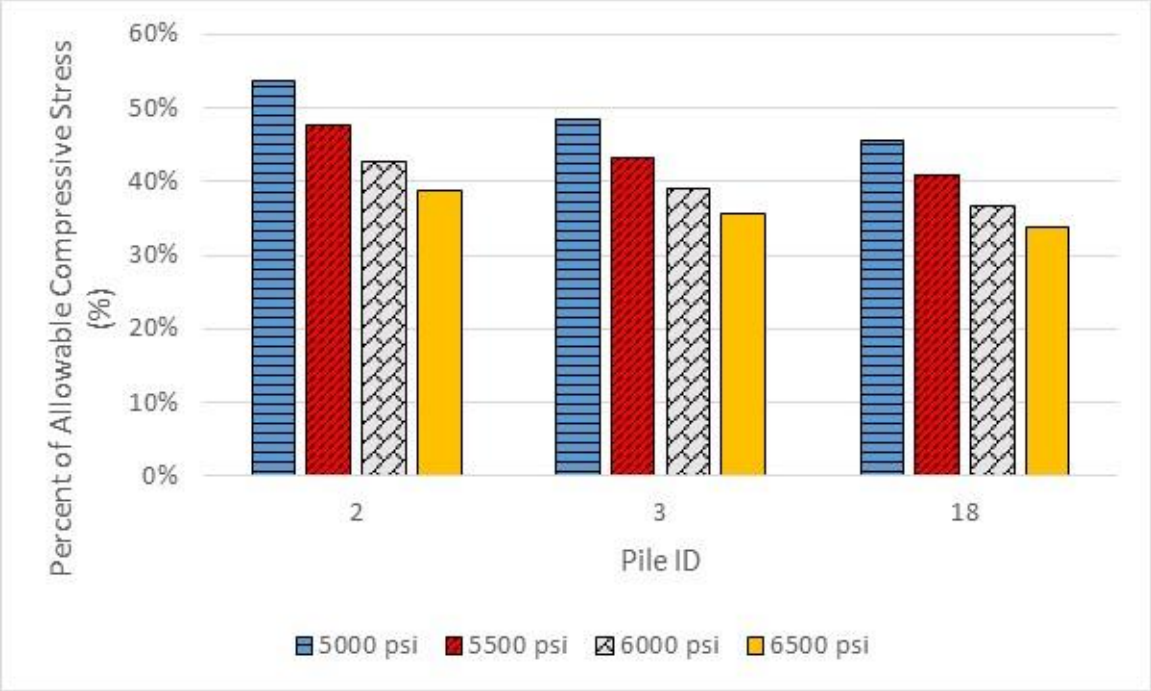

Figure 7-35: Percentage of allowable compressive stress achieved during 20” inch reduced size pile installations.

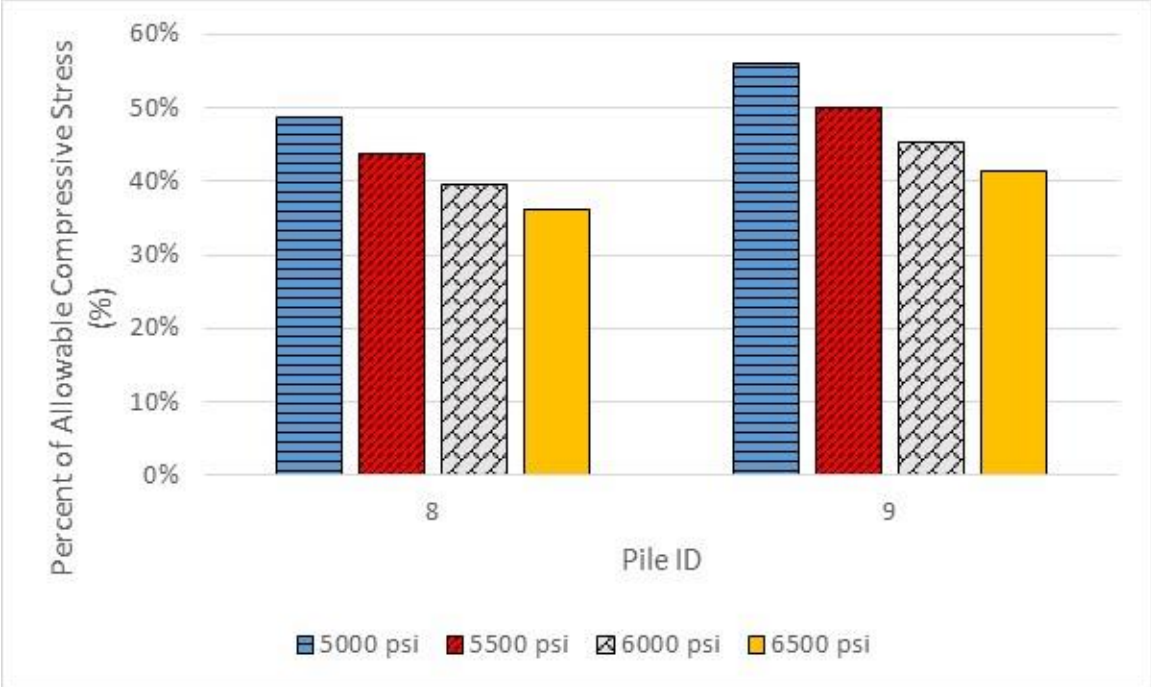

Figure 7-36: Percentage of allowable compressive stress achieved during 24” inch reduced size pile installations.

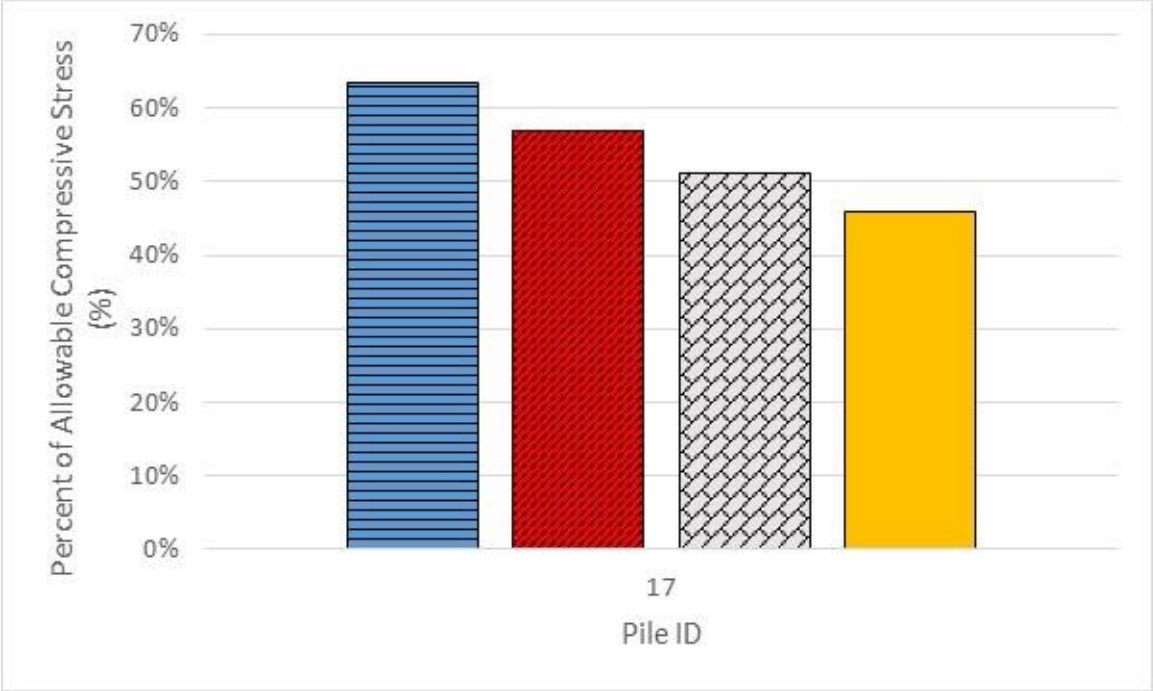

Figure 7-37: Percentage of allowable compressive stress achieved during 30" inch reduced size pile installations.

Figure 7-32 to Figure 7-37 reveal that none of the reduced size piles experienced maximum compressive driving stress exceeding estimated allowable compressive stress limits. Consistent with the original test pile analysis, the majority of the reduced size piles experienced maximum compressive driving stress that fell well short of exceeding estimated allowable compressive stress limits. Thus, results indicate that extending the embedment of the reduced size piles did not subject the piles to damaging compressive driving stress. The results also reveal that for each reduced size pile installation the percentage of achieved allowable compression decreased as compressive concrete strength increased. Consistent with the test pile analysis, increasing the compressive concrete strength of the reduced size pile had a more pronounced impact upon the allowable compressive driving stress limit of the pile than it did the actual maximum compressive driving stress incurred by the pile during installation. On average, a 500 psi increase in compressive concrete strength increased the allowable compressive stress limit of the reduced size piles by 11.3 percent, while the maximum compressive driving stress incurred by the pile only increased by 0.22 percent. As a result, the percentage of achieved allowable compression decreased with each increase in compressive concrete strength. The percentage of allowable tension achieved during each reduced size pile installation is presented in Figure 7-38 to Figure 7-43.

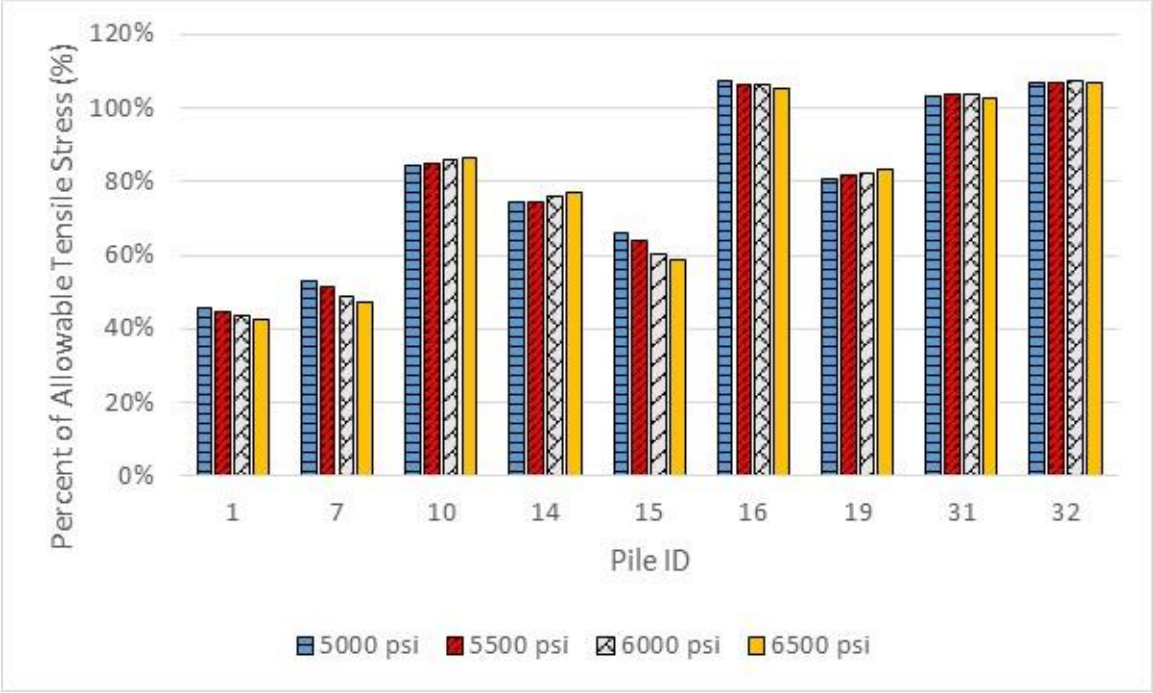

Figure 7-38: Percentage of allowable tensile stress achieved during 12 inch reduced size pile installations.

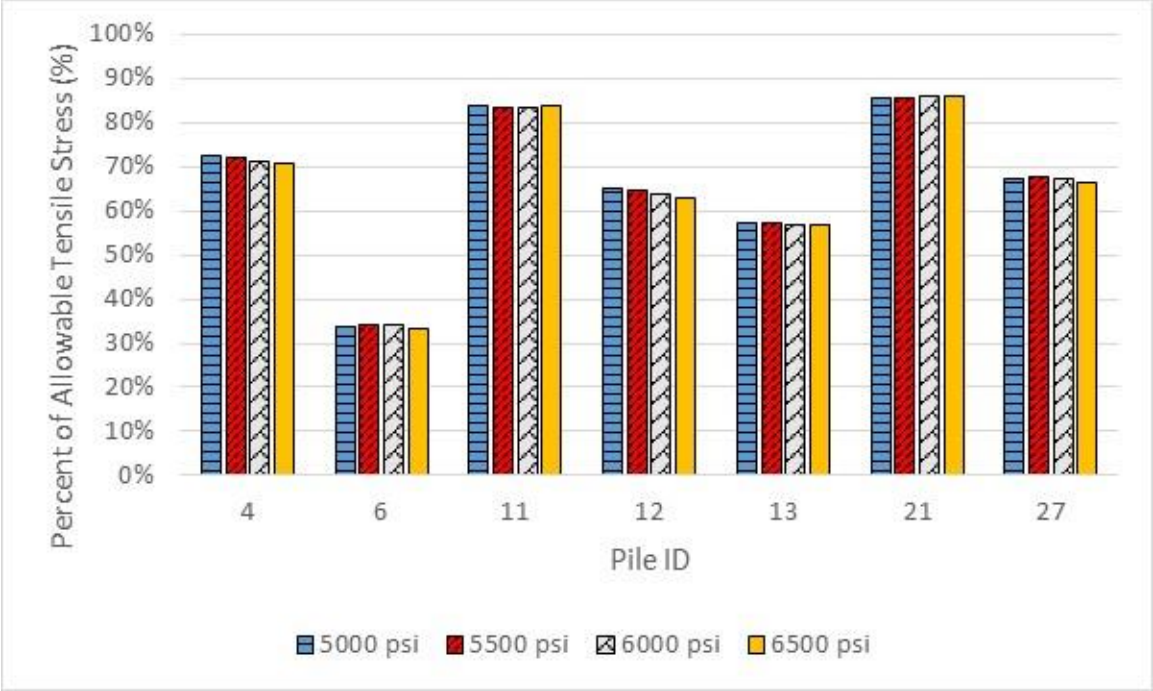

Figure 7-39: Percentage of allowable tensile stress achieved during 14 inch reduced size pile installations.

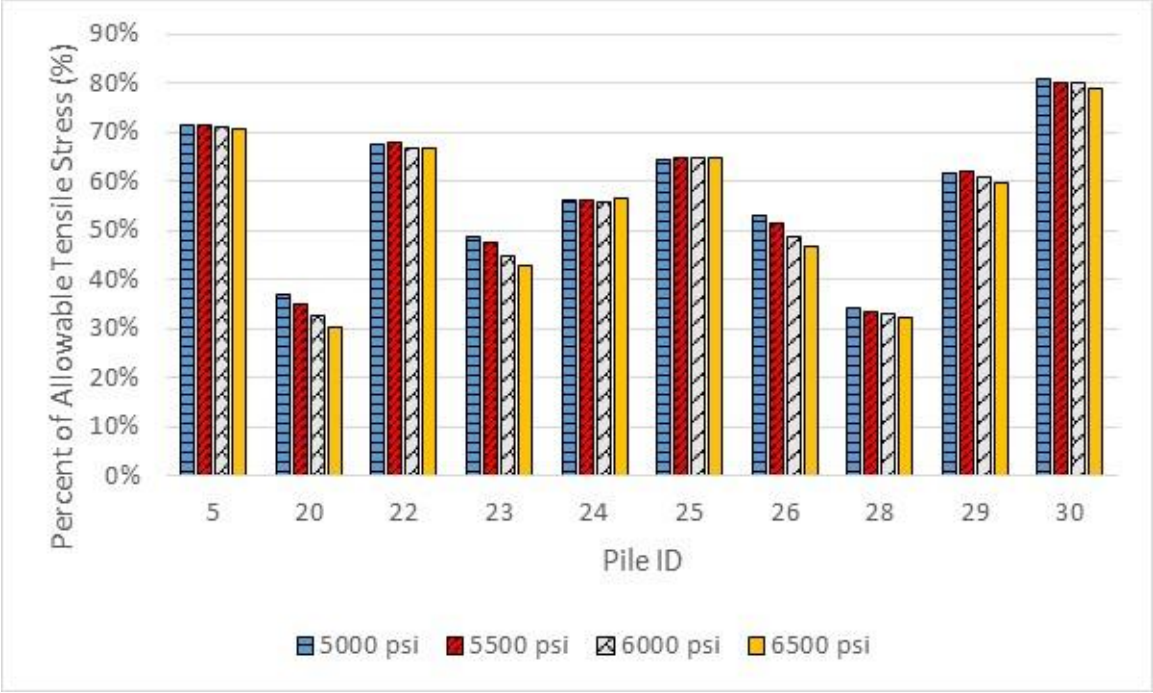

Figure 7-40: Percentage of allowable tensile stress achieved during 18 inch reduced size pile installations.

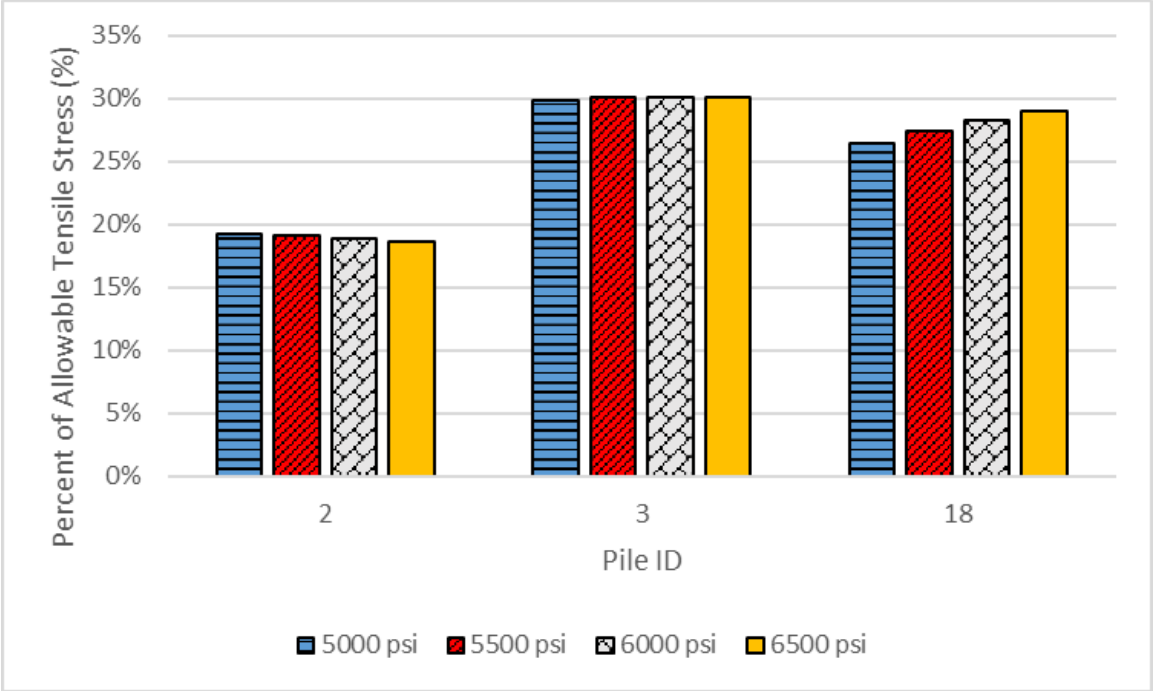

Figure 7-41: Percentage of allowable tensile stress achieved during 20 inch reduced size pile installations.

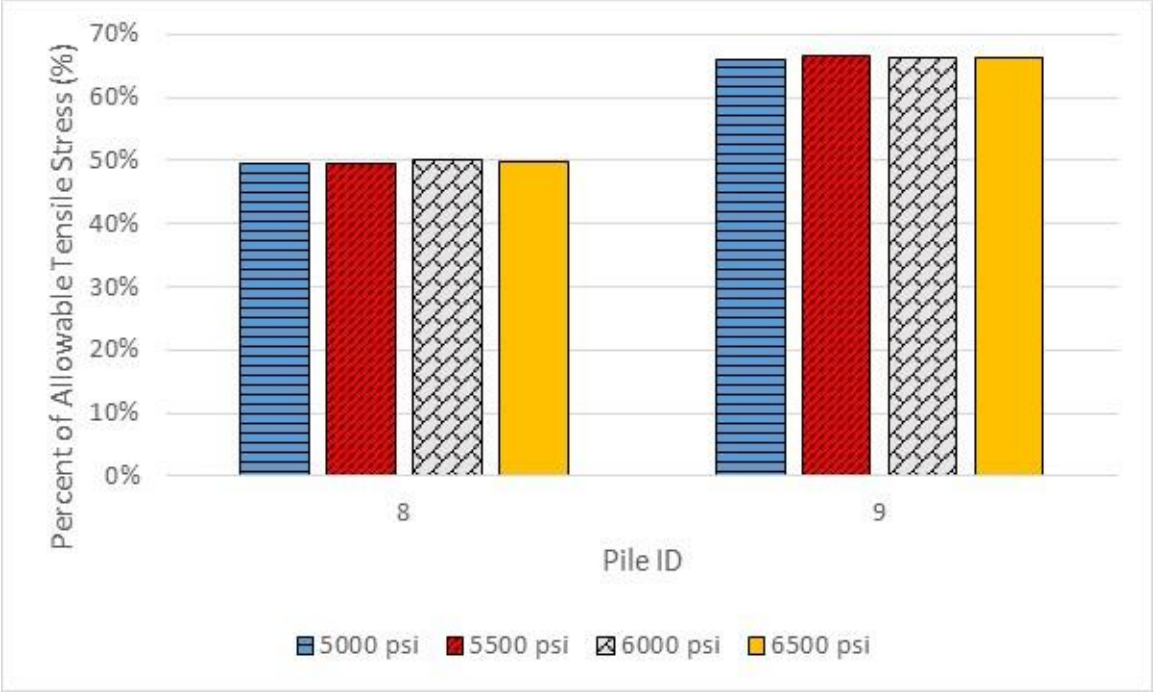

Figure 7-42: Percentage of allowable tensile stress achieved during 24 inch reduced size pile installations.

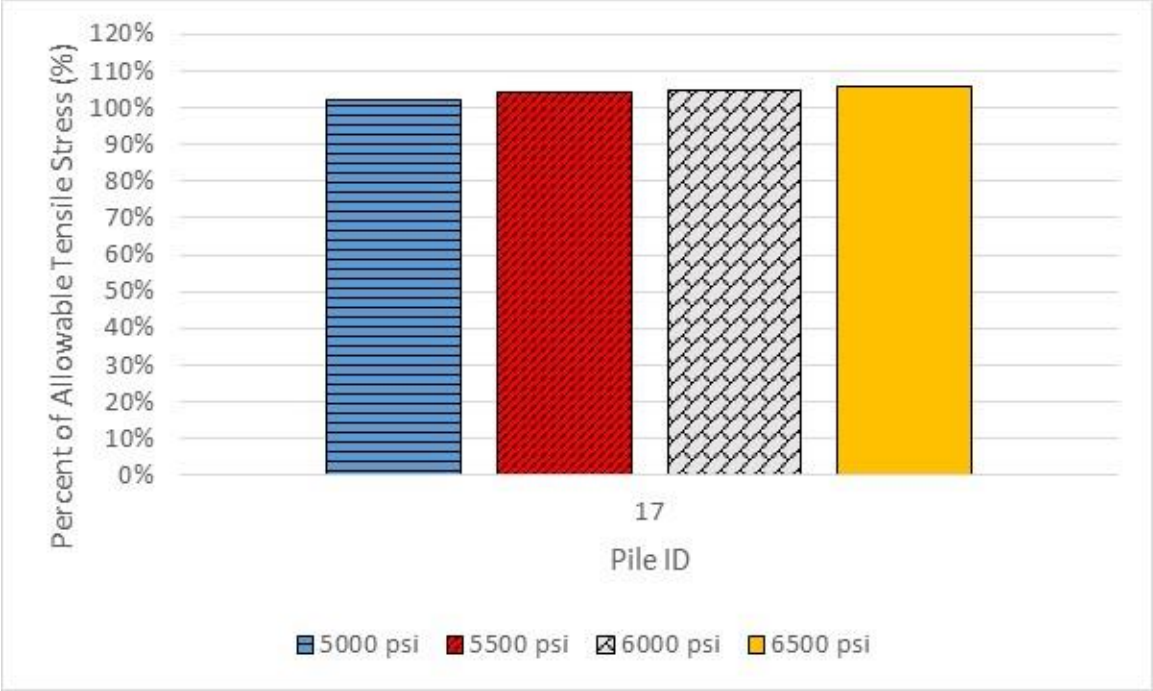

Figure 7-43: Percentage of allowable tensile stress achieved during 30 inch reduced size pile installations.

Figure 7-38 to Figure 7-43 reveal that all but four reduced size piles experienced maximum tensile driving stresses within allowable tensile stress limits. The four reduced size piles that exceed allowable tensile stress limits included the solitary 30 inch pile (Pile 17) and three 12 inch piles (Pile

16, 31, and 32). As previously mentioned, pile 17 was a research pile installed for research purposes only. Therefore, its installation may not have aligned with restrictions placed upon piles installed as a structural support member. It is important to note that ALDOT does not currently allow the use of 12 inch square PPC piles. As such, there were no 12 inch square PPC pile installations included within the historical records from which an appropriate hammer and driving system components could be determined. In the absence of 12 inch pile data, each twelve inch pile installation was modelled using hammer and driving system parameters commonly used for 14 inch square PPC pile installations. Though six of the nine 12 inch reduction piles, installed with the 14 inch pile components, experienced maximum driving stresses within allowable stress limits, it is possible that excessive tensile driving stresses experienced by piles 16, 31, and 32 were the direct result of being installed with the larger 14 inch pile components. Therefore, it is possible that all 12 inch reduction piles could have been safely installed had appropriately sized driving components been utilized for their modelled installations.

For reduced size piles, the change in the percentage of achieved allowable tension resulting at incremental increases in concrete strength was less uniform than that of achieved allowable compression. In response to incremental increases in compressive concrete strength, the percentage of achieved allowable tension slightly increased for 30 inch test piles and fluctuated between increasing and decreasing values for 12, 14, 18, 20, and 24 inch piles. Consistent with the analysis of the original test piles, this varied response can be attributed to subtle changes in both the allowable tensile stress limits and maximum tensile driving stresses resulting at each incremental increases in concrete strength. On average, a 500 psi increase in compressive concrete strength increased the allowable tensile stress limit of the reduced size piles by 1.2 percent and the maximum tensile driving stress incurred by the pile by 0.43 percent. Therefore, the percentage of achieved allowable tension varied little with increased compressive concrete strength.

The driving stress analysis performed on the reduced size pile installations revealed that the maximum driving stresses incurred during installation were often well below allowable stress limits. Though four reduced size piles were found to exceed tensile stress limits, it is possible that their subjection to excessive tensile stress was the product of analysis error.

The percentage of allowable stress achieved by original test piles and reduced size piles at a compressive concrete strength of 5000 psi were compared to evaluate the change in the percentage of achieved allowable stress resulting from pile size reduction. Table 7-15 provides a comparison of the percentage of achieved allowable compressive driving stress utilizing 5000 psi compressive strength concrete for original and reduced size piles.

Table 7-15 indicates the varied response of the percentage of achieved allowable compressive stress to pile size reduction. Some piles responded to pile size reduction with an increase in achieved allowable compressive stress, while others responded with a decrease in achieved allowable compressive stress. Through analysis of the soil existing between original test and reduced size pile depths of embedment, it was revealed that the installations experiencing the greatest increase in achieved allowable compressive stress were those in which the test pile was tipped in a soil possessing a strength much weaker than that of the soil into which the reduced size pile was advanced. Therefore, as anticipated, the advancement of a pile into a higher strength soil increased compressive driving stress. Accounting for all analyzed pile installations, the installation of reduced size piles resulted in a 3 percent average increase in achieved allowable compressive stress.

Table 7-16 provides a comparison of the percentage of achieved allowable tensile driving stress when utilizing a 5000 psi compressive strength concrete for original and reduced size piles. Table 7-16

indicates that for 25 of the 32 analyzed pile installations, pile size reduction resulted in an increase in achieved allowable tensile stress. Analysis of the soil existing between original test and reduced size pile embedment revealed that the piles experiencing the greatest increase in achieved allowable tension were those in which the test pile was tipped in a soil possessing a strength much stronger than that of the soil into which the reduced size pile was advanced. Therefore, as anticipated, the advancement of a pile into weaker soil increased tensile driving stress. Accounting for all analyzed pile installations, the installation of reduced size piles resulted in a 16 percent average increase in achieved allowable tensile stress.

Table 7-15: Comparison of the percentage of allowable compressive stress achieved by original and reduced sized piles utilizing 5000 psi concrete.

Size (in)	Pile ID	Percentage of Allowable Compressive Stress (%)		Difference (Red. - Orig.)
		Original Size Pile	Reduced Size Pile	
14"-12"	1	57%	76%	19%
	7	58%	63%	5%
	10	78%	80%	2%
	14	71%	64%	-6%
	15	49%	65%	16%
	16	54%	62%	7%
	19	88%	79%	-10%
	31	75%	61%	-14%
	32	76%	62%	-15%
	Avg.	**67%**	**68%**	**1%**
16"-14"	4	55%	59%	4%
	6	65%	69%	3%
	11	59%	67%	8%
	12	47%	59%	12%
	13	44%	58%	13%
	21	49%	61%	12%
	27	53%	53%	0%
	Avg.	**53%**	**61%**	**8%**
20"-18"	5	54%	59%	5%
	20	40%	46%	6%
	22	42%	47%	5%
	23	41%	46%	5%
	24	36%	34%	-1%
	25	51%	48%	-3%
	26	36%	44%	8%
	28	37%	46%	9%
	29	41%	58%	17%
	30	64%	62%	-2%
	Avg.	**44%**	**49%**	**5%**
24"-20"	2	58%	54%	-4%
	3	54%	49%	-5%
	18	62%	46%	-17%
	Avg.	**58%**	**49%**	**-9%**
30"-24"	8	50%	49%	-1%
	9	57%	56%	-1%
	Avg.	**53%**	**52%**	**-1%**
36"-30"	17	60%	63%	3%
	Avg.	**60%**	**63%**	**3%**

Table 7-16: Comparison of the percentage of allowable tensile stress achieved by original and reduced sized piles utilizing 5000 psi concrete.

Size (in)	Pile ID	Percentage of Allowable Tensile Stress (%)		Difference (Red. - Orig.)
		Original Size Pile	Reduced Size Pile	
14"-12"	1	19%	46%	26%
	7	44%	53%	9%
	10	13%	85%	71%
	14	59%	74%	15%
	15	47%	66%	19%
	16	72%	107%	35%
	19	72%	81%	9%
	31	40%	103%	63%
	32	75%	107%	32%
	Avg.	**49%**	**80%**	**31%**
16"-14"	4	28%	72%	44%
	6	33%	34%	1%
	11	16%	84%	67%
	12	45%	65%	20%
	13	19%	57%	38%
	21	72%	86%	14%
	27	67%	67%	0%
	Avg.	**40%**	**66%**	**26%**
20"-18"	5	51%	72%	21%
	20	32%	37%	5%
	22	61%	68%	7%
	23	46%	49%	2%
	24	60%	56%	-4%
	25	57%	65%	7%
	26	46%	53%	7%
	28	8%	34%	27%
	29	51%	62%	11%
	30	95%	81%	-14%
	Avg.	**51%**	**58%**	**7%**
24"-20"	2	38%	19%	-19%
	3	51%	30%	-21%
	18	30%	26%	-4%
	Avg.	**40%**	**25%**	**-15%**
30"-24"	8	21%	49%	29%
	9	70%	66%	-4%
	Avg.	**46%**	**58%**	**12%**
36"-30"	17	102%	102%	0%
	Avg.	**102%**	**102%**	**0%**

7.8. Cost Analysis of Installing Reduced Size Piles

Establishing the required depth of embedment and length of each reduced size pile provided the data necessary to calculate and compare the estimated cost of original test piles to that of reduced size piles installed at the same locations. Typically, material and installation costs decrease directly with pile size. For each analyzed pile, estimated material cost per foot was multiplied by pile length and estimated installation cost per foot was multiplied by pile embedment. Summation of material and installation costs provided the estimated total cost of each pile installation. Table 7-17 presents a comparison of the estimated total cost associated with original test pile installations to that of the reduced size piles installed at the same locations to depth at which original test pile capacity could be achieved. Negative change in cost values indicate the installation of the reduced size pile generated a cost savings.

Table 7-17: Material and installation cost comparison of original and reduced sized piles.

Size (in)	Pile ID	Total Cost of Orig. Pile	Change of Embedment (ft)	Total Cost of Red. Pile	Change in Total Cost (Red. - Orig.)
14"-12"	1	$1,644.00	13.5	$1,751.25	$107.25
	7	$2,157.00	5	$1,868.00	-$289.00
	10	$1,837.50	57	$3,343.95	$1,506.45
	14	$2,317.50	32	$2,899.75	$582.25
	15	$2,082.00	6	$1,834.00	-$248.00
	16	$3,222.00	6	$2,752.50	-$469.50
	19	$2,910.00	18	$2,899.50	-$10.50
	31	$2,107.50	27	$2,575.50	$468.00
	32	$3,094.50	8	$2,715.50	-$379.00
16" - 14"	4	$2,080.00	7.6	$2,095.20	$15.20
	6	$2,591.00	31	$3,519.00	$928.00
	11	$1,792.00	31	$2,835.00	$1,043.00
	12	$2,237.00	3	$2,043.00	-$194.00
	13	$2,261.00	5	$2,142.00	-$119.00
	21	$3,059.20	36.4	$4,147.80	$1,088.60
	27	$2,802.00	21	$3,279.00	$477.00
20" - 18"	5	$4,850.08	30.56	$5,811.08	$961.00
	20	$5,862.00	5	$4,931.00	-$931.00
	22	$6,850.00	20	$6,682.00	-$168.00
	23	$5,360.00	9	$4,827.00	-$533.00
	24	$5,796.00	24.5	$6,125.50	$329.50
	25	$6,778.00	22	$6,722.00	-$56.00
	26	$5,876.00	4	$4,866.00	-$1,010.00
	28	$4,072.00	9	$3,778.00	-$294.00
	29	$6,542.80	2.6	$5,366.80	-$1,176.00
	30	$6,362.00	22	$7,057.00	$695.00
24" - 20"	2	$6,200.00	13	$5,036.00	-$1,164.00
	3	$7,045.00	14	$5,686.00	-$1,359.00
	18	$9,905.00	14	$7,420.00	-$2,485.00
30" - 24"	8	$6,225.00	1.5	$5,102.50	-$1,122.50
	9	$9,097.00	9.4	$8,390.00	-$707.00
36" - 30"	17	$18,222.50	42.5	$21,312.50	$3,090.00

Generating a cost savings through pile size reduction required that a reduced size pile achieve original test pile capacity at a depth of embedment in which the cost saving generated by a reduction

in pile cross-sectional area offset the cost generated by extending reduced size pile length and embedment. As previously mentioned, pile capacity is the result of resistance developed between the pile and the soil surrounding it. In general, higher strength soils generate higher resistance and therefore higher pile capacity. As such, the ability of a reduced size pile to generate a cost savings depended upon soil layers possessing adequate strength existing at a reasonable depth beyond original test pile embedment from which the reduced size pile could generate original test pile capacity. Therefore, the results of cost analysis were site specific, meaning they were dependent upon the soil composition at the installation site. Table 7-17 reveals that reducing the pile size at 19 of the 32 or roughly 60 percent of the analyzed locations generated a cost savings. The average change of embedment for the reduced size piles generating a cost savings was 9.2 feet, whereas the average change of embedment for the reduced size piles generating a cost increase was 28.9 feet. Of the 14 locations for which the installation of a reduced size pile did not generate a cost savings, the size reduction of pile 17 generated the greatest increase in total cost of $3,090.00. This relatively large increase in cost can be attributed to both the high material and installation costs associated with the large piles as well as the soil stratigraphy at the installation site. The soil beyond the depth of original test pile 17 embedment consisted of a thin medium strength sand layer and a low strength clay layer extending to the terminal depth of boring. Therefore, achieving original 36 inch test pile capacity with reduced 30 in pile required a substantial increase in pile length and embedment into the low bearing capacity clay layer which dramatically increased cost. If pile 17 were removed from the dataset, the average cost savings per pile analyzed is approximately $145. Results also indicated an increased likelihood of generating a substantial cost savings through the size reduction of piles 24 inches and larger. This can be attributed to the fact that there is a greater price difference between the larger size piles resulting from the increased size differences. For example, 24 inch piles can be reduced to 20 inch piles, 30 inch piles can be reduced to 24 inch piles, and 36 inch piles can be reduced to 30 inch piles.

8. Summary and Conclusions

Through the previously discussed research, a far better understanding of standard DOT practices has been developed when it comes to the design and use of prestressed, precast, concrete piles. This has been accomplished from a thorough review of available DOT resources, AASHTO Standard Specifications for Highway Bridges (17th Edition), AASHTO LRFD Bridge Design Specifications (8th Edition), other industry guides, and survey responses collected from DOTs, as well as structural analysis carried out utilizing the current standard pile details.

Based on the structural analysis conducted within this document, Alabama's standard structural pile capacities can be increased for PPCPs. For future projects, ALDOT engineers have excellent opportunities to optimize their pile usage by considering increasing the permissible structural capacities of the piles as determined by licensed professionals. To understand the industry applications of the knowledge this research has generated thus far, a survey was developed and distributed to pile producers and pile drivers. This survey was formulated and dispersed in a similar manner to the one that was sent to DOT representatives. The questions within the survey though focus on logistical considerations for transporting the piles, production capabilities, and preliminary cost information. There currently are not many responses to draw information from, and so their analysis and discussion remain for future work beyond what is considered for this report.

Driving stresses were assessed to determine the effect of increasing pile compressive concrete strength on driving stress, as well as whether smaller piles could be safely installed to support heavier loads. The costs of original test pile installations and reduced size pile installations were calculated and compared to see if using reduced size piles resulted in an economic benefit.

8.1. Conclusions

The research sought to fulfill several objectives and has produced several corresponding conclusions. First, a state of practice review demonstrated that ALDOT's PPCP capacities were lower than most DOTs considered. Then, a detailed consideration of ALDOT's particular capacity values produced the plausible explanation for their current table values. It appears that the AASHTO ASD capacities were calculated, then an additional safety factor of approximately 2.25 was applied to generate their ALDOT ASD capacities listed in their 2008 SDM. From there, a factor of about 1.5 was likely applied to account for the factored loads used with LRFD analysis, thereby determining LRFD capacities for ALDOT's piles. This analysis and corresponding moment-axial interaction diagram development confirmed the theory that ALDOT's structural capacities of their piles are substantially lower than the AASHTO LRFD allowed capacities, and thus could be increased. Table 8-1 below includes a possible new table of values that ALDOT could consider adopting for their structural PPCP capacity for fully supported piles. Table 8-2 shows these possible values compared with ALDOT's current values and Florida and Georgia current values. From this table, it is apparent that increasing the ALDOT values would bring them closer to the values used by their neighbors.

Table 8-1: Possible New ALDOT PPCP Capacities

Possible New ALDOT Standard Capacities		
Pile Size	Factored Axial Capacity	
	kips	tons
14-inch Pile	468	234
16-inch Pile	631	315
18-inch Pile	783	391
20-inch Pile	989	494
24-inch V. Pile	1200	600
30-inch V. Pile	1702	851
36-inch V. Pile	2214	1107

Table 8-2: Comparing ALDOT Possible Values with Current Values and Other DOTs

Possible New ALDOT Standard Capacities				
Pile Size	Alabama		Florida	Georgia
	Current	Possible		
14-inch Pile	180	468	550	473
16-inch Pile	240	631	N/A	636
18-inch Pile	300	783	900	820
20-inch Pile	360	989	1100	1006
24-inch V. Pile	440	1200	1575	1158
30-inch V. Pile	620	1702	1800	1706
36-inch V. Pile	820	2214	N/A	2224

Driving stress analysis was performed on both original test piles and reduced size piles, yielding consistent results. Incrementally increasing the piles' compressive concrete strength had little effect on the intensity of the resulting driving stresses. However, increasing the piles' compressive concrete strength increased the allowable driving stress limits. On average, increasing a pile's concrete compressive strength by 500 psi increased its allowable compressive stress limit by 11.3% and allowable tensile stress limit by 1.3%. As a result, increasing a pile's compressive concrete strength had a greater impact on its ability to withstand compressive driving stress than it did on its ability to withstand tensile stress. This finding is especially significant because it calls into question the rationale for increasing a pile's compressive concrete strength above 5000 psi. The driving stress

analysis revealed that neither the original test piles nor the reduced size piles exceeded compressive stress limits. This result was even consistent for smaller piles with a minimum compressive stress limit of 5000 psi and driven to greater depths of embedment. As is typical of most concrete elements, tensile stress appears to be the most important factor governing PPC pile design and installation. However, the results of the driving stress analysis conducted in this study show that increasing a pile's compressive concrete strength may be a futile attempt to compensate for tensile driving stress. Only five of the 64 pile installations analyzed (Original Test and Reduced Size Piles) produced tensile driving stresses that exceeded allowable tensile stress limits. It is worth noting that all five of these installations exceeded tensile stress limits at each analyzed compressive concrete strength, including 5000, 5500, 6000, and 6500 psi. As a result, there were no instances, where increasing a pile's compressive concrete strength from 5000 to 6500 psi significantly improved or compromised pile integrity.

Driving stress analysis on reduced-size piles revealed that 28 of the 32 analyzed piles could be safely installed to a depth of embedment sufficient to achieve the original test pile capacity. The installation of three 12 inch reduced size piles (Piles 16, 31, and 32) and a single 30 inch reduced size pile (Pile 17) resulted in maximum tensile driving stresses that exceeded allowable stress limits at each analyzed compressive concrete strength. The fact that these pile installations exceeded tensile stress limits could be attributed to the conditions of their modelled installation. As a result, it is possible that all reduced-size piles could have been safely installed if properly sized driving components had been used for their modelled installations. The percentage of achieved allowable stress at a compressive concrete strength of 5000 psi was determined by comparing the original test and reduced size piles. It was found that pile size reduction had a greater impact on achieved allowable tensile stress than achieved allowable compressive stress. On average, pile size reduction increased the percentage of achieved allowable compressive and tensile stress. However, the resulting increase in the percentage of achieved allowable stress was only significant for the previously discussed reduced size piles that exceeded tensile stress limits. As a result, the results of driving stress analysis on reduced size piles make a compelling case for considering pile size reduction. As a result, driving stress results suggest that the consideration of pile size reduction should not be hampered by concerns about exceeding pile stress limits.

From the structural perspective, ALDOT Project 930-929's overarching objective of optimizing PPCP usage has already been achieved by demonstrating that the analytical structural capacities of these piles are higher than those capacities currently in use. With this information, ALDOT engineers have the opportunity to update and enhance their PPCP design practices to make them more efficient. In conclusion, the results of driving stress analysis and the potential cost savings resulting from the utilization of reduced size piles make a strong case for ALDOT's consideration of increasing the axial load limits placed on square PPC pile sizes. Increasing square PPC pile axial load limits has the potential to provide a safe and cost-efficient alternative for the selection of concrete piles installed within the State of Alabama.

REFERENCES

1. Alabama Department of Transportation (ALDOT). *Bridge Bureau Structures Design and Detailing Manual*. 2008
2. Alabama Department of Transportation (ALDOT). *Bridge Special Project Drawings*. 2015. https://www.dot.state.al.us/brweb/bspd.html
3. Alabama Department of Transportation (ALDOT). *Precast Prestressed Concrete Piles: 14-16-18-20-30 & 36 Inches*. Bridge Special Project Drawing No. PSCP-1. 2017a.
4. Alabama Department of Transportation (ALDOT). *Structural Design Manual*. 2017b.
5. American Association of State Highway and Transportation Officials (AASHTO). *AASHTO LRFD Bridge Design Specifications*, 8th. ed. (Washington: AASHTO, 2017). Retrieved from https://app.knovel.com/hotlink/toc/id:kpAASHTO94/aashto-lrfd-bridge-design/aashto-lrfd-bridge-design
6. American Association of State Highway and Transportation Officials (AASHTO). *AASHTO LRFD Bridge Design Specifications* 6th. ed. (Washington: AASHTO, 2013). Foreword, pg. v. Retrieved from https://app.knovel.com/hotlink/toc/id:kpAASHTO32/aashto-lrfd-bridge-design/aashto-lrfd-bridge-design
7. American Association of State Highway and Transportation Officials (AASHTO). *Standard Specifications for Highway Bridges*, 17th. ed. (Washington: AASHTO, 2002). Retrieved from https://app.knovel.com/hotlink/toc/id:kpSSHBE001/standard-specifications/standard-specifications
8. American Concrete Institute Committee 318 (ACI). *Building Code Requirements for Structural Concrete*. Standard No. ACI 318-14. Farmington Hills: ACI. 2014.
9. American Institute of Steel Construction (AISC). *Steel Construction Manual.* 15th ed. (Chicago: AISC 2016).
10. American Society for Testing and Materials (ASTM). *Behavior of Deep Foundations*. STP 670. Baltimore: ASTM. 1979.
11. Das, Braja M. *Principles of Foundation Engineering*. 8th ed. (Boston: Cengage Learning, 2014).
12. Federal Highway Safety Administration (FHWA). *Geotechnical Engineering Circular No. 6 Shallow Foundations*. Report No. FHWA-SA-02-054. 2002. https://www.fhwa.dot.gov/engineering/geotech/pubs/010943.pdf
13. Federal Highway Safety Administration (FHWA). *Design and Construction of Driven Pile Foundations – Lessons Learned on the Central Artery/Tunnel Project*. Publication No. FHWA-HRT-05-159. 2006. https://www.fhwa.dot.gov/publications/research/infrastructure/geotechnical/05159/chapter4.cfm
14. Florida Department of Transportation (FDOT). "LRFD Design Example #1: Prestressed Precast Concrete Beam Bridge Design." 2011.
15. Florida Department of Transportation (FDOT). "Notes and Details for Square Prestressed Concrete Piles." Index No. 20600. 2016.
16. Florida Department of Transportation (FDOT). *Instructions for Design Standards - Index 20600 Series Concrete Piles.* "Design Aids" Topic Number: 625-010-003. pg 299 – 305. 2018a. https://fdotwww.blob.core.windows.net/sitefinity/docs/default-source/content2/roadway/ds/18/ids/ids-20600.pdf?sfvrsn=67aae288_0
17. Florida Department of Transportation (FDOT). *Standard Specifications for Road and Bridge Construction*. 2018b.
18. Florida Department of Transportation (FDOT). *Structural Design Guidelines*. 2018c.

19. Georgia Department of Transportation (GDOT). *Square Prestressed Concrete Piles*. Standard No. 3215. 1984.
20. Georgia Department of Transportation (GDOT). "Load Resistance Factor Design for Bridge Foundation Investigation Template Guidelines." 2016.
21. Georgia Department of Transportation (GDOT). *Bridge and Structures Design Manual*. 2017.
22. Likins, Garland. "Safety Factors for Pile Testing". Pile Driving Contractors Association. PileDriver. Volume 4. No. 2.(Spring). 34-43. 2003. https://www.pile.com/wp-content/uploads/2017/03/safteyFactors.pdf
23. Louisiana Department of Transportation and Development (LADOTD). *Bridge Design and Evaluation Manual*. 2017.
24. Meetz, B. Jr. "24 in. Octagonal Prestressed Concrete Piles and 14 in. Square Prestressed Concrete Piles." Official memorandum. South Carolina Department of Highways and Transportation. 1993.
25. Mishra, Gopal. "Types of Shallow Foundations and their Uses." The Constructor. Accessed December 17, 2018. https://theconstructor.org/geotechnical/shallow-foundations-types/5308/
26. Mississippi Department of Transportation (MDOT). *Bridge Design Manual*. 2010.
27. Nawy, Edward G. *Prestressed Concrete: A Fundamental Approach*. Upper Saddle River: Prentice Hall. 1995.
28. North Carolina Department of Transportation (NCDOT). "12 in. Prestressed Concrete Pile." 2017.
29. Parola, Jerry F. 1970, "Mechanics of Impact Driving." PhD thesis, The University of Illinois at Urbana-Champaign. Viewed August 2018. https://vulcanhammerinfo.files.wordpress.com/2017/08/parola.pdf
30. Portland Cement Association (PCA). "Report on Allowable Stresses in Concrete Piles." 1971.
31. Precast/Prestressed Concrete Institute (PCI). *PCI Design Handbook*. 2010.
32. Precast/Prestressed Concrete Institute (PCI). *Bridge Design Manual*. 2011.
33. Precast/Prestressed Concrete Institute (PCI). PCI Prestressed Concrete Pile Interaction Diagram Spreadsheet, version 1.2.15. Chicago, IL. 2015.
34. Rabun, Benjamin F, III. "LRFD Maximum Factored Structural Resistances and Drivability Stress Limits for Piles." Interdepartmental Correspondence. Georgia Department of Transportation. 2013.
35. Saatcioglu, M. "Chapter 4: Design of Slender Columns". University of Ottawa. Ottawa, Canada. n.d. http://by.genie.uottawa.ca/~murat/CHAPTER%204%20-%20SLENDER%20COLUMNS%20-%20SP17%20-%2009-07.pdf.
36. South Carolina Department of Transportation (SCDOT). "Prestressed Concrete Piles." Standard Drawing No. 704-01. 2014.
37. Tennessee Department of Transportation (TDOT). "Standard Pile Details." Standard Drawing No. STD-5-1. 1990.
38. Texas Department of Transportation (TxDOT). *Geotechnical Manual*. 2018.
39. Virginia Department of Transportation (VDOT). "Prestressed Concrete Piles Square: 12 in. thru 24 in." Plan No. BPP-1. 2016.
40. Virginia Department of Transportation (VDOT). Geotechnical Manual. "*Chapter 9 – Pile Foundations*." 2011.
41. Zickler, Andy. "LRFD NOW!" PowerPoint Presentation, VDOT Structure and Bridge Division. 2006. www.virginiadot.org/business/resources/LRFDNOW.ppt.

42. ASTM. (2011). Standard Test Method for Standard Penetration Test (SPT) and Split Spoon Sampling of Soils. West Conshohocken, PA: ASTM International.
43. ASTM. (2013). Standard Test Methods for Deep Foundations Under Static Axial Compressive Load. West Conshohocken, PA: ASTM International.
44. Coduto, D. P. (2001). Foundation Design Principles and Practices. Upper Saddle River, NJ: Prentice-Hall, Inc.
45. Coduto, D. P., Kitch, W. A., & Yeung, M. R. (2016). Foundation Design Principles and Practices-Third Edition. Upper Saddle River, NJ: Pearson Education, Inc.
46. Daniel, D. (2018, October 22). Jordan Pile Driving. (A. Weatherford, Interviewer)
47. Das, B. M. (2014). Principles of Foundation Engineering, Eigth Edition. Boston, MA: Cengage Learning.
48. Hannigan, P. J., Rausche, F., Likins, G. E., Robinson, B. R., & Becker, M. L. (2016). Geotechnical Engineering Circular No.12 - Volume 1& 2 Design and Construction of Driven Pile Foundations. National Highway Institute, U.S. Department of Transportation. Washington, DC: Federal Highway Administration.
49. McClelland, B., Focht, J.A. and Emrich, W.J. (1969). Problems in Design and Installation of Offshore Piles. American Society of Civil Engineers (ASCE), Journal of the Soil Mechanics and Foundations Division, Vol. 94, No.6, pp. 1491-1514.
50. Naylor, Nicholas. 2018. Map of Test Pile Installation Sites. Alabama: United States Geological Survey.
51. Pement, B. J., EVALUATION OF WBUZPILE DESIGN METHODOLOGY AND THE DEVELOPMENT OF A LRFD DRIVEN PILE RESISTANCE FACTOR CALIBRATION FOR ALABAMA SOILS.M.S. Thesis, Department of Civil, Coastal, and Environmental Engineering, University of South Alabama, Mobile, Al, 2017.
52. Pile Dynamics, I. (2010). GRLWEAP 2010 Background Report. Cleveland, OH: Pile Dynamics, Inc.Pile Dynamics, I. (2018, October 15). GRLWEAP Wave Equation Analysis. Retrieved from Pile.com: http://www.pile.com/wp-content/uploads/2017/09/GRLWEAP-Product-Details.pdf
53. PCI Committee on Prestressed Concrete Piling (1993). Recommended Practice for Design, Manufacture and Installation of Prestressed Concrete Piling. PCI Journal
54. Poulos, H.G. and Davis, E.H. (1980). Pile Foundation Analysis and Design. John Wiley and Sons, New York, NY, pp. 18-51.
55. Svinkin, M. (2017). Modulus of Elasticity and Stiffness of Composite Hammer Cushions. Cleveland, OH: VibraConsult.
56. Vesic, A. S. (1977). Design OF Pile Foundations. Washington, DC: Transportation Research Board.
57. Yang, N. C. (1970). Relaxation of Piles in Sand and Inorganic Silt. Journal of the Soil Mechanics and Foundations Division, 395-409.

APPENDIX A: Survey for DOTs Regarding PPCP Design and Use

The following survey was distributed to various state DOTs requesting information on their PPCP design and use. Formatting has been modified to facilitate inclusion with this document.

Survey Title: Prestressed Precast Concrete Piles Research for ALDOT

Table 0A-0-1: DOT Survey Logic

Survey Flow
Standard: 0. Default Block (1 Question) Standard: 1. Contact Information: (6 Questions) Standard: 2. DOT Documents & Resources: (11 Questions) Standard: 3. Pile Types Used (Please Check All That Apply) : (3 Questions) Standard: 4. Prestressed Precast Concrete Piles (Please Select All That Apply): (13 Questions) Standard: 5. Pile Capacity Calculations & General Design Considerations: (7 Questions) Standard: 6. Standard Capacity Dichotomy (3 Questions)
Branch: New Branch If If Does your DOT utilize a table or list of standard capacities for PPCPs? Yes Is Selected Standard: 6a. Standard Capacities Used for PPCPs: (7 Questions)
Branch: New Branch If If Does your DOT utilize a table or list of standard capacities for PPCPs? No Is Selected Standard: 6b. No Standard Pile Capacity Values Used: (4 Questions)
Branch: New Branch If If Does your DOT utilize a table or list of standard capacities for PPCPs? Not Sure Is Selected Standard: 6a. Standard Capacities Used for PPCPs: (7 Questions) Standard: 6b. No Standard Pile Capacity Values Used: (4 Questions)
Branch: New Branch If If Does your DOT utilize a table or list of standard capacities for PPCPs? It Depends Is Selected Standard: 6a. Standard Capacities Used for PPCPs: (7 Questions) Standard: 6b. No Standard Pile Capacity Values Used: (4 Questions)
Standard: 7. Construction & Driving Practices for Prestressed Precast Piles: (18 Questions) Standard: 0. Survey Completion: (2 Questions)

- Survey Content to Follow -

Start of Block: 0. Default Block

0. Prestressed Precast Concrete Piles Research for ALDOT

Thank you very much for filling out this survey. We have been looking into various southeastern DOTs' Prestressed Precast Concrete Pile usage, but it is important that we gather additional information and confirm what we have found matches your DOT's current design practice.

We are looking to gather information from a variety of perspectives, (namely structural, geotechnical, and construction/installation), and so the following questions touch on all 3 areas. If you do not know the answer to a question, please feel free to leave it blank and focus on those that fall under your area of expertise.

For the questions that have an "Other" option, please use the box provided to specify or explain what your response would be as it was not listed as another choice.

At the end of question sections, you will see a box for "Any Additional Comments". Please use this space to elaborate on your responses above or otherwise share any additional relevant information if you feel it is needed.

If you have any questions while you are filling out the survey, please feel free to contact us:

Emily Gould
Graduate Research Assistant - The University of Alabama
eagould@crimson.ua.edu

Dr. Sri Aaelti
Assistant Professor - The University of Alabama
Phone: (205) 348-5110
saaleti@eng.ua.edu

End of Block: 0. Default Block

Start of Block: 1. Contact Information:

1. Contact Information:

1.1 Which state's Department of Transportation are you responding for?
▼ Alabama, Arkansas, Florida, Georgia, Louisiana, Mississippi, North Carolina, South Carolina, Tennessee, Texas, Virginia, West Virginia, Other

1.2 Your Contact Information:

Name: _____
Job Title (Please include area of expertise: structural, geotechnical, construction, other): _____
Email: _____
Phone Number (Can put N/A if you prefer not to share): _____

1.3 Is there anyone else within your DOT we should contact? If so, please provide their information below.

1.3a Alternate Contact 1
Name: _____
Job Title (Please include area of expertise: structural, geotechnical, construction, other): _____
Email: _____

Phone Number (Can put N/A if you prefer not to share): _____

1.3b Alternate Contact 2
Name: _____
Job Title (Please include area of expertise: structural, geotechnical, construction, other): _____
Email: _____
Phone Number (Can put N/A if you prefer not to share): _____

End of Block: 1. Contact Information:

Start of Block: 2. DOT Documents & Resources:

2. DOT Documents & Resources:

We would like to ensure that the information and documents we have reflect current design practices with your DOT. Please attach web links to the currently used documents for each category below, if available, or alternatively you can upload files here directly.

If web links or files are not available or able to be shared through this survey for the documents below, please let us know how copies could be obtained in the "Any Additional Comments" section.

2.1a Web Link for Current Structural Design Manual: _____
2.1b File Upload for Current Structural Design Manual:
2.2a Web Link for Current Geotechnical Design Manual: _____
2.2b File Upload for Current Geotechnical Design Manual:
2.3a Web Link for Current Prestressed Precast Concrete Pile Construction Drawings: _____
2.3b File Upload for Current Prestressed Precast Concrete Pile Construction Drawings:
2.4a Web Link for Current Construction Specifications Pertaining to Driving Piles: _____
2.4b File Upload for Current Construction Specifications Pertaining to Driving Piles:
2.5 Please use this link if you would like to upload an additional file regarding PPCPs.
Any Additional Comments: _____

End of Block: 2. DOT Documents & Resources:

Start of Block: 3. Pile Types Used (Please Check All That Apply):

3. Pile Types Used by Your DOT:
3.1 Please check all driven pile types your DOT utilizes:

- Prestressed Precast Concrete Piles (PPCPs)
- Steel - Tube or Rectangular Pipe, or H Piles
- Timber Piles
- Other: _____

0 Any Additional Comments: _____

End of Block: 3. Pile Types Used (Please Check All That Apply):

Start of Block: 4. Prestressed Precast Concrete Piles (Please Select All That Apply):

4. Prestressed Precast Concrete Piles (If Applicable: Please Select All That Apply):

4.1 Typical or Allowable Square Pile Gross Dimensions:
- 14 in.
- 16 in.
- 18 in.
- 20 in.
- 24 in.
- 30 in.
- 36 in.
- Other: _____

4.2 Typical Minimum Cover for Cross Section:
- 2.0 in.
- 2.25 in.
- 2.5 in.
- 3.0 in.
- Other: _____

4.3 Allowable/Required Concrete Strength (f'c at 28 days) :
- 5,000 psi
- 5,500 psi
- 6,000 psi
- 6,500 psi
- 7,000 psi
- 7,500 psi
- 8,000 psi
- 8,500 psi
- Other: _____

4.5 Most Common Concrete Strength (f'c at 28 days) Used:
- 5,000 psi
- 5,500 psi
- 6,000 psi
- 6,500 psi
- 7,000 psi
- 7,500 psi
- 8,000 psi
- 8,500 psi
- Other: _____

4.6 Required Concrete Strength Used at Release/Transfer of Prestress:
- 3,000 psi

- 3,500 psi
- 4,000 psi
- 4,500 psi
- Other: _____

4.7 Minimum Age of Pile Before Shipping from Manufacturing Plant (days): _____

4.8 Minimum Age of Pile Before Driving (days): _____

4.9 Prestressing Strand Diameter Allowed in Piles:
- 3/8 in.
- 7/16 in.
- 0.5 in.
- 0.6 in.
- Other: _____

4.10 Allowable Prestressing Strand Material Properties:
- Stress Relieved Strand
- Low-Lax Strand
- Grade 270
- Grade 250

4.11 Do you prescribe required initial prestress in the strands? If so, please briefly explain how that value is determined. _____

4.12 What losses do you account for in transitioning from initial prestress to effective prestress?
- Lump Sum or Percentage (If so, please elaborate): _____
- Detailed Loss Calculations Based on AASHTO Equations (LRFD Bridge Design Specifications, 8th Edition, Section 5.9.3. - Including Creep, Elastic Shortening, Shrinkage, & Relaxation)
- Other (In-house methods? Please explain): _____

0 Any Additional Comments: _____

End of Block: 4. Prestressed Precast Concrete Piles (Please Select All That Apply):

Start of Block: 5. Pile Capacity Calculations & General Design Considerations:

5. Pile Capacity Calculations & General Design Considerations:

5.1 What considerations are incorporated into the capacity determination of a pile? Please check all that apply.
- Structural Capacity (Axial Only - When Piles are Fully Embedded)
- Structural Capacity (Axial and Moment - When Some Piles Continue Above Ground)
- Geotechnical Capacity Specific to the Site
- General Soil Conditions of the Region
- Driving Stresses
- Transportation Stresses

- Other: _____

5.2 To what degree do the following factors typically affect the design or selection of piles?

	Not a Factor	Minor Impact	Moderate Impact	Significant Impact	Typically Controls
Structural Capacity					
Geotechnical Capacity Specific to the Site					
General Soil Conditions of the Region					
Driving Stresses					
Transportation Stresses					
Availability from Manufacturers					
Ease of Installation					
Cost					

5.3 Does your DOT use a table of standard PPCP pile capacities? Why or why not? If yes, please name the design specification or provide the web link where it can be found. _____

5.4 If your DOT has documents detailing design procedures aside from what has been provided previously, please provide a description of how they can be accessed, or provide a link below.
_____

5.5 Please use this space to upload a file detailing design procedures if available.

0 Any Additional Comments: _____

End of Block: 5. Pile Capacity Calculations & General Design Considerations:

Start of Block: 6. Standard Capacity Dichotomy

6. Does your DOT utilize a table or list of standard capacities for PPCPs?
▼ Yes, No, Not Sure, It Depends

You will be directed to a particular set of questions based on your response above. If you selected "Not Sure" or "It Depends" you will be directed through both tracks of questions. Please fill them out to the best of your ability.

0 Any Additional Comments: _____

End of Block: 6. Standard Capacity Dichotomy

Start of Block: 6a. Standard Capacities Used for PPCPs:

6a. Standard Capacities Used for PPCPs:

Please complete this section if your DOT **DOES** use a table or other list of standard capacities for PPCPs.

6a.1 If your DOT uses a table or list of standard PPCP pile capacities, please explain what precisely is meant by those values. Are they listed in terms of LRFD design capacities?
_____

6a.2 How were those standard capacity values calculated? Were they originally determined via ASD then transitioned to LRFD? Please explain methodology.
_____

6a.3 Which considerations are incorporated into the standard capacity values of the piles? Please check all that apply.

- o Structural Capacity (Axial Only)
- o Structural Capacity (Axial and Moment)
- o Geotechnical Capacity Specific to the Site
- o General Soil Conditions of the Region
- o Driving Stresses
- o Transportation Stresses
- o Other: _____

6a.4 Please briefly explain the design process for your piles. Who has primary responsibility for the pile designs? How are the standard capacities checked against demands specific to the project?
_____

6a.5 What conditions warrant additional design work for piles or deviation from standard capacities? _____

0 Any Additional Comments: _____

End of Block: 6a. Standard Capacities Used for PPCPs:

Start of Block: 6b. No Standard Pile Capacity Values Used:

6b. No Standard Pile Capacity Values Used:

Complete this section if your DOT **DOES NOT** use a table or list of standard capacities for PPCPs.

6b.1 In the recent past, has your DOT used a table of standard capacities for piles? If so, why did your DOT move away from that practice? _____

6b.2 Please briefly explain the design process for your piles. Who has primary responsibility for the pile designs? _____

0 Any Additional Comments: _____

End of Block: 6b. No Standard Pile Capacity Values Used:

Start of Block: 7. Construction & Driving Practices for Prestressed Precast Piles:

7. Construction & Driving Practices for Prestressed Precast Piles:
7.1 What analysis methods are used to check the driving stresses which will be imparted to the piles?

- WEAP Analysis
- Other: _____

7.2 Who is ultimately responsible for ensuring the pile can withstand driving stresses?

- Structural/Bridge Engineer
- Geotechnical Engineer
- Contractor
- Other: _____

7.3 Please describe the frequency of use for each hammer type listed below:

	Not at All	Rarely	Occasionally	Regularly	Most Often	Always/with Few Exceptions
Diesel						
Hydraulic						
Air						
Steam						

Gravity						

7.4 Are there any other types of hammers your DOT utilizes? If so, please list them and the frequency of their use based on the scale above. _____

7.5 What dynamic analysis and static load test methods are typically employed for determining nominal pile bearing resistance? Please check all that apply. (Corresponding to AASHTO LRFD Bridge Design Specifications, 8th Edition Table 10.5.5.2.3.1)

- Static load test of at least one pile per site condition and dynamic testing of at least 2 piles per site condition, but no less than 2% of the production piles
- Static load test of at least one pile per site condition without dynamic testing
- Dynamic testing on 100% of production piles
- Dynamic testing, quality control by dynamic testing of at least 2 piles per site condition, but no less than 2% of the production piles
- Wave equation analysis, without pile dynamic measurements or load test but with field confirmation of hammer performance
- FHWA-modified Gates dynamic pile formula
- Engineering News dynamic pile formula
- Other: _____

0 AASHTO Bridge Design Specification Table 10.5.5.2.3.1

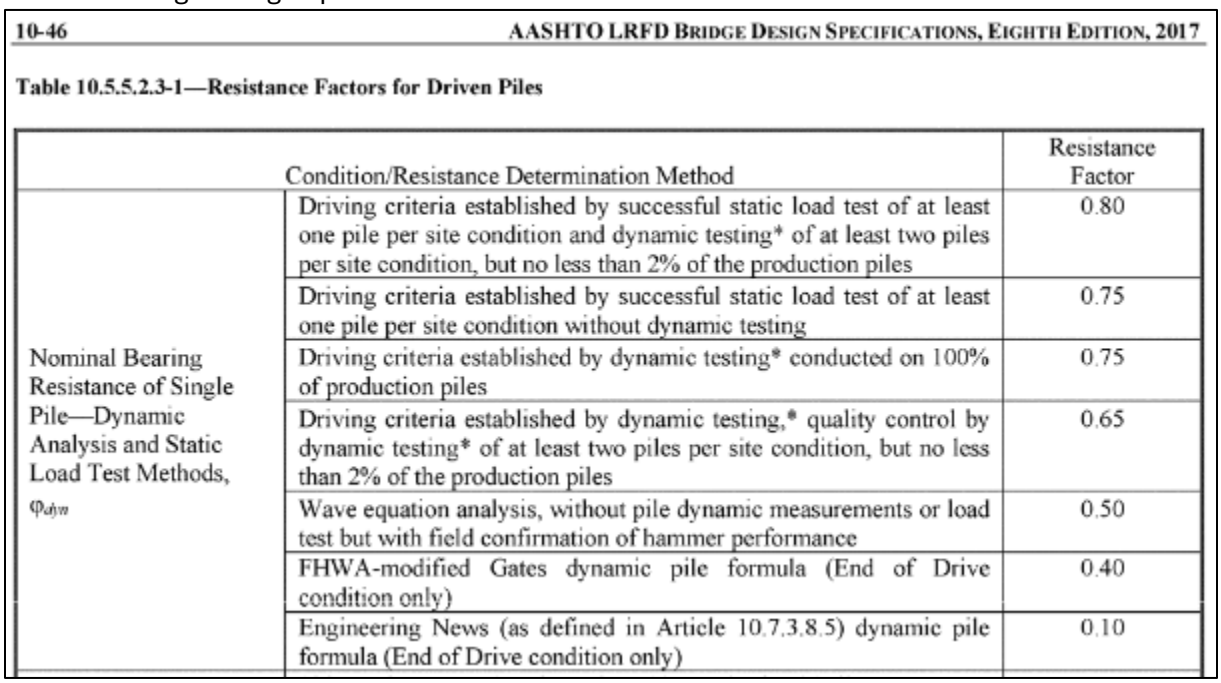

10-46 AASHTO LRFD BRIDGE DESIGN SPECIFICATIONS, EIGHTH EDITION, 2017

Table 10.5.5.2.3-1—Resistance Factors for Driven Piles

	Condition/Resistance Determination Method	Resistance Factor
Nominal Bearing Resistance of Single Pile—Dynamic Analysis and Static Load Test Methods, φ_{dyn}	Driving criteria established by successful static load test of at least one pile per site condition and dynamic testing* of at least two piles per site condition, but no less than 2% of the production piles	0.80
	Driving criteria established by successful static load test of at least one pile per site condition without dynamic testing	0.75
	Driving criteria established by dynamic testing* conducted on 100% of production piles	0.75
	Driving criteria established by dynamic testing,* quality control by dynamic testing* of at least two piles per site condition, but no less than 2% of the production piles	0.65
	Wave equation analysis, without pile dynamic measurements or load test but with field confirmation of hammer performance	0.50
	FHWA-modified Gates dynamic pile formula (End of Drive condition only)	0.40
	Engineering News (as defined in Article 10.7.3.8.5) dynamic pile formula (End of Drive condition only)	0.10

7.6a Does your DOT use the corresponding AASHTO LRFD resistance factors for the above dynamic analysis and static load test methods?

- Yes
- No
- Other (locally calibrated or other): _____

7.6b If you chose "No" or "Other" above, how can your resistance factors be accessed?

- See Previous Files Uploaded (Name of File): _____
- Web Link: _____
- Other: _____

7.7 Approximately what percentage of piles are statically tested for a project? _____

7.8 Approximately what percentage of piles are dynamically tested for a project? _____

7.9 Has your DOT experienced any cases when the measured driving stresses exceeded the WEAP predicted stresses? Please explain. _____

7.10 Has your DOT experienced damage to piles when the hammer selection analysis provided a safe condition? Please explain. _____

7.11a Does your DOT complete field inspector driving log sheets with hammer stroke, finish elevation, blow counts with embedment, EOD bearing capacity, and other driving information for each pile?

- Yes
- No
- I Don't Know

7.11b If you responded "Yes" to 7.10a: has your DOT experienced difficulty in completing some of the driving information? Please briefly explain. _____

7.12 Does your DOT complete a pile driving and equipment data form with hammer cushion and pile cushion specifications including area, elastic modulus, thickness, coefficient of restitution, and stiffness?

- Yes
- No
- I Don't Know

0 Any Additional Comments: _____

End of Block: 7. Construction & Driving Practices for Prestressed Precast Piles:

Start of Block: 0. Survey Completion:

0 **Survey Completion:**

Thank you very much for completing this survey. Your responses will prove extremely valuable in this project pertaining to PPCP usage. You will be directed to a report of your responses which you may save for your records.
Please feel free to leave any final comments in the space provided below.
If you have any questions after completing this survey, please feel free to contact us:

Emily Gould
Graduate Research Assistant - The University of Alabama
eagould@crimson.ua.edu

Dr. Sri Aaelti
Assistant Professor - The University of Alabama
Phone: 205-348-5110
saaleti@eng.ua.edu

0 Any Additional Comments: _____

End of Block: 0. Survey Completion:

APPENDIX B: Moment-Axial Interaction Diagrams for Standard ALDOT PPCPs

The following interaction diagrams were generated using Moment-Axial Interaction Diagram Generator (v9.3). Table 0B-0-1 shows the inputs which were used to generate these diagrams.

Table 0B-0-1 – Pile Inputs for Standard ALDOT Piles

Pile Inputs							
Pile Name:	14 inch ALDOT Standard	16 inch ALDOT Standard	18 inch ALDOT Standard	20 inch ALDOT Standard	24 inch Voided ALDOT Standard	30 inch Voided ALDOT Standard	36 inch Voided ALDOT Standard
Concrete Material Properties							
Concrete Strength (ksi)	5	5	5	5	5	5	5
Weight of Concrete (kcf)	0.15	0.15	0.15	0.15	0.15	0.15	0.15
Ultimate Strain of Concrete	0.003	0.003	0.003	0.003	0.003	0.003	0.003
Reinforcing Material Properties							
Grade Of Prestressing (ksi)	270	270	270	270	270	270	270
Modulus of Elasticity (ksi)	28500	28500	28500	28500	28500	28500	28500
Compression Limit	0.002	0.002	0.002	0.002	0.002	0.002	0.002
Tension Limit	0.005	0.005	0.005	0.005	0.005	0.005	0.005
Ties or Spiral	Spiral	Spiral	Spiral	Spiral	Spiral	Spiral	Spiral
Stress and Strain Information							
fpe (ksi)	-162	-162	-162	-162	-162	-162	-162
Section Properties							
Length (in.)	14	16	18	20	24	30	36
Width (in.)	14	16	18	20	24	30	36
Concrete Cover (in.)	3	3	3	3	3	3	3
Voided or Solid	Solid	Solid	Solid	Solid	Voided	Voided	Voided
Void Diameter (in.)	0	0	0	0	10.5	16.5	22.5
Strand Layout							
Number of Strands	8	8	12	12	16	20	28
Number of Spaces	2	2	3	3	4	5	7
Strand Diameter (in.)	0.5	0.5	0.5	0.5	0.5	0.5	0.5
Strand Area ($in.^2$)	0.153	0.153	0.153	0.153	0.153	0.153	0.153
Tie/Spiral Diameter	0.252	0.252	0.252	0.252	0.252	0.252	0.252
Layer 1 Strand #	3	3	4	4	5	6	8
Layer 2 Strand #	2	2	2	2	2	2	2
Layer 3 Strand #	3	3	2	2	2	2	2
Layer 4 Strand #	0	0	4	4	2	2	2
Layer 5 Strand #	0	0	0	0	5	2	2
Layer 6 Strand #	0	0	0	0	0	6	2
Layer 7 Strand #	0	0	0	0	0	0	2
Layer 8 Strand #	0	0	0	0	0	0	8
Layer 9 Strand #	0	0	0	0	0	0	0
Layer 10 Strand #	0	0	0	0	0	0	0

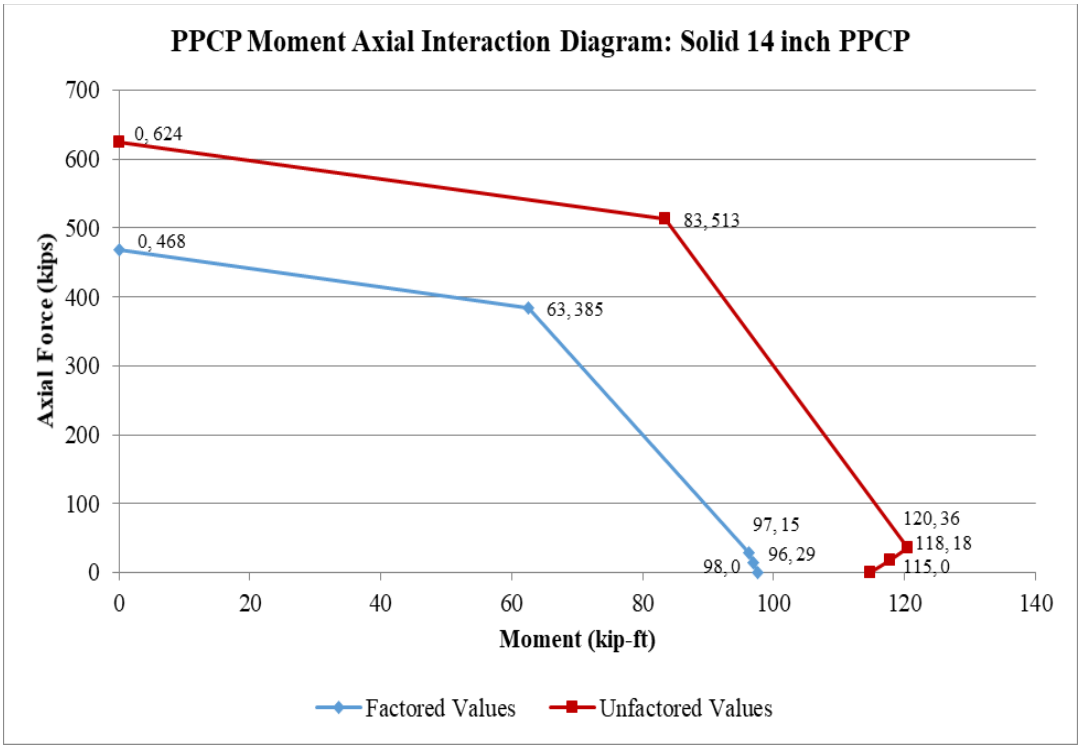

Figure 0B-0-1 – M-P Diagram: ALDOT Std. 14 in. PPCP

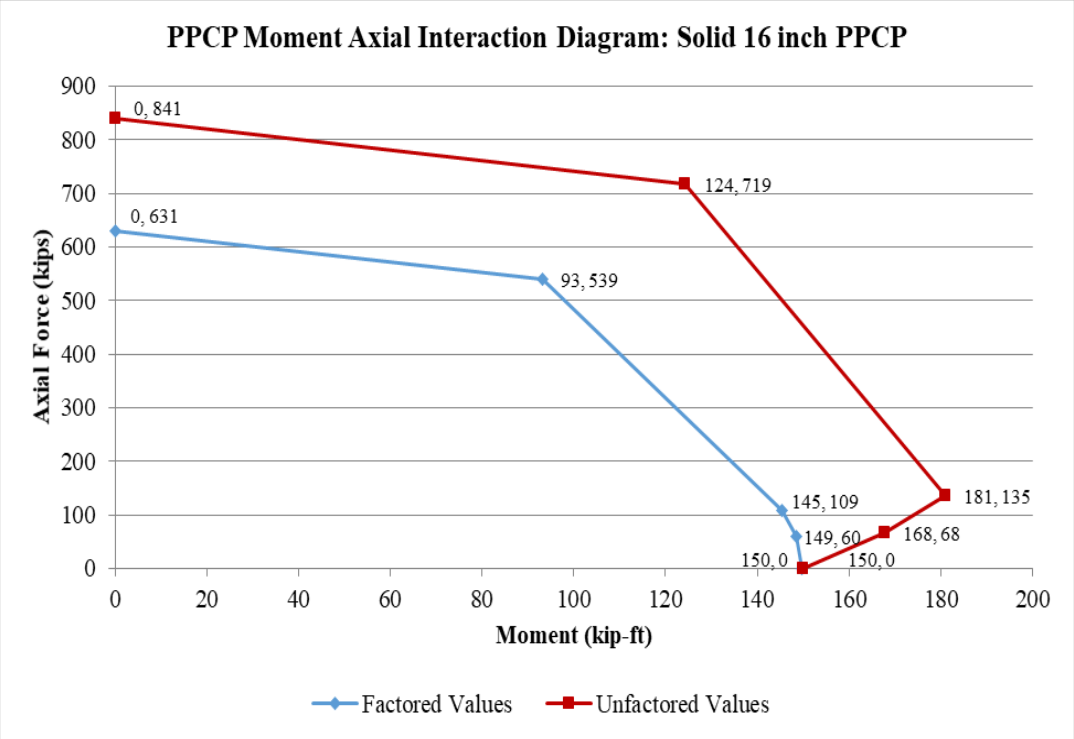

Figure 0B-0-2 – M-P Diagram: ALDOT Std. 16 in. PPCP

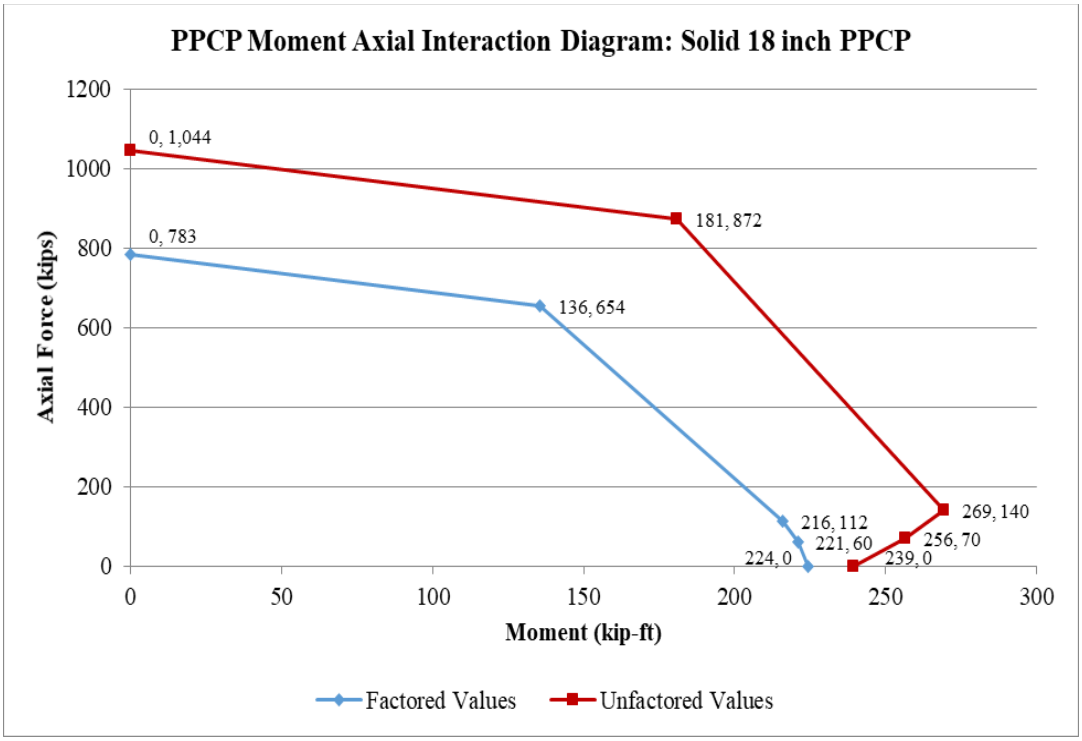

Figure 0B-0-3 – M-P Diagram: ALDOT Std. 18 in. PPCP

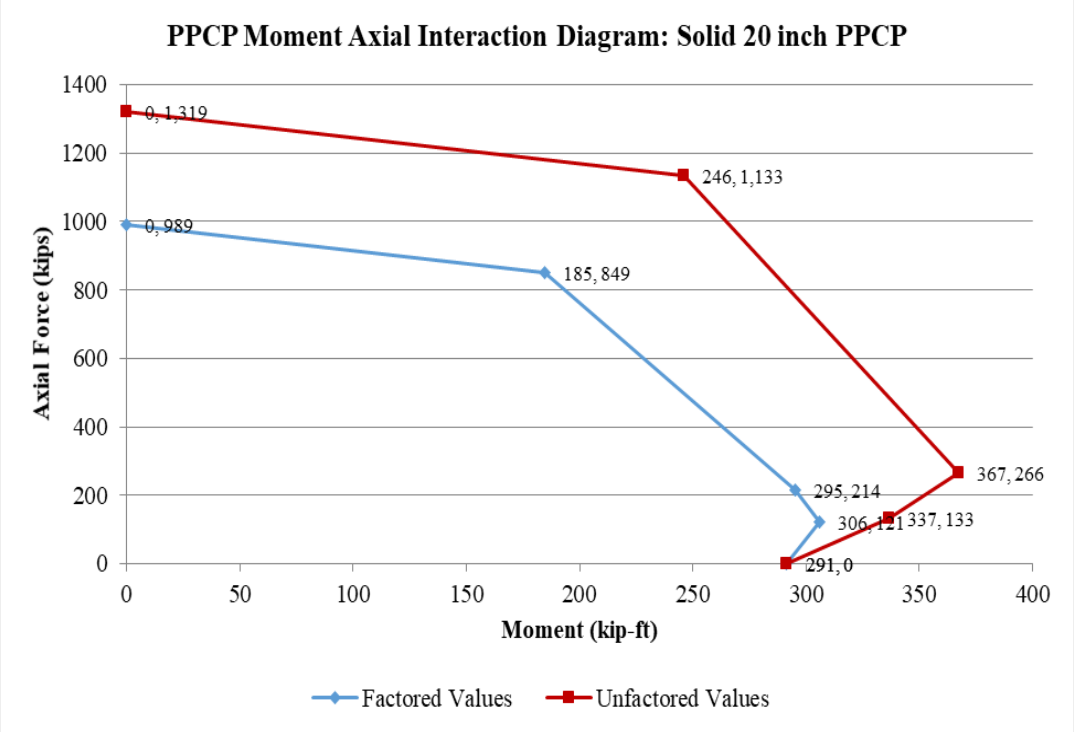

Figure 0B-0-4 – M-P Diagram: ALDOT Std. 20 in. PPCP

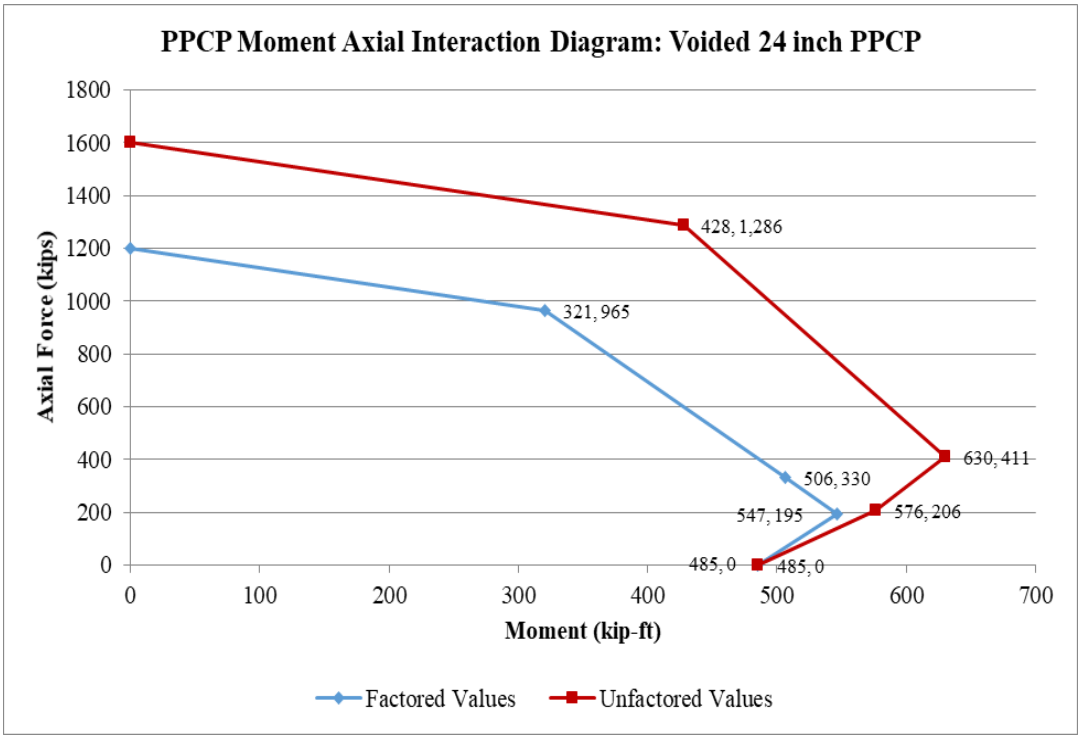

Figure 0B-0-5 – M-P Diagram: ALDOT Std. 24 in. PPCP

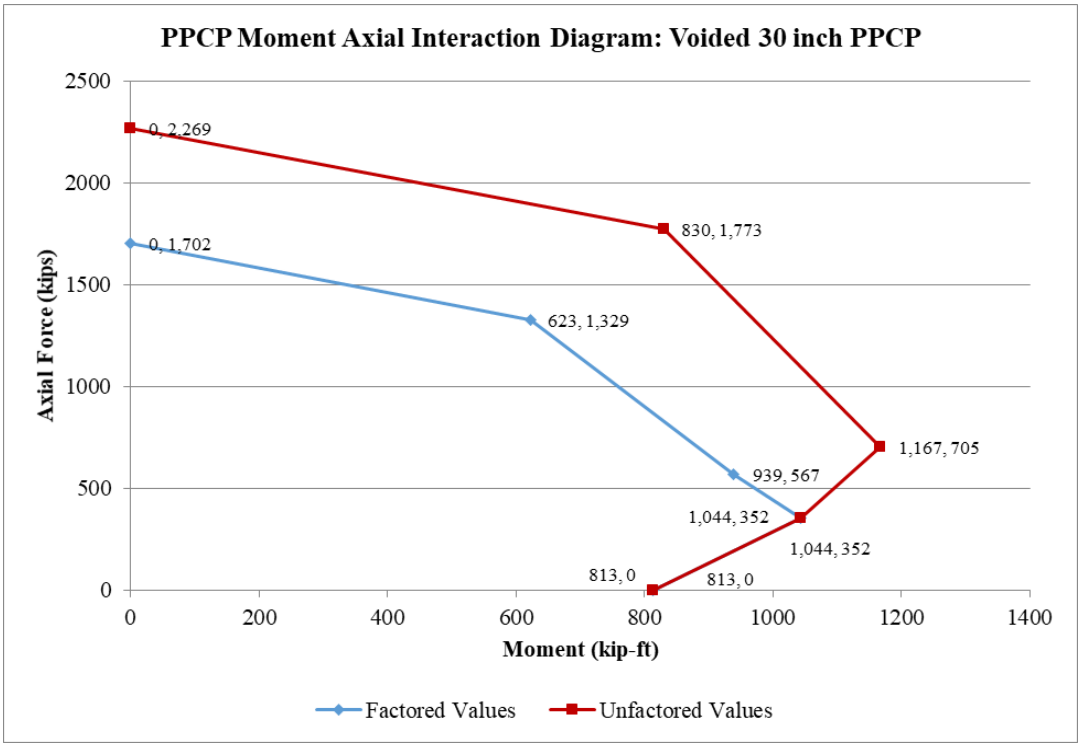

Figure 0B-0-6 – M-P Diagram: ALDOT Std. 30 in. PPCP

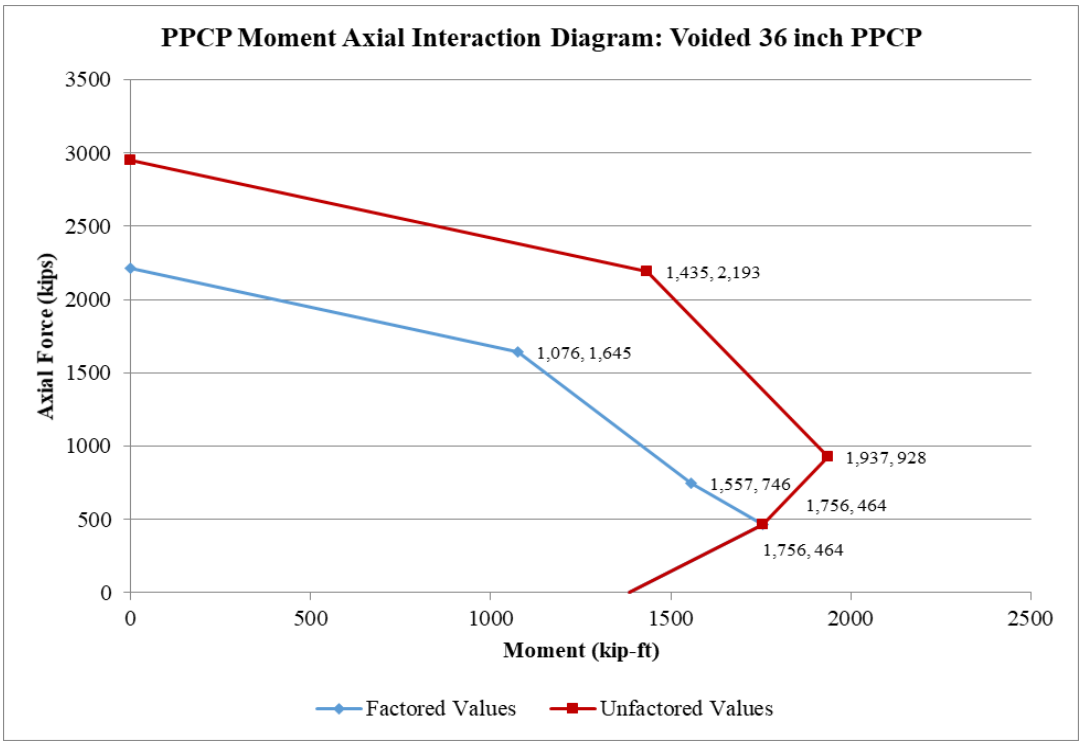

Figure 0B-0-7 – M-P Diagram: ALDOT Std. 36 in. PPCP

APPENDIX C: Analytical Pile Reactions for Prototype Bridges

For each of the load cased and bridges, reactions were estimated using the same loads for each pile size, varying only the analytical members' properties (area and effective moment of inertia). Within each table, the "Max. Bent" row indicates the maximum values experienced by a single pile in each category. These maximum values may not occur for the same pile.

Table 0C-0-1 – Bridge Analysis Reactions with Varying Pile Size

Two-Lane Bridge Analysis

	20-in. Pile	18-in. Pile	16-in. Pile	14-in. Pile
Primary Dim.	20	18	16	14
Ig, in.^{4}	13333	8748	5461	3201
I eff.	9333	6124	3823	2241
A, in.^{2}	400	324	256	196
LP Ieff:	46667	30618	19115	11205
LP Area	2000	1620	1280	980

	2-Lane	4-Lane	6-Lane
Number of Girders/Piles	5	9	13

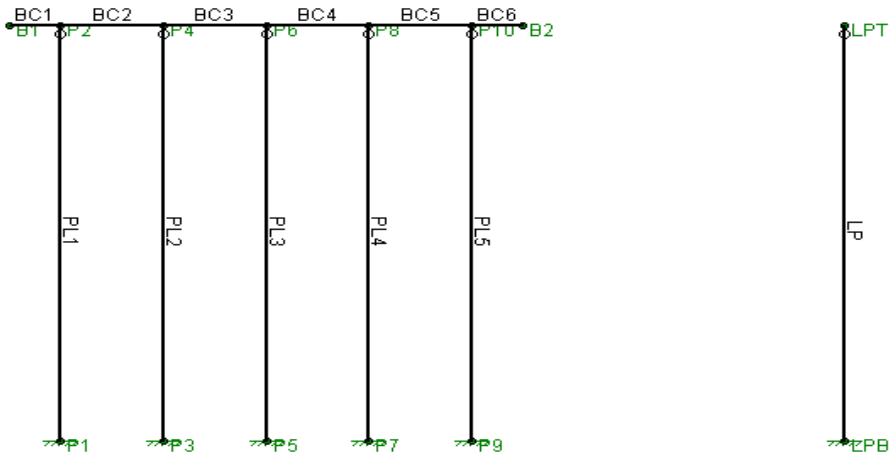

2-Lane - Strength I Case													Trend Moving Down in Pile Size		
2-Lane Bridge - Fixed Base, Pinned Top															
	20 in.			18 in.			16 in.			14 in.					
	X, k	Y, k	M, k-ft.	X, k	Y, k	M, k-ft.	X, k	Y, k	M, k-ft.	X, k	Y, k	M, k-ft.	X	Y	M
P1	-0.05	167.20	0.66	-0.05	168.19	0.66	-0.05	169.37	0.66	-0.05	170.77	0.66	=	+	=
P3	-0.05	264.76	0.66	-0.05	262.09	0.66	-0.05	259.06	0.66	-0.05	255.66	0.66	=	-	=
P5	-0.05	224.77	0.66	-0.05	228.14	0.66	-0.05	231.87	0.66	-0.05	235.89	0.66	=	+	=
P7	-0.05	267.61	0.66	-0.05	264.90	0.66	-0.05	261.82	0.66	-0.05	258.36	0.66	=	-	=
P9	-0.05	170.33	0.66	-0.05	171.35	0.66	-0.05	172.55	0.66	-0.05	173.99	0.66	=	+	=
LPB	-37.80	1094.70	1134.00	-37.80	1094.70	1134.00	-37.80	1094.70	1134.00	-37.80	1094.70	1134.00	=	=	=
Max. Bent	0.05	267.61	0.66	0.05	264.90	0.66	0.05	261.82	0.66	0.05	258.36	0.66	Trend Moving Down in Pile Size		
2 Lane Bridge - Fixed Base, Fixed Top															
	20 in.			18 in.			16 in.			14 in.					
	X, k	Y, k	M, k-ft.	X, k	Y, k	M, k-ft.	X, k	Y, k	M, k-ft.	X, k	Y, k	M, k-ft.	X	Y	M
P1	0.54	169.39	-5.42	0.44	169.96	-4.35	0.33	170.72	-3.29	0.23	171.75	-2.28	-	+	+
P3	0.01	262.59	-0.04	0.00	260.42	-0.02	0.00	257.85	0.01	0.00	254.85	0.04	-	-	+
P5	-0.05	224.71	0.49	-0.05	227.93	0.49	-0.05	231.55	0.50	-0.05	235.53	0.51	-	+	+
P7	-0.11	265.37	1.11	-0.11	263.17	1.08	-0.10	260.57	1.05	-0.10	257.51	1.01	-	-	-
P9	-0.66	172.61	6.56	-0.55	173.19	5.47	-0.44	173.97	4.39	-0.34	175.03	3.37	+	+	-
LPB	-37.80	1094.70	1134.00	-37.80	1094.70	1134.00	-37.80	1094.70	1134.00	-37.80	1094.70	1134.00	=	=	=
Max. Bent	0.66	265.37	6.56	0.55	263.17	5.47	0.44	260.57	4.39	0.34	257.51	3.37			

2-Lane - Strength V Case													Trend Moving Down in Pile Size		
2-Lane Bridge - Fixed Base, Pinned Top															
	20 in.			18 in.			16 in.			14 in.					
	X, k	Y, k	M, k-ft.	X, k	Y, k	M, k-ft.	X, k	Y, k	M, k-ft.	X, k	Y, k	M, k-ft.	X	Y	M
P1	-3.12	153.17	87.75	-3.12	153.94	87.74	-3.12	154.85	87.73	-3.12	155.93	87.73	=	+	-
P3	-3.12	228.31	87.73	-3.12	226.25	87.73	-3.12	223.92	87.73	-3.12	221.31	87.73	=	-	-
P5	-3.12	197.53	87.72	-3.12	200.13	87.72	-3.12	203.00	87.72	-3.12	206.09	87.72	=	+	+
P7	-3.12	230.51	87.71	-3.12	228.42	87.71	-3.12	226.05	87.72	-3.12	223.39	87.72	=	-	+
P9	-3.12	155.59	87.71	-3.12	156.37	87.71	-3.12	157.30	87.72	-3.12	158.40	87.72	=	+	+
LPB	-29.16	965.11	874.80	-29.16	965.11	874.80	-29.16	965.11	874.80	-29.16	965.11	874.80	=	=	=
Max. Bent	3.12	230.51	87.75	3.12	228.42	87.74	3.12	226.05	87.73	3.12	223.39	87.73	Trend Moving Down in Pile Size		
2-Lane Bridge - Fixed Base, Fixed Top															
	20 in.			18 in.			16 in.			14 in.					
	X, k	Y, k	M, k-ft.	X, k	Y, k	M, k-ft.	X, k	Y, k	M, k-ft.	X, k	Y, k	M, k-ft.	X	Y	M
P1	-2.51	145.14	40.66	-2.63	145.53	41.56	-2.75	146.14	42.47	-2.85	147.04	43.33	-	+	+
P3	-3.18	229.43	47.29	-3.15	227.74	46.72	-3.13	225.63	46.26	-3.11	223.04	45.93	+	-	-
P5	-3.21	197.48	47.64	-3.19	199.96	47.13	-3.17	202.75	46.71	-3.16	205.81	46.38	+	+	-
P7	-3.26	226.03	48.15	-3.23	224.34	47.54	-3.21	222.47	47.05	-3.19	220.39	46.67	+	-	-
P9	-3.43	167.03	49.76	-3.38	167.54	49.04	-3.34	168.13	48.32	-3.28	168.84	47.65	+	+	-
LPB	-29.16	965.11	874.80	-29.16	965.11	874.80	-29.16	965.11	874.80	-29.16	965.11	874.80	=	=	=
Max. Bent	3.43	229.43	49.76	3.38	227.74	49.04	3.34	225.63	48.32	3.28	223.04	47.65			

Four-Lane Bridge Analysis

	20-in. Pile	18-in. Pile	16-in. Pile	14-in. Pile
Primary Dim.	20.00	18.00	16.00	14.00
Ig, in.^{4}	13333	8748	5461	3201
I eff.	9333	6124	3823	2241
A, in.^{2}	400.00	324.00	256.00	196.00
LP Ieff:	84000	55112	34406	20168
LP Area	3600	2916	2304	1764

	2-Lane	4-Lane	6-Lane
Number of Girders/Piles:5	5	9	13

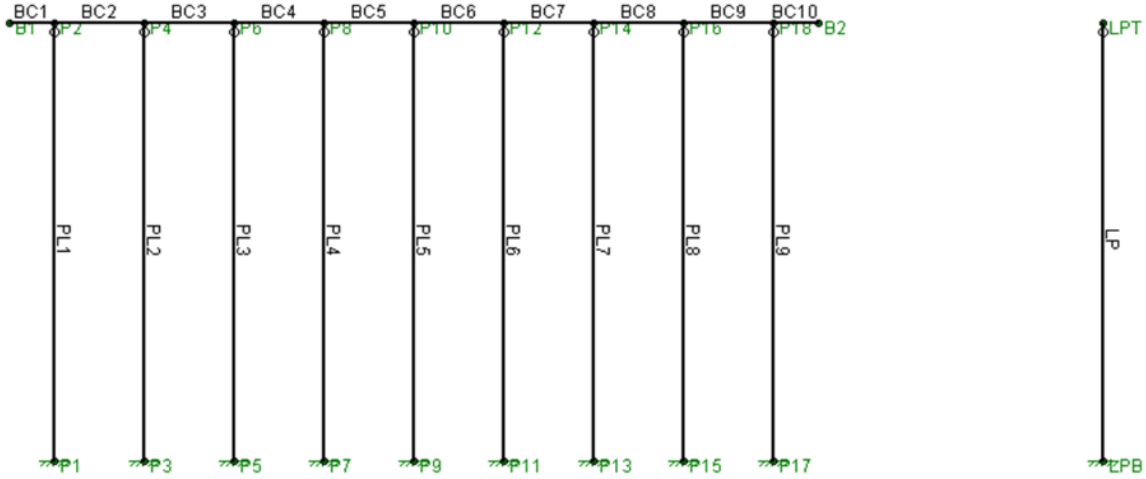

4-Lane - Strength I Case

4-Lane Bridge - Fixed Base, Pinned Top

	20 in.			18 in.			16 in.			14 in.			Trend Moving Down in Pile Size		
	X, k	Y, k	M, k-ft.	X, k	Y, k	M, k-ft.	X, k	Y, k	M, k-ft.	X, k	Y, k	M, k-ft.	X	Y	M
P1	-0.05	178.72	0.66	-0.05	180.10	0.66	-0.05	181.80	0.66	-0.05	183.92	0.66	=	+	=
P3	-0.05	329.07	0.66	-0.05	325.94	0.66	-0.05	322.24	0.66	-0.05	317.86	0.66	=	-	=
P5	-0.05	295.34	0.66	-0.05	297.78	0.66	-0.05	300.37	0.66	-0.05	303.01	0.66	=	+	=
P7	-0.05	306.01	0.66	-0.05	304.43	0.66	-0.05	302.88	0.66	-0.05	301.46	0.66	=	-	=
P9	-0.05	268.70	0.66	-0.05	270.50	0.66	-0.05	272.43	0.66	-0.05	274.53	0.66	=	+	=
P11	-0.05	308.38	0.66	-0.05	306.79	0.66	-0.05	305.23	0.66	-0.05	303.79	0.66	=	-	=
P13	-0.05	298.78	0.66	-0.05	301.20	0.66	-0.05	303.77	0.66	-0.05	306.38	0.66	=	+	=
P15	-0.05	331.91	0.66	-0.05	328.80	0.66	-0.05	325.12	0.66	-0.05	320.75	0.66	=	-	=
P17	-0.05	181.34	0.66	-0.05	182.72	0.66	-0.05	184.42	0.66	-0.05	186.55	0.66	=	+	=
LPB	-63.00	2498.30	1890.00	-63.00	2498.30	1890.00	-63.00	2498.30	1890.00	-63.00	2498.30	1890.00	=	=	=
Max Bent	0.05	331.91	0.66	0.05	328.80	0.66	0.05	325.12	0.66	0.05	320.75	0.66	Trend Moving Down in Pile Size		

4-Lane Bridge - Fixed Base, Fixed Top

	20 in.			18 in.			16 in.			14 in.			Trend Moving Down in Pile Size		
	X, k	Y, k	M, k-ft.	X, k	Y, k	M, k-ft.	X, k	Y, k	M, k-ft.	X, k	Y, k	M, k-ft.	X	Y	M
P1	0.82	182.25	-8.21	0.67	182.96	-6.71	0.52	184.00	-5.19	0.37	185.52	-3.74	-	+	+
P3	0.18	325.56	-1.83	0.15	323.18	-1.46	0.11	320.21	-1.11	0.08	316.46	-0.79	-	-	+
P5	-0.16	294.81	1.65	-0.14	297.25	1.44	-0.12	299.86	1.24	-0.10	302.55	1.04	+	+	-
P7	-0.13	306.36	1.26	-0.12	304.71	1.15	-0.11	303.09	1.05	-0.10	301.61	0.95	+	-	-
P9	-0.05	269.00	0.48	-0.05	270.77	0.48	-0.05	272.68	0.49	-0.05	274.74	0.50	=	+	+
P11	0.03	308.71	-0.27	0.02	307.06	-0.16	0.00	305.43	-0.04	-0.01	303.92	0.06	-	-	+
P13	0.06	298.22	-0.56	0.04	300.64	-0.37	0.02	303.24	-0.17	0.00	305.90	0.02	-	+	+
P15	-0.30	328.37	2.96	-0.26	326.02	2.57	-0.22	323.06	2.21	-0.19	319.34	1.87	+	-	-
P17	-0.93	184.96	9.29	-0.78	185.66	7.78	-0.63	186.70	6.26	-0.48	188.22	4.81	+	+	-
LPB	-63.00	2498.30	1890.00	-63.00	2498.30	1890.00	-63.00	2498.30	1890.00	-63.00	2498.30	1890.00	=	=	=

Max. Bent	0.93	328.37	9.29	0.78	326.02	7.78	0.63	323.06	6.26	0.48	319.34	4.81	

4-Lane - Strength V Case

	4-Lane Bridge - Fixed Base, Pinned Top												Trend Moving Down in Pile Size		
	20 in.			18 in.			16 in.			14 in.					
	X, k	Y, k	M, k-ft.	X, k	Y, k	M, k-ft.	X, k	Y, k	M, k-ft.	X, k	Y, k	M, k-ft.	X	Y	M
P1	-2.38	161.28	63.10	-2.38	162.34	63.09	-2.38	163.65	63.07	-2.38	165.29	63.06	+	+	-
P3	-2.38	277.14	63.09	-2.38	274.73	63.07	-2.38	271.89	63.06	-2.38	268.51	63.06	+	-	-
P5	-2.38	251.23	63.07	-2.38	253.11	63.06	-2.38	255.10	63.06	-2.38	257.13	63.05	=	+	-
P7	-2.38	259.43	63.05	-2.38	258.21	63.05	-2.38	257.02	63.05	-2.38	255.93	63.05	=	-	-
P9	-2.38	230.63	63.04	-2.38	232.02	63.04	-2.38	233.51	63.05	-2.38	235.13	63.05	=	+	+
P11	-2.38	261.25	63.03	-2.38	260.02	63.04	-2.38	258.81	63.04	-2.38	257.71	63.05	-	-	+
P13	-2.38	253.84	63.02	-2.38	255.71	63.03	-2.38	257.69	63.04	-2.38	259.70	63.04	-	+	+
P15	-2.38	279.33	63.02	-2.38	276.93	63.03	-2.38	274.10	63.04	-2.38	270.74	63.04	-	-	+
P17	-2.38	163.30	63.02	-2.38	164.36	63.03	-2.38	165.67	63.04	-2.38	167.31	63.04	-	+	+
LPB	-48.60	2137.50	1458.00	-48.60	2137.50	1458.00	-48.60	2137.50	1458.00	-48.60	2137.50	1458.00	=	=	=
Max. Bent	2.38	279.33	63.10	2.38	276.93	63.09	2.38	274.10	63.07	2.38	270.74	63.06			
	4-Lane Bridge - Fixed Base, Fixed Top												Trend Moving Down in Pile Size		
	20 in.			18 in.			16 in.			14 in.					
	X, k	Y, k	M, k-ft.	X, k	Y, k	M, k-ft.	X, k	Y, k	M, k-ft.	X, k	Y, k	M, k-ft.	X	Y	M
P1	-1.58	157.35	26.82	-1.73	157.84	28.10	-1.87	158.64	29.40	-2.01	159.86	30.62	-	+	+
P3	-2.24	276.26	33.40	-2.26	274.41	33.37	-2.27	272.02	33.38	-2.29	268.96	33.44	-	-	?
P5	-2.50	250.96	35.99	-2.48	252.92	35.56	-2.46	255.04	35.20	-2.43	257.24	34.88	+	+	-
P7	-2.47	259.66	35.61	-2.45	258.37	35.28	-2.44	257.12	35.00	-2.42	255.99	34.78	+	-	-
P9	-2.41	230.86	34.98	-2.40	232.23	34.74	-2.39	233.70	34.56	-2.39	235.29	34.42	+	+	-
P11	-2.35	261.57	34.38	-2.35	260.30	34.24	-2.35	259.04	34.14	-2.35	257.86	34.09	-	-	-

P13	-2.33	253.29	34.20	-2.34	255.06	34.11	-2.35	256.95	34.08	-2.35	258.87	34.08	-	+	-
P15	-2.61	274.80	36.98	-2.56	273.00	36.39	-2.53	270.81	35.89	-2.49	268.12	35.47	+	-	-
P17	-2.92	172.70	40.10	-2.84	173.31	39.13	-2.75	174.13	38.12	-2.66	175.25	37.16	+	+	-
LPB	-48.60	2137.50	1458.00	-48.60	2137.50	1458.00	-48.60	2137.50	1458.00	-48.60	2137.50	1458.00	=	=	=
Max. Bent	2.92	276.26	40.10	2.84	274.41	39.13	2.75	272.02	38.12	2.66	268.96	37.16			

Six-Lane Bridge Analysis

	20-in. Pile	18-in. Pile	16-in. Pile	14-in. Pile
Primary Dim.	20	18	16	14
Ig, in.^{4}	13333	8748	5461	3201
I eff.	9333	6124	3823	2241
A, in.^{2}	400	324	256	196
LP Ieff:	121333	79607	49698	29132
LP Area	5200	4212	3328	2548

	2-Lane	4-Lane	6-Lane
Number of Girders/Piles:	5	9	13

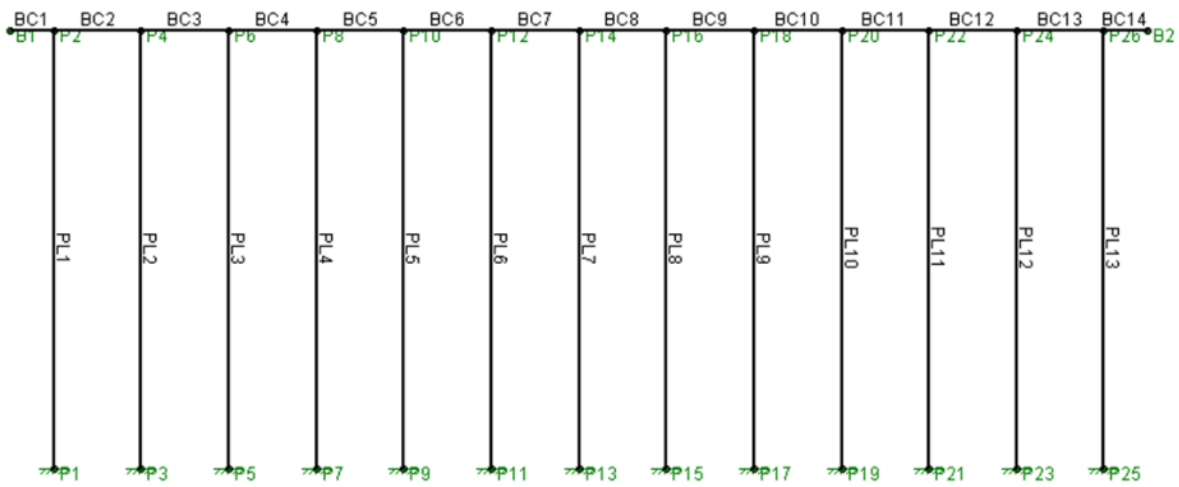

6-Lane - Strength I Case													Trend Moving Down in Pile Size		
	6-Lane Bridge - Fixed Base, Pinned Top														
	20 in.			18 in.			16 in.			14 in.					
	X, k	Y, k	M, k-ft.	X, k	Y, k	M, k-ft.	X, k	Y, k	M, k-ft.	X, k	Y, k	M, k-ft.	X	Y	M
P1	-0.05	193.31	0.66	-0.05	195.19	0.66	-0.05	197.49	0.66	-0.05	200.36	0.66	=	+	=
P3	-0.05	393.03	0.66	-0.05	388.70	0.66	-0.05	383.57	0.66	-0.05	377.47	0.66	=	-	=
P5	-0.05	345.76	0.66	-0.05	349.07	0.66	-0.05	352.65	0.66	-0.05	356.40	0.66	=	+	=
P7	-0.05	367.19	0.66	-0.05	365.72	0.66	-0.05	364.40	0.66	-0.05	363.36	0.66	=	-	=
P9	-0.05	342.59	0.66	-0.05	344.07	0.66	-0.05	345.54	0.66	-0.05	346.97	0.66	=	+	=
P11	-0.05	365.63	0.66	-0.05	363.50	0.66	-0.05	361.23	0.66	-0.05	358.81	0.66	=	-	=
P13	-0.05	318.91	0.66	-0.05	321.45	0.66	-0.05	324.23	0.66	-0.05	327.23	0.66	=	+	=
P15	-0.05	368.18	0.66	-0.05	366.04	0.66	-0.05	363.74	0.66	-0.05	361.29	0.66	=	-	=
P17	-0.05	346.07	0.66	-0.05	347.53	0.66	-0.05	348.99	0.66	-0.05	350.40	0.66	=	+	=
P19	-0.05	370.08	0.66	-0.05	368.62	0.66	-0.05	367.31	0.66	-0.05	366.30	0.66	=	-	=
P21	-0.05	348.27	0.66	-0.05	351.59	0.66	-0.05	355.19	0.66	-0.05	358.97	0.66	=	+	=
P23	-0.05	395.99	0.66	-0.05	391.64	0.66	-0.05	386.50	0.66	-0.05	380.38	0.66	=	-	=

P25	-0.05	196.27	0.66	-0.05	198.16	0.66	-0.05	200.47	0.66	-0.05	203.34	0.66	=	+	=
LPB	-94.50	4351.30	2835.00	-94.50	4351.30	2835.00	-94.50	4351.30	2835.00	-94.50	4351.30	2835.00	=	=	=
Max. Bent	0.05	395.99	0.66	0.05	391.64	0.66	0.05	386.50	0.66	0.05	380.38	0.66			

6-Lane Bridge - Fixed Base, Fixed Top													Trend Moving Down in Pile Size		
	20 in.			18 in.			16 in.			14 in.					
	X, k	Y, k	M, k-ft.	X, k	Y, k	M, k-ft.	X, k	Y, k	M, k-ft.	X, k	Y, k	M, k-ft.	X	Y	M
P1	1.12	198.06	-11.20	0.92	199.02	-9.17	0.71	200.44	-7.12	0.52	202.49	-5.18	-	+	+
P3	0.26	388.28	-2.54	0.21	384.98	-2.05	0.16	380.84	-1.60	0.12	375.61	-1.18	-	-	+
P5	-0.21	345.31	2.10	-0.18	348.56	1.78	-0.15	352.11	1.47	-0.12	355.89	1.18	+	+	-
P7	-0.03	367.72	0.33	-0.04	366.14	0.41	-0.05	364.69	0.48	-0.06	363.54	0.55	-	-	-
P9	-0.05	342.34	0.48	-0.05	343.90	0.49	-0.05	345.45	0.50	-0.05	346.94	0.52	-	+	+
P11	-0.14	365.61	1.44	-0.13	363.49	1.25	-0.11	361.22	1.08	-0.09	358.82	0.92	+	-	+
P13	-0.05	319.30	0.47	-0.05	321.75	0.48	-0.05	324.44	0.48	-0.05	327.37	0.49	-	+	+
P15	0.05	368.12	-0.46	0.03	365.99	-0.26	0.01	363.71	-0.08	-0.01	361.28	0.09	-	-	+
P17	-0.06	345.79	0.61	-0.06	347.35	0.59	-0.06	348.88	0.56	-0.05	350.36	0.54	+	+	-
P19	-0.08	370.61	0.79	-0.07	369.04	0.70	-0.06	367.61	0.61	-0.05	366.48	0.53	+	-	-
P21	0.10	347.83	-1.03	0.07	351.09	-0.72	0.04	354.66	-0.41	0.01	358.46	-0.13	-	+	+
P23	-0.36	391.21	3.60	-0.31	387.90	3.11	-0.27	383.74	2.66	-0.22	378.51	2.24	+	-	-
P25	-1.23	201.10	12.27	-1.02	202.06	10.23	-0.82	203.48	8.18	-0.62	205.53	6.23	+	+	-
LPB	-94.50	4351.30	2835.00	-94.50	4351.30	2835.00	-94.50	4351.30	2835.00	-94.50	4351.30	2835.00	=	=	=
Max. Bent	1.23	391.21	12.27	1.02	387.90	10.23	0.82	383.74	8.18	0.62	378.51	6.23			

6-Lane - Strength V Case

6-Lane Bridge - Fixed Base, Pinned Top													Trend Moving Down in Pile Size		
	20 in.			18 in.			16 in.			14 in.					
	X, k	Y, k	M, k-ft.	X, k	Y, k	M, k-ft.	X, k	Y, k	M, k-ft.	X, k	Y, k	M, k-ft.	X	Y	M
P1	-1.64	172.24	43.30	-1.64	173.68	43.28	-1.64	175.46	43.25	-1.64	177.67	43.24	+	+	-
P3	-1.64	326.19	43.28	-1.64	322.85	43.26	-1.64	318.89	43.25	-1.64	314.19	43.24	+	-	-
P5	-1.64	289.77	43.27	-1.64	292.32	43.25	-1.64	295.08	43.24	-1.64	297.97	43.23	+	+	-
P7	-1.64	306.31	43.25	-1.64	305.18	43.24	-1.64	304.16	43.23	-1.64	303.36	43.23	+	-	-
P9	-1.64	287.34	43.23	-1.64	288.48	43.23	-1.64	289.61	43.23	-1.64	290.72	43.22	+	+	-

P11	-1.64	305.11	43.22	-1.64	303.47	43.22	-1.64	301.71	43.22	-1.64	299.85	43.22	=	-	=
P13	-1.64	269.07	43.21	-1.64	271.03	43.21	-1.64	273.17	43.22	-1.64	275.49	43.22	=	+	+
P15	-1.63	307.08	43.20	-1.64	305.42	43.21	-1.64	303.65	43.21	-1.64	301.77	43.21	-	-	+
P17	-1.63	290.02	43.19	-1.63	291.15	43.20	-1.64	292.27	43.21	-1.64	293.36	43.21	-	+	+
P19	-1.63	308.55	43.18	-1.63	307.43	43.20	-1.64	306.41	43.20	-1.64	305.63	43.21	-	-	+
P21	-1.63	291.73	43.18	-1.63	294.30	43.19	-1.64	297.07	43.20	-1.64	299.98	43.21	-	+	+
P23	-1.63	328.49	43.17	-1.63	325.14	43.19	-1.64	321.17	43.20	-1.64	316.46	43.21	-	+	+
P25	-1.63	174.55	43.17	-1.63	176.00	43.19	-1.63	177.78	43.20	-1.64	180.00	43.21	-	+	+
LPB	-72.90	3656.40	2187.00	-72.90	3656.40	2187.00	-72.90	3656.40	2187.00	-72.90	3656.40	2187.00	=	=	=
Max. Bent	1.64	328.49	43.30	1.64	325.14	43.28	1.64	321.17	43.25	1.64	316.46	43.24	Trend Moving Down in Pile Size		

6-Lane Bridge - Fixed Base, Fixed Top															
	20 in.			18 in.			16 in.			14 in.					
	X, k	Y, k	M, k-ft.	X, k	Y, k	M, k-ft.	X, k	Y, k	M, k-ft.	X, k	Y, k	M, k-ft.	X	Y	M
P1	-0.65	171.33	13.98	-0.83	172.04	15.62	-1.00	173.13	17.28	-1.17	174.75	18.86	-	+	+
P3	-1.43	323.77	21.76	-1.46	321.21	21.92	-1.48	317.95	22.10	-1.51	313.80	22.30	-	-	+
P5	-1.78	289.53	25.26	-1.75	292.09	24.84	-1.72	294.91	24.47	-1.70	297.91	24.14	+	+	-
P7	-1.64	306.68	23.83	-1.64	305.45	23.73	-1.64	304.34	23.67	-1.64	303.46	23.62	-	-	-
P9	-1.65	287.15	23.92	-1.65	288.35	23.77	-1.64	289.54	23.67	-1.64	290.68	23.60	+	+	-
P11	-1.72	305.10	24.63	-1.70	303.46	24.35	-1.69	301.71	24.10	-1.67	299.86	23.90	+	-	-
P13	-1.64	269.37	23.86	-1.64	271.25	23.73	-1.64	273.33	23.63	-1.64	275.59	23.56	+	+	-
P15	-1.57	307.04	23.13	-1.58	305.40	23.15	-1.60	303.63	23.19	-1.61	301.76	23.25	-	-	+
P17	-1.65	289.81	23.93	-1.65	291.01	23.79	-1.65	292.21	23.68	-1.64	293.35	23.58	+	+	-
P19	-1.67	309.00	24.06	-1.66	307.79	23.87	-1.65	306.69	23.71	-1.64	305.80	23.58	+	-	-
P21	-1.53	291.30	22.68	-1.55	293.75	22.81	-1.57	296.42	22.95	-1.59	299.26	23.09	-	+	+
P23	-1.89	323.59	26.29	-1.85	321.05	25.76	-1.81	317.90	25.30	-1.77	313.98	24.89	+	-	-
P25	-2.44	182.77	31.78	-2.31	183.57	30.38	-2.17	184.68	28.95	-2.04	186.24	27.57	-	+	-
LPB	-72.90	3656.40	2187.00	-72.90	3656.40	2187.00	-72.90	3656.40	2187.00	-72.90	3656.40	2187.00	=	=	=
Max. Bent	2.44	323.77	31.78	2.31	321.21	30.38	2.17	317.95	28.95	2.04	313.98	27.57			